Coupling Paleoecological Proxies to Infer Competition, Niche Partitioning and Ecosystem Structure in Extinct Mammalian Communities

By

Gregory James Smith

Dissertation

Submitted to the Faculty of the

Graduate School of Vanderbilt University

in partial fulfillment of the requirements

for the degree of

DOCTOR OF PHILOSOPHY

in

Earth and Environmental Sciences

August 9, 2019

Nashville, Tennessee

Approved:

Steven Goodbred, Ph.D.

Simon A.F. Darroch, Ph.D.

Jessica Oster, Ph.D.

Patrick Abbot, Ph.D.

For Harvey

ACKNOWLEDGMENTS

This research was supported in part by National Science Foundation grant #1053839. Additionally, financial support was provided by the Larry Agenbroad Legacy Fund for Research, the Theodore Roosevelt Memorial Fund for Research. a Paleontological Society student research grant, a Geological Society of America student research grant, and Vanderbilt University.

This thesis could not have been completed without an extraordinary amount of assistance from many helpful, knowledgeable, and capable people. I am particularly grateful to Steven Goodbred and Guilherme Gualda, who have always supported me in what has otherwise been a very tumultuous journey. I thank my committee members, Simon Darroch, Jessica Oster, and Patrick Abbott for many fruitful conversations and excellent advice during my time at Vanderbilt. You are all remarkable educators and have inspired me more than you can know.

I am grateful to the amazing graduate students I have worked alongside at Vanderbilt. Jen, you have forever changed my life for the better. Brandt, thanks for your friendship and support. Eva, thanks for always being a beacon of sunshine. I'm grateful to my fellow GTFs for keeping me sane and smiling during me last year - Robert, Alex, and Chelsea, thanks for the cupcakes, the laughter, and the *Stegomastodon*.

Nobody has been more supportive and more instrumental in the successful completion of this dissertation than my family. I thank my parents, Arthur and Kathleen Smith, for always inspiring me and pushing me to follow my dreams. Thank you to my mother-in-law and father-in-law, Connie and Ashby Clanton. Thank you to Rooty, Masaya, and Charlie for snuggles, kisses, and love.

Finally, thank you to Lauren. I love you with all of my heart. You are an amazing wife, friend, and confidant and I am so thankful for you every day. You will make an amazing mother. Harvey - this is for you.

NOTE ON FORMATTING

Chapter 1 of this dissertation has been published, and Chapters 2 and 3 of this dissertation are currently in submission to peer-reviewed journals. Some structural changes have been made from the published format and the background sections for each publication explaining the paleoecological proxies used have been combined into one introductory section in Section 1.2. Despite these structural changes, the content of the individual chapters have been preserved. The references for these chapters are listed below:

Chapter 1: Smith, G.J. and DeSantis, L.R.G. 2018. Dietary ecology of Pleistocene mammoths and mastodons as inferred from dental microwear textures. Palaeogeography, Palaeoclimatology, Palaeoecology 492:10-25.

Chapter 2: Smith, G.J. and DeSantis, L.R.G. Extirpation of the gomphotheres: evidence for competition between sympatric proboscideans in Pleistocene North America. Paleobiology (in review)

Chapter 3: Smith, G.J., DeSantis, L.R.G., Green, J.L., and Dooley, A.C. Paleoecology of the Late Pleistocene Diamond Valley Lake Local Fauna in southern California as evidenced by dental mesowear analysis and dental microwear texture analysis. Palaeogeography, Palaeoclimatology, Palaeoecology (in review)

TABLE OF CONTENTS

LIST OF TABLES

LIST OF FIGURES

Chapter 1

INTRODUCTION

1.1 Motivation and Objectives

Megafauna (i.e., animals $\geq$44 kg in body mass; Martin (1967)) are extremely efficient resource consumers that play a significant role in the lateral transport of nutrients, often transporting them from areas of high to low abundance (e.g., Naiman 1988; Wolf et al. 2013). Because of this, modern megafauna, including Asian and Africa elephants, sustain high ecological diversity and productivity in their environments (e.g., Pringle 2008; Campos-Arceiz and Blake 2011). Given their disproportionate impacts on regional ecology and economic tourism, modern elephants are a critical component of conservation strategies (e.g., Hillborn et al. 2006; Wasser et al. 2010; Challender et al. 2014; Naidoo et al. 2016). However, a full understanding of how modern elephants might respond to anthropogenic stressors such as habitat loss due to farming or climate change is limited without a better appreciation for how their relatives responded to biotic and abiotic stressors in the past.

Paleoecology uses the fossil record as a tool to develop and test models of biotic response to climate and environmental change. When compared to modern (or neontological) ecology, a strength of paleoecology is the ability for researchers to acquire a long-term perspective on species, communities, and ecosystems, well beyond the limited timeframe of direct human observation (Kowalewski 2004; Dietl and Flessa 2009, 2011). The fossil record offers us perspective in a world of shifting baselines, where changing human perceptions of biological systems due to loss of experience about past conditions can lead towards a perception of normalcy despite constantly-changing ecological and environmental conditions (Papworth et al. 2009). Paleoecology studies generally take one of two approaches: the "near-time" approach, which uses fossil remains from within the last two million years

to compare conditions "before" and "after" a major disturbance; and the "deep-time" approach, which uses the longer geological record to investigate biological responses to system perturbations of diverse kinds and magnitudes (Conservation Paleobiology Workshop 2012).

This research examines the paleoecology and ecological structure of North American mammal communities throughout the Cenozoic at local, regional, and continental scales. The overall goal of this dissertation is to interrogate past ecosystems and their response to disturbance using both a "near-time" approach (Chapters 1-3) and a "deep-time" approach (Chapter 4). Under this framework, my specific research objectives are as follows:

Objective 1: Improve our understanding of megaherbivore paleoecology using geochemical and textural proxies for diet.

Objective 2: Use these proxy records to reconstruct the dietary niches of extinct megafauna and infer competition and niche partitioning in past mammalian communities.

Objective 3: Assess whether and how past biotic crises impacted ecosystem structure and function in North American mammals.

I used these objectives to examine paleoecological community structure at increasing geographic and temporal scales. Chapters 1 and 3 focus on particularly rich fossil sites that are time-averaged across tens of thousands of years, and are thus considered to be "local scale" studies. Chapter 2 combines multiple fossil assemblages distributed throughout the Pleistocene, and is thus considered to be a "regional scale" study. Finally, Chapter 4 examines North American mammal communities throughout the Cenozoic, and is thus considered to be a "continental scale" study. In the next section, I provide an overview of the paleoecological proxies used in Chapters 1-3.

1.2 Explanation of Paleoecological Proxies

1.2.1 Stable Oxygen Isotopes

Oxygen isotopes in animal tissues reflect a physiological balance between oxygen inputs and outputs whose proportions may differ among species (Bryant and Froelich 1995; Kohn and Cerling 2002); however, body water $\delta^{18}O$ values are linearly related to drinking water $\delta^{18}O$ values (Ayliffe et al. 1992; Longinelli 1984; Luz et al. 1984). Geography impacts $\delta^{18}O$ values of meteoric water ($\delta^{18}O_{mw}$), such that values decline with increased altitude, increased distance from the coast, increased precipitation (especially in tropical or subtropical regions), and decreased surface air temperature (Dansgaard 1964). In eastern North America, $\delta^{18}O_{mw}$ fluctuates seasonally, with lower values in the fall and winter months and higher values in the spring and summer months (Dorale et al. 1998; Sjostrom and Welker, 2009). This seasonal fluctuation is strongly controlled by moisture source, as reflected in $\delta^{18}O$ values recorded in speleothems ($\delta^{18}O_{spel}$) from the Atlantic Coastal Plain and Caribbean (Oster et al., 2019). Specifically, increases in $\delta^{18}O_{spel}$ during the summer months reflect precipitation primarily sourced from the Gulf of Mexico and subtropical Atlantic Ocean, while decreases in $\delta^{18}O_{spel}$ during the winter months reflect the intermixing of these subtropical sources with Pacific and Arctic air masses moving eastward across the polar jet stream (Liu et al. 2010; Aharon et al. 2012; Aharon and Dhugana 2017). Because of the controlling effects of climate on meteoric water, $\delta^{18}O_{enamel}$ preserved in fossil teeth can be useful for paleoenvironmental reconstructions (Higgins and MacFadden 2004; Hoppe 2004; Levin et al. 2006; Murphy et al. 2007; DeSantis et al. 2009; Yann et al. 2013). Large mammals, including proboscideans, are obligate drinkers with low metabolisms and are thus heavily reliant on surface water (Sukumar 2003); as a result, $\delta^{18}O_{enamel}$ values in proboscidean teeth more accurately reflects $\delta^{18}O_{mw}$ values as compared to smaller or drought-tolerant mammals (Bryant and Froelich 1995; Levin et al. 2006). Proboscidean $\delta^{18}O_{enamel}$ values can therefore be used to separate glacial and interglacial periods (Ayliffe

et al. 1992, 1994) and infer temporal changes in relative temperature and/or aridity (e.g., Koch et al. 1998; DeSantis et al. 2009; Metcalfe et al. 2011; Fisher et al. 2014; Baumann and Crowley 2015), although the multiplicity of compounding effects (aridity, temperature, and altitude, for example; as shown in Iacumin et al. 2010) can make predicting accurate conditions difficult. That being said, aridity can be teased apart from temperature via the aridity index (Levin et al. 2006; Yann et al. 2013). An additional strength of oxygen isotopes is in identifying populations that have been spatially mixed (via migration, for example) or time-averaged; generally, when standard deviations in $\delta^{18}O_{enamel}$ are large (e.g., $1\sigma \geq 2‰$ *sensu* Koch et al., 2004), although more seasonally variable climates often exceed this number (DeSantis et al., 2017).

1.2.2 Stable Carbon Isotopes

Stable carbon isotope values recorded in herbivorous animal tissues, including tooth enamel (specifically, enamel hydroxyapatite, $\delta^{13}C_{enamel}$), are derived from vegetation consumed during the life of the animal with an enrichment factor that is partially dependent on organismal body mass (Cerling and Harris 1999; Passey et al. 2005; Tejada-Lara et al. 2018). The two dominant photosynthetic pathways of plants fractionate stable isotopes of carbon differently, with C_3 plants discriminating more against the heavy ^{13}C isotope than C_4 plants (Bender 1971; Ehleringer et al. 1991). Modern C_3 plant $\delta^{13}C_{veg}$ values average approximately -27.0‰ and typically range from -35‰ to -22‰ (O'Leary 1988; Farquhar et al. 1989; Kohn 2010). Modern C_4 plants, in contrast, have average $\delta^{13}C_{veg}$ values of approximately -14.0‰ and generally range between -19‰ and -9‰ (O'Leary 1988; Farquhar et al. 1989; Ehleringer and Monson 1993). In tropical and subtropical regions, C_3 photosynthesis is the dominant photosynthetic pathway of most dicotyledonous shrubs, trees, and herbs (including those that produce fruit), while C_4 photosynthesis characterizes most monocotyledonous grasses and forbs (Teeri and Stowe 1976; Stowe and Teeri 1978; Sage 2017). As a result, stable carbon isotopes in mammalian enamel are a powerful tool

for discriminating between dietary habits in herbivores (Table 1.1) - particularly after the global expansion of C_4 grasses (*ca.* 9 - 5 million years ago; Cerling et al. 1997; Strömberg and McInerney 2011) and in the low-latitude localities targeted in this dissertation. Carbon isotope values of vegetation may be influenced by the isotopic composition of CO_2 in the atmosphere ($\delta^{13}C_{atm}$) (Kohn 2010, 2016) and pCO_2 within cell walls in C_3 plants (Schubert and Jahren 2012, 2015); however, multiple studies (Diefendorf et al. 2015; Voelker et al. 2015; Kohn 2016) have shown that the impact of pCO_2 on C_3 land plant $\delta^{13}C_{veg}$ is likely to be minimal on evolutionary timescales. Atmospheric $\delta^{13}C_{atm}$ values fluctuate with time and over climatic cycles (e.g., decreasing during glacial periods and increasing during climatic optimums; Tipple et al. 2010); therefore, calibration of $\delta^{13}C_{veg}$ values using independent estimates of $\delta^{13}C_{atm}$ are necessary to compare specimens across time.

Table 1.1: Dietary categories and the expected $\delta^{13}C$ or DMTA response variable for specialist populations in tropical or temperate locations where C_3 grasses and C_4 dicots are rare.

Dietary Category	**Expected $\delta^{13}C$**	**Expected *Asfc***	**Expected *epLsar***
Grazer	High	Low	High
Woody Browser	Low	Intermediate	Low
Mixed Feeder	Intermediate	Intermediate	Intermediate
Frugivore	Low	Very High	Low

Asfc, area-scale fractal complexity; *epLsar*, exact proportion length-scale anisotropy of relief. Dietary interpretations for DMTA follow those interpreted for bovids (Scott 2012) while stable isotope expectations are based on data from O'Leary 1988 and Kohn and Cerling 2003.

1.2.3 Dental Microwear

Dental microwear refers to the microscopic features on the wear facet of a tooth surface that result from food processing, recognizable as patterns of pits and scratches on a tooth surface. The study of dental microwear provides a 'snapshot' in time of the diet of an organism because dissolution from food and saliva has not yet remodeled the tooth surface

(Grine 1986). The prominence and density of scratches, pits, and gauges (i.e., deeper or more prominent pits) on the wear facet can thus be used to summarize the textural properties of diet during the last few days to weeks of an organism's life (e.g., Walker et al. 1978; Grine 1981, 1986; Solounias et al. 1988). In herbivores, a high incidence of scratches indicates the consumption of tougher or more pliant food items, such as phytolith-rich grasses that require shear force to rupture tissues (Teaford and Walker 1984). On the other hand, pits or gauges tend to form as a result of the crushing of hard and/or brittle objects – such as woody bark, seeds, or fruit pits – with the size of the pit dependent on the size and/or hardness of the food being consumed (e.g., Walker et al. 1978; Grine 1981, 1986; Solounias and Semprebon 2002; Semprebon et al. 2004). Taken together, quantification of the prevalence of scratches to pits on the wear facet of a tooth can discriminate between feeding ecologies in mammalian herbivores.

Microwear has historically been quantified through either two dimensional or user-based methods, where an observer counts the number of pits and scratches left on the surface of enamel as captured via SEM images (e.g., Walker et al. 1978; Teaford and Walker 1984; Grine 1981, 1986) or through the lens of a stereomicroscope (e.g., Solounias and Semprebon 2002; Semprebon et al. 2004; Rivals et al. 2007, 2010, 2012). In these studies, a higher ratio of pits to scratches in herbivores corresponds with a diet high in woody browse; by contrast, a lower ratio of pits and scratches indicates a diet composed of tougher food items like grass (Walker et al. 1978; Grine 1981; Teaford and Walker 1984). Despite attempts to standardize this method (Teaford and Walker 1984; Gordon 1988), observers of varying experience levels have been shown to record significantly different numbers of pits and scratches on identical scans (Grine et al. 2002; Galbany et al. 2005; Mihlbachler et al. 2012; DeSantis et al. 2013). However, the results of traditional microwear analyses may be robust so long as the counts of pits and scratches used are those of one researcher adopting methods that ensure observer blindness (Mihlbachler et al. 2012); studies incorporating such methods continue to yield important insights into the dietary ecology of both extinct

and extant organisms (e.g., Mihlbachler et al. 2016, 2018).

Dental microwear texture analysis (DMTA) arose over 15 years ago as the result of an effort to develop a more accurate and repeatable method quantifying dental microwear textures (Ungar et al. 2003; Scott et al. 2005, 2006). DMTA captures the surfaces of replica casts of tooth wear facets using a scanning white-light microscope with confocal capabilities, then analyzes the point clouds using scale-sensitive fractal analysis (Scott et al. 2005, 2006). The output variables (or 'DMTA attributes') most often reported are *epLsar* (exact-proportion length-scale anisotropy of relief; the orientation of wear features) and *Asfc* (area-scale fractal complexity; surface roughness at varying scales) (Ungar et al. 2003; Scott et al. 2005, 2006). The relationship between *Asfc* and *epLsar* values can be used to identify a ground-dwelling herbivorous animal as consuming tougher (i.e., grass) or more brittle foods (i.e., woody browse, fruits and/or seeds): high *epLsar*, low *Asfc* for grazers; low *epLsar*, high *Asfc* for frugivores; moderate *epLsar* and *Asfc* for browsers and mixed-feeders (Ungar et al. 2003, 2008; Scott et al. 2005, 2006; Prideaux et al. 2009; Scott 2012; DeSantis 2016; DeSantis et al. 2017) (Table 1.1). Other DMTA attributes include *Tfv* (textural fill volume; quantifies the total depth of microwear features) and *HAsfc* (heterogeneity of complexity; compares microwear signatures between sub-surfaces of a scanned area) (Scott et al. 2006; DeSantis 2016). *Tfv* is useful for distinguishing gouges from pits, which has the potential to differentiate between consumption of foods with different fracture properties (leaves versus fruit pits, for example) (Ungar et al. 2007, 2008; Scott et al. 2006). *HAsfc* is calculated by splitting individual scanned areas into smaller sections with equal numbers of rows and columns (from 2 x 2 up to 11 x 11) and comparing *Asfc* values between subregions (Scott et al. 2006). Low values in *HAsfc* have been shown to be indicative of either high grit loads or grass consumption (Scott 2012; Merceron et al. 2016); *HAsfc* has also been linked to dietary variability in both omnivores and herbivores (Souron et al. 2015).

1.2.4 Dental Mesowear

Dental mesowear refers to the macroscopic wear patterns in herbivorous mammal teeth, traditionally regarding the shape and relief of upper premolar and molar cusps. The study of dental mesowear provides evidence to the average dietary preferences of an individual over the course of its life, as cusps are gradually worn down from the moment of eruption by a combination of attritive (i.e., tooth-on-tooth) wear and abrasive (i.e., tooth-on-food) wear (Butler 1972; Walker 1984; Fortelius and Solounias 2000; Lucas 2004). A low-abrasive browsing diet allows attrition to dominate, causing sharp and high occlusal relief to develop, while abrasive plant material (like silica-rich grass) causes to cusps to wear down lower and rounder, eventually ending up very low and blunt in specialized grazing mammals (Fortelius and Solounias 2000). Further, mesowear analysis offers us a tool for discriminating between dry and wet environments, with more dust and particulate matter accumulating on plant food in drier environments, thus resulting in blunter, rounder cusps (Kaiser and Schulz 2006). Dental mesowear may be employed in conjunction with other dietary proxies such as microwear analysis (e.g., Valli and Palombo 2008; DeMiguel et al. 2011) or stable isotope analysis (e.g., Louys et al. 2012, Loffredo and DeSantis 2014; Ecker et al. 2013), although it is often used as a stand-alone method for interpreting diet (e.g., Blondel et al. 2010; Mihlbachler et al. 2011).

Dental mesowear methods were initially developed for use in dietary studies focusing on ungulates with either selenodont (molars with anteroposteriorly elongated, crescent-shaped cusps) or ectolophodont (molars with anteroposterior buccal lophs) tooth morphology, because these teeth have obvious cusps showing occlusal relief when observed buccally (Fortelius and Solounias 2000). The original formulation involved classifying cusp apices by two categories: cusp shape (CS) (with values of sharp, round, and blunt) and occlusal relief (OR) (with values of high and low) (Fortelius and Solounias 2000). Because CS and OR tend to be correlated, later studies adopted the practice of treating mesowear as a single variable. This can be done in one of two ways: the first is the mesowear univariate

score (MWS) (Kaiser et al. 2009) and the second is the mesowear numerical score (MNS) (Mihlbachler et al. 2011). The MWS involves transforming CS and OR values to a 0 – 4 scale, with the combinations as follows: 0; high and sharp; 1, high and rounded; 2, low and sharp; 3, low and rounded; 4, low and blunt (Kaiser et al. 2009). The MNS is based on qualitatively comparing tooth samples to a reference "ruler" of seven equid teeth on a continuum ranging from zero to six, with six representing the bluntest, lowest relief cusp and zero representing the sharpest, highest relief cusp (Mihlbachler et al. 2011). As with two-dimensional microwear studies, level of experience and bias may result in intra-observer variability of mesowear scores; however, this variability can be reduced significantly by including at least five observers (of any experience level) in mesowear analysis and averaging the scores (Loffredo and DeSantis 2014).

Recent studies have expanded the use of mesowear analysis to a broader range of tooth positions and taxonomic groups as well as developed a more quantitative (i.e., measured) component (Loffredo and DeSantis 2014). In theory, the principles of tooth wear should remain constant across lineages: abrasive vegetation (i.e., grass) accelerates the wear rates of enamel and dentin, causing a flatter occlusal relief to develop, whereas nonabrasive vegetation (i.e., dicotylenous browse) enables attrition to dominate so that the more wear-resistant enamel ridges scour deeper valleys into the softer dentin, thus maintaining a higher relief. By applying these principles of wear to other organisms, studies have measured mesowear angles in notoungulates (Croft and Weinstein 2008), marsupials (Butler et al. 2014; DeSantis et al. 2018), hominoid primates (Merceron et al. 2007), proboscideans (Saarinen et al. 2015), and even xenarthrans (Saarinen et al. 2017). While mesowear was originally intended to examine the labial cusps of upper second molars (M^2), later studies expanded the method to four upper cheek teeth (P^4-M^3) as well as to the lingual cuspids of lower molars (Franz-Odendaal and Kaiser 2003; Kaiser and Solounias 2003; Kaiser and Fortelius 2003). However, lower teeth wear differently than upper teeth, particularly in mixed feeders; thus, comparing signatures from upper and lower teeth may be misleading.

1.2.5 Microwear - Mesowear Congruence

Because microwear and mesowear patterns are formed over different periods of time during the life of an individual, congruence between interpretations made using these two dietary proxy methods should be expected only if the feeding ecology of the individual examined was similar during both periods of time (Mihlbacher et al. 2018). An organism might experience near-death shifts in feeding ecology as a result of seasonal fluctuations in diet or episodes of ecological stress such as drought (Gogarten and Grine 2013; Saunders and DeSantis 2017). In such a case, the individual's mesowear-derived dietary interpretation would be inconsistent with its microwear-derived dietary interpretation. Neither interpretation would be incorrect nor would the inconsistency indicate a flaw in either proxy – particularly since both mesowear and microwear have been shown to correlate well with known dietary ecology in modern ungulates and proboscideans (e.g., Fortelius and Solounias 2000; Kaiser and Fortelius 2003; Kaiser and Solounias 2003; Kaiser et al. 2009, 2013; Louys et al. 2012; Scott 2012; Merceron et al. 2014; Saarinen et al. 2015; Mihlbachler et al. 2016). Instead, the coupled use of both dental-wear proxies in paleoecological studies offers researchers a tool for reconstructing long-term dietary habits of extinct populations (mesowear) and documenting short-term changes in diet due to seasonal mixed-feeding or rapid changes in environment (microwear) (Mihlbachler et al. 2018).

1.3 Structure of Dissertation

Following this introductory Chapter (1), Chapter 2 uses paleodietary proxy data (stable isotopes and dental microwear) to better understand the degree to which Columbian mammoths (*Mammuthus columbi*) and American mastodons (*Mammut americanum*) consumed tough and/or hard food items, including grass, leaves, and woody browse, in their respective environments in the Late Pleistocene. I find that despite having disparate geochemical signatures indicating C_3 browsing in mastodons and C_4 grazing in mammoths, the textural

properties of diet indicate that both proboscideans were extreme dietary generalists. Additionally, juvenile mammoths and mastodons consumed neither softer nor tougher foods than their adult counterparts. Finally, I find that mammoths on the Channel Islands of California ate food items with more variable textural properties (including a greater incidence of hard foods) than Columbian mammoths from ecotonal regions in Texas, suggesting the Channel Island mammoths inhabited a closed-forest environment. The results of this work suggests that microwear alone may not be sufficient to reconstruct "browsing" or "grazing" habits in mastodons and mammoths; thus, multiple dietary proxies may be needed to reconstruct the diets of proboscideans, which consume a wide variety of foods with diverse textural and photosynthetic properties.

Chapter 3 uses stable isotopes and dental microwear of specimens from the Gulf Coastal Plain of Texas and Florida to test whether the extirpation of gomphotheres from North America can be explained as resulting from a competitive exclusion with sympatric mammoths and/or mastodons. Results suggest that gomphotheres consumed a wide range of resources with variable textural and photosynthetic properties and were not specialized on either grasses or browse. Further, both isotopes and microwear indicate the consumption of similar foods between contemporaneous gomphotheres and mammoths, and niche plasticity in gomphotheres prior to their disappearance from North America. In this chapter, I show that the generalist feeding strategy of gomphotheres may have been advantageous early in their history but rendered them inferior competitors to the larger-bodied, more efficient generalists (mammoths and mastodons) during the Late Pleistocene.

Chapter 4 reconstructs the dietary ecology of 5 large mammals occupying a remarkable Late Pleistocene assemblage from the American southwest - the Diamond Valley Lake Local Fauna in Southern California. Specifically, I test: (1) whether the dietary habits of focal taxa changed between two stratigraphic units dating to before and after the last glacial maximum; and, (2) whether diets of these fauna are consistent with dietary interpretations of these fauna from elsewhere in the United States during the Late Pleistocene. I find that,

while the average dietary habits of herbivores do not differ between the older and younger units, the short-term dietary habits of two taxa (bison and horses) do. Additionally, I present evidence for disparate microwear signatures between Diamond Valley fauna and La Brea fauna, which might be explained by seasonal migration and/or niche partitioning. The results of this chapter highlight the combined use of dental-wear dietary proxies to document changes in mammal communities before and after an interval of dramatic climatic change and demonstrate the resilient nature of this population of large mammals to past climate change.

Chapter 5 asks whether a given source of stress during critical moments (biotic crises) in the Cenozoic results in predictable patterns of extinction and/or origination for mammalian families. To answer this question, I test for phylogenetic conservatism (i.e., the tendency for descendant species to retain ancestral traits) by quantifying two metrics of phylogenetic clustering using over 46,000 mammalian records from the North American fossil record. I find evidence for two intervals of significantly clustered extinction: the first occurring during the 10-million-year period following the Cretaceous-Paleogene extinctions, and the second coinciding with the Eocene-Oligocene transition. These results suggest periods of time where abiotic factors may have been more important than biotic factors in driving speciation or extinction. Critically, this chapter suggests that phylogenetic clustering provides a mechanism - loss in evolutionary history - for why there is sometimes a disconnect between the taxonomic severity of an extinction and its ecological severity.

Chapter 6 synthesizes findings from this dissertation, discusses the broader impacts of this work, and offers ideas for future work.

Chapter 2

DIETARY ECOLOGY OF PLEISTOCENE MAMMOTHS AND MASTODONS AS INFERRED FROM DENTAL MICROWEAR TEXTURES

2.1 Introduction

A wide diversity of large-bodied herbivorous taxa including bovids, camelids, and proboscideans occupied North America during the Pleistocene (Anderson 1984). Proboscideans in particular experienced a three-pronged dispersal across the Bering Land Bridge from Eurasia, with subsequent colonization events introducing the mastodons, gomphotheres, and mammoths to North America (Shoshani 1998). The earliest Mammutids (*Zygolophodon spp.*) arrived in North America sometime during the early Barstovian Land Mammal Age (Tedford et al. 2004), although *Mammut americanum* does not appear until the Blancan (Bell et al. 2004). Mammoths (*Mammuthus spp.*) were the final and most highly derived proboscideans to arrive, having tracked the expansion of grasslands out of Africa and into Eurasia *ca.* 3 Ma and arriving to North America as early as $\sim$1.5 - 1.3 Ma (Agenbroad, 2005; Lister and Sher 2015). The presence of *Mammuthus* south of 55° latitude defines the lower limit of the Irvingtonian Land Mammal Age (Bell et al. 2004).

Proboscideans in general are thought to have played a considerable role in shaping past ecosystems due to their classification as megaherbivores (i.e., $>$ 1000 kg in body mass) (Owen-Smith 1987) and current role as ecosystem engineers (Jones et al. 1994). Modern African elephants (*Loxodonta spp.*) and Asian elephants (*Elephas maximus*) are capable of large-scale turnover of vegetation and ecosystem transformations (Naiman 1988). Elephants selectively consume a wide range of fruits and other species of plant, playing a large role in seed dispersal (Campos-Arceiz and Blake 2011) while also selectively consuming specific plant parts over a wide diversity of species (Owen-Smith and Chafota 2012). Additionally, they physically disturb and destroy trees and shrubs, leading to widespread

vegetation changes and alteration of fire regimes (Laws 1970), impacting food supply and population dynamics of other animals (Pringle 2008), altering soil formation and biogeochemical cycling, and ultimately changing the ecological regime of their habitats (Naiman 1988).

Because of their close phylogenetic and morphologic affinities, extinct species of proboscideans are similarly likely to have acted as ecosystem engineers (Haynes 2012). However, such behavioral and ecological inferences are difficult to interpret in the fossil record. Understanding the paleoecological roles played by fossil proboscideans has largely been based on tooth morphology (Maglio 1972; Saunders, 1996; Tobien 1996; Todd and Roth 1996) and, more recently, stable isotopes (e.g., Baumann and Crowley 2015; Bocherens et al. 1996; Connin et al. 1998; DeSantis et al. 2009; Fisher et al. 2014; Fox-Dobbs et al. 2008; Fox and Fisher 2001, 2004; Koch et al. 1998, 2004; Metcalfe et al. 2013; Drucker et al. 2015; Pérez-Crespo et al. 2012; Trayler et al. 2015; Yann and DeSantis 2014). For example, the zygolophodont dentition of mastodons suggests adaptation for browsing (Tobien 1996) while the hypsoloxodont dentition of mammoths is thought to have been an adaptation to more abrasive plants, such as grass (Maglio 1972; Todd and Roth 1996). Inferences into the stable isotope ecology of North American mammoths reveal a wide range of dietary preferences commensurate with the cosmopolitan nature of the genus. For example, stable carbon isotopes suggest the consumption of primarily C_4 vegetation (likely grass) in Florida (Koch et al. 1998; DeSantis et al. 2009; Yann and DeSantis 2014), predominately C_3 vegetation in California (Trayler et al. 2015), and mixed C_3/C_4 vegetation during the Last Glacial Maximum (LGM) in the Cincinnati region (Baumann and Crowley 2015). Further, mammoths consumed primarily C_4 vegetation from the Mojave Desert (in California and Nevada) through to the Southern High Plains (Arizona and New Mexico) and into Texas (Connin et al. 1998; Koch et al. 2004). Both C_3 and C_4 grasses have been hypothesized to have been a large component of the diet of *Mammuthus* in these and other localities (including central Utah and the subarctic; e.g., Kubiak 1982; Gillette and Madsen

1993).

A third means of inferring the diet of extinct organisms is dental microwear. Dental microwear, the microscopic wear patterns formed during the processing of food, can be used to make inferences regarding foods consumed during the last days to weeks of an organism's life (e.g., Grine 1986). Microwear can be examined quantitatively via counting the number of pits and scratches on a 2-dimensional surface using a scanning electron microscope (SEM) or by user recognition while looking directly through the lens of a stereomicroscope. Alternatively, one may use a white light scanning confocal microscope and scale-sensitive fractal analysis (SSFA) in a more automated and repeatable process known as dental microwear texture analysis (DMTA) (Scott et al. 2005, 2006; Ungar et al. 2003), which allows for more nuanced differences in diets to be detected and is less prone to issues of observer variability (DeSantis et al. 2013). DMTA has been used to reconstruct diets in a wide range of disparate extant and extinct taxa (see DeSantis 2016 for a review of DMTA and studies utilizing this approach). Several studies have used dental microwear to analyze dietary tendencies in fossil proboscideans using the 2D analysis of SEM images (Capozza 2001; Filippi et al. 2001; Palombo et al. 2005; Calandra et al. 2008), low-magnification user-based methods on a light microscope (Green et al. 2005; Todd et al. 2007; Rivals et al. 2010, 2012, 2015; Semprebon et al. 2016) and DMTA on a confocal microscope (Zhang et al. 2017; Green et al. 2017). These studies reveal a wealth of dietary preferences in mammoths ranging from predominately browsing to strictly grazing, while establishing evidence for more dietary flexibility in mastodons than had previously been inferred from dental morphology.

Here, we aim to test the following hypotheses: 1) mammoths and mastodons with inferred differences in diet (via stable carbon isotopes indicating C_4 grass or C_3 browse consumption) have disparate dental microwear attributes; 2) juvenile proboscidean microwear differs significantly from adult proboscideans, tested by examining a unique late Pleistocene site (Friesenhahn Cave in Texas) with exceptionally well preserved juvenile mam-

moth and mastodon teeth; and, 3) the pygmy mammoth (*Mammuthus exilis*) consumed texturally disparate foods from either of the larger mainland taxa examined here (*Mammuthus columbi* and *Mammut americanum*). Collectively, DMTA data can help clarify the dietary preferences of Pleistocene mammoths and mastodons, including any size or age correlation with the textural properties of food consumed.

2.2 Materials and Methods

2.2.1 Fossil Proboscidean Populations

A population recovered from Late Pleistocene deposits on the Gulf Coastal Plain near Ingleside, Texas (TMM Site #30967; Figure 2.1; Table 2.1) was examined to compare the microwear signatures of sympatric mammoths and mastodons. Previous work (Koch et al. 2004; Hoppe 2004; Yann et al. 2016) has revealed a clear dietary disparity between mammoths and mastodons at this site, with mastodons displaying $\delta^{13}C_{enamel}$ values of -12.6‰ to -7.4‰ and mammoths displaying $\delta^{13}C_{enamel}$ values of between -2.6‰ and +0.2‰. Further, there is little evidence for spatial or temporal mixing of these proboscideans based on low variation in $\delta^{1O}O_{enamel}$ values for mammoths (1σ = 0.8‰; Koch et al. 2004) and mastodons (1σ = 0.9‰; Yann et al. 2016). The age of Ingleside deposits is between 75,000 and 30,000 years BP (uncalibrated radiocarbon years before present) based on faunal correlation (Lundelius 1972), temporally prior to the Last Glacial Maximum (LGM). Koch et al. (2004) suggested that the Texas Gulf Coastal Plain was 70 to 90% C_4 biomass during this time based on carbon isotope values in mammalian enamel and climate-vegetation models. Bryant and Holloway (1985), on the basis of pollen records from elsewhere along the Gulf Coast, posited two hypotheses for the vegetation of east Texas *ca.* 30 ka: either, 1) a closed oak-hickory-pine forest, or 2) an ecotonal region between grasslands and scrubby vegetation to the west and deciduous forests to the east. Taken together, Ingleside is probably best considered to have been an ecotonal region consisting of predominately C_4 grasses inter-

spersed by stands of C_3 forest (likely mixed coniferous). Thus, mammoths at Ingleside may have been predominately C_4 grazers, while mastodons at Ingleside were predominately C_3 browsers. This makes Ingleside an ideal location to discern whether dental microwear has the potential to discriminate between browse and grass in proboscideans or if the textural properties of food consumed were similar.

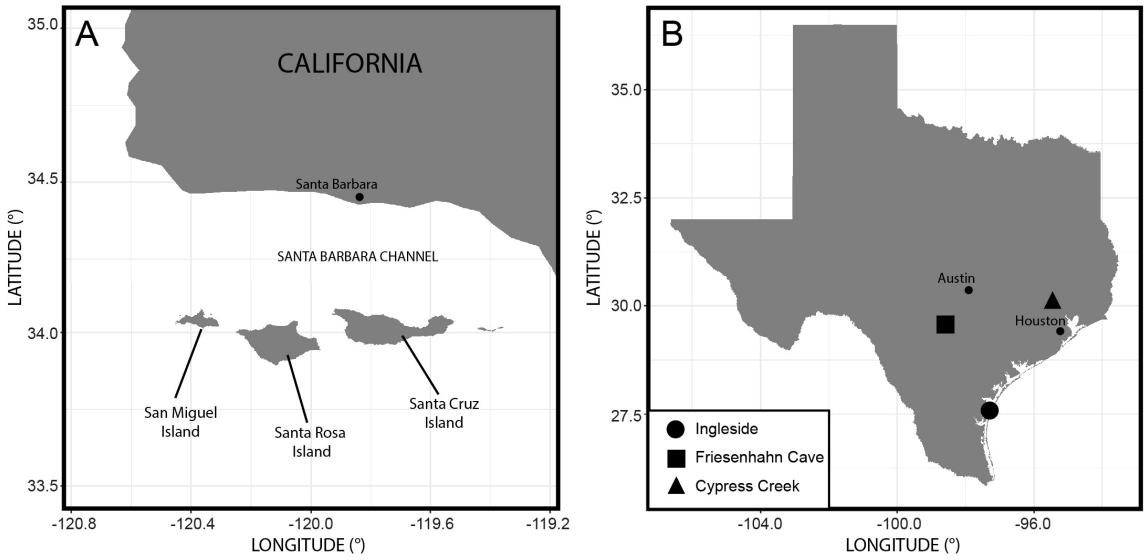

Figure 2.1: Site map for all proboscidean populations examined in this study. (A) The California Channel Islands as they appear today (all samples come from Santa Rosa Island); and, (B) the late Pleistocene Texas sites of Ingleside, Friesenhahn Cave, and Cypress Creek.

We also examined mammoths and mastodons from Friesenhahn Cave (TMM Site #933; Figure 2.1; Table 2.1), a site on the Edwards Plateau that acted as a den cave for the Pleistocene scimitar cat *Homotherium serum* (Evans 1961; Meade 1961). Friesenhahn is unique in that its mammoth and mastodon population is overwhelmingly comprised of juvenile individuals (Graham 1976). Initial radiocarbon dates of mammoth material from Friesenhahn indicated multiple sedimentation events, with the two horizons bearing mammoth remains dated to 17,800 $\pm$ 880 and 19,600 $\pm$ 710 years BP (excavation units 3B and 3A, respectively; Graham 1976). Subsequent re-interpretations of these initial ages suggest that the reported dates are probably inaccurate since collagen is unpreserved and the material dated (bioapatite) is generally unreliable (Graham et al. 2013). However, Graham et al. (2013)

still consider an age estimate of full glacial (15 - 20 ka) to be a reasonable estimate for the mammoth and mastodon remains from Friesenhahn. Pollen analyses of Friesenhahn LGM sediments are consistent with modern grassland assemblages, including 19% Asteraceae, 18% Poaceae, and 15% Ambrosia (Hall and Valastro 1995); although Graham et al. (2013) reasoned that riparian woodlands must also have been present near the edge of the plateau based upon the presence of woodland mammals such as *Mammut*, *Tapirus*, and *Mylohyus*. The presence of pollen from conifers such as *Pinus* ($\sim$16%) and *Juniperus* (7%) supports this reasoning (Hall and Valastro 1995). Previously published stable carbon isotopes on mammoths from Friesenhahn suggest a predominantly C_4 (probably grazing) signature (-1.8 $\pm$ 1.4‰; Hoppe 2004); however, no studies have as of yet compared the juvenile dietary signature to that of the adults. The high sample size of juvenile *Mammuthus* and *Mammut*, published pollen record, and previously published δ^{13}C values make Friesenhahn an ideal location to test for ontogenetic shifts in diet of proboscideans with well-resolved diets.

Table 2.1: Localities of Texas proboscidean populations analyzed for DMTA.

Site/Taxon	**n**	**Age***	**Paleoenvironment***
Cypress Creek, TX *Mammuthus columbi*	 13	LGM 24 – 17 ka	Mesic open grassland with abundant sedges
Ingleside, TX *Mammut americanum* *Mammuthus columbi*	 32 26	Pre-LGM 75 – 30 ka	Open C4 grassland interspersed by areas of C3 forest
Friesenhahn Cave, TX *Mammut americanum* juvenile *Mammuthus columbi* adult juvenile	 7 7 32 9 22	LGM 20 – 15 ka	Open C4 grassland with some forests likely occupying canyons and riparian zones
Santa Rosa Island, CA *Mammuthus columbi* *Mammuthus exilis*	 1 15	Pre-to Post-LGM 150 – 11 ka	Cypress, pine, and Douglas Fir forest during the pre-LGM transitioning to a grassland, shrubland, and parkland mosaic during the post-LGM

*See text for references for age estimates and paleoenvironmental interpretations.

In addition to previously-published δ^{13}C values from Ingleside and Friesenhahn Cave, we analyzed a sample of *Mammuthus columbi* recovered from a locality along Cypress Creek on the Gulf Coastal Plain near Hockley, Texas (TMM Site #47200; Figure 2.1; Table 2.1). The Cypress Creek deposits are equivalent to the Deweyville Formation, whose individual units are described by Blum and Aslan (2006) as representing former floodplain surfaces cut by channels and aggraded during the late Pleistocene falling stage to lowstand. Lundelius et al. (2013) reported the discovery of a toxodont, *Mixotoxodon sp.*, from one of the Cypress Creek outcroppings. Strata at this location where described as being horizontally-bedded but convoluted due to spring activity (Lundelius et al. 2013). Recovery efforts evidently were made from multiple locations, as the toxodont was found associated with other mammalian genera (including *Equus*, *Bison*, *Cuvieronius*, *Mammuthus*, *Eremotherium*, *Camelops*, and *Paleolama*) and wood samples that were collected upstream, with "little variation" in the stratigraphy between localities (Lundelius et al. 2013). These wood samples yielded AMS radiocarbon ages of 17,080 $\pm$ 90 cal ka BP (calibrated ^{14}C years) and 23,730 $\pm$ 100 cal ka BP (Lundelius et al. 2013); along with the stratigraphic interpretation (Blum and Aslan 2006), the fauna recovered from the Cypress Creek locality likely represent an LGM assemblage. Lundelius et al. (2013) interpreted the Cypress Creek environment to have been a mesic open grassland during the LGM based on the associated fauna and pollen, although they mention the possibility that large mammals from this locality could have been migrating inland when lower sea levels ($\sim$100 meters) pushed the coastline 80 - 160 km east of present. An interpretation of open grassland with scattered areas of riparian parklands or woodlands is in agreement with pollen recovered from LGM sediment cores to the north and west of Cypress Creek (Bryant and Holloway 1985).

Mammuthus exilis, the pygmy mammoth, was endemic to the California Channel Islands (CHIS) of Santa Rosa, San Miguel, and Santa Cruz, all of which once comprised the Late Pleistocene "super island" of Santarosae (Orr 1968; Agenbroad 2001). The pygmy mammoth is suggested to have been a descendent of the mainland *Mammuthus columbi*

(Roth 1982, 1996), which swam to Santarosae during periods of lower eustatic sea level when the distance between the island and the mainland was less (Johnson 1978); likely either during the glacial periods of Marine Isotope Stage (MIS) 6 (∼150 ka) or MIS 8 (∼250 ka) (Muhs et al. 2015). The Columbian mammoths which made it to the island would then have left a line of descendants of decreasing size due to resource constraints regarding food availability and land area - the Island Rule (Foster 1964; McNab 2010) - leading eventually to the pygmy *Mammuthus exilis* (Agenbroad 2012).

We collected dental microwear molds of 16 individuals of *Mammuthus* (15 *M. exilis*, including 'intermediate' forms, and 1 *M. columbi*) from Santa Rosa Island, CA (these 16 individuals had portions of their wear facets that were well preserved, in contrast to other available teeth which had a chalky texture and did not preserve dental microwear) and compared them to Pleistocene adult mammoth populations from the three Texas sites (Ingleside, Friesenhahn Cave, and Cypress Creek) as well as adult mastodons from Ingleside (Table 2.1). The dietary preferences of the CHIS mammoths have been examined elsewhere (Semprebon et al. 2016) via user-based light microscopy analysis, and results suggested that the CHIS mammoths' microwear signature resembled that of browsing proboscideans such as Florida mastodon (*Mammut americanum*) and African forest elephants (*Loxodonta cyclotis*). We analyzed a sample of the CHIS mammoth population and compared it with a large sample of mammoths and mastodons from Texas via 3D DMTA.

2.2.2 Assignment of Ontogenetic Stages

Mammoth cheek teeth are molariform, with deciduous premolars differing from permanent molars in maximum length, maximum width, and number of plates (Laws 1966; Maglio 1973; Graham 1986). To determine the approximate age of a mammoth from isolated teeth, we measured these characters and compared them to previously published populations of extant African elephants (Laws 1966; Lee et al. 2012) and Columbian mammoths (Graham 1986; Smith and Graham 2017) to assign tooth position and the mandibular vs.

maxillary setting (e.g., dp4/DP4, m1/M1, m2/M2). An inherent uncertainty in this method is that elephantid teeth are sexually dimorphic and thus male teeth tend to be larger than female teeth (Maglio 1973); however, differences are usually small and thus amount to little difference for the first four cheek teeth (Lee et al. 2012; Stansfield 2015). We then used the morphology of the occlusal surface of each tooth to assign wear stages to each molar following Laws (1966), with updated approximate ages assigned to each tooth following Stansfield (2015; see Haynes 2017 for discussion). These ages were then used to assign each tooth to an age category as originally presented by Saunders (1977a), which considers mammoth ages in African [elephant] Equivalent Years (AEY). Sukumar (2003) considered weaning to comprise a significant portion of modern African elephant diets until approximately 3 years of age (Laws Wear Stage I - V), and stable nitrogen work by Metcalfe et al. (2010) corroborates this for woolly mammoths (*Mammuthus primigenius*); to discern differences in weaning, we separate the juvenile age group used by Saunders (1977a) into two sub-categories. The five categories we delineate are: "Weaning Juvenile" (0 - 3 AEY), "Post-Weaning Juvenile" (4 - 7 AEY), "Youth" (8 - 17 AEY), "Young Adult" (18 - 34 AEY), and "Mature" (>34 AEY).

Mastodon teeth differ in morphology along the tooth row as well as in their maximum length and maximum width (Green and Hulbert 2005). The relative tooth position, as well as the amount of wear the tooth has experienced, can be used to separate molars into relative developmental age groupings (Saunders 1977b; Green and Hulbert 2005). We measured the length and width of each mastodon tooth included in our study and assigned a wear stage to each tooth following descriptions first proposed by Saunders (1977b) and later expanded upon by Green and Hulbert (2005). We then assigned each tooth to a developmental stage as outlined by Saunders (1977b) and Green and Hulbert (2005). Whereas Green and Hulbert (2005) subdivided their "Juvenile" stage into 5 subdivisions and their "Youth" into 2 subdivisions, we refrained from doing so because of sample size limitations at Friesenhahn Cave (n = 7) and because we were largely interested in discerning between

weaning juveniles and non-weaning adults. We used the same age categories as in mammoths ("Juveniles", "Youth", "Young Adult", and "Mature"), but refrain from assigning African [elephant] Equivalent Years (AEY) to each grouping because of larger uncertainties in the life history differences between *Mammut* and elephantids.

2.2.3 Stable Isotope Analysis

While the majority of stable isotope data included here are from published sources (i.e., Hoppe 2004; Koch et al. 2004; Yann et al. 2016), additional isotopic data were collected from 10 specimens of *Mammuthus columbi* at Cypress Creek for this study. All methods for enamel collection and treatment follow procedures described by DeSantis et al. (2009). Approximately 2 - 3 mg of enamel powder was drilled over a $\sim$1 cm sampling transect oriented parallel to the tooth's growth axis using a variable speed rotary tool with a 1 mm diameter carbide bit. Samples were taken no less than 1 cm from the occlusal surface on the exposed exterior portion of the most well-preserved loph of each molar. The powder was collected and treated with 30% hydrogen peroxide to remove organic material. Following hydrogen peroxide treatment, the samples were rinsed with distilled water and then treated with 0.1N acetic acid for exactly 18 hours to remove secondary carbonates, and subsequently rinsed with distilled water (similar to Koch et al. 1997 and DeSantis et al. 2009). After being left to air-dry, the treated samples were analyzed using a VG Prism stable isotope ratio mass spectrometer with an in-line ISOCARB automatic sampler in the Department of Geological Sciences at the University of Florida. The standard deviation (1σ) of the laboratory standard (NBS-19) included with these samples was $< 0.05‰$. The analytical precision is $\pm$ 0.1‰, based upon replicate analyses of samples and standards (NBS-19). Stable isotope data were normalized to the laboratory standard (NBS-19) and are reported in conventional delta (δ) notation against V-PDB for $\delta^{13}C_{enamel}$ and V-SMOW for $\delta^{18}O_{enamel}$.

2.2.4 Dental Microwear Texture Analysis

Ante-mortem wear facets on the occlusal surface of proboscidean molars were sampled using polyvinylsiloxane dental impression material (Regular-Body President's Jet, Coltene-Whaledent Corporation, Alstatten, Switzerland). The resultant molds were reinforced with a polyvinylsiloxane dental putty to stabilize them and prevent leaking. The molds were then cast using a high-resolution epoxy (Epotek 301, Epoxy Technologies Corporation, Billerica, MA, USA), which were left to harden in a fume hood for 72 hours prior to scanning. Previous work determined that a significant amount of variability is present in microwear features across extant elephantid teeth (Todd et al., 2007); to reduce this variability, maintain consistency with previous results by Semprebon et al. (2016), and allow for comparison with other proboscidean DMTA studies (e.g., Green et al. 2017), the center portions of the central enamel bands were preferentially sampled on each mammoth and mastodon molar.

The replica casts were scanned using a Sensofar PLu neox optical profiler at Vanderbilt University in the Department of Earth and Environmental Sciences (Solarius Development, Inc, Sunnyvale, CA). Only enamel wear facets were scanned, as the underlying dentine is not as robust and differs from enamel (Haupt et al. 2013). A total area of 285.5 x 381 μm^2 was scanned on the surface of each cast; we then extracted a smaller area of 204 x 276 μm^2 and split it into a 2 x 2 grid so as to be comparable to prior work (e.g., Ungar et al. 2003; Scott 2012). Further, scans from the Sensofar PLu neox optical profiler at Vanderbilt University (colloquially referred to as "Dolly") are not significantly different in dental microwear textural attributes as compared to scans acquired at the University of Arkansas on a white-light confocal microscope referred to as "Connie" (Arman et al. 2016). The scans underwent scale-sensitive fractal analysis (SSFA) using toothfrax and Sfrax software (http://www.surfract.com/), and were then analyzed for complexity (*Asfc*), anisotropy (*epLsar*), textural fill volume (*Tfv*), and heterogeneity (*HAsfc*) (Ungar et al. 2003; Scott et al. 2005, 2006; DeSantis 2016). Like other studies (e.g., Scott et al. 2006),

we report both $HAsfc_{3x3}$ and $HAsfc_{9x9}$ values (comparison among 9 and 81 sub-surfaces, respectively).

2.2.5 Statistical Analyses

Stable isotope values for all proboscidean populations were normally distributed (Shapiro-Wilks, all $p \geq 0.05$; Table 2.2, Table 2.3); thus, Student's t-tests were used to compare the stable isotope values of each population. Spearman Rank correlation tests were used to assess the correlation between DMTA values and stable isotope values. DMTA data are typically non-normally distributed. Therefore, we used non-parametric tests to compare DMTA attribute values (instead employing parametric tests when normally distributed, Shapiro-Wilks tests).

The Ingleside mammoth population was compared to other Texas mammoth localities (Friesenhahn, Cypress Creek) using a Kruskal-Wallis test with post hoc comparisons using Dunn's procedure (Dunn 1964). Because *Asfc* and *epLsar* values were normally distributed for each of these populations (Table 2.4), we also compared the distributions of these attributes using an ANOVA with post hoc Tukey HSD tests. Mann-Whitney U tests were used to compare Ingleside mammoths and mastodons to test the null hypothesis that the distributions of DMTA variables for both taxa were equal. Ingleside mastodons were also compared to all Texas adult mammoths (i.e., non-weaning individuals) using a Mann-Whitney U test to see if mainland mammoths differed significantly from mastodons in the textural properties of their diet.

We compared "Weaning Juvenile" mammoths at Friesenhahn to Friesenhahn adults (collectively, the "Post-Weaning Juvenile", "Youth", "Young Adult", and "Mature" developmental age groups) using parametric or non-parametric Mann Whitney U tests to see if a diet partly supplemented by milk would impact the microwear signature of weaning individuals (based on inferences from Sukumar 2003 and Metcalfe et al. 2010). We also compared the "Weaning Juvenile" Friesenhahn mammoths to Ingleside adult mammoths to test

for environmental differences between the two groups. We then compared the "Juvenile" mastodons at Friesenhahn to adults at Ingleside using parametric t-tests or non-parametric Mann Whitney U tests to see if the two populations differed due to either environment or ontogeny. Further, all Texas adult *Mammuthus columbi* specimens were collectively compared to the Santa Rosa specimens using Mann-Whitney U tests (*epLsar* was normally distributed for these two populations; thus, a t-test was also used to compare between them). In addition, we implemented a Levene's Test on all comparisons to test whether the variances of the populations being compared were equal. For all tests, the Bonferroni correction factor was withheld as it can result in an increase in Type II errors (Cabin and Mitchell 2000; Nakagawa 2004). P-values of <0.05 were considered significant.

2.3 Results

2.3.1 Stable Isotopes

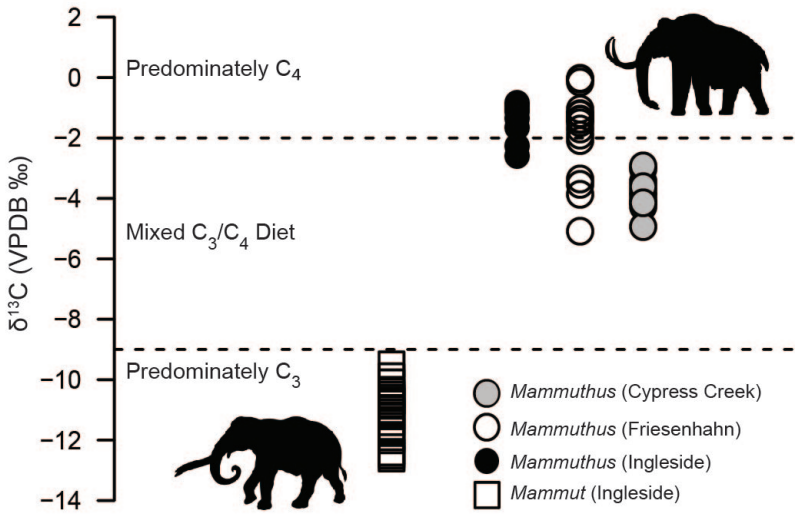

Figure 2.2: Stable carbon isotope values for Texas proboscidean populations. Horizontal dotted lines denote the boundary for predominately C_3 consumers, mixed C_3/C_4 consumers, and predominately C_4 consumers.

Stable isotope data for all taxa are summarized in Tables 2.2 and 2.3; primary stable isotope data are included in Supplemental Table 1. Stable carbon isotope values of Cypress

Table 2.2: Stable carbon isotope summary statistics for Texas proboscidean populations.

			$\delta^{13}C_{enamel}$ V-PBD (‰)						
Site	**Taxon**	**n**	**mean**	**min**	**max**	**range**	**sd**	**sem**	**p-value**
Cypress Creek	*Mammuthus*	10	–3.8	–4.9	–2.9	2.0	0.6	0.2	0.930
Friesenhahn Cave	*Mammuthus*	16	–1.9	–5.1	0.0	5.1	1.4	0.4	0.118
Ingleside	*Mammut*	19	–11.1	-12.6	–9.5	3.1	0.9	0.2	0.726
Ingleside	*Mammuthus*	9	–1.3	–2.6	0.2	2.8	0.8	0.3	0.732

n, number of specimens; min, minimum; max, maximum; sd, one standard deviation (1σ); sem, standard error of the mean ($\sigma/\sqrt{n}$). All samples are non-normally distributed (Shapiro-Wilks p-value ≥ 0.05).

Creek mammoths ranged from -4.9‰ to -2.9‰ (total range of 2‰) with an average of -3.8‰ (Figure 2.2, Table 2.2). Friesenhahn and Ingleside mammoths are statistically indistinguishable from one another in $\delta^{13}C$ (p = 0.239). Ingleside mastodons (total $\delta^{13}C_{enamel}$ range of -12.6‰ to -9.5‰) have significantly lower $\delta^{13}C$ values than Ingleside, Cypress Creek, and Friesenhahn mammoth populations (all $p < 0.001$). Cypress Creek mammoths have significantly lower $\delta^{13}C$ values than either Friesenhahn mammoths or Ingleside mammoths (all $p < 0.001$). Stable oxygen isotopes of Cypress Creek mammoths ranged from 28.6‰ to 31.5‰ (total range of 2.5‰) with an average of 29.8‰ and were not significantly different from any of the other populations (Ingleside mammoths, p = 0.9033; Friesenhahn mammoths, p = 0.7696; Ingleside mastodons, p = 0.238). The standard deviations (1σ) of $\delta^{18}O_{enamel}$ for all proboscidean populations are ≤ 1.0‰ (Table 2.3).

2.3.2 Dental Microwear

Dental microwear data for all proboscidean populations are summarized in Table 2.4; Table 2.5 breaks down dental microwear data for adult and juvenile proboscidean populations; primary DMTA data are included in Supplemental Table 2. Supplemental Table 3 lists molar dimensions, wear stage, and developmental age group for all Texas mammoth and mastodon molars used in this study. Examples of color 3D images for all proboscideans are shown in Supplemental Figure 1 with biplots of complexity and anisotropy exhibited

Table 2.3: Stable oxygen isotope summary statistics for Texas proboscidean populations.

		$\delta^{18}O_{enamel}$ V-PBD (‰)							
Site	**Taxon**	**n**	**mean**	**min**	**max**	**range**	**sd**	**sem**	**p-value**
Cypress Creek	*Mammuthus*	10	29.8	28.6	31.1	2.5	0.8	0.3	0.395
Friesenhahn Cave	*Mammuthus*	16	29.7	28.1	31.1	3.0	0.7	0.2	0.592
Ingleside	*Mammut*	19	30.2	28.5	31.7	3.2	0.9	0.2	0.715
Ingleside	*Mammuthus*	9	29.8	28.0	31.4	3.4	1.0	0.3	0.210

n, number of specimens; min, minimum; max, maximum; sd, one standard deviation (1σ); sem, standard error of the mean ($\sigma/\sqrt{n}$). All samples are non-normally distributed (Shapiro-Wilks p-value ≥ 0.05).

in Figure 2.3. Summaries of comparisons between mainland mammoth populations are in Supplemental Table 4; summary of comparisons between ontogenetic groups of mammoths and mastodons are in Supplemental Tables 5 and 6, respectively.

Among all populations, the Channel Island mammoths (*Mammuthus exilis* and *Mammuthus columbi*) have the highest mean complexity value (5.698) followed by Friesenhahn *Mammuthus columbi* (2.885) and Ingleside *Mammut americanum* (2.684; Figure 2.3; Table 2.4). The lowest mean complexity value is for *Mammut americanum* from Friesenhahn (1.275). Mean anisotropy values ranged between 0.003 and 0.005 for all populations.

All Texas adult mammoth populations have indistinguishable mean complexity and anisotropy values (all p $\geq$ 0.335; Supplemental Table 4). Cypress Creek mammoths have significantly greater textural fill values than Ingleside mammoths (p = 0.008). Friesenhahn mammoths have significantly greater heterogeneity values than both Cypress Creek mammoths ($HAsfc_{3x3}$, p = 0.036) and Ingleside mammoths ($HAsfc_{3x3}$, p = 0.005; $HAsfc_{9x9}$, p = 0.032). Excepting textural fill volume (*Tfv*, p = 0.005), variances of DMTA attribute values between populations were similar (*Asfc*, p = 0.651; *eplsar*, p = 0.290; $HAsfc_{3x3}$, p = 0.181; $HAsfc_{9x9}$, p = 0.160). No other significant differences exist between populations (all p $>$ 0.05; Supplemental Table 4).

Ingleside mastodons are indistinguishable from mammoths for all DMTA attributes, whether compared to only Ingleside mammoths (*Asfc*, p = 0.692; *eplsar*, p = 0.684, *Tfv*,

p = 0.895; $HAsfc_{3x3}$, p = 0.291; $HAsfc_{9x9}$, p = 0.662) or all Texas mammoths as a whole (*Asfc*, p = 0.798; *eplsar*, p = 0.301, *Tfv*, p = 0.071; $HAsfc_{3x3}$, p = 0.868; $HAsfc_{9x9}$, p = 0.625). There are no significant differences in variance between Ingleside mastodons and mammoths (*Asfc*, p = 0.260; *eplsar*, p = 0.735, *Tfv*, p = 0.787; $HAsfc_{3x3}$, p = 0.061; $HAsfc_{9x9}$, p = 0.210).

Friesenhahn "weaning juvenile" mammoths are indistinguishable from adult mammoths in all DMTA attributes (all $p > 0.05$; Supplemental Table 5). Additionally, there are no significant differences in variance between the two ontogenetic age groups (*Asfc*, p = 0.945; *eplsar*, p = 0.968; *Tfv*, p = 0.341; $HAsfc_{3x3}$, p = 0.440; $HAsfc_{9x9}$, p = 0.852). Friesenhahn "weaning juvenile" mammoths have significantly greater *epLsar* values than Ingleside adults (Table 2.5; Supplemental Table 5). Friesenhahn juvenile mastodons have significantly lower *Asfc* values than Ingleside adult mastodons (p = 0.016), but are indistinguishable from one another in all other DMTA attributes (*eplsar*, p = 0.993; *Tfv*, p = 0.359; $HAsfc_{3x3}$, p = 0.199; $HAsfc_{9x9}$, p = 0.647; Supplemental Table 6).

CHIS mammoth DMTA attribute mean values are not significantly different from adult specimens of *Mammuthus columbi* from Texas (*Asfc*, p = 0.881; *eplsar*, p = 0.663; *Tfv*, p = 0.629; $HAsfc_{3x3}$, p = 0.729; $HAsfc_{9x9}$, p = 0.915) or adult *Mammut americanum* specimens from Ingleside, Texas (*Asfc*, p = 0.983; *eplsar*, p = 0.759; *Tfv*, p = 0.302; $HAsfc_{3x3}$, p = 0.686; $HAsfc_{9x9}$, p = 0.577); however, complexity values are significantly more variable in CHIS mammoths than in either Texas proboscidean (*Mammuthus columbi* Levene's Test, p = 0.003; *Mammut americanum* Levene's Test, p = 0.034). The variance of all other DMTA attributes is indistinguishable between CHIS mammoths and adult specimens of either *Mammuthus columbi* from Texas (*eplsar*, p = 0.649; *Tfv*, p = 0.154; $HAsfc_{3x3}$, p = 0.931; $HAsfc_{9x9}$, p = 0.113) or *Mammut americanum* from Ingleside, Texas (*eplsar*, p = 0.578; *Tfv*, p = 0.382; $HAsfc_{3x3}$, p = 0.546; $HAsfc_{9x9}$, p = 0.466).

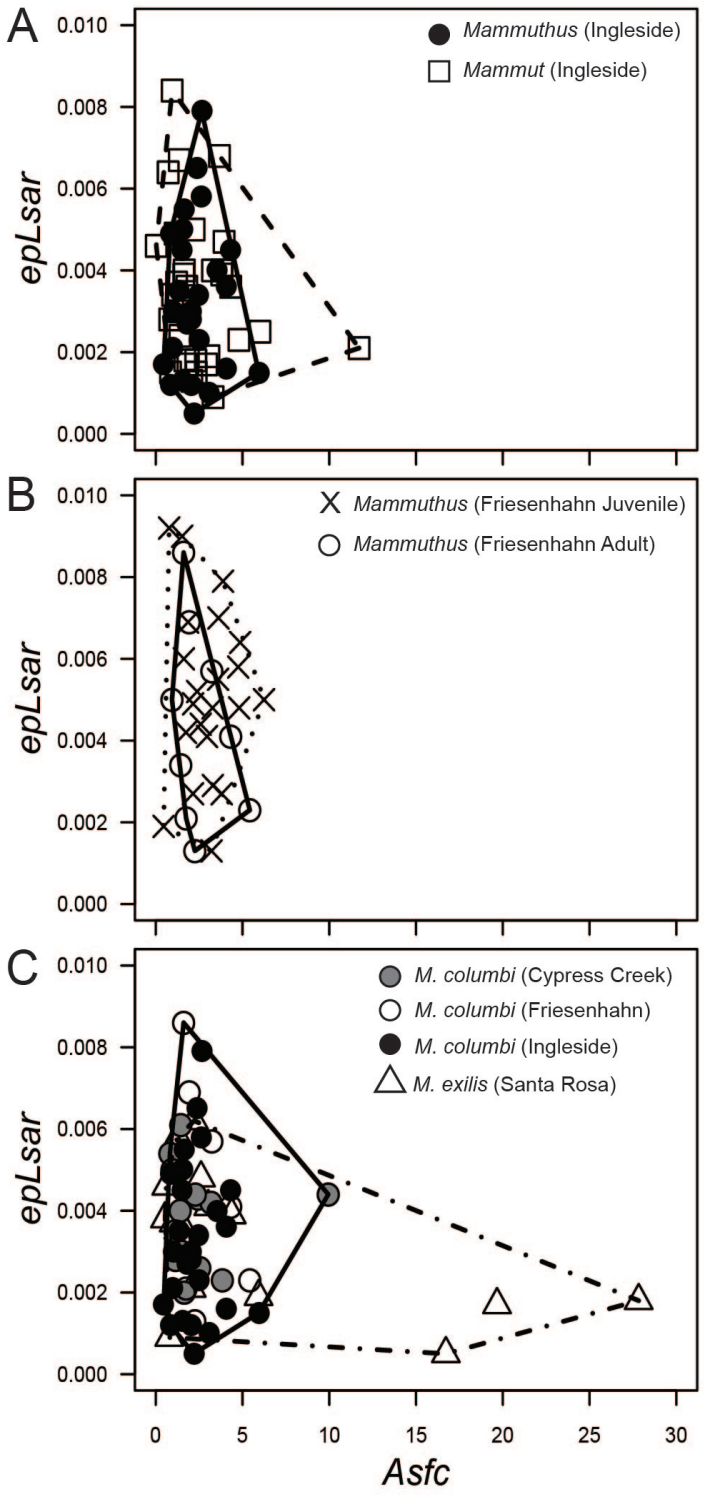

Figure 2.3: Bivariate plots of *epLsar* and *Asfc* for (A) Ingleside mammoths and mastodons; (B) Friesenhahn juvenile and adult mammoths; and (C) Santa Rosa pygmy mammoths and all mainland adult mammoths in this study.

2.3.3 Relationships between DMTA and Stable Isotope Data

There are no significant relationships observed between DMTA attribute values and δ^{13}C values for either *Mammuthus* (*Asfc*, p = 0.284; *eplsar*, p = 0.120; *Tfv*, p = 0.185; $HAsfc_{3x3}$, p = 0.506; $HAsfc_{9x9}$, p = 0.320) or *Mammut* (*Asfc*, p = 0.559; *eplsar*, p = 0.456; *Tfv*, p = 0.415; $HAsfc_{3x3}$, p = 0.178; $HAsfc_{9x9}$, p = 0.135) (Figure 2.4). Heterogeneity ($HAsfc_{9x9}$) is negatively correlated with δ^{18}O in *Mammut* (ρ = –0.524, p = 0.031); all other relationships between δ^{18}O and DMTA attribute values are not significant for either *Mammut* (*Asfc*, p = 0.212; *epLsar*, p = 0.138; *Tfv*, p = 0.547; $HAsfc_{3x3}$, p = 0.087) nor *Mammuthus* (*Asfc*, p = 0.260; *eplsar*, p = 0.067; *Tfv*, p = 0.615; $HAsfc_{3x3}$, p = 0.109; $HAsfc_{9x9}$, p = 0.247).

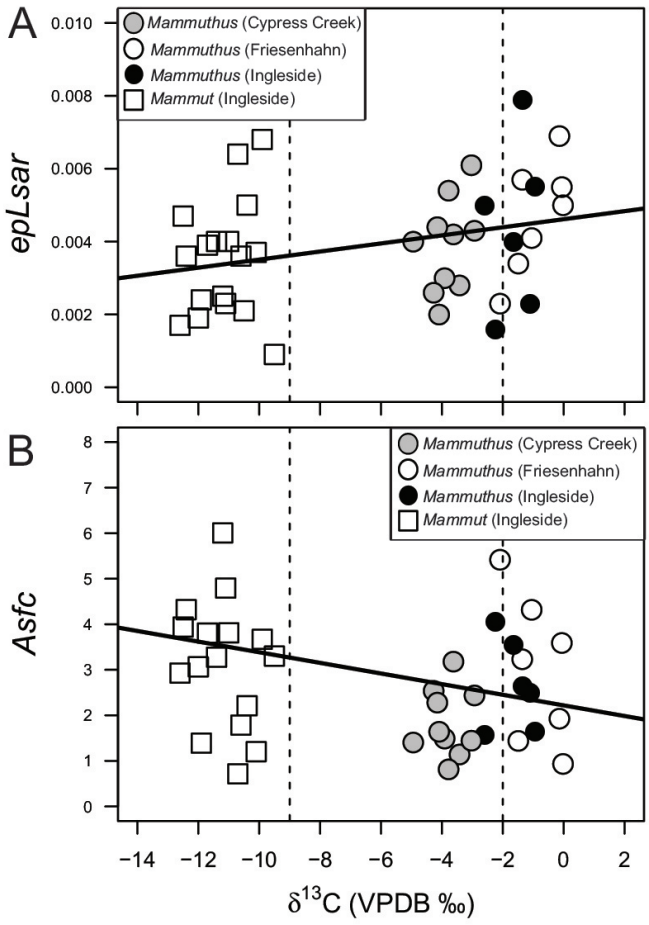

Figure 2.4: Bivariate plots of (A) anisotropy and (B) complexity versus δ^{13}C for all fossil proboscideans in this study. See text for rank correlations and significances.

2.4 Discussion

2.4.1 Ingleside *Mammuthus columbi* and *Mammut americanum*

The dental microwear signatures of mammoths and mastodons from Ingleside are remarkably similar, with similar mean values and ranges (Table 2.4, Figure 2.3). The high degree of overlap in DMTA attribute values is in stark contrast to the disparate geochemical signatures of tooth enamel. The δ^{13}C signature of *Mammut americanum* at Ingleside is indicative of C_3 vegetation while *Mammuthus columbi* consumed a significant portion of C_4 vegetation and was likely a mixed C_3/C_4 feeder (Koch et al. 2004; Yann et al. 2016). Specifically, in Texas during the late Pleistocene, carbon isotope signatures of mastodons most likely result from the consumption of dicotyledonous trees and shrubs; although it could also reflect water-dependent C_3 grasses such as reeds, sedges, and rushes, the low mean anisotropy value of the Ingleside population (Table 2.4) suggests that grasses were unlikely to have made up a large portion of their diet. The δ^{13}C signature of *Mammuthus columbi* from Ingleside is at the high end of C_3/C_4 mixed feeding, and is dominated by C_4 vegetation (applying a mixing model of pure C_3 and pure C_4 vegetation (following Koch et al. 2004), mammoths consumed approximately 74% C_4). C_4 signatures are typically inferred to result from warm-adapted (mostly monocotyledonous) grasses due to the unlikely presence of CAM plants in Late Pleistocene Texas environments (Yann et al. 2016).

In past studies of DMTA in ungulates, grazers and browsers occupied distinct morphospaces on an *Asfc*/*epLsar* biplot, leading towards the dietary niche expectations summarized in Table 1.1. For example, Scott (2012) showed that among African bovids, the grazing common tsessebe (*Damaliscus lunatus*) had low *Asfc* values (< 2.0) and high *epLsar* values (0.006 to 0.009), while the browsing common duiker (*Sylvicapra grimmia*) had moderate *Asfc* values (1.0 to 5.0) and low *epLsar* values (0.001 to 0.004). The range in complexity and anisotropy values for both Ingleside mastodons and mammoths completely encapsulates the ranges of all bovids with disparate diets from Scott (2012). The high

Table 2.4: DMTA attribute summary statistics for proboscidean populations in this study. Bold values indicate a non-normal distribution (Shapiro-Wilks; $p < 0.05$ is significant).

Taxon	**n**	**Statistic**	***Asfc***	***epLsar***	***Tfv***	***HAsfc*$_{3x3}$**	***HAsfc*$_{9x9}$**
Mammut americanum	7	mean	1.275	0.003	11300	0.33	0.71
Friesenhahn Cave		median	1.047	0.004	12658	0.21	0.57
		sd	0.873	0.002	3074	0.22	0.46
		min	0.429	0.001	4847	0.18	0.34
		max	2.759	0.005	13725	0.81	1.66
		range	2.330	0.004	8878	0.63	1.33
		p (normality)	0.120	0.144	**0.018**	**0.005**	0.057
Mammut americanum	32	mean	2.684	0.003	10370	0.41	0.78
Ingleside		median	2.146	0.003	11028	0.35	0.61
		sd	2.110	0.002	3581	0.23	0.54
		min	0.715	0.001	507	0.14	0.28
		max	11.717	0.008	16547	0.99	3.05
		range	11.002	0.007	16040	0.84	2.77
		p (normality)	**<0.001**	**0.019**	**0.017**	**<0.001**	**<0.001**
Mammuthus columbi	12	mean	1.989	0.004	16507	0.42	0.73
Cypress Creek		median	1.8	0.004	16362	0.35	0.64
		sd	0.905	0.001	7652	0.21	0.31
		min	0.794	0.002	3870	0.19	0.34
		max	3.84	0.007	32492	0.86	1.33
		range	3.046	0.005	28621	0.67	1.00
		p (normality)	0.614	0.355	0.913	0.130	0.641
Mammuthus columbi	32	mean	2.885	0.005	12619	0.48	0.87
Friesenhahn Cave		median	2.489	0.005	12596	0.41	0.77
		sd	1.52	0.002	2654	0.27	0.39
		min	0.457	0.001	4432	0.20	0.38
		max	6.471	0.009	16973	1.66	2.10
		range	6.014	0.008	12542	1.47	1.72
		p (normality)	0.142	0.458	**<0.001**	**<0.001**	0.122
Mammuthus columbi	26	mean	2.285	0.003	10456	0.33	0.64
Ingleside		median	2.062	0.003	11304	0.33	0.59
		sd	1.273	0.002	3711	0.11	0.23
		min	0.456	0.001	739	0.16	0.37
		max	5.937	0.008	18020	0.55	1.40
		range	5.481	0.007	17280	0.39	1.03
		p (normality)	0.057	0.306	0.107	0.485	**0.002**
Mammuthus exilis/	16	mean	5.698	0.003	11476	0.42	0.97
Mammuthus columbi		median	2.143	0.004	12002	0.37	0.68
Santa Rosa Island		sd	8.197	0.002	2654	0.20	0.93
		min	0.537	0.001	5345	0.18	0.35
		max	27.829	0.006	15271	0.98	3.50
		range	27.292	0.005	9925	0.80	3.15
		p (normality)	**<0.001**	0.433	0.603	**0.009**	**<0.001**

Table 2.5: DMTA attribute summary statistics for proboscidean age groups in this study. Bold values indicate a non-normal distribution (Shapiro-Wilks; $p < 0.05$ is significant).

Taxon	**n**	**Statistic**	***Asfc***	***epLsar***	***Tfv***	***HAsfc3x3***	***HAsfc9x9***
Mammut americanum	7	mean	1.275	0.003	11299	0.33	0.71
Friesenhahn, TX		median	1.047	0.004	12658	0.21	0.57
(Juveniles)		sd	0.873	0.002	3074	0.22	0.46
		min	0.429	0.001	4847	0.18	0.34
		max	2.759	0.005	13725	0.81	1.66
		range	2.330	0.004	8878	0.63	1.33
		p (normality)	0.120	0.144	**0.018**	**0.005**	0.057
Mammut americanum	20	mean	2.558	0.004	9431	0.47	0.89
Ingleside, TX		median	1.966	0.004	10076	0.36	0.65
(Adults)		sd	2.398	0.002	4046	0.25	0.64
		min	0.715	0.001	507	0.19	0.38
		max	11.717	0.007	16547	0.99	3.05
		range	11.002	0.006	16040	0.80	2.67
		p (normality)	**<0.001**	0.147	0.228	**0.002**	**<0.001**
Mammuthus columbi	13	mean	2.871	0.005	12349	0.47	0.88
Friesenhahn, TX		median	2.254	0.005	12462	0.41	0.73
(Adults)		sd	1.759	0.002	2695	0.21	0.45
		min	0.457	0.001	6891	0.26	0.47
		max	6.241	0.009	16973	1.06	2.10
		range	5.784	0.007	10082	0.80	1.63
		p (normality)	0.535	0.954	0.964	**0.011**	**0.012**
Mammuthus columbi	18	mean	2.958	0.005	12690	0.48	0.83
Friesenhahn, TX		median	2.775	0.005	12468	0.40	0.77
(Juveniles)		sd	1.395	0.002	2713	0.32	0.35
		min	0.774	0.001	4432	0.20	0.38
		max	6.471	0.009	16966	1.66	1.98
		range	5.697	0.008	12535	1.47	1.61
		p (normality)	0.507	0.583	**0.019**	**<0.001**	**0.002**
Mammuthus columbi	21	mean	2.436	0.004	10973	0.35	0.67
Ingleside, TX		median	2.191	0.003	11528	0.34	0.66
(Adults)		sd	1.348	0.002	3523	0.10	0.24
		min	0.456	0.001	739	0.16	0.37
		max	5.937	0.008	18020	0.55	1.40
		range	5.481	0.007	17280	0.39	1.03
		p (normality)	0.252	0.725	0.085	0.836	**0.015**

anisotropy values for both proboscideans suggests a high proportion of tough foods likely dominated the diets of both organisms, although the disparity in $\delta^{13}C$ values suggests that such food came from different plant sources and/or habitats (e.g., forests vs. grasslands). Tough food is expected for a partly C_4 grazing *Mammuthus*, but higher complexity values than the grazing common tsessebe (Scott, 2012) suggest that mammoths at Ingleside were likely highly generalized in their diets. On the other hand, the predominately C_3-browsing *Mammut* might be expected to have had higher *Asfc* values if individuals were specialized on woody browse. Higher and more variable *Asfc* values than the browsing common duiker (Scott 2012) suggests that Ingleside mastodons were also highly generalized and consumed a high proportion of brittle or hard components of vegetation such as bark, nuts, or fruits.

Mammut americanum, although displaying evolutionarily conservative tooth morphology as compared to *Mammuthus columbi*, has been shown to have a wide array of dietary preferences. Analysis of mastodon dung recovered from the late Pleistocene Page-Ladson site in Florida revealed a broad diversity of consumed vegetation, including the wood, bark, seeds, fruit, vines, stems, leaves, thorns, and fine woody debris of at least 57 different taxa including trees, shrubs, lianas, vines and aquatic and terrestrial herbs (Newsom and Mihlbachler 2006). Critically, the dung samples from this site were overwhelmingly ($\geq$ 98% by volume) composed of distal growth twigs. By comparison, the "Burning Tree" mastodon dung from Ohio largely consisted of non-coniferous leaves and twigs, mosses, and low herbaceous growth (Lepper et al. 1991), suggesting a selective diet with both browsing and grazing habits. Another study on mastodon digesta from three boreal forest sites in New York State showed an overall reliance on *Picea* and *Pinus* with seasonal preferences for *Salix* and *Populus* (winter) and *Alnus* (spring; Teale and Miller 2012). Further, a mastodon tooth from Washington was found with pollen primarily represented by *Pinus*, *Salix*, *Shepherdia canadensis*, Rosaceae, Compositae, Cyperaceae, and Gramineae (Petersen et al. 1983). Additional work examining opal phytoliths preserved in mastodon tooth calculus suggests that some mastodons were capable of a predominately grazing

lifestyle, if the environment demanded it (Gobetz and Bozarth 2001). Low magnification stereomicrowear work on *Mammut americanum* from the Pleistocene of Florida revealed that mastodon microwear most closely aligned with the folivorous browsing morphospace, followed by mixed grazers/folivores and then fruit browsers (Green et al. 2005). Recent work employing DMTA suggests that still subtler dietary differences exist when comparing *Mammut* populations from cypress swamps, boreal forests, and open-pine parklands (Green et al. 2017). *Mammut* is probably best considered as a proboscidean with significant adaptability in its browsing niche, capable of expanding its dietary choices outside of the typical "browsing" dietary niches (e.g., folivore, frugivore, mixed feeder) depending on environmental and/or climatic conditions.

Our results, in accordance with the findings of the aforementioned studies utilizing multiple proxies for paleodiet, suggest an overall reliance of *Mammut americanum* on tough and/or hard foods, likely dominated by leaves (tough) and bark/woody browse (brittle and hard). *Mammut* foraging strategy in Late Pleistocene Texas likely paralleled that of modern monogastric herbivores. In this sense, Ingleside and Friesenhahn mastodon diets were mostly comprised of low-quality but chemically undefended species (regionally local conifers) supplemented by broadleaf and herbaceous species when toxin levels decreased on a seasonal basis (Teale and Miller 2012). DMTA data support the prevailing view of mastodons as displaying considerable adaptability in their ecological resistance during changing climates and environments in the Late Pleistocene (e.g., Baumann and Crowley 2015; Metcalfe et al. 2013; Newsom and Mihlbachler 2006; Green et al. 2017; Widga et al. 2017a). These data also support the reconstruction of mammoths as generalist mixed feeders in Late Pleistocene Texas, likely consuming a wide array of foods with varying textural and photosynthetic properties. While δ^{13}C values suggest that C_4 grasses were a dominant component of their diet, DMTA data demonstrate that they consumed food with a broader range of textures than just tough grasses. These findings corroborate past studies showing a trend toward mixed feeding for elephantids in the Late Pleistocene despite be-

ing evolutionarily adapted for efficient grazing (Cerling et al. 1999; Kingston and Harrison 2007). Whether mastodons or mammoths were indiscriminate in their dietary choices, consuming the roots, tubers, stems, leaves, needles, bark, and seeds of every species of plant they relied upon or only some of these components distributed across hundreds of specific species (as modern elephants do; Owen-Smith and Chafota 2012) remains to be tested.

An additional aspect that could play a critical role in how dental microwear manifests on a wear facet is the manner in which the organism processed its food. In mammoths (as in modern elephants), the power stroke is concentrated in a fore-aft movement, wherein the lower molars contact the posterior portion of the upper molars and are brought forward (Maglio 1972). The enamel cross-lophs of the molars contact one another at an oblique angle, shearing foods and wearing the tooth crowns to a flat surface crossed by low-relief enamel ridges (Maglio 1972). Thus, wear features such as scratches should be preferentially aligned antero-posteriorly if the rear-to-front movement of the jaw brings foods along the way. By contrast, American mastodon mastication was evolutionarily conservative and characterized by a bucco-lingual movement of the jaw during the power stroke (Laub 1996). Laub (1996) suggested that the power stroke could only be fully executed when the teeth fully occluded, which would have only been possible at higher wear stages when the cones and conules were not as pronounced. The highly generalized microwear signature of *Mammut* in our study might therefore have resulted from differing orientations of the power stroke at different stages of relative tooth wear.

A further complicating factor in dental microwear studies is the potential role of grit, which has previously been suggested to be the main controlling factor in forming dental microwear features (Lucas et al. 2013). Exogenous grit has been suggested to be capable of leaving microwear features on enamel surfaces, although such features might not necessarily be similar to those left from the phytoliths in plant opal (Grine 1986; Solounias and Semprebon 2002). Grit increases in abundance due to geographic (e.g., increased loess input) and/or climactic changes (e.g., increased aridity), which would be an important caveat

to consider when looking at time-averaged assemblages. However, stable oxygen isotopes suggest that these Texas proboscidean populations were not significantly time-averaged (all δ^{18}O standard deviations $1\sigma \leq 1.0‰$, Table 2.3) and that significantly different climatic conditions were not experienced by individuals in these assemblages. As a result, there is no evidence to suggest that grit load would have changed appreciably over time at either Friesenhahn, Ingleside, or Cypress Creek. Further, recent studies clearly show that not only can food items create microwear (Xia et al. 2015), but that variability of microwear features is positively associated with variation of dietary abrasiveness (Schultz et al. 2013). Additionally, controlled feeding studies in rabbits (Schultz et al. 2013) and sheep (Ramdarshan et al. 2016; Merceron et al. 2016) demonstrate that dietary signals are not overwhelmed by the ingestion of grit. Even wild koalas, which are known to ingest dust and grit on leaves (and primarily consume eucalyptus which lacks phytoliths), exhibit DMTA that records textural properties of consumed foods (Hedberg and DeSantis 2017). It is therefore unlikely that exogenous grit is solely responsible for the microwear signatures of the proboscideans in this study, and that the wide range of *Asfc* and *epLsar* values is instead a true reflection of the highly generalized textural properties of the diets of both *Mammut* and *Mammuthus* from the late Pleistocene of Texas.

2.4.2 Ontogenetic shifts in *Mammuthus columbi* and *Mammut americanum*

Dietary partitioning between individuals at different stages of life prevents intraspecific competition, allowing an individual to avoid direct overlap in resource use with members of its own species (Werner and Gilliam 1984). Additionally, size has a predominant influence on an animal's energetic requirements – large-bodied organisms require a high abundance of food, which can be of low quality, while smaller individuals require less food but of higher nutrient quality (Peters 1983). It follows that the change in body size during ontogeny could change the resource intake rate (e.g., Peters 1983) and composition (Werner and Gilliam 1984) of an individual. Ontogenetic diet shifts are widespread in nature, al-

though they are most often found in invertebrates and lower vertebrates living in freshwater communities (Werner and Gilliam 1984). There is some evidence of ontogenetic dietary partitioning in mammals with precocial youth such as deer mice (Van Horne 1982) and fur seals (de Albernaz et al. 2017). Some primates similarly show variations in feeding between juveniles and adults that is related to food toughness (Chalk-Wilayto et al. 2016).

Our data do not support the hypothesis that juvenile mammoths consumed foods of different textural properties than their adult counterparts at Friesenhahn Cave (Figure 2.3; Table 2.5). However, we do find evidence that Friesenhahn juvenile mammoths had significantly higher anisotropy than Ingleside adult mammoths (Table 2.5; ; Supplemental Table 5), suggesting two possible scenarios. The first possibility is that a higher proportion of tough foods comprised the diet of Friesenhahn juveniles as compared to Ingleside adults. The second possibility is that differing loads of exogenous grit were present in the environment at Friesenhahn during the LGM as were present at Ingleside pre-LGM, increasing the dietary *epLsar* signature of Friesenhahn mammoths. If the latter case were true, than we would expect grit to have caused an increase in *epLsar* values in both Friesenhahn adults and juveniles, as the grit would have been nonselective in being incorporated in the diets of all individuals at that site. Additionally, grit has been shown to play a minor (and non-significant) role in altering *epLsar* values of grazers in controlled feeding studies (Merceron et al., 2016). Because Ingleside and Friesenhahn adult mammoths are indistinguishable in all DMTA attributes (Supplemental Table 4), the first scenario of a dietary discrepancy is the more likely one. As Friesenhahn exhibited a very high percentage of grasses and sedges (64%) compared to modern regional shortgrass prairies (47%) and modern regional tallgrass prairies (38%) (Hall and Valastro 1995), it is very likely that Friesenhahn juvenile mammoths were consuming predominantly grasses. Ingleside mammoths, likely inhabiting an open C_4 grassland interspersed by stands of C_3 forest (Bryant and Holloway 1985; Koch et al. 2004), would have encountered a variety of foods of varying textures, resulting in dampened *epLsar* values.

In addition, we find evidence that Friesenhahn juvenile mastodons had significantly lower complexity than Ingleside adult mastodons (Table 2.5; Supplemental Table 6). This suggests that Friesenhahn mastodons were consuming less brittle and/or harder foods than Ingleside mastodons. However, as we lack an adult mastodon population at Friesenhahn, we cannot say for sure whether this phenomenon is due to a true ontogenetic difference between juveniles and adults or whether it is due to an environmental difference between the two sites. Juvenile mastodons could have been restricted to consuming less hard foods due to difficulties accessing and/or processing such foods; on the other hand, Ingleside may have had an abundance of harder foods – such as bark, seeds, fruit pits, or nuts – as compared to Friesenhahn due to either climatic differences (pre-LGM vs. LGM conditions) or geographic location (coastal vs. plateau setting). Because of the multiplicity of these compounding effects, we cannot explicitly state whether mastodons displayed an ontogenetic difference in diet. We encourage a future study focusing on dental microwear of juvenile and adult mastodons recovered from the same location, much as we were able to do with the Friesenhahn mammoth assemblage.

Juveniles and adults might not be expected to exhibit dietary partitioning for one of three reasons. First, elephant juveniles are highly precocial - newborns are capable of walking and feeding themselves almost immediately after birth, although juveniles rely at least partially on their mother's milk for the first 2 - 3 years of life (Sukumar 2003). Second, individual elephant diets (regardless of age) within a population are not likely to vary significantly due to their herd's social structure. Newborns stay with their mothers and a herd of mostly female adults, roaming and foraging together as a unit (Sukumar 2003). Thus, the vegetation spectra that individuals come into contact with are, on average, the same across a herd. This relationship might not hold true in closed forest-dwelling browsing mastodons because more resources might be available to full-sized individuals (for example, fruits hanging on high branches); however, it is equally likely that adults might knock these resources down and rupture fruit or seed hard skins for juveniles, much as modern

elephant mothers do for their young (Sukumar 2003). Third, being a large-bodied forager with a cecal digestive system necessitates that elephants consume as much food as possible, as they are less limited by the amount of food consumed or rate of ingestion as compared to ruminants (Hanley 1982). Elephants are therefore likely to consume whatever vegetation is available to them and would be expected to show little resource discrimination amongst the members of the herd.

Elephantids (including mammoths) might also be likely to show similar patterns in dental microwear from the juvenile through adult stage because of their molariform premolars and molars (Maglio 1972). Deciduous premolars (i.e., dp2, dp3 and dp4) are composite organs of similar morphology and structure to permanent molars (i.e., m1, m2 and m3), with subsequent molars essentially acting as scaled-up versions of the previous cheek tooth. Thus, the masticatory process is likely unchanged with age as is the bulk morphology of the wear facet, limiting the potential for differential wear mechanisms between adults and juveniles. On the other hand, the molar morphology of mammutids does change from the juvenile through adult stage, with bilophodont DP2/dp2 and DP3/dp3, trilophodont DP4/dp4, M1/m1, and M2/m2, and tetralophodont (or greater) M3/3 tooth forms (Saunders 1977b; Green and Hulbert 2005). However, Laub (1996), who conducted the most in-depth consideration of mastodon chewing mechanics, did not mention any potential difference in the power strokes between juveniles and adults. It also seems unlikely that the mere addition of lophs from second deciduous premolars through permanent third molars would give cause for a significant alteration in the manner in which adult mastodons processed their foods as compared to juveniles. Laub (1996) considered prominent cusps preventing an efficient bucco-lingual shear stroke to be the most important aspect controlling microwear signatures in *Mammut*. Thus, any amount of variation in microwear signature among different cheek teeth along the toothrow in proboscideans (e.g., deciduous premolars or permanent molars) is likely to be at least as much as would be seen when comparing among lophs (at potentially differing wear stages) on a singular molar. However, as Todd et al. (2007) did

find significant variability among lophs of extant elephant molars, to yield the most comparable methods for researchers it is best to standardize the tooth position and/or loph that they choose to examine in dental microwear signatures – typically, the central enamel band in *Mammuthus* and the metaloph/id in *Mammut* (as is typically the practice in proboscidean microwear studies; e.g., Sembrebon et al. 2016; Green et al. 2017).

2.4.3 Dietary comparison of Late Pleistocene *Mammuthus* and *Mammut* to Santa Rosa *Mammuthus exilis*

Semprebon and colleagues (2016; their figure 4C) demonstrated via stereomicroscopic analysis that *Mammuthus exilis* had similar textural properties to *Loxodonta cyclotis* and *Mammut americanum*, the three of which fell within the extant ungulate browsing morphospace (Semprebon 2002; Solounias and Semprebon 2002). None of the 53 *Mammuthus exilis* or the singular *Mammuthus columbi* from Santa Rosa, Santa Cruz, and San Miguel fell within the smaller grazing morphospace defined by extant grazers (Semprebon et al. 2016; their figure 4B). Because of the pygmy mammoth's similarity in stereomicrowear to both mastodons and African forest elephants, Semprebon and colleagues suggested that Santa Rosa Island was more than likely a closed-forest environment during the Late Pleistocene and that mammoths there were likely consumers of tough vegetation such as spruce, cypress, and Douglas Fir (Semprebon et al. 2016). However, the authors noted that the stereomicrowear pattern of modern elephants (*Loxodonta cyclotis*, *L. africana*, *Elephas maximus*) and the pygmy mammoth (*Mammuthus exilis*) were unique compared to other herbivorous mammals studied via steromicrowear to date (Semprebon et al. 2016; p. 7).

Our data similarly show that the CHIS mammoths (*Mammuthus exilis* and *Mammuthus columbi*) are unique in having a wider range, higher variability, and higher mean values of complexity (*Asfc*) than either population of Texas *Mammuthus* or *Mammut* (Figure 2.3; Table 2.4). Further, the significantly higher variability in *Asfc* values for CHIS mammoths as compared to both populations of Texas proboscideans suggests a higher variability in diet

for the island-restricted population of pygmy mammoths (and one Columbian mammoth).

There are some caveats to treating the Santa Rosa Island mammoths as a discrete population in space and time. Specimens of *Mammuthus exilis* are not well-constrained temporally, arriving on Santarosae at least 150 ka and perhaps as much as 250 ka (Muhs et al. 2015). The youngest dated mammoth specimen from Santa Rosa Island was reported as 11,030 $\pm$ 50 ka (Agenbroad 2005); thus, this "population" is highly time-averaged, spanning multiple glacial-interglacial cycles and their associated transgressions and regressions. The microwear signature of mammoths from Santa Rosa therefore represents different environmental signatures - some likely during the warmer interstadials and others during cool interglacials. This may explain the higher variability in Santa Rosa complexity values because our sample likely represents a longer environmental and dietary history than any of the Texas mammoth or mastodon populations (Table 2.1).

Anderson et al. (2010) summarizes the LGM vegetation of southwestern California based on previous studies from multiple mainland sites (including Rancho La Brea and McKittrick) as being dominated by multiple coniferous species (*Pinus*, *Abies*, and *Juniperius* or *Cupressus*) and resembling mixed conifer forests of the higher elevation San Jacinto and San Bernardino mountains today. During the LGM, the interpretation of Santa Rosa Island as a mixed coniferous forest with a lower abundance of grasses (Anderson et al. 2010) suggests that mammoths on the island were exposed to a greater abundance of hard foods including bark, twigs, and seeds than the Texas *Mammuthus columbi* and *Mammut americanum* populations examined in this study. Between 17 and 13 ka, Santarosae was characterized by Douglas fir (*Pseudotsuga menziesii*), Gowen cypress (*Cupressus governiana*), and bishop pine (*Pinus muricata*) with a diverse understory of forbs and shrubs (Chaney and Mason 1930; Anderson et al. 2008). By the latest Pleistocene (*ca.* 11,800 cal. yrs BP), the mixed conifer forest was beginning to fragment into multiple plant communities, including pine stands, coastal sage scrub and grassland (Anderson et al. 2010), introducing a wide array of foods with highly variable structural properties and/or textures.

The pygmy mammoths (*M. exilis*) occupying Santarosae during this period would have almost certainly been subsisting on a wide variety of resources, and our complexity values are reflective of this highly generalized diet.

Although our sample size of pygmy mammoths (n = 16) was considerably smaller than the previous user-based light microscopy study (n = 51), the overall environmental signature of Santa Rosa pygmies was similar between the two studies. One of the strengths of DMTA is its ability to discern dietary patterns with relatively small sample sizes (Scott 2012; DeSantis et al. 2013). The hypothesis that *Mammuthus exilis* had a diet distinct in textural properties as compared to Texas *Mammuthus columbi* or *Mammut americanum* is supported via DMTA insofar as the variability in complexity values exceeds any other known artiodactyl, perissodactyl, or proboscidean previously studied (e.g., Scott 2012; DeSantis and Schubert 2015; Zhang et al. 2017; Jones and DeSantis 2017; Green et al. 2017). As higher complexity values are expected from an organism feeding on bark, seeds, and woody material, our data support previous interpretations of the feeding habits of pygmy mammoths (Semprebon et al. 2016).

Although the pygmy mammoth is the end-result of a long history of insular dwarfism and is considered to be a distinct species (*Mammuthus exilis*), the CHIS collections are time-averaged and record multiple colonization events (Muhs et al. 2015). Thus, dwarfism likely occurred several times on Santarosae. The CHIS mammoths are therefore comprised mostly of intermediate individuals represented by only a few 'pure' *M. columbi* and a few 'pure' *M. exilis* individuals. Indeed, not all mammoths we measured belong to *M. exilis* as evidenced by measurements of length, width, and other diagnostic dental characters outlined in Widga et al. (2017b). These measurements are part of an ongoing study on the character of the Channel Island mammoths (J. Hoffman, personal communication). This complication hints at the larger issue of identifying mammoth material to the species level, which has been previously suggested to have been a difficult task in the Late Pleistocene, when mammoths varied in size and morphology more due to phenetic conditions than ge-

netic differences (Enk et al. 2011, 2016; Smith and Graham 2017; Lister 2017) – although there are promising methods in the works (Widga et al. 2017b). As result, it is possible that some specimens originally referred to *M. exilis* are in fact simply smaller or intermediate *M. columbi*. This complicating factor should not significantly impact our results because it is likely that *M. exilis* and *M. columbi* would have displayed similar feeding and foraging behavior on Santa Rosa Island due to similarities in feeding habits (Agenbroad 2012).

2.5 Conclusions

We demonstrate that Ingleside mastodons were likely highly generalized in their consumption of C_3 woody browse, while mammoths were C_3/C_4 mixed feeders; however, both proboscideans consumed a wide variety of foods with varying textural properties. The overlap in DMTA signatures of the two organisms suggests that both mammoths and mastodons had generalized diets of tough and hard foods. There is no evidence for ontogenetic differences in the diet of *Mammuthus columbi*, despite large differences in size between juvenile and adult mammoths. There may be evidence that dietary choices between Friesenhahn juvenile mammoths and mastodons differed from their adult counterparts at Ingleside, although whether this difference is due to ontogenetic or environmental differences (or some combination of the two) is unclear. Finally, the pygmy mammoths on Santa Rosa Island had a more variable diet with extensive hard object feeding as compared to late Pleistocene *Mammuthus columbi* and *Mammut americanum* from Texas, consistent with previous reconstructions of the dietary behavior of *Mammuthus exilis* using user-based stereomicrowear methods. Our work suggests that microwear alone may not be sufficient to reconstruct "browsing" or "grazing" habits in proboscideans, as they were likely highly generalized in consuming a wide variety of plant parts while remaining somewhat specialized on the isotopic source of those plants. Thus, multiple dietary proxies may be needed to reconstruct the diets of proboscideans and potentially other large-bodied taxa, which consume a wide variety of foods to sustain themselves.

Chapter 3

EXTIRPATION OF THE GOMPHOTHERES: EVIDENCE FOR COMPETITION BETWEEN SYMPATRIC PROBOSCIDEANS IN THE LATE PLEISTOCENE OF NORTH AMERICA

3.1 Introduction

Gomphotheres (subfamily Gomphotheriinae *sensu lato*) are temporally and spatially prolific, dominant in North America since the Miocene and emigrating to South America from North America during the closure of the Isthmus of Panama between 1.8 and 0.125 Ma (Webb 1985; Woodburne 2010; Mothé et al. 2017). Their dietary flexibility is hypothesized to have facilitated their successful migration in contrast to mammoths and mastodons, which remained in Central and North America despite the continental connection (Pérez -Crespo et al. 2016). On the other hand, gomphothere abundance, diversity, and geographic range in North America rapidly drops off after the arrival of mammoths and the gomphotheres are rarely represented in Rancholabrean faunal assemblages (*ca.* 0.3 – 0.012 Ma *sensu* Bell et al. 2004) (Carrasco et al. 2005). The success of the mammoth radiation and its apparent correlation with the demise of the gomphothere clade in North America has led some to argue that competition from early mammoths caused the extirpation of the gomphotheres (i.e., competitive exclusion; Kurtén and Anderson 1980). However, others have argued that cooling climates and the emergence of steppe/prairie habitats would have displaced the gomphotheres from North America even in the absence of competition (i.e., ecological displacement; Dudley 1996). These two competing hypotheses have yet to be fully tested or resolved.

The competitive exclusion principle attests that when closely-related species with similar niches coexist, one of these taxa will either outcompete the other or they will partition their niches to exploit different resources (Hardin 1960). Niche partitioning studies in

fossil ungulates are commonly carried out through a reconstruction of diet using similar methods to those implemented here, and often show the alteration of dietary preference by one or multiple organisms to facilitate coexistence with other organisms (e.g., in bovids, camelids, and horses; MacFadden et al. 1999; Bibi 2007; DeSantis et al. 2009, Yann and DeSantis 2014). Similarly, studies of proboscidean dietary niche partitioning often indicate high dietary flexibility amongst focal taxa (e.g., Calandra et al. 2008; Rivals et al. 2015; Pérez -Crespo et al. 2016). Most paleoecological studies on gomphotheres suggest that they were already highly flexible in their dietary choices, capable of fluctuating between grazing, browsing, and mixed-feeding habits (e.g., MacFadden and Cerling 1996; Koch et al. 1998, 2004; MacFadden 2000; Fox and Fisher 2001, 2004; Sánchez et al. 2004; Calandra et al. 2008; DeSantis et al. 2009; Rivals et al. 2015; Pérez-Crespo et al. 2016; Zhang et al. 2017; González-Guarda et al. 2018). However, on a smaller spatial and temporal scale, gomphotheres tended to restrict their dietary preferences due to abiotic (climatic) or biotic (competitive) factors; for example, South American populations of *Notiomastodon* showed an adaptive trend toward either grazing or browsing habits in the late Pleistocene due to habitat differentiation (Sánchez et al. 2004), South China populations of *Sinomastodon* were restricted to the consumption of browse due to competition with co-occurring *Stegodon* (Zhang et al. 2017), and the East Asian gomphotherid *Protonancus* was competitively displaced by the amebelodont *Platybelodon* (Wang et al. 2015). Recognizing this pattern of dietary restriction in smaller populations, we therefore limit our analysis herein to Pleistocene populations of gomphothere (*Cuvieronius hyodon*), mammoth (*Mammuthus columbi*), and mastodon (*Mammut americanum*) occupying the Atlantic Coastal Plain (ACP) physiogeographic province of North America (Figure 3.1A).

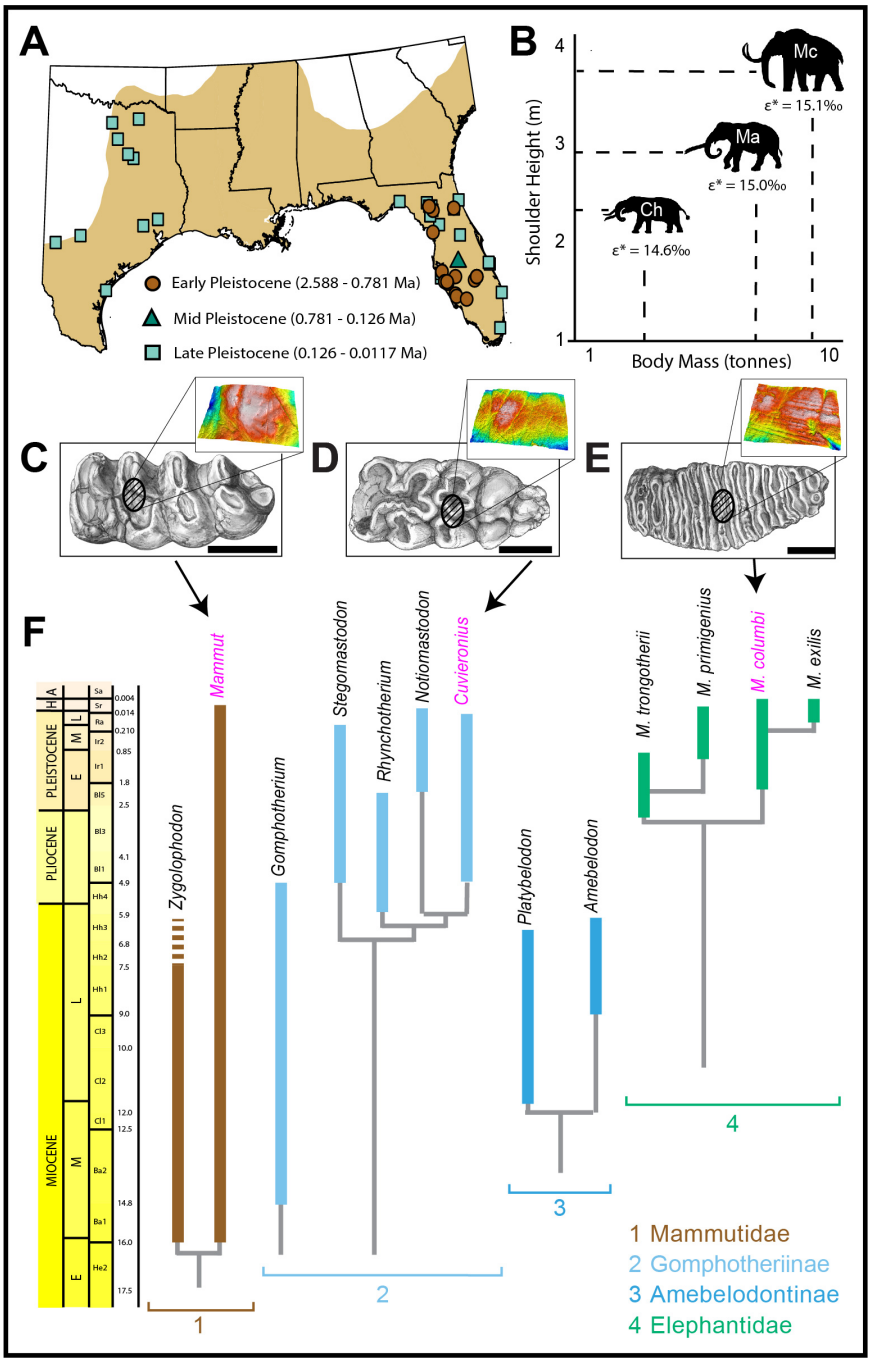

Figure 3.1: Geography, body size, and phylogeny related to the study material. (A) Overview of the study area, with the Atlantic Coastal Plain in orange and sites delineated by their geologic age. (B) Average body size and shoulder height of the focal proboscideans with enrichment factor (ε*) obtained using body size estimates. Ch = *Cuvieronius hyodon*; Ma = *Mammut americanum*; Mc = *Mammuthus columbi*. (C) UF 80004, left m3. Scale bar = 10 cm. Cross-hatching represents area where DMTA mold was sampled, with 3D surface model of wear facet. (D) TMM 47200-172, right m3. (E) UF 86825, right m1. (F) Temporal ranges of North American proboscidean taxa, modified from Fisher (2018). Solid bars show known range of taxa; interrupted bars show uncertain range extensions.

This study aims to fill an important spatial and temporal gap in the paleoecological record of proboscideans. In this paper, we present a quantitative analysis of dietary differences among Pleistocene proboscideans in North America using the integration of stable isotope geochemistry and dental microwear texture analysis (DMTA). The design of this study allows for both a regional comparison over time (from the Early to Late Pleistocene) and local, site-based assessments. Specifically, multi-proxy data are used to test the following hypotheses: 1) North American *Cuvieronius* consumed similar resources as sympatric *Mammuthus*, and, 2) *Cuvieronius*, *Mammuthus*, and *Mammut* altered their dietary habits in the ACP throughout the Pleistocene. Evidence for the consumption of similar resources by *Cuvieronius* and *Mammuthus*, as inferred via stable isotopes and dental microwear textures, may suggest that competition was a primary driver of the early demise of North American gomphotheres - particularly if either taxa displays shifting dietary habits over time.

3.2 Materials and Methods

3.2.1 Fossil Populations

Our study uses specimens recovered from numerous fossil mammal sites in the Atlantic Coastal Plain of the United States (Figure 3.1A). We first compiled a list of published bulk stable isotope data (n = 168; MacFadden and Cerling 1996; Koch et al. 1998; Feranac and MacFadden 2000; Hoppe 2004; Koch et al. 2004; DeSantis et al. 2009; Yann and DeSantis 2014; Yann et al. 2016; Smith and DeSantis 2018) and DMTA data previously analyzed on the confocal microscope located at Vanderbilt University (n = 117; Green et al. 2017; Smith and DeSantis 2018) for proboscideans from this area (Supplemental Table 7). Focusing on localities from one physiogeographic province below 35° N limits the possible inclusion of C_3 grass, which increases in abundance in more northern and western regions with decreased growing season temperatures (Teeri and Stowe 1976; Stowe and Teeri 1978; Still et al. 2003). New targeted samples of primarily under sampled *Cuvieronius*, and co-

occurring *Mammuthus* and/or *Mammut* from the same locality were added to published data, resulting in a total of 244 bulk stable isotope samples and 241 DMTA samples.

3.2.2 Stable Isotope Geochemistry

Geochemical bulk samples of the carbonate portion of enamel hydroxyapatite were removed from well-preserved proboscidean samples from the Texas Memorial Museum (TMM) in Austin, TX and the Florida Museum of Natural History (FLMNH) in Gainesville, FL. All sampled teeth were drilled using a variable speed rotary drill with carbide dental burrs (1 mm burr width), which was used to create a 1 cm x 1 mm sample oriented parallel to the growth axis of the tooth. The collected enamel powder was pretreated with 30% H_2O_2 to remove organics, then rinsed with distilled water and treated with 0.1N acetic acid for 18h to remove secondary carbonates (similar to Koch et al. 1997), followed by an additional rinse. Samples were left to air dry, and 1mg per sample was analyzed on a VG Prism stable isotope ratio mass spectrometer with an in-line ISOCARB automatic sampler in the Department of Geological Sciences at the University of Florida. The standard deviation (1σ) of the laboratory standard (NBS-19) included with these samples was $<0.05‰$ for both carbon and oxygen. The analytical precision is $\pm 0.1‰$, based on replicate analyses of samples and standards (NBS-19). Stable isotope data were normalized to NBS-19 and are reported in conventional delta notation.

Carbon values from enamel ($\delta^{13}C_{enamel}$) are reported relative to V-PDB (Coplen, 1994). Consumer $\delta^{13}C_{enamel}$ values were converted to the carbon isotope value of vegetation consumed ($\delta^{13}C_{veg}$) using enrichment factors (ε*) of 15.1‰, 15.0‰, and 14.6‰ for *Mammuthus columbi*, *Mammut americanum*, and *Cuvieronius hyodon*, respectively. These enrichment factors were obtained using the regression equation for hindgut fermenters from Tejada-Lara et al. (2018): $\ln \varepsilon^* = 2.42 + 0.032 * (BM)$, where BM is body mass in kg and is log-transformed. Average body mass for each proboscidean taxon was derived from volumetric method estimates reported by Larramendi (2016); the body mass values we used are

9500 kg for *M. columbi*, 8000 kg for *M. americanum*, and 3500 kg for *C. hyodon* (Figure 3.1B). To correct for the effects of differing $\delta^{13}C_{atm}$ values over time on $\delta^{13}C_{veg}$ values, we used estimates of past $\delta^{13}C_{atm}$ values from benthic foraminifera (Tipple et al. 2010) to convert paleodietary vegetation to their modern equivalent values ($\delta^{13}C_{vmeq}$) based on an AD 2000 $\delta^{13}C_{atm}$ of -8‰ (following methods outlined in Kohn, 2010). Sample age came from site age estimates (see Section 3.2.4); we used the estimates of minimum and maximum site age (Supplemental Table 7) to calculate average $\delta^{13}C_{atm}$ value over the age range of the sample. This value was inserted into Equation 3 from Kohn (2010) and used to calculate Δ. We then calculated $\delta^{13}C_{vmeq}$ using the following linear regression equation, obtained using the dataset in the supplemental material from Kohn (2010): $\delta^{13}C_{vmeq}$ = -0.9543* Δ – 8.3617. Oxygen isotope values ($\delta^{18}O_{enamel}$) are reported relative to V-SMOW. Previously published $\delta^{18}O_{enamel}$ values reported relative to V-PDB were converted using the following equation: $\delta^{18}O_{V\text{-}SMOW}$ = 1.03086 * $\delta^{18}O_{V\text{-}PBD}$ + 30.86 (Friedman and O'Neil 1977).

3.2.3 Dental Microwear Texture Analysis

Microwear molds were collected from the jaws and isolated teeth of proboscidean fossils held at TMM (n = 13) and FLMNH (n = 103). Sampling methods for DMTA followed procedures outlined in prior studies (Jones and DeSantis 2017; Smith and DeSantis 2018). Briefly summarized here, the wear facets of mammoth, mastodon, and gomphothere molars were cleaned with acetone and then sampled with Regular Body President's Jet to create a mold. We prioritized sampling the central enamel bands for all specimens (Figure 3.1C-E) to maintain consistency with past studies of DMTA in proboscideans (Zhang et al. 2017; Green et al. 2017; Smith and DeSantis 2018) and because sampling these areas reduces the amount of variation in microwear features attributable to differences in the direction of the power stroke during mastication (e.g., Laub 1996; Todd et al. 2007; von Koenigswald 2016). The molds were then cast at Vanderbilt University using a high-resin epoxy (Epotek 301) and dried in a fume hood for at least 72 hours prior to analysis.

All specimens were scanned in three dimensions in four adjacent fields of view for a total sampled area of 204 x 276 μm^2 using the Plu NEOX white-light microscope with confocal capabilities at Vanderbilt University. Scans were analyzed using scale sensitive fractal analysis (SSFA) software (ToothFrax and SFrax, Surfract Corporation, www.surfract.com), which characterizes wear surfaces according to variables including complexity (*Asfc*), anisotropy (*epLsar*), textural fill volume (*Tfv*), and heterogeneity of complexity (*HAsfc*). Complexity is a quantification of the change in surface roughness with increasing scale and is used to distinguish taxa that consume hard/brittle foods from those that eat softer/tougher foods (Ungar et al. 2003, 2007; Scott et al. 2005; Prideaux et al. 2009; Scott 2012; DeSantis 2016). Anisotropy is the degree to which surface features share a similar orientation, such that a predominance of parallel striations leads towards highly anisotropic surfaces – typical in grazers and other consumers of tough food items (Ungar et al. 2003, 2007; Prideaux et al. 2009; Scott 2012; DeSantis 2016; Hedberg and DeSantis 2017). Textural fill volume is a measure of the total volume of square cuboids of a given scale that fill surface features and is useful for distinguishing deeper microwear features (such as gouges from pits), which has the potential to distinguish between consumption of foods with different fracture properties (leaves versus fruit pits, for example) (Ungar et al. 2007, 2008; Scott et al. 2006). Heterogeneity of complexity is calculated by splitting individual scanned areas into smaller sections with equal numbers of rows and columns (from 2 x 2 up to 11 x 11) and comparing *Asfc* values between subregions (Scott et al. 2006). Low values in heterogeneity have been shown to be indicative of either high grit loads or grass consumption (Scott 2012; Merceron et al. 2016). We report heterogeneity at two scales, 3 x 3 (*HAsfc3x3*) and 9 x 9 (*HAsfc9x9*), as has been the practice in previous studies (e.g., Green et al. 2017; Smith and DeSantis 2018).

3.2.4 Assignment to Biochronologic Intervals ('Biochrons')

Each proboscidean individual sampled for stable isotopes or DMTA was referred to a specific locality (Supplemental Table 7). For published samples, the minimum and maximum ages for that locality were inferred from the publication that contained the sample reference. For new samples, the age of the site was either determined from the literature (e.g., Kissimmee River 6 age and geography from Appendix 1 of Hulbert (2010)) or from personal communication with the Collections Manager of the FLMNH (R. Hulbert). DeSoto Shell Pit, Devil's Elbow, Haile 7C, and Brighton Canal were all considered to date to the latest Blancan (Bl5). Following Lucas (2008), we consider all gomphotheriids from Florida from Bl5 or younger to be *Cuvieronius hyodon*. We therefore include the samples referred to *Rhynchotherium* in MacFadden and Cerling (1996) as samples of *Cuvieronius hyodon*. Site ages were used to bin samples to the following biochrons, with ages from Bell et al. (2004): Bl5 (Late Blancan), minimum age = 1.6 Ma, maximum age = 2.5 Ma; Ir1 (Early Irvingtonian), minimum age = 0.85 Ma, maximum age = 1.6 Ma; Ir2 (Late Irvingtonian), minimum age = 0.3 Ma, maximum age = 0.85; Ra (Rancholabrean), minimum age = 0.010 Ma, maximum age = 0.3 Ma.

3.2.5 Statistical Analyses

All published and new data were combined for statistical comparisons. We carried out two statistical comparisons of $\delta^{13}C_{vmeq}$, $\delta^{18}O_{enamel}$, and DMTA attributes for each genus: first, within each biochron to test for consumption of similar foods in sympatric populations; and, second, across biochrons to assess whether dietary niche was conserved over time for each taxon. When comparing between normally-distributed attributes, parametric tests (e.g., t-test or ANOVA) were employed; otherwise, nonparametric equivalent tests (e.g., Mann-Whitney U or Kruskal-Wallis) were used. P-values of <0.05 were considered significant.

Table 3.1: Stable carbon isotope summary statistics for ACP proboscideans, broken down by biochronologic interval.

		$\delta^{13}C_{vmeq}$ V-PDB (‰)							
Age	**Taxon**	**n**	**mean**	**min**	**max**	**range**	**SD (1σ)**	**SE**	**p-value**
Bl5	*Cuvieronius hyodon*	20	-20.7	-27.4	-17.6	9.8	2.3	0.5	**0.004**
Ir1	*Cuvieronius hyodon*	28	-19.2	-21.1	-17.6	3.5	1.1	0.2	**0.034**
	Mammut americanum	6	-28.3	-29.5	-27.0	2.5	1.0	0.4	0.389
	Mammuthus columbi	19	-18.6	-21.1	-17.1	4.0	1.0	0.2	0.231
Ir2	*Mammut americanum*	6	-26.6	-28.4	-22.2	6.2	2.3	0.9	0.081
	Mammuthus columbi	5	-21.1	-24.4	-17.0	7.4	2.9	1.3	0.853
Ra	*Cuvieronius hyodon*	23	-21.9	-27.1	-16.5	10.6	2.8	0.6	0.228
	Mammut americanum	44	-27.0	-28.7	-25.1	3.6	1.1	0.2	0.092
	Mammuthus columbi	93	-18.5	-23.9	-15.7	8.2	1.7	0.2	**<0.001**

Bold values indicate a non-normal distribution (Shapiro-Wilks; $p < 0.05$ is significant). Bl5, Late Blancan (2.6 – 1.8 Ma); Ir1, Early Irvingtonian (1.8 – 0.85 Ma), Ir2, Late Irvingtonian (0.85 – 0.3 Ma); Ra, Rancholabrean (0.3 – 0.011 Ma).

3.3 Results

3.3.1 Stable Isotope Ecology

Mammut $\delta^{13}C_{vmeq}$ values are statistically indistinguishable through time in contrast to *Mammuthus*, which exhibits higher $\delta^{13}C_{vmeq}$ values during the Rancholabrean (0.3 – 0.011 Ma) as compared to the Late Irvingtonian (0.85 – 0.3 Ma), and *Cuvieronius*, which has significantly lower $\delta^{13}C_{vmeq}$ values during the Rancholabrean than the Early Irvingtonian (1.8 – 0.85 Ma) (Table 3.1). Further, *Mammut* consistently has lower $\delta^{13}C_{vmeq}$ values than both *Cuvieronius* and *Mammuthus* through time, while *Mammuthus* has significantly greater $\delta^{13}C_{vmeq}$ values than *Cuvieronius* during the Rancholabrean (note, $\delta^{13}C_{vmeq}$ values are indistinguishable when compared to the Early Irvingtonian).

Oxygen isotope values of *Cuvieronius* are significantly greater during the Early Irvingtonian (1.8 – 0.85 Ma) than both the Late Blancan (2.6 – 1.8 Ma) and Rancholabrean (Table 3.2). In contrast, *Mammut* has significantly higher $\delta^{18}O_{enamel}$ values during the Late Irvingtonian than both the Early Irvingtonian and Rancholabrean. *Mammuthus* has the highest $\delta^{18}O_{enamel}$ values during the Late Irvingtonian followed by the Early Irving-

Table 3.2: Stable oxygen isotope summary statistics for ACP proboscideans, broken down by biochronologic interval.

		$\delta^{18}O_{enamel}$ V-SMOW (‰)							
Age	**Taxon**	**n**	**mean**	**min**	**max**	**range**	**SD (1σ)**	**SE**	**p-value**
Bl5	*Cuvieronius hyodon*	20	29.6	27.8	32.9	5.1	1.1	0.3	0.058
Ir1	*Cuvieronius hyodon*	28	31.5	30.2	32.6	2.4	0.6	0.1	0.873
	Mammut americanum	6	28.6	27.4	30.6	3.2	1.3	0.5	0.343
	Mammuthus columbi	19	30.0	28.3	31.6	3.3	0.9	0.2	0.929
Ir2	*Mammut americanum*	6	32.2	31.6	32.8	1.2	0.5	0.2	0.302
	Mammuthus columbi	5	32.2	31.1	33.8	2.7	1.0	0.5	0.670
Ra	*Cuvieronius hyodon*	23	29.9	27.6	32.6	5	1.2	0.3	0.922
	Mammut americanum	44	29.9	28.0	31.8	3.8	1.0	0.1	0.600
	Mammuthus columbi	93	29.7	25.9	33.3	7.4	1.3	0.1	0.428

Bold values indicate a non-normal distribution (Shapiro-Wilks; $p < 0.05$ is significant). Bl5, Late Blancan (2.6 – 1.8 Ma); Ir1, Early Irvingtonian (1.8 – 0.85 Ma), Ir2, Late Irvingtonian (0.85 – 0.3 Ma); Ra, Rancholabrean (0.3 – 0.011 Ma).

tonian and Rancholabrean (all significantly different from one another). Overall, all proboscideans examined have indistinguishable $\delta^{18}O_{enamel}$ values from one another during the Late Irvingtonian and Rancholabrean, with only *Cuvieronius* yielding significantly higher $\delta^{18}O_{enamel}$ values than both *Mammut* and *Mammuthus* during the Early Irvingtonian.

3.3.2 Textural Properties of Food Resources

Cuvieronius and *Mammut* both have *Asfc*, *epLsar*, *Tfv*, and *HAsfc* (both $HAsfc_{3x3}$ and $HAsfc_{9x9}$) values that are indistinguishable over time (Table 3.3). Only *Mammuthus* exhibits significantly greater *Tfv* during the Early Irvingtonian as compared to both the Late Irvingtonian and Rancholabrean. During the Early Irvingtonian, *Cuvieronius* has significantly higher *Asfc* values than *Mammut*, while *Mammuthus* has significantly higher Tfv than *Cuvieronius*. *Mammut* and *Mammuthus* have *Asfc*, *epLsar*, *Tfv*, and *HAsfc* (both $HAsfc_{3x3}$ and $HAsfc_{9x9}$) values that are indistinguishable from one another during the Late Irvingtonian. During the Rancholabrean, *Mammuthus* has significantly higher *Asfc* values than *Mammut*, *Cuvieronius* has significantly lower *epLsar* than both *Mammut* and *Mam-*

muthus, and *Mammuthus* has significantly higher *Tfv* than *Cuvieronius* and *Mammut*.

3.4 Discussion

Despite an oft-mentioned viewpoint that the extinction of gomphotheres was tied to competition with other megaherbivores, particularly mammoths (Kurtén and Anderson 1980; Cerling et al. 2003; Sanders 2007; Lister 2013), there are few studies that have searched for signatures of that competition in the fossil record. Interspecific competition is notoriously difficult to prove when examining fossil populations, as paleoecologists can neither directly observe interference competition (e.g., male-male combat or other acts of aggression towards a competitor) nor precisely quantify the magnitude of resource limitation leading towards exploitative competition (e.g., consumption of similar resources by two potential competitors). Because of these limitations, evidence of interspecific competition in the fossil record is usually either modelled using phylogenetic hypotheses (e.g., Rabosky 2013) or inferred from character displacement (Schluter 2000; Grant and Grant 2006). However, the paleontological record offers a potential strength in documenting the signs of exploitative and interference competition over geological time scales if one makes a few assumptions about how competition between megaherbivores would manifest in the fossil record. First, if one assumes via the principle of limiting similarity that there is a limit to how similar species can be and still coexist (MacArthur and Levins 1967; May and MacArthur 1972; May 1974), then it follows that there is an upper limit of shared niche space that would facilitate co-existence between two species. Above this limit, the more likely it is that one species will exclude the other through competition for resources. Second, if one assumes that competition promotes the use of different resources (as opposed to complete exclusion) (Schoener 1974, 1982; Pianka 1976), then shifting dietary habits over geologic time scales may be correlated with the intensity of interspecific competition. In this case, demonstrating such shifts in response to the presence of a potential competitor can be considered to be evidence of competition (Pianka 1976). Finally, if we assume that

Table 3.3: DMTA attribute summary statistics for ACP proboscidean populations, broken down by biochronologic interval.

Age	Taxon	n	Statistic	*Asfc*	*epLsar*	*Tfv*	*HAsfc3x3*	*HAsfc9x9*
Bl5	*Cuvieronius*	23	mean	2.648	0.003	11033	0.52	0.97
			median	1.799	0.002	11093	0.46	0.88
			sd	1.976	0.002	2593	0.24	0.41
			min	0.734	0.001	3849	0.16	0.37
			max	8.932	0.007	15525	1.14	2.08
			range	8.198	0.006	11676	0.98	1.71
			p (normal)	**<0.001**	**<0.001**	0.507	0.128	0.188
Ir1	*Cuvieronius*	26	mean	2.922	0.003	11542	0.43	0.85
			median	2.383	0.003	8558	0.39	0.76
			sd	1.502	0.002	10074	0.19	0.36
			min	0.980	0.001	262	0.18	0.42
			max	6.863	0.008	38565	1.15	2.06
			range	5.883	0.007	38303	0.97	1.64
			p (normal)	**0.006**	**0.009**	**0.006**	**<0.001**	**<0.001**
	Mammut	6	mean	1.568	0.004	20116	0.50	0.85
			median	1.806	0.004	17796	0.36	0.56
			sd	0.455	0.002	13446	0.36	0.69
			min	0.736	0.002	2165	0.19	0.39
			max	1.880	0.007	35815	1.18	2.22
			range	1.144	0.005	33650	0.99	1.83
			p (normal)	**0.020**	0.811	0.500	**0.037**	**0.004**
	Mammuthus	28	mean	2.165	0.004	19001	0.41	0.68
			median	2.131	0.003	18913	0.33	0.57
			sd	0.988	0.001	12606	0.26	0.37
			min	0.520	0.001	544	0.17	0.34
			max	4.142	0.007	55980	1.38	2.12
			range	3.622	0.006	55436	1.21	1.78
			p (normal)	0.096	0.790	0.097	**<0.001**	**<0.001**
Ir2	*Mammut*	5	mean	2.243	0.003	12480	0.38	0.72
			median	1.705	0.003	12062	0.33	0.83
			sd	1.361	0.002	2037	0.16	0.30
			min	1.229	0.001	10631	0.20	0.38
			max	4.588	0.006	15937	0.56	1.02
			range	3.359	0.005	5306	0.36	0.64
			p (normal)	**0.062**	0.295	0.157	0.299	0.236
	Mammuthus	5	mean	3.932	0.003	114780	0.39	0.90
			median	3.317	0.003	12012	0.38	0.92
			sd	2.214	0.002	2945	0.12	0.30
			min	1.863	0.001	6672	0.26	0.54
			max	6.737	0.005	14755	0.55	1.20
			range	4.874	0.004	8083	0.29	0.66
			p (normal)	0.296	0.245	0.231	0.737	0.324

Age	Taxon	n	Statistic	*Asfc*	*epLsar*	*Tfv*	*HAsfc3x3*	*HAsfc9x9*
Ra	*Cuvieronius*	23	mean	2.227	0.003	7691	0.44	0.57
			median	1.841	0.003	9594	0.41	0.70
			sd	1.389	0.001	5242	0.21	0.40
			min	0.670	0.001	181	0.17	0.39
			max	6.388	0.005	17000	0.98	1.86
			range	5.718	0.004	16819	0.81	1.47
			p (normal)	**0.009**	0.126	0.220	0.128	**0.003**
	Mammut	56	mean	2.056	0.004	10082	0.40	0.81
			median	1.403	0.004	11324	0.35	0.62
			sd	1.846	0.002	3906	0.21	0.53
			min	0.032	0.001	168	0.14	0.28
			max	11.717	0.008	16547	0.99	3.05
			range	11.685	0.007	16379	0.85	2.77
			p (normal)	0.062	0.295	0.157	0.299	0.236
	Mammuthus	69	mean	2.503	0.004	12369	0.41	0.75
			median	2.156	0.004	12210	0.38	0.71
			sd	1.387	0.002	4738	0.22	0.33
			min	0.456	0.001	739	0.16	0.33
			max	6.471	0.009	32491	1.66	2.10
			range	6.015	0.008	31752	1.50	1.77
			p (normal)	**0.001**	0.101	**<0.001**	**<0.001**	**<0.001**

n, number of individuals sampled; sd, one standard deviation (1σ); *Asfc*, area-scale fractal complexity; *epLsar*, anisotropy; *Tfv*, textural fill volume, $HAsfc_{3x3}$, $HAsfc_{9x9}$, heterogeneity of complexity in a 3x3 and 9x9 grid, respectively. Bold values indicate a non-normal distribution (Shapiro-Wilk; $p < 0.05$ is significant.

where mammoths are abundant, they may be considered keystone competitors (*sensu* Bond 1993), then mammoths should limit large herbivore abundances via monopolizing resource utilization in their local communities (Fritz 1997, Fritz et al. 2002). Bearing these assumptions in mind, we elaborate below on the evidence for interspecific competition between sympatric megaherbivores in Pleistocene North America.

Although we are unable at present to generalize beyond the ACP, our results comprise two lines of evidence that support the competitive exclusion hypothesis (as opposed to the ecological displacement hypothesis; (Dudley 1996)). First, data presented here supports the hypothesis that Columbian mammoth (*Mammuthus columbi*) and gomphothere (*Cuvieronius hyodon*) populations consumed foods of similar geochemical and textural properties

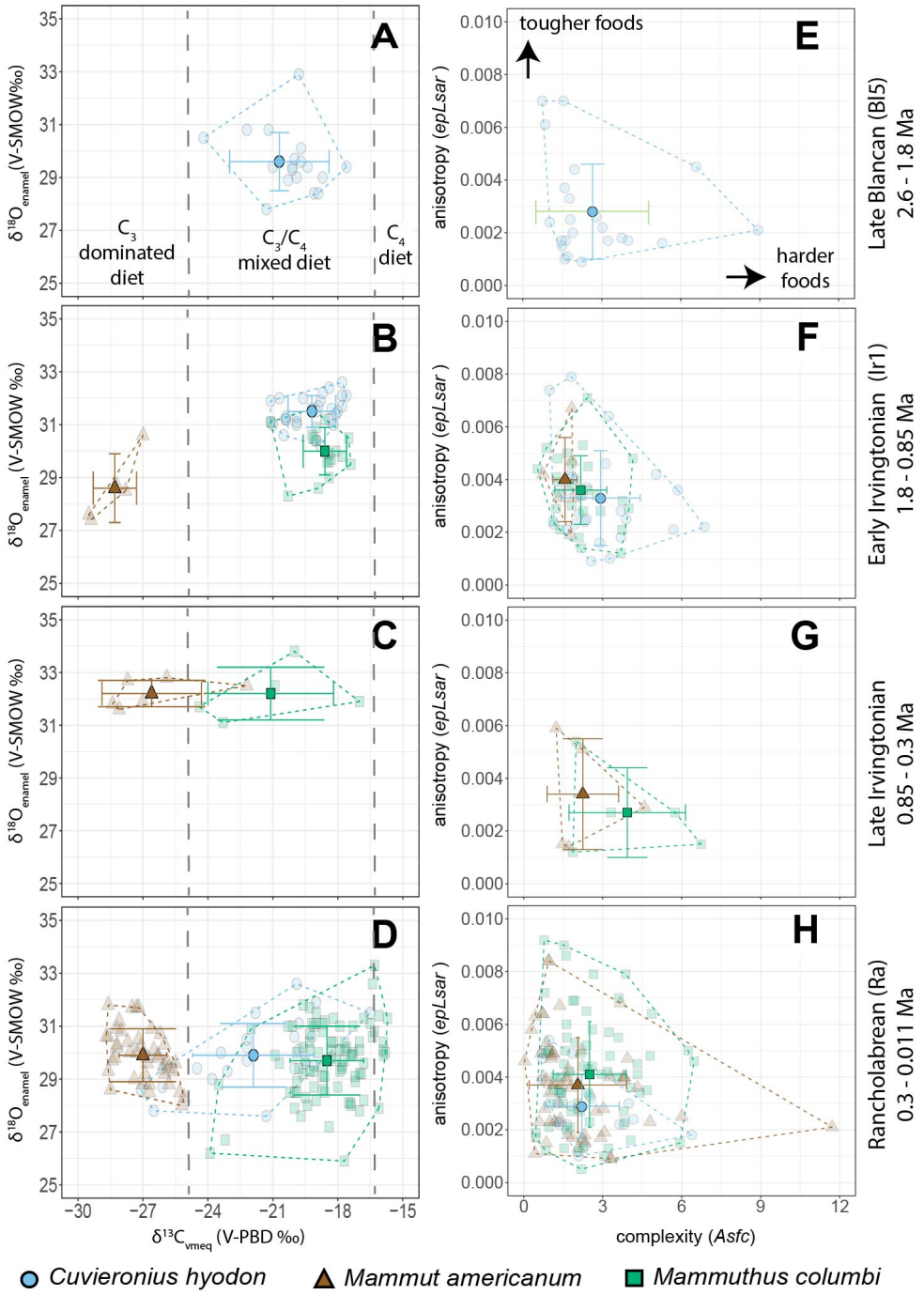

Figure 3.2: Bivariate plots of stable oxygen vs. stable carbon (A-D) and anisotropy (*epLsar*) vs. complexity (*Asfc*) (E-H) for proboscideans from the Atlantic Coastal Plain of North America. Blue circles, *Cuvieronius hyodon*; brown triangles, *Mammut americanum*; green squares, *Mammuthus columbi*. Mean values for each population are shown with error bars for the standard deviation; individual sample values are slightly transparent. Convex hulls overlay the range of values for each taxon. (A, E) Late Blancan (2.6 – 1.8 Ma) samples. (B, F) Early Irvingtonian (1.8 – 0.85 Ma) samples. (C, G) Late Irvingtonian (0.85 – 0.3 Ma) samples. (D, H) Rancholabrean (0.3 – 0.011 Ma) samples.

during the Early Irvingtonian (1.6 – 1.0 Ma), when mammoths first appear in North America. Specifically, mean $\delta^{13}C_{vmeq}$ values of -19.2‰ and -18.6‰ for gomphotheres and mammoths, respectively, indicate a predominately C_4 grazing signature supplemented with C_3 resources (Figure 3.2B, Table 3.1), while moderate *Asfc* and *epLsar* values that both have a high range similarly suggest a highly generalized mixed-feeding signature for both proboscideans (Figure 3.2F, Table 3.3). All of these proxy data (i.e., $\delta^{13}C_{vmeq}$, *Asfc*, and *epLsar*) are statistically indistinguishable for gomphotheres and mammoths. We interpret these results to show that, upon arrival in the ACP, mammoths began to exploit similar resources as the endemic gomphotheres.

All Early Irvingtonian samples in our dataset come from two assemblages from Florida – the Leisey Shell Pit Local Fauna (LSPLF) (Morgan and Hulbert 1995) and the Punta Gorda Local Fauna (PGLF) (Webb 1974). The LSPLF were deposited during an interglacial period *ca.* 1.6 – 1.0 Ma, as supported by magnetic polarity dates; strontium isotope values on marine bivalves; stratigraphic evidence of a high-stage sea level stand; vertebrate chronology, including the presence of warm-adapted vertebrates such as alligators; and ^{18}O-enriched values in mammalian herbivore enamel, consistent with a drier climate (Morgan and Hulbert 1995; DeSantis et al. 2009). Our data show no statistically significant difference in $\delta^{18}O_{enamel}$ values between LSPLF and PGLF *Cuvieronius* (mean $\delta^{18}O_{enamel}$ = 31.5‰ and 31.4‰, respectively; p = 0.867) or *Mammuthus* (mean $\delta^{18}O_{enamel}$ = 30.1‰ and 29.9‰, respectively; p = 0.534) (Table 3.2). This may indicate that a similar climatic setting was experienced by both faunas, which would support the inference by Morgan and Hulbert (1995) that the two sites are of similar ages. DeSantis et al. (2009) reported significant differences in the $^{13}C/^{12}C$ isotopic signatures of browsers (*Palaeolama*, *Tapirus*, *Mammut*, *Odocoileus*), mixed-feeders (*Mylohyus*, *Platygonus*, *Hemiauchenia*), and grazers (*Equus*, *Mammuthus*, *Cuvieronius*) of the LSPLF, but noted no significant differences when browsers were compared to one another or when grazers were compared to one another. The authors suggested that the high degree of niche partitioning among the mam-

malian community, facilitated by the abundance of C_4 grass and the diversity of C_3 dietary resources, may have contributed to the high mammalian diversity of the LSPLF (DeSantis et al. 2009). Our results corroborate this suggestion and specifically indicate that *Cuvieronius* and *Mammuthus* were able to co-exist during the Early Irvingtonian despite consuming foods of similar geochemical and textural properties. This suggests that there must have been an abundance of dietary resources in the ACP, as both proboscideans were large monogastric-caecalid grazers with high dietary resource intake requirements (Guthrie 1984). As large mammalian herbivores are primarily food-limited (Sinclair 1975) (as opposed to predator-limited; (Sinclair et al. 2003; Fritz et al. 2011)), warm climates and long growing seasons likely produced a diverse floral habitat with considerable local heterogeneity needed to support such a high abundance of closely-related and ecologically similar taxa (a 'vegetative mosaic'; (Guthrie 1984)).

The second line of evidence in support of the competitive exclusion hypothesis is niche plasticity in *Cuvieronius* populations from the ACP. While stable isotope and dental microwear data do support the hypothesis of shifting dietary habits over time, the magnitude and direction of this shift varies by taxon. *Mammut* exhibits the narrowest dietary niche of the three proboscideans, with the smallest range in $\delta^{13}C_{vmeq}$ values of all taxa in each NALMA (Table 3.1) and statistically unchanging DMTA attribute values for all NALMAs (Table 3.3, Supplemental Table 8). Further, *Mammut* $\delta^{13}C_{vmeq}$ values are consistently significantly lower than either *Cuvieronius* or *Mammuthus*, implying a persistent preference for C_3 dietary resources over time - interpreted here as woody-browse. Because of the high abundance of *Mammut* remains recovered in the ACP, our interpretation of these data is that mastodons successfully dominated the "large monogastric browser" niche up until the end-Pleistocene, even during periods of resource limitation. Similarly, *Mammuthus* $\delta^{13}C_{vmeq}$, *Asfc*, and *epLsar* values do not change significantly from the Early Irvingtonian to the Rancholabrean (Table 3.3, Supplemental Table 8), suggesting a similar dietary niche of C_4 grazing supplemented with C_3 resources of varying textural properties; thus, mammoths

are interpreted as having occupied the "large monogastric grazer" niche. Since mammoths lack a rumen (and can therefore not avoid absorbing toxic plant defenses including alkaloids and cyanogens into the bloodstream; (Guthrie 1984)), this likely would have required a diet consisting of grass as a staple and supplemented by other plant species with complementary nutrients and less toxic defenses. In contrast to mammoths and mastodons, *Cuvieronius* populations show a statistically significant decrease in $\delta^{13}C_{vmeq}$ values from the Early Irvingtonian to the Rancholabrean while more than doubling the standard deviation of mean $\delta^{13}C_{vmeq}$ values (Table 3.1, Supplemental Table 8). During the Rancholabrean, *Cuvieronius* populations in the ACP consumed a diet that was geochemically intermediate between *Mammut* and *Mammuthus* diets (Figure 3.2D) and texturally indistinguishable from either (Figure 3.2H). Rancholabrean gomphothere $\delta^{13}C_{vmeq}$ values are statistically equitable to their Late Blancan $\delta^{13}C_{vmeq}$ values (Supplemental Table 8). Our interpretation of these data is that Late Pleistocene gomphotheres in the ACP were mixed-feeding C_3/C_4 generalists (similar to the Early Pleistocene, prior to the arrival of mammoths), covering a dietary spectrum that was overlapped by mammoths on the grazing end and mastodons on the browsing end.

During the Pleistocene, rapid climate changes may have disturbed vegetative mosaics and led to floral community restructuring, resulting in periodic resource scarcity and affecting niche partitioning among large mammalian herbivores. Pleistocene glacial-interglacial dynamics became especially pronounced beginning *ca.* 70-60 ka, with the onset of 2-3 kyr warm-cool oscillations (Dansgaard-Oescher, or DO, events) punctuated by abrupt ($\sim$ 1 kyr) cool phases characterized by Heinrich events (i.e., the fracturing of ice shelves into the North Atlantic) (Heinrich 1988; Dansgaard et al. 1993; Bond and Lotti 1995; Elliot et al. 1998; Alley et al. 2003). These climatic changes likely led to phenological shifts in plant communities (e.g., earlier flowering or emergence dates) and individualistic shifts in the reproductive habits and geographic ranges of mammals, as is currently occurring in modern biota (Graham 2005; Post 2013). Further, there is evidence from a $\sim$60 kyr palyno-

logical record from South Florida that ACP pollen changes and the warming effects of DO events were out-of-sync with the rest of North America (Grimm et al. 1993, 2006; Arnold et al. 2018). Heterogeneous climatic and environmental changes in North America served to breakdown the Pleistocene vegetative mosaics that had supported the co-evolution of a high diversity of specialized groups of organisms (Graham and Lundelius 1984; Graham and Grimm 1990). As seasonal mixed-feeders, proboscideans depend on the right composition of low-quality grass and high-quality (but chemically defended) browse emerging at the right time of year (e.g., Janzen and Martin 1982; Guthrie 1984; Owen-Smith 1988; Teale and Miller 2012; Metcalfe 2017); disruption of this timing would have limited the abundance of these dietary resources at critical times, leading to increased intra- and interspecific competition.

The large body size of mammoths and mastodons may have provided these taxa with a competitive advantage over sympatric gomphotheres. *Cuvieronius hyodon* was the smallest of the three proboscidean taxa in the ACP – on average, between 57% and 68% less massive than *Mammuthus columbi* and 48% to 62% less massive than *Mammut americanum* based on volumetric estimates of body mass (Larramendi 2016). *Mammut* and *Mammuthus* were also considerably higher at the shoulder than *Cuvieronius* (Figure 3.2B) (Larramendi 2016). As a result, gomphothere populations were more likely to suffer from both interference competition and exploitative competition with mammoths and mastodons. Modern African elephants (Loxodonta africana) are known to aggressively attack and kill smaller large herbivores such as rhinoceroses, particularly when adult males enter musth (a periodic condition characterized by a sharp rise in aggressive behavior, temporin secretion, and the continuous discharge of urine) (Poole 1987; Berger and Cunningham 1998; Slotow and van Dyke 2001). Mammoths and mastodons likely engaged in similar violence; fossil evidence of the kind of male-on-male violence typical of musth includes two bull mammoths that died after their tusks became locked during combat (Agenbroad and Mead 1994) and pathologies on the mandible of the holotype of the Pacific mastodon (*Mammut*

pacificus; (Dooley et al. 2019)) consistent with tusk strikes from another bull. Additionally, Fisher (2004) has shown through examination of the dentin layers from tusks that male mammoths in the Great Lakes regularly fasted, as modern elephants do during musth. Exploitative competition was also likely; assuming dietary intake scales with body mass at a rate of $BM^{0.75}$ (according to the Jarman-Bell Principle; (Geist 1974)), mammoths and mastodons would have consumed significantly more food than gomphotheres. Using regression equations based on modern herbivores (Müller et al. 2013) and body mass estimates from Larramendi (2016), we estimate that *Mammuthus* and *Mammut* consumed roughly twice as much dry matter per day as *Cuvieronius* (49.9 ± 4.5 kg/day and 43.7 ± 4.9 kg/day for mammoths and mastodons, respectively, as compared to 23.3 kg/day in *Cuvieronius*). This may have created food scarcity during resource-limited intervals if mammoth and mastodon abundance remained high; for example, modern African elephants with large population densities have been shown to impact the foraging patterns of black rhinoceroses (*Diceros bicornis*), with rhinos switching from a diet comprised of mostly browse to one consisting of mostly grass during seasons of resource scarcity, when elephants have monopolized their food sources (Landman et al. 2013). This reduced intake of preferred foods and change in diet along the grass-browse continuum may have reduced gomphothere diet quality, causing reduced body mass and/or reduced fecundity (as has been shown to occur in modern ungulates (Simard et al. 2008; Christianson and Creel 2009)).

3.5 Conclusions

In conclusion, dietary proxy data from proboscideans indicate that the Early Pleistocene co-existence of mammoths and gomphotheres in the ACP was potentially made possible by both proboscideans exhibiting a generalist mixed-feeding dietary habit permitted by abundant resources, but that dramatic climatic and ecologic changes in the Late Pleistocene may have limited resource availability and led to increased interspecific competition. The ultimate extinction of the gomphothere family was likely due to the culmination of millions

of years of environmental turnovers and biotic stressors (competitive exclusion as well as human-gomphothere predation; (Sánchez et al. 2014)). Gomphotheres were part of a highly co-evolved ecological food web that began to experience disruption due to dramatic climatic and ecologic changes in the Late Pleistocene. The results of this study demonstrate that competition between mammoths and the gomphothere *Cuvieronius* was prevalent in the ACP of North America throughout the Pleistocene. *Cuvieronius* may have migrated into South America in the Late Pleistocene tracking a preferred environmental habitat (Mothé et al. 2017), but populations in the ACP of North America experienced heavy competition from *Mammuthus* and *Mammut* before disappearing entirely. Using multiple dietary proxies from sympatric megaherbivores, interspecific interactions including niche partitioning and competition can be inferred and here provide compelling evidence for gomphotheres being competitively excluded in North America prior to the Late Pleistocene megafaunal extinction.

Chapter 4

PALEOECOLOGY OF THE DIAMOND VALLEY LAKE LOCAL FAUNA IN SOUTHERN CALIFORNIA AS EVIDENCED BY DENTAL MESOWEAR ANALYSIS AND DENTAL MICROWEAR TEXTURE ANALYSIS

4.1 Introduction

An aim of paleoecological research is to clarify the ecological dynamics of fossil communities in order to better understand modern ecosystems. Paleoecological studies involving large herbivorous mammals ('megafauna,' i.e., mammals $\geq$ 44 kg in body mass, after Martin (1967)) are particularly informative, as the loss of these organisms resulted in a variety of ecological consequences (Johnson 2009). For example, megafauna have disproportionate impacts on biogeochemical cycling and the lateral transport of nutrients, disperse seeds and promote spatial heterogeneity in vegetation formations, create habitat for smaller animals, and ultimately shape the ecological structure and character of their communities (e.g., Naiman 1988; Jones et al. 1994; Knapp et al. 1999; Hester et al. 2006; Pringle 2008; Campos-Arceiz and Blake 2011; Wolf et al. 2013). Past megafauna played similar ecological roles (e.g., Janzen and Martin 1982; Owen-Smith 1987; Haynes 2012) and faced stressors similar to today's megafauna (Barnosky et al. 2011). It is therefore vital to document the effects of environmental change on ancient megafauna during the recent past (e.g., the Late Pleistocene).

The Diamond Valley Lake Local Fauna (DVLLF) is the largest non-asphaltic, open-environment Late Pleistocene terrestrial vertebrate assemblage known from the American southwest (Springer et al. 2009). The DVLLF is a unique assemblage with a preponderance of large herbivorous mammals, including at least two species of *Equus*, two species of *Bison*, *Camelops*, *Mammuthus*, and *Mammut* (Springer et al. 2010). The character of the fauna is something of a middle ground between the abundant *Bison* and *Equus* assemblage

at Rancho La Brea (to the northwest) and the *Camelops*-dominated localities of the Mojave Desert (to the northeast) (Figure 4.1) (Springer et al., 2010); furthermore, the DVLLF is unique in its extraordinary abundance of the chronospecies *Mammut pacificus* (Springer et al. 2010; Dooley et al. 2019) and the co-occurrence of three species of ground sloth (*Paramylodon halani*, *Megalonyx jeffersonii*, and *Nothrotheriops shastensis*) (Springer et al. 2009). The local fauna is comprised of >2500 discrete localities (Springer et al. 2010) that were collected from two contiguous valleys during the excavation of Diamond Valley Lake, the largest freshwater reservoir in southern California. Fauna collected on either end of the two valleys (∼4 miles apart) come from stratigraphic layers that have been dated via AMS on associated plant macrofossil remains and represent two distinct temporal units deposited in different geologic settings (Springer et al. 2009). The thickly-bedded lacustrine sediments of the Diamond Valley (>48.1 – 37.8 calibrated ^{14}C years (hereafter, cal ka BP)) lie to the east, and the interbedded fluvial sediments of the Domenigoni Valley (*ca*. 16.8 – 15.9 cal ka BP) lie to the west (Springer et al. 2009, 2010; Dooley et al. 2019) (Table 4.1). A pollen record for the older Diamond Valley sediments was also published (Anderson et al. 2002), although a more thorough paleobotanical analysis of the younger sediments from the Domenigoni Valley is needed.

Table 4.1: Site context for the two distinct faunal units of Diamond Valley Lake.

	Diamond Valley			**Domenigoni Valley**		
Geological Setting	Thick deposits of lacustrine organic clays			Interbedded silts and clays intercalated with coarse-grained stream channel sediments		
Conventional AMS age range	>48.1– 37.8 cal ka BP			∼16.8– 15.9 cal ka BP		
Depth below surface for AMS dates	12.5 m – 16.8 m			2.14 m – 4.31 m		
Palynological Setting	Vegetative mosaic dominated by cypress, juniper, and pines with open grasslands; comparable to lower montane forests of the local mountains today			Transition from open pine-juniper-cypress woodland to an oak-chaparral mosaic with periodic bursts of alder and pine; vegetation that locally rare today		
Paleoclimate Setting	Warm and comparatively more arid interval in southern California between HS 5 and HS 4			Transition from the warm/dry "Big Dry" to the cold/wet "Big Wet" during HS 1.		
Large Mammal Abundances	**% NISP**	**% MNI**	**% MNI-L**	**% NISP**	**% MNI**	**% MNI-L**
Bison	31%	26%	35%	16%	21%	22%
Camelops	17%	31%	25%	19%	24%	23%
Equus	20%	16%	27%	22%	22%	28%
Mammut	20%	10%	5%	22%	14%	11%
Mammuthus	<1%	<1%	2%	11%	5%	4%

% NISP, percentage of total number of identified specimens; % MNI percentage of total minimum number of individuals; % MNI-L, percentage of MNI by locality (see Springer et al., 2010 for discussion). Geological setting references: Springer et al., 2009, 2010. Palynological setting references: Diamond Valley, Anderson et al., 2002; Domenigoni Valley, Heusser, 1995, 1998; Heusser and Sirocko, 1997. Paleoclimate setting references: Diamond Valley, Glover et al., 2017; Domenigoni Valley, Oster et al., 2009, 2015a.

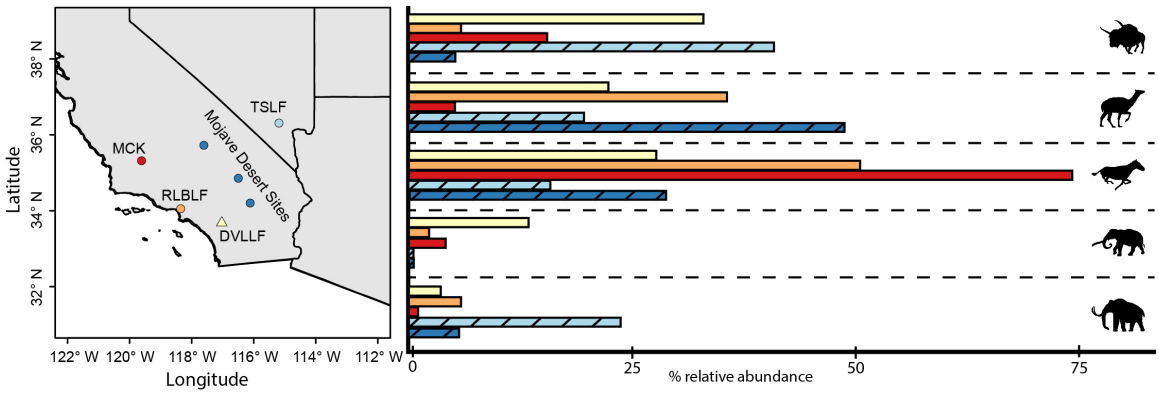

Figure 4.1: (A) Geographic setting for Diamond Valley Lake and other nearby late Pleistocene sites with a significant large mammal component. DVLLF, Diamond Valley Lake Local Fauna; RLBLF, Rancho La Brea Local Fauna; MCK, McKittrick and Maricopa Tar Seeps; TSLF, Tule Springs Local fauna. Mojave Desert Sites include (from northwest to southeast): China Lake, Twentynine Palms, and Lake Manix. (B) Percent relative abundance for (from top to bottom): *Bison*, *Camelops*, *Equus*, *Mammut*, and *Mammuthus* from each site. Percentages are relative to: minimum number of individuals (MNI) for DVLLF, RLBLF (Numbers from Springer et al., 2010, and references therein), and MCK (Torres, 1989); and number of identified specimens (NISP) for TSLF (Scott et al., 2017) and the Mojave Desert Sites (Jefferson, 2003). Silhouettes from PhyloPic.org.

The disparity in ages between the two separate valley units within the DVLLF allows the paleoecology of the fauna to be compared during two different climatic and environmental settings (Table 4.1). The Diamond Valley sediments correspond to an interval of time in between Heinrich Stadial (HS) 5 (50 – 47 ka) and HS 4 (40.2 – 38.3 ka) (Glover et al. 2017). Locally, the paleoenvironment was characterized by a mix of conifer stands (cypress, juniper, and pines) and grasslands (grasses and sedges) similar to the lower montane forests of the nearby San Bernardino Mountains today (Anderson et al. 2002). The microfossil assemblage recovered from Diamond Valley sediments suggests cooler temperatures (4° –5° C cooler than today) and is interpreted to correspond to a portion of the cooling phase of a Dansgaard-Oeschger (DO) event (Anderson et al. 2002).

In contrast, plant macrofossils from the Domenigoni Valley sediments were dated to an interval of time within HS 1 straddling the "Big Dry" (a warm and locally dry interstadial *ca.* 17.5 – 16.1 ka) and the succeeding "Big Wet" (comparatively colder and wetter *ca.* 16.1 – 15 ka) (Oster et al. 2015a). The paleoenvironment (as recorded in offshore sediment cores

from nearby Santa Barbara basin), was transitioning from an open pine-juniper-cypress woodland to the oak-chaparral mosaic of the San Bernardino Valley today (Heusser 1995, 1998; Heusser and Sirocko 1997). Additionally, periodic bursts in the abundance of alder and pine - trees that grow along streams in southern California today (Baldwin et al. 2012) - suggest brief episodes of increased rainfall in southern California (Heusser 1995, 1998), consistent with evidence of increased precipitation in the southwest as a result of a shift in the steering of westerly storms during the LGM (Oster et al. 2015b).

The co-occurrence of multiple megafauna with apparently differing dietary niches (e.g., grazers: *Equus*, *Mammuthus*, *Bison*; browsers: *Mammut*, *Camelops*; mixed feeders: *Paramylodon*) in both Diamond and Domenigoni Valley (Springer et al. 2010) suggests that some degree of niche partitioning may have facilitated the co-existence of these organisms. However, the period coinciding with the last glacial maximum (LGM, *ca.* 26.5 – 19 ka) (Clark et al. 2009) was characterized by millennial-scale changes in plant species distributions and community composition in southern California (Jiménez-Moreno et al. 2010; Millar and Woolfenden 2016). These floral community shifts may have stressed resident mammal populations, leading to an increase in competitive interactions among taxa. A preliminary study incorporating the DVLLF used stable carbon and oxygen isotopes to suggest niche partitioning facilitated the co-existence of two species of *Bison* (*B. latifrons* and *B. antiquus*) (Hardy 2015); however, the focus of that study was on spatial heterogeneity of diet in species of *Bison* and did not comment on any differences between *Bison* from the two valleys.

The overall goals of this study are to characterize the paleoecology of the megafauna in the DVLLF before and after the LGM, and to place the DVLLF into paleoenvironmental context as compared to other Late Pleistocene communities in the southwestern United States. Here, we assess the diets of five megafauna genera (*Equus*, *Bison*, *Camelops*, *Mammut*, and *Mammuthus*) using a combination of dental mesowear and dental microwear textures, which reflect the textural properties of foods consumed and can be used to infer

grazing, mixed-feeding, and browsing habits. Dietary information was subsequently used to test the following null hypotheses: 1) diets of examined megafauna are consistent over time, regardless of global/local climate change; and, 2) the paleoecological interpretation of the large mammal genera of the DVLLF is consistent with previous interpretations of these genera at other Late Pleistocene sites in the region. Accurate reconstructions of the paleoecology of mammal faunas in Late Pleistocene North America are critical to understanding mammalian response to abrupt climate change on geologic time scales.

4.2 Materials and Methods

4.2.1 Dental Microwear

All new microwear samples examined for this study were collected from the jaws and isolated teeth of *Equus*, *Bison*, *Camelops*, *Mammut*, and *Mammuthus* fossils held at the Western Science Center (WSC) in Hemet, California (Supplemental Table 9). Sampling methods for DMTA followed procedures outlined in prior studies (Jones and DeSantis 2017; Smith and DeSantis 2018). Briefly summarized here, the wear facets of molars were cleaned with acetone and then sampled using a polyvinylsiloxane dental impression material (President's Jet, Coltene-Whaledent Corp., Alstatten, Switzerland) to create a mold. The molds were reinforced with a polyvinylsiloxane dental putty to prevent leakage and cast using a high-resolution epoxy (Epotek 301, Epoxy Technologies Corp., Billerica, MA, USA) at Vanderbilt University. The exact replica casts were left to harden in a fume hood for at least 72 hours prior to being scanned.

All specimens were scanned in three dimensions in four adjacent fields of view for a total sampled area of 204 x 276 μm^2 using the Plu NEOX white-light microscope with confocal capabilities at Vanderbilt University. For ungulates, the lingual enamel area of the paracone was scanned as it is the most representative of diet in living ungulates (Valli et al. 2012). For proboscideans, we prioritized sampling the central enamel band to maintain

consistency with past studies of DMTA in proboscideans (Zhang et al. 2017; Green et al. 2017; Smith and DeSantis 2018) and because sampling these areas reduces the amount of variation in microwear features attributable to differences in the direction of the power stroke during mastication (e.g., Laub 1996; Todd et al. 2007; von Koenigswald 2016). Scans were analyzed using scale sensitive fractal analysis (SSFA) software (ToothFrax and SFrax, Surfract Corporation, www.surfract.com), which characterizes wear surfaces according to the DMTA attributes described above: complexity (*Asfc*), anisotropy (*epLsar*), textural fill volume (*Tfv*), and heterogeneity of complexity (*HAsfc*). We report heterogeneity at two scales, 3 x 3 ($HAsfc_{3x3}$) and 9 x 9 ($HAsfc_{9x9}$), as has been the practice in previous studies (e.g., Jones and DeSantis 2017; Smith and DeSantis 2018). Each reported attribute value for each specimen is the median value of that attribute for the four adjacent fields of view (Supplemental Table 9).

4.2.2 Dental Mesowear

Dental mesowear measurements were collected from the premolars and molars of *Equus*, *Bison*, and *Camelops* fossils from the DVLLF. All specimens were photographed in buccal view using a high resolution using a Canon EOS Rebel T6 DSLR camera. We chose only those specimens with at least one unbroken cusp and with a moderate degree of wear (i.e., neither unworn nor completely worn down to the root). We prioritized photographing the M^2 for ungulates as these are preferable for dental mesowear analysis (Fortelius and Solounias 2000); however, we included P^4-M^3 increase sample sizes and because mesowear values from these teeth are not statistically significantly different from the M^2s in extant taxa (Kaiser and Solounias 2003). In total, we sampled 7 specimens of *Bison*, 9 specimens of *Camelops*, and 21 specimens of *Equus*. Although it was originally suggested that a minimum sample size of 10 was required to obtain a robust mesowear signal (Fortelius and Solounias 2000; Kaiser et al. 2000), a later study suggested that smaller sample sizes are sufficient to offer insights into paleodiet and paleoecology (Bernor et al. 2014), and many

studies since then have presented mesowear results for extinct populations using sample sizes of less than 10 (e.g., Danowitz et al. 2016; Díaz-Sibaja et al. 2018; Mihlbachler et al. 2018).

We conducted mesowear analysis on all ungulate specimens using these photographs. Following recommendations made by Loffredo and DeSantis (2014), five different observers were asked to assign each tooth a cusp shape (CS) value (sharp, round, or blunt), an occlusal relief (OR) value (high or low), and an overall mesowear numerical score (MNS), as done in prior studies (e.g., Mihlbachler et al. 2011; Loffredo and DeSantis 2014; Jones and DeSantis 2017). The observers ranged in experience level and familiarity with paleontological material, but were each provided with a PowerPoint file with images of each tooth cusp and instructions for how to score CS, OR, and MNS values. In addition to an image of the cusp, each PowerPoint slide contains the reference scales in Figure 4.2 (adapted from Mihlbachler et al. 2011 and Kaiser and Solounias 2003) and the genus, catalog number, and tooth position for the sample. Observers worked independently to score teeth and were instructed to score only the sharper cusp when conducting their analysis; this cusp was clearly identified on each image. We assigned numeric values to CS (1 = sharp, 0.5 = round, 0 = blunt) and to OR (1 = high, 0 = low) to allow for statistical comparisons. For each observer, CS and OR values were transformed to univariate MWS values following Kaiser et al. (2009): 0 for high and sharp cusps; 1 for high and rounded cusps; 2 for low and sharp cusps; 3 for low and rounded cusps; and, 4 for low and blunt cusps (Supplemental Table 10).

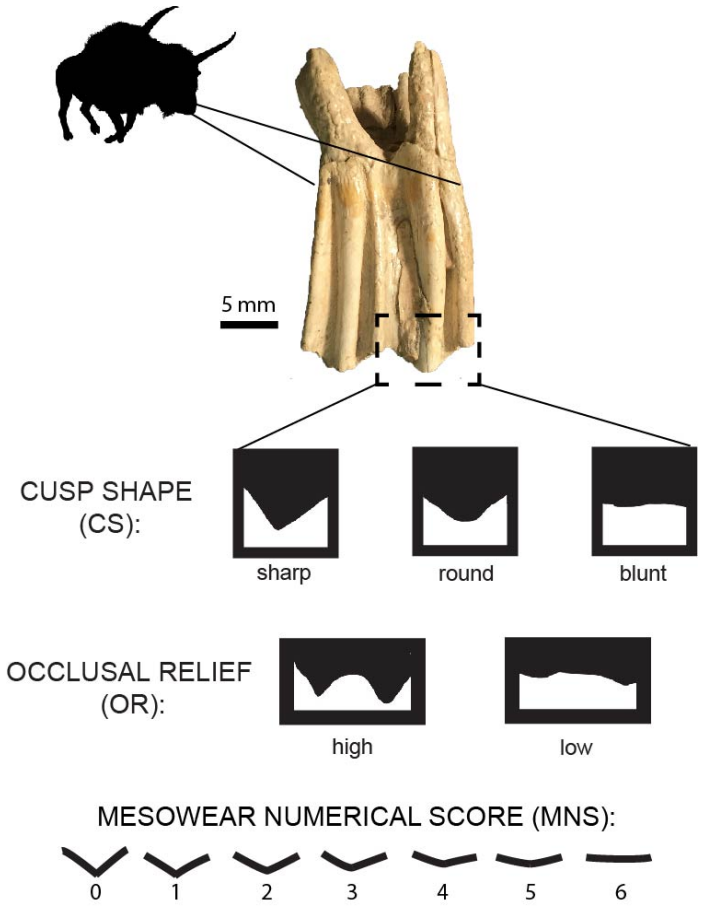

Figure 4.2: Visual summaries of the comparative scales used for mesowear analysis in ungulates. Modified from Kaiser and Solounias (2003) and Mihlbachler et al. (2011). *Bison* silhouette from PhyloPic.org.

4.2.3 Statistical Analysis

We computed summary statistics of all DMTA attributes for all taxa from the Domenigoni Valley and Diamond Valley (Table 4.2). Shapiro-Wilks tests were run to confirm whether DMTA data were non-normally distributed (Table 4.2). Non-parametric Mann-Whitney U tests were used to compare DMTA data when at least one sample was non-normally distributed; otherwise, parametric t-tests were used to compare samples between the same taxa in different time periods (Supplemental Table 11) and between different taxa in the DVLLF as a whole (Supplemental Table 12). We also compared our results to published DMTA data for *Bison*, *Equus* and *Camelops* from the nearby Rancho La Brea Local Fauna

(RLBLF) (Table 4.3) and to DMTA data for *Mammut* and *Mammuthus* from disparate environmental settings (e.g., boreal spruce forest, cypress-dominated swamp, open pine parkland, and closed coniferous forest) (Jones and DeSantis 2017; Green et al. 2017; Smith and DeSantis 2018). These data were scanned on the same confocal microscope at Vanderbilt University and should thus minimize inter-microscope variability (Arman et al. 2016). Statistical comparisons were made using non-parametric or parametric tests, where appropriate (Supplemental Table 13).

For mesowear summary statistics, we calculated the mean, standard deviation, and standard error of the mean for CS, OR, MWS, and MNS values for each specimen assigned by the five observers (Table 4.4). As sample sizes, and thus the likelihood of a normal distribution, were low, we used non-parametric tests to compare MWS and MNS values in *Bison*, *Camelops*, and *Equus* between the Diamond and Domenigoni Valleys (i.e., time-dependent) (Supplemental Table 11) as well as for the DVLLF ungulates as a whole (i.e., time-independent) (Supplemental Table 12). We also compared our results to published mesowear values for RLBLF *Bison*, *Equus* and *Camelops* (Jones and DeSantis 2017) (Table 4.5) using non-parametric tests (Supplemental Table 13).

We employed Spearman Rank correlation tests to assess the degree of congruence between dental mesowear variables and dental microwear attributes. We compared MNS and MWS values to DMTA attribute values (*Asfc*, *epLsar*, *Tfv*, $HAsfc_{3x3}$, $HAsfc_{9x9}$) for each taxon in the Domenigoni and Diamond Valleys. P-values <0.05 were considered statistically significant.

4.3 Results

4.3.1 Dental Microwear

Diamond Valley *Bison* has significantly higher *epLsar* values than Domenigoni Valley *Bison*, while Diamond Valley *Equus* has significantly lower *Asfc* values than Domenigoni Valley *Equus* (Table 4.2, Figure 4.3). All other differences in microwear attributes between taxa from the two valleys are non-significant (all $p > 0.05$, Supplemental Table 11).

When examining the DVLLF as a whole (i.e., time-independent), *Mammut* has significantly lower *Asfc* and *Tfv* values than all other taxa and *Camelops* has significantly lower *epLsar* values than all other taxa (Supplemental Table 12, Figure 4.4A). *Bison* has significantly lower *Tfv* values than *Camelops* and *Equus*, significantly higher *Tfv* values than *Mammut*, and is indistinguishable from *Mammuthus* in *Tfv* values (Table 4.3, Supplemental Table 12). *Camelops* and *Equus* are indistinguishable from one another in *Tfv* values but both have significantly higher *Tfv* values than either *Mammut* or *Mammuthus* (Table 4.3, Supplemental Table 12). *Mammuthus Tfv* values are significantly lower than *Camelops* and *Equus* and significantly higher than *Mammut*. All other comparisons are non-significant (all $p > 0.05$, Supplemental Table 12).

DVLLF *Equus* has significantly higher *epLsar* values than RLBLF *Equus* (Table 4.3, Supplemental Table 13). Additionally, *Bison* and *Equus* from the DVLLF both have significantly higher heterogeneity values (both $HAsfc_{3x3}$ and $HAsfc_{9x9}$) than their RLBLF counterparts (Table 4.3, Supplemental Table 13).

Table 4.2: DMTA summary statistics for all taxa analyzed from the Diamond Valley Lake Local Fauna.

Taxon	**n**	**Statistic**	***Asfc***	***epLsar***	***Tfv***	***HAsfc$_{3x3}$***	***HAsfc$_{9x9}$***
Bison	18	mean	3.455	0.005	12853	0.35	0.63
Diamond		median	2.732	0.006	12376	0.31	0.50
		sd	2.090	0.002	1597	0.16	0.28
		min	1.732	0.002	10908	0.15	0.34
		max	9.319	0.007	16715	0.62	1.16
		range	7.587	0.005	5807	0.47	0.82
		p (normality)	**0.002**	0.091	0.095	0.248	0.071
Bison	15	mean	4.462	0.003	12890	0.30	0.55
Domenigoni		median	3.188	0.003	13115	0.24	0.47
		sd	3.560	0.001	1669	0.16	0.21
		min	2.531	0.002	9952	0.15	0.33
		max	14.271	0.005	15863	0.69	0.98
		range	11.740	0.003	5912	0.54	0.65
		p (normality)	<**0.001**	0.866	0.998	**0.009**	0.160
Camelops	12	mean	5.349	0.002	14065	0.38	0.70
Diamond		median	5.984	0.002	14662	0.36	0.61
		sd	2.498	0.001	3193	0.14	0.25
		min	1.655	0.001	7324	0.20	0.48
		max	8.448	0.004	16748	0.59	1.09
		range	6.793	0.003	9423	0.39	0.60
		p (normality)	0.697	0.124	**0.031**	0.505	**0.043**
Camelops	8	mean	4.402	0.003	13974	0.28	0.53
Domenigoni		median	4.677	0.003	14734	0.26	0.49
		sd	1.861	0.001	2584	0.08	0.16
		min	2.113	0.001	8862	0.19	0.35
		max	6.411	0.004	16214	0.39	0.75
		range	4.298	0.003	7352	0.20	0.40
		p (normality)	0.226	0.174	**0.009**	0.542	0.453
Equus	21	mean	3.302	0.005	14067	0.37	0.65
Diamond		median	3.234	0.005	14490	0.35	0.67
		sd	1.419	0.002	2533	0.13	0.18
		min	1.554	0.002	7614	0.22	0.38
		max	6.836	0.008	17753	0.76	1.01
		range	5.282	0.006	10140	0.55	0.63
		p (normality)	0.268	0.320	0.339	**0.010**	0.727
Equus	18	mean	4.871	0.004	14433	0.37	0.70
Domenigoni		median	4.345	0.003	14173	0.34	0.66
		sd	1.565	0.002	1258	0.12	0.24
		min	2.771	0.001	11969	0.23	0.38
		max	7.776	0.007	16937	0.64	1.33
		range	5.005	0.006	4968	0.42	0.95
		p (normality)	0.275	0.939	0.916	0.126	0.053

Taxon	**n**	**Statistic**	***Asfc***	***epLsar***	***Tfv***	***HAsfc$_{3x3}$***	***HAsfc$_{9x9}$***
Mammut	8	mean	2.935	0.004	10754	0.39	0.71
Diamond		median	2.707	0.004	10553	0.29	0.62
		sd	1.323	0.001	4253	0.24	0.34
		min	1.659	0.002	4565	0.24	0.47
		max	4.562	0.006	17365	0.86	1.37
		range	2.903	0.004	12800	0.63	0.90
		p (normality)	0.121	0.568	0.926	**0.003**	**0.011**
Mammut	20	mean	2.486	0.003	10109	0.34	0.64
Domenigoni		median	2.125	0.004	9958	0.30	0.58
		sd	1.019	0.002	3664	0.16	0.22
		min	1.281	0.001	4402	0.17	0.41
		max	4.854	0.007	18353	0.79	1.30
		range	3.573	0.006	13951	0.62	0.89
		p (normality)	0.072	0.780	0.475	**0.004**	**<0.001**
Mammuthus	3	mean	6.967	0.003	13613	0.30	0.54
Diamond		median	6.967	0.003	13613	0.30	0.54
		sd	5.141	0.002	291	0.04	0.07
		min	3.332	0.002	13407	0.27	0.49
		max	10.603	0.005	13819	0.33	0.58
		range	7.271	0.003	412	0.06	0.10
		p (normality)	**n/a**	**n/a**	**n/a**	**n/a**	**n/a**
Mammuthus	8	mean	5.705	0.004	12331	0.4	0.79
Domenigoni		median	5.236	0.004	11724	0.45	0.67
		sd	3.399	0.002	1798	0.11	0.31
		min	1.767	0.002	10541	0.27	0.47
		max	10.424	0.008	14691	0.53	1.16
		range	8.657	0.006	4150	0.26	0.68
		p (normality)	0.345	0.198	0.086	0.098	0.070

n, number of individuals sampled; sd, one standard deviation (1σ); *Asfc*, area-scale fractal complexity; *epLsar*, *anisotropy*; *Tfv*, textural fill volume, *HAsfc$_{3x3}$*, *HAsfc$_{9x9}$*, heterogeneity of complexity in a 3x3 and 9x9 grid, respectively. Bold values indicate a non-normal distribution (Shapiro-Wilk; $p < 0.05$ is significant; n/a, sample size too small for a reliable p-value estimate).

Table 4.3: DMTA summary statistics for all taxa analyzed from Southern California.

Taxon	**n**	**Statistic**	***Asfc***	***epLsar***	***Tfv***	***HAsfc$_{3x3}$***	***HAsfc$_{9x9}$***
Bison	33	mean	3.913	0.004	12870	0.33	0.59
DVLLF		median	2.828	0.004	12615	0.27	0.49
		sd	2.825	0.002	1591	0.16	0.25
		min	1.732	0.002	9952	0.15	0.33
		max	14.271	0.007	16715	0.69	1.16
		range	12.539	0.005	6763	0.54	0.83
		p (normality)	<**0.001**	0.139	0.612	**0.014**	**0.008**
Bison	44	mean	2.962	0.003	13451	0.53	0.91
RLBLF		median	2.364	0.003	13303	0.50	0.80
		sd	1.696	0.001	1548	0.25	0.40
		min	0.91	0.001	9324	0.17	0.31
		max	8.454	0.007	16634	1.24	1.99
		range	7.544	0.006	7310	1.07	1.68
		p (normality)	<**0.001**	0.066	0.787	**0.023**	**0.005**
Bison	77	mean	3.279	0.004	13257	0.46	0.81
So. Cal.		median	2.652	0.003	13103	0.41	0.72
		sd	2.165	0.002	1575	0.24	0.38
		min	0.91	0.001	9324	0.15	0.31
		max	14.271	0.007	16715	1.24	1.99
		range	13.361	0.006	7391	1.09	1.68
		p (normality)	<**0.001**	**0.003**	0.810	<**0.001**	<**0.001**
Camelops	20	mean	4.912	0.002	14023	0.33	0.62
DVLLF		median	5.786	0.002	14662	0.31	0.54
		sd	2.192	0.001	2807	0.13	0.23
		min	1.655	0.001	7324	0.19	0.35
		max	8.448	0.004	16748	0.59	1.09
		range	6.793	0.003	9423	0.40	0.74
		p (normality)	0.484	0.060	**0.003**	0.120	0.089
Camelops	43	mean	3.963	0.003	13251	0.54	0.96
RLBLF		median	2.843	0.003	13644	0.45	0.80
		sd	3.109	0.002	2637	0.31	0.50
		min	1.106	0.000	3587	0.18	0.36
		max	13.625	0.008	16650	1.81	2.62
		range	12.519	0.008	13063	1.64	2.26
		p (normality)	<**0.001**	**0.008**	**<0.001**	<**0.001**	<**0.001**
Camelops	63	mean	4.184	0.003	13430	0.49	0.88
So. Cal.		median	2.966	0.003	13899	0.41	0.73
		sd	2.931	0.002	2671	0.29	0.47
		min	1.106	0.00	3587	0.18	0.35
		max	13.625	0.008	16748	1.81	2.62
		range	12.519	0.008	13161	1.64	2.27
		p (normality)	<**0.001**	<**0.001**	<**0.001**	<**0.001**	<**0.001**

Taxon	n	Statistic	*Asfc*	*epLsar*	*Tfv*	*HAsfc$_{3x3}$*	*HAsfc$_{9x9}$*
Equus	39	mean	3.982	0.004	14226	0.37	0.67
DVLLF		median	3.671	0.005	14476	0.35	0.66
		sd	1.658	0.002	2057	0.13	0.20
		min	1.554	0.001	7614	0.22	0.38
		max	7.776	0.008	17753	0.76	1.33
		range	6.222	0.007	10140	0.55	0.95
		p (normality)	0.152	0.188	0.072	**0.003**	0.053
Equus	33	mean	3.763	0.003	13968	0.49	0.87
RLBLF		median	3.359	0.003	13883	0.47	0.83
		sd	1.83	0.002	1847	0.19	0.29
		min	0.901	0.001	10193	0.18	0.43
		max	7.823	0.007	18047	1.13	1.62
		range	6.922	0.006	7854	0.95	1.19
		p (normality)	0.139	**0.018**	0.988	**0.002**	0.151
Equus	72	mean	3.867	0.004	14091	0.43	0.78
So. Cal.		median	3.509	0.003	14173	0.39	0.75
		sd	1.74	0.002	1938	0.17	0.27
		min	0.901	0.001	7614	0.18	0.38
		max	7.823	0.008	18047	1.13	1.62
		range	6.922	0.007	10433	0.95	1.24
		p (normality)	**0.027**	**0.004**	0.390	<**0.001**	**0.002**
Mammut	29	mean	2.603	0.004	10277	0.35	0.66
DVLLF		median	2.125	0.004	10466	0.30	0.59
		sd	1.093	0.002	3736	0.18	0.25
		min	1.281	0.001	4402	0.17	0.41
		max	4.854	0.007	18353	0.86	1.37
		range	3.573	0.006	13951	0.69	0.96
		p (normality)	**0.017**	0.450	0.573	<**0.001**	<**0.001**
Mammuthus	11	mean	5.985	0.004	12616	0.38	0.73
DVLLF		median	5.236	0.004	13407	0.33	0.58
		sd	3.504	0.002	1660	0.11	0.29
		min	1.767	0.002	10541	0.27	0.47
		max	10.603	0.008	14691	0.53	1.16
		range	8.836	0.006	4150	0.26	0.68
		p (normality)	0.118	0.119	0.072	0.061	**0.015**

n, number of individuals sampled; sd, one standard deviation (1σ); *Asfc*, area-scale fractal complexity; *epLsar*, anisotropy; *Tfv*, textural fill volume, *HAsfc$_{3x3}$*, *HAsfc$_{9x9}$*, heterogeneity of complexity in a 3x3 and 9x9 grid, respectively. Bold values indicate a non-normal distribution (Shapiro-Wilk; $p < 0.05$ is significant. RLBLF data are from Jones and DeSantis (2017).

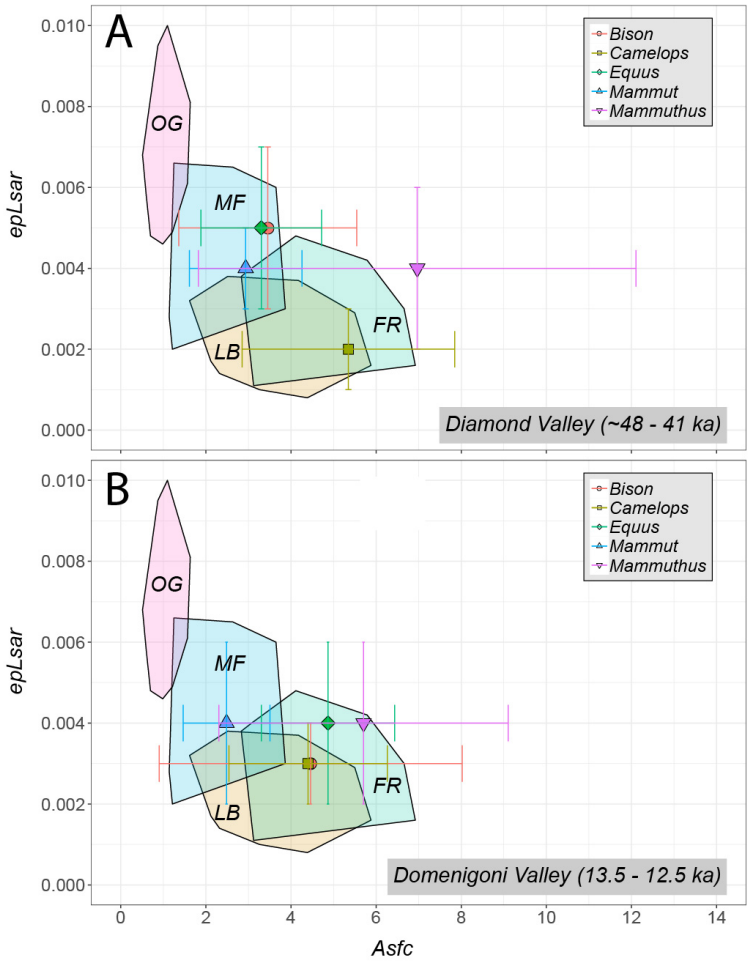

Figure 4.3: Means (filled circles) and standard deviations (horizontal and vertical bars) of anisotropy (*epLsar*) and complexity (*Asfc*) values for DVLLF taxa in relation to Gaussian confidence ellipses (p = 0.95) on the centroid for extant bovid obligate grazers (OG), mixed feeders (MF), leaf browsers (LB), and frugivores (FR) (bovid data from Scott 2012 and DeSantis et al. 2013). (A) Diamond Valley specimens. (B) Domenigoni Valley specimens.

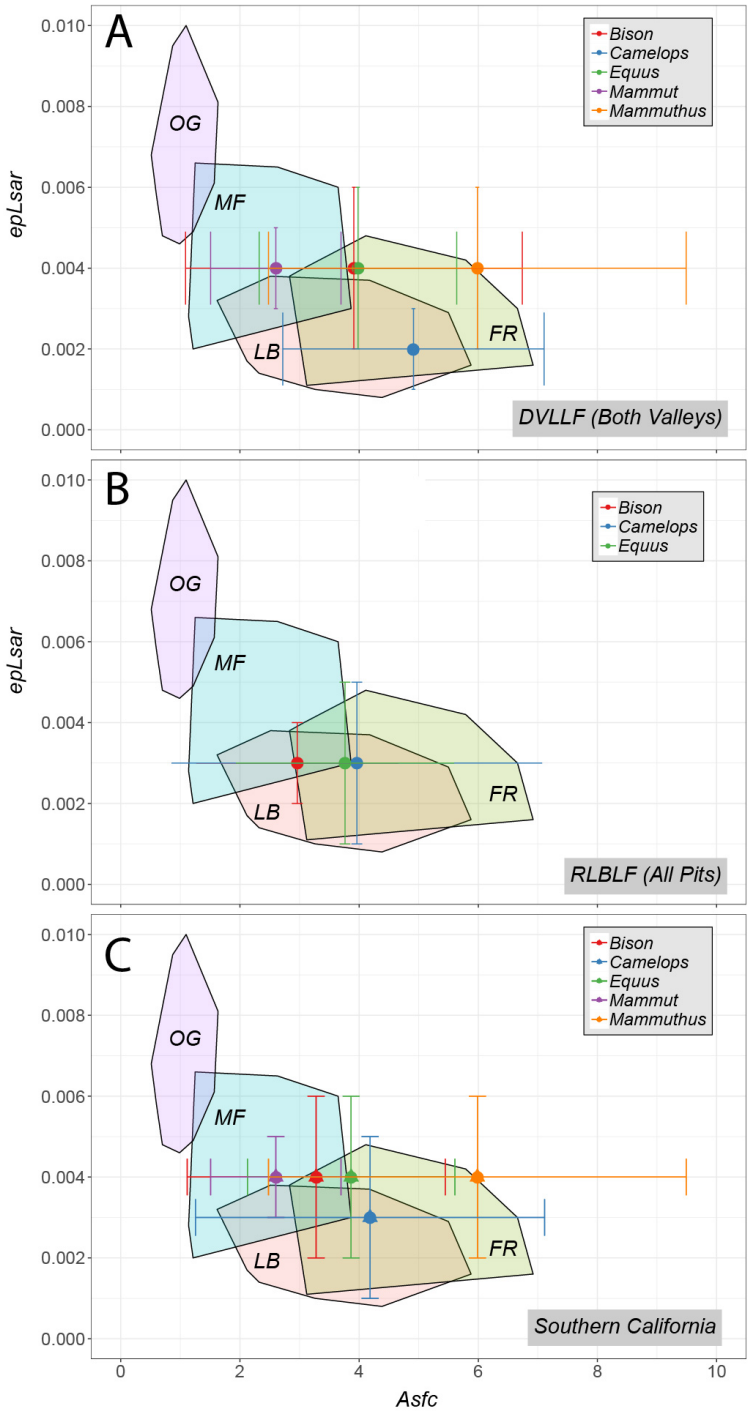

Figure 4.4: Means (filled circles) and standard deviations (horizontal and vertical bars) of anisotropy (*epLsar*) and complexity (*Asfc*) values for Southern California taxa in relation to Gaussian confidence ellipses (p = 0.95) on the centroid for extant bovid obligate grazers (OG), mixed feeders (MF), leaf browsers (LB), and frugivores (FR) (bovid data from Scott 2012 and DeSantis et al. 2013). (A) Diamond Valley Lake Local Fauna specimens. (B) Rancho La Brea Local Fauna specimens (data from Jones and DeSantis 2017). (C) DVLLF and RLBLF specimen data pooled.

Table 4.4: Summary of dental mesowear attributes for DVLLF ungulates.

Taxon	n	Statistic	Cusp Shape (CS)	Occlusal Relief (OR)	MWS	MNS
Bison	4	mean	0.6	0.8	1.3	2.3
Diamond		sd	0.2	0.5	1.4	1.7
		sem	0.1	0.2	0.7	0.9
Bison	3	mean	0.3	0.6	2.1	3.7
Domenigoni		sd	0.3	0.5	1.6	1.6
		sem	0.1	0.2	0.7	0.9
Camelops	6	mean	0.7	0.5	1.7	2.8
Diamond		sd	0.2	0.5	1.4	1.5
		sem	0.1	0.2	0.6	0.6
Camelops	3	mean	0.7	0.3	2.0	3.7
Domenigoni		sd	0.2	0.3	1.0	0.9
		sem	0.1	0.2	0.6	0.5
Equus	11	mean	0.3	0.1	3.2	4.9
Diamond		sd	0.2	0.2	0.6	0.7
		sem	0.1	0.1	0.2	0.2
Equus	10	mean	0.4	0.3	2.8	4.3
Domenigoni		sd	0.3	0.4	1.2	1.0
		sem	0.1	0.1	0.4	0.3

n, number of specimens; sd, one standard deviation (1σ); sem, standard error of the mean; MWS, mesowear univariate scale (0-4); MNS, mesowear numerical score (0-6).

4.3.2 Dental Mesowear

There are no statistically significant differences in mesowear signatures between any ungulate taxa from the Diamond Valley and Domenigoni Valleys (Supplemental Table 11, Figure 4.5). When examining the mesowear signatures for the DVLLF as a whole (i.e., time-independent), *Equus* has significantly higher MWS and MNS values than *Camelops* and significantly higher MNS values than *Bison* (Table 4.5, Supplemental Table 12). *Bison* and *Camelops* mesowear scores are indistinguishable from one another in all comparisons (all $p > 0.05$).

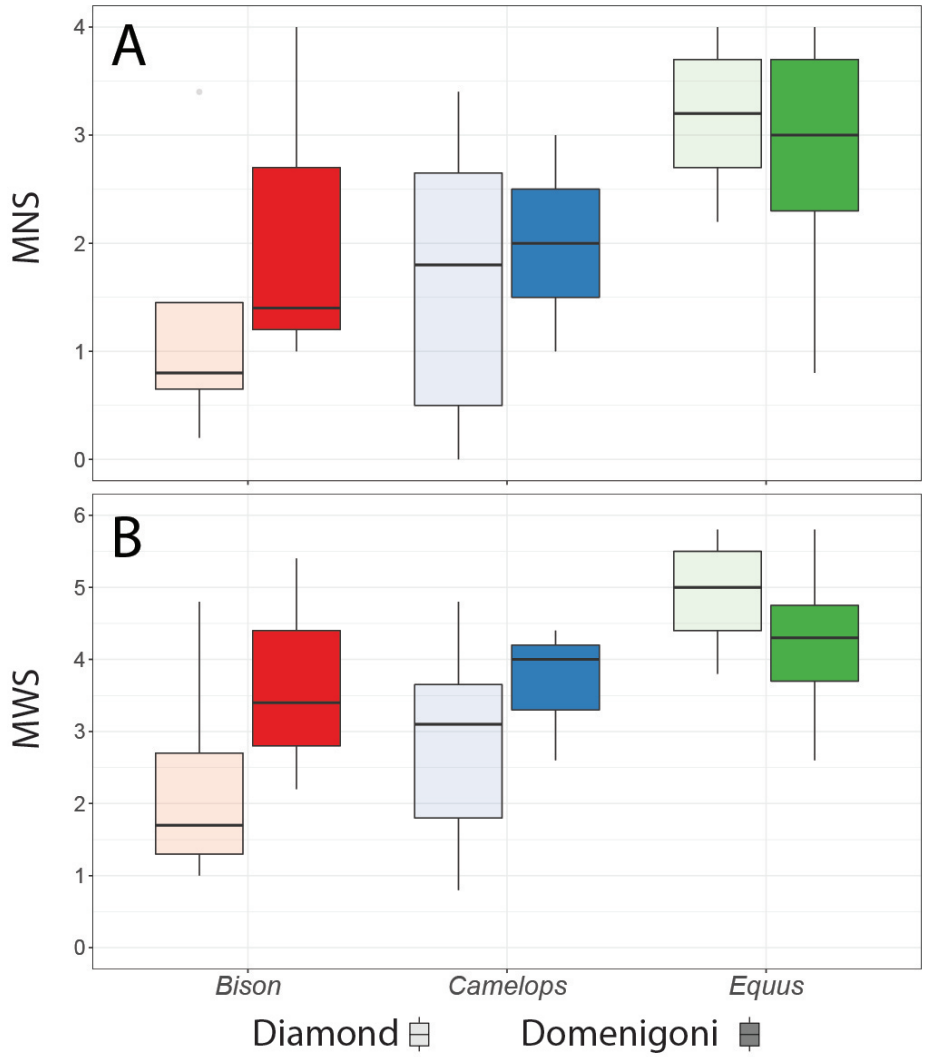

Figure 4.5: Box and whisker plots for Diamond Valley specimens (translucent) and Domenigoni Valley specimens (opaque). (A) MNS values. (B) MWS values.

Compared to their RLBLF counterparts, *Equus* from DVLLF have significantly lower MNS and MWS scores and *Camelops* from DVLLF have significantly higher MNS and MWS values (Table 4.5, Supplemental Table 12, Figure 4.6). There are no significant differences between DVLLF and RLBLF *Bison* for any mesowear variables (all $p > 0.546$).

Table 4.5: Summary of dental mesowear attributes for all taxa analyzed from Southern California.

Taxon	n	Statistic	Cusp Shape (CS)	Occlusal Relief (OR)	MWS	MNS
Bison	7	mean	0.5	0.7	1.7	2.9
DVLLF		sd	0.3	0.5	1.5	1.7
		sem	0.1	0.2	0.5	0.6
Bison	33	mean	0.6	0.7	1.4	2.3
RLBLF		sd	0.2	0.3	0.8	1.0
		sem	0.0	0.0	0.1	0.2
Bison	40	mean	0.6	0.7	1.5	2.4
So. Cal.		sd	0.2	0.3	1.0	1.2
		sem	0.0	0.0	0.2	0.2
Camelops	9	mean	0.7	0.4	1.8	3.1
DVLLF		sd	0.2	0.4	1.2	1.3
		sem	0.1	0.1	0.4	0.4
Camelops	23	mean	0.7	0.7	1.2	2.1
RLBLF		sd	0.2	0.3	1.0	1.0
		sem	0.0	0.0	0.2	0.2
Camelops	32	mean	0.7	0.6	1.3	2.4
So. Cal.		sd	0.2	0.4	1.1	1.2
		sem	0.0	0.1	0.2	0.2
Equus	21	mean	0.3	0.2	3.0	4.6
DVLLF		sd	0.2	0.3	0.9	0.9
		sem	0.1	0.1	0.2	0.2
Equus	24	mean	0.2	0.4	3.6	5.0
RLBLF		sd	0.2	0.2	0.6	1.0
		sem	0.0	0.0	0.1	0.2
Equus	45	mean	0.2	0.1	3.3	4.8
So. Cal.		sd	0.2	0.3	0.8	1.0
		sem	0.0	0.0	0.1	0.1

n, number of specimens; sd, one standard deviation (1σ); sem, standard error of the mean; MWS, mesowear univariate scale (0-4); MNS, mesowear numerical score (0-6).

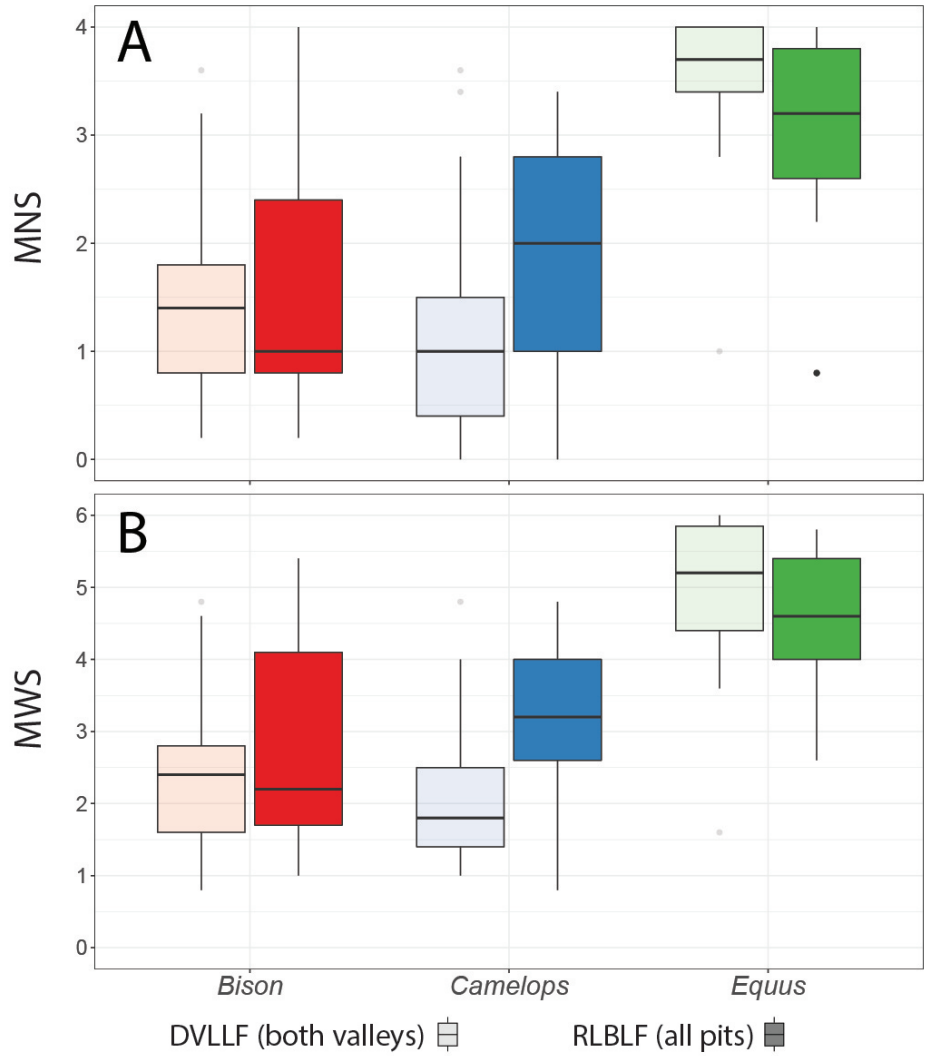

Figure 4.6: Box and whisker plots for Diamond Valley Lake specimens (translucent) and Rancho La Brea specimens (opaque). (A) MNS values. (B) MWS values.

4.3.3 Microwear - Mesowear Congruence

As we are primarily interested in the degree to which the two proxy methods correlate with one another, we do not compare microwear attributes to one another or mesowear attributes to one another. We compared all DMTA attributes to mesowear MNS and MWS values for *Bison*, *Camelops*, and *Equus* from the Domenigoni Valley unit and the Diamond Valley unit. For all comparisons, there are no significant correlations between any DMTA attributes and dental mesowear variables (all $p > 0.102$).

4.4 Discussion

4.4.1 Paleoecology of DVLLF herbivores before and after the LGM

The dietary interpretation of the large mammal fauna from the older Diamond Valley sediments (>48.1 – 37.8 cal ka BP) is broadly consistent with the dietary interpretation of these fauna from the younger Domenigoni Valley sediments (*ca.* 16.8 – 15.9 cal ka BP), although there are some key differences. Notably, DMTA data document a significant decrease in *epLsar* values in *Bison* and a significant increase in *Asfc* values in *Equus*, suggesting a relative decrease in tough foods (i.e., grass) in *Bison* diets and an increase in hard foods (i.e., woody browse) in horse diets over time (Figure 4.3). In contrast, neither DMTA data nor dental mesowear data suggest significant changes in the dietary ecology of *Camelops*, *Mammut*, or *Mammuthus* before and after the LGM. There are no statistically significant changes in mesowear scores (MWS and MNS) for any ungulate taxa when comparing the Diamond Valley unit to the Domenigoni Valley unit (i.e., all p-values > 0.05, Supplemental Table 12). Collectively, these data suggest that while the dietary preferences of *Bison* and horses may have changed during the last few days to weeks of their lives (as evidenced by significant changes in *eplsar* and *Asfc*, respectively), the average lifetime dietary habits of DVLLF ungulates (as recorded by mesowear signatures) did not.

The shift in microwear signatures in the DVLLF grazers (*Bison* and horses) over time suggests a decrease in grass consumption in populations occupying the intermontane basins of southern California. Palynological data from the Diamond Valley sediments support the presence of a nearby grassland habitat *ca.* 42.7 $\pm$ 1.8 cal ka BP, with an average pollen percentage of $\sim$10% Poaceae (grasses) and $\sim$15- 20% Cyperaceae (sedges) throughout the record (Anderson et al. 2002) and a similar range of fossil pollen samples as is found in modern samples from grassland communities west of Mt. San Jacinto (Anderson and Koehler 2003). A shallow-water lake setting existed at this time, with evidence including: an abundance of pollen from sedges, which tend to prefer growing in wet environ-

ments; the presence of warm water, epiphytic, and low-energy adapted diatoms (Anderson et al. 2002); and, an organic clay-rich lacustrine sedimentary record (Springer et al. 2009). Moderate-to-high *epLsar* values in *Bison*, horses, and mammoths from the Diamond Valley sediments (Figure 4.3A) support an interpretation of these grazing-adapted taxa consuming a diet rich in the non-woody grasses and sedges that would have grown around the lake margin. By contrast, a statistically significant decrease in Domenigoni Valley *Bison epLsar* values is counterintuitive, as grass and sedge abundance in inland southern California remains relatively consistent from ∼40 ka to ∼13 ka (Heusser, 1998). Domenigoni Valley *Equus* and *Bison Asfc* values are moderately high and suggest the consumption of hard foods such as seed pits or woody browse (Figure 4.3B). Millennial-scale shifts in temperature and precipitation amount in southern California during HS 1 (Oster et al. 2015a; Glover et al. 2017) may have promoted the increase in chaparral and oak as well as the periodic bursts in pines and alders observed in sediments coeval with the Domenigoni Valley unit (Heusser 1995, 1998; Heusser and Sirocko 1997). The resultant spread of low-growing heathland (similar to vegetation found in the California interior chaparral and woodlands ecoregion today; Baldwin et al. 2012) likely provided abundant woody forage for the large mammal fauna occupying the region surrounding the Domenigoni Valley.

Microwear and mesowear data support the null hypothesis that DVLLF camel, mastodon, and mammoth dietary niches did not change significantly over time (i.e., niche conservatism; Peterson et al. 1999; Martinez Meyer et al. 2004; Weins et al. 2010; DeSantis et al. 2012). In Diamond Valley mastodons, moderate *Asfc* and *epLsar* values suggest a browsing diet falling within the range of leaf-browsing (folivorous) and mixed-feeding ungulates (Scott 2012) (Figure 4.3A). Further, high *Asfc* values in Diamond Valley *Camelops* and *Mammuthus* (Figure 4.3B) suggest a mixed-feeding diet supplemented with substantial woody browse, as seen in modern bovids (Scott 2012). Pollen data support a high percentage of *Pinus* (pine), *Juniperus* (juniper), and *Cupressus* (cypress) in the Diamond Valley sediments (Anderson et al. 2002), all of which are coniferous trees with woody

bark, seeds, and new-growth tissues for browsers and mixed-feeders to consume. It is interesting that diets (as inferred from dental mesowear and dental microwear textures) do not change significantly for *Camelops*, *Mammut*, and *Mammuthus* from the Diamond Valley to the Domenigoni Valley, despite the vegetation changes between the two units. Both *Mammut* and *Mammuthus* relative abundance increase in the younger Domenigoni Valley deposits (Table 4.1), with the profusion of *Mammut* representing a unique outlier compared to other Late Pleistocene sites from southern California (see below). The increase in proboscidean abundances may have been a product of the increase in the diversity of woody forage around Domenigoni Valley; as large-bodied monogastric mixed-feeders, both mastodons and mammoths would have benefited from a wider diversity of chemically defended shrubs, trees, and sedges to spread out the toxic impacts of alkaloids present in plant tissues (e.g., Guthrie 1984).

Both the Diamond Valley and Domenigoni Valley units are attritional, time-averaged assemblages that accumulated gradually over space and time (Springer et al. 2010). The high abundance of herbivores recovered from the DVLLF (Table 4.1) stands in contrast to nearby asphaltic assemblages including Rancho La Brea, McKittrick, and Maricopa, where entrapment regimes preferentially trap carnivores as well as juvenile individuals (Shaw and Quinn 1986; Torres 1989). Because attritional assemblages capture regional paleocommunity structure over space and time, the DVLLF is a representative sample of population density and diversity in southern California. Fauna recovered from the DVLLF may have been seasonal migrants, an inference supported by serial sampled stable carbon and oxygen isotopes in *Bison* teeth showing substantial vegetational and environmental changes (Hardy 2015; also see below). DMTA attributes are useful in that they capture a "last supper effect" for organisms' diets, as compared to the average dietary trends examined using mesowear; thus, DMTA data likely reflect the local vegetation signature of the Diamond and Domenigoni Valleys, while mesowear inferences paint a more representative picture of the paleoenvironmental setting of southern California during the late Pleistocene.

4.4.2 Dietary ecology of DVLLF herbivores in comparison to nearby sites

Bison

Although modern *Bison* inhabiting short and tall grass prairies are predominately grazers (Nowak 2018), the decrease in *epLsar* values over time documented here is consistent with prior studies suggesting more flexible dietary habits in extinct *Bison* populations. Direct dietary evidence preserved in dental boluses in Rancho La Brea *Bison* teeth suggested a preference for gymnosperms and dicotyledons (i.e., non-grasses) including legume seed pods, conifer tissues, and chenopods (Akersten et al. 1988). Stable isotope studies confirm a C_3/C_4 mixed-feeding habit for *Bison* from Rancho La Brea (mean $\delta^{13}C_{enamel}$ = -6.8‰; Feranec et al. 2009; Jones and DeSantis 2017), the nearby McKittrick Tar Seeps ($\delta^{13}C_{enamel}$ = -4.9‰; Trayler et al. 2015), and the DVLLF (mean $\delta^{13}C_{enamel}$ = -9.8‰; Hardy 2015). As inferred from dental microwear and dental mesowear data, geographically widespread populations of the extinct *Bison antiquus* ate a variable mixed-feeding diet that was more diverse in textural properties than the grass-dominated diet of modern *Bison Bison* (Rivals et al. 2007; Rivals and Semprebon 2011). *Bison* from Middle Wisconsinan (*ca.* 36 - 18 ka) sites in Mexico were also variable grazers and mixed-feeders as evidenced by dental mesowear analysis (Díaz-Sibaja et al. 2018). La Brea *Bison antiquus* have intermediate *Asfc* values and moderate *epLsar* values, suggesting the consumption of woody browse as well as some tough grass and/or leaves (Figure 4.4B; Jones and DeSantis 2017). Additionally, La Brea *Bison* have significantly higher *Hasfc* values than DVLLF *Bison*, suggesting that *Bison* in the Los Angeles basin consumed a diet with more variable mechanical properties. Mesowear attributes are indistinguishable between DVLLF and RLBLF *Bison* (Supplemental Table 13), suggesting that the average diets of both populations are representative of the larger *Bison* population living in southern California in the Late Pleistocene (Figure 4.4C).

Based on an assessment of the eruption sequence and wear patterns in the teeth of *Bison antiquus*, Jefferson and Goldin (1989) argued that La Brea *Bison* were seasonal late spring

migrants to the Los Angeles Basin. Later isotopic studies confirmed that they were seasonal migrants as evidenced by comparatively more variable serial-sampled stable oxygen and carbon isotope values (Feranec et al. 2009). The mixed C_3/C_4 diet of La Brea *Bison* apparently resulted from the consumption of C_4 vegetation during the winter months (Feranec et al. 2009). One likely culprit is C_4 photosynthetic shrubs like chenopods (Chenopodiaceae), which were found in high abundance in the Diamond Valley pollen record (Anderson et al. 2002) and as tissue in the dental boluses of Rancho La Brea *Bison* teeth (Akersten et al. 1988). The San Bernardino Valley may have been a fall/winter refuge for *Bison*, with the Los Angeles Basin being their primary spring/summer habitat. Because the geology of these two areas differs substantially, a future study incorporating strontium isotopes preserved in *Bison* bones and teeth may be able to test this hypothesis.

Camelops

In combination with previous studies, microwear and mesowear data collectively confirm a browsing habit for *Camelops*. Camels have significantly lower *epLsar* values than all other DVLLF taxa (all $p < 0.045$) and consistently low maxillary MWS and MNS values (Table 4.4), with both proxy methods confirming that grass was not a substantial portion of their diets. Further, *Camelops* has significantly higher *Asfc* and *Tfv* values than *Mammut* (Table 4.3, Supplemental Table 12), suggesting that camels may have consumed harder browse that left deeper gouges in their wear facets than mastodons (Scott et al. 2006). These deeper gouges may have resulted from *Camelops* consuming seed pods or fruit pits, evidence of which was found in plant tissue preserved in the teeth of La Brea *Camelops* (Akersten et al. 1988). Microwear and mesowear analysis of *Camelops* teeth from the American southwest further support an opportunistic browsing habit (Semprebon and Rivals 2010). At nearby McKittrick, stable carbon isotopes suggest a C_3/C_4 mixed diet for *Camelops* ($\delta^{13}C_{enamel}$ = -5.0 $\pm$ 2.7‰; Trayler et al. 2015; Yann et al. 2016); the enriched ^{13}C signature in this case is unlikely to result from C_4 grasses, which are rare in California

due to the cool Mediterranean climate (Collatz et al. 1998). Rather, McKittrick *Camelops* may have specialized on C_4 chenopods including the saltbrush (*Atriplex*), the most common fossil plant material found at McKittrick and a shrub still native to the area today (Mason 1944; Baldwin et al. 2012). Trayler et al. (2015) showed that *Camelops* shifted diet seasonally and suggested that *Atriplex* could have provided adequate winter forage. Chenopods were abundant in the Diamond Valley area (Anderson et al. 2002) and may have been a seasonal staple for *Camelops* populations there, as well. The diet of *Camelops* in southern California was likely similar to modern *Camelus dromedarius* (as suggested by Akersten et al. 1988): browsers that prefer shrubby vegetation including *Atriplex* (Iqbal and Khan 2001).

The textural properties of *Camelops* diets do not differ significantly between sites or through time (Supplemental Table 11, Supplemental Table 13), suggesting a potential link between populations. *Camelops* may have been a seasonal migrant to the San Bernardino Valley like *Bison*, which could explain the similarity in DMTA and mesowear attributes between DVLLF and RLBLF if populations were encountering and consuming similar foods. McKittrick and La Brea *Camelops* show little evidence of intermingling, as evidenced by the dissimilar carbon isotopic signatures of diet between the two populations (Trayler et al. 2015; Yann et al. 2016; Jones and DeSantis 2017). However, while McKittrick is located 220 km northwest of La Brea, Diamond Valley is geographically situated between the coast (with few *Camelops*-rich sites) and the Mojave Desert (with several vertebrate faunas with a high abundance of *Camelops*) (Springer et al. 2010). Because of this, *Camelops* from the DVLLF may represent a time-averaged assemblage of seasonal migrants between the desert and the coast. Future studies assessing the dietary habits and environmental preferences of *Camelops* from high desert sites (e.g., Tule Springs Local Fauna, Lake Mannix, Twenty-nine Palms, or China Lake; Figure 4.1) may be able to resolve this. Since *Camelops* diets show no significant differences in any microwear attributes between glacial and interglacial deposits at either La Brea (Jones and DeSantis 2017) or Diamond Valley (this study), we

suggest that niche conservatism in this taxon may be the rule, rather than the exception.

Equus

While horses have high-crowned (hypsodont) teeth that can withstand an abrasive diet, they were not necessarily obligate grazers in the past. Although stable isotope studies confirm a preference for C_4 grasses in Pleistocene horses from the Gulf Coastal Plain (e.g., MacFadden and Cerling 1996; Koch et al. 1998; 2004; MacFadden et al. 1999b; Feranec and MacFadden 2000), extinct horses displayed considerable adaptability and often altered their dietary habits when sympatric with potential competitors (e.g., *Bison*, mammoths, and other horses) (McFadden et al. 1999a; Feranec 2004; Feranec et al. 2009; Barrón-Ortiz et al. 2014). Horses in southern California likely consumed a high quantity of C_3 grass, which would explain both the high mesowear scores in La Brea and Diamond Valley *Equus* (Table 4.5) as well as the depleted ^{13}C signature of horses from La Brea ($\delta^{13}C_{enamel}$ = -8.6 $\pm$ 0.9‰; Jones and Desantis 2017; Feranec et al. 2009) and McKittrick ($\delta^{13}C_{enamel}$ = -6.4 $\pm$ 2.1‰; Trayler et al. 2015).

Like *Bison*, microwear data suggest shifting dietary habits in DVLLF *Equus*, adding to an increasing body of evidence documenting dietary niche plasticity in extinct horses. Specifically, higher *Asfc* values in Domenigoni Valley *Equus* suggests an increase in the consumption of hard, woody browse after the LGM (Figure 4.3). This is chronologically out of sync with horses at Rancho La Brea, which were found to have incorporated a larger proportion of woody browse in their diet during the Wisconsin glacial as compared to the warm interglacial $\sim$11 ka (Jones and DeSantis 2017). When compared independent of time, DVLLF *Equus* exhibit significantly higher *epLsar* values and significantly lower *Hasfc* values than RLBLF *Equus* (Table 4.3, Supplemental Table 13), supporting a greater preference for grass and less dietary variability in San Bernardino Valley horse populations. As horses may not have migrated outside of the Los Angeles Basin (Jefferson and Goldin 1989; Feranec et al. 2009), it is possible that DVLLF horses and RLBLF horses did not

intermingle despite living only ∼80 km apart. Alternatively, because microwear is able to pick up more nuanced dietary differences than mesowear, it is possible that local changes in vegetation (e.g., low-growing woody heathland or abundance of hardwood) are driving the observed differences. Further work, including strontium isotope analysis or serial sampled carbon and oxygen isotope analysis, is needed to better resolve potential migratory behavior of ungulates from the Diamond Valley Lake assemblage.

Mammut

Indistinguishable microwear and mesowear values for Diamond Valley and Domenigoni Valley mastodons suggests dietary niche conservatism between the two populations despite significant environmental and climatic changes during the Wisconsin glaciation (Supplemental Table 11). The findings here parallel the results of previous work that documented dietary niche conservatism in mastodons from the Great Lakes region in the Late Pleistocene (Green et al. 2017). *Mammut* was less abundant in the older Diamond Valley sediments (Table 4.1), perhaps due to restricted or intermittent forest stands (Anderson et al. 2002). However, *Mammut* is highly abundant in the younger Domenigoni Valley sediments, which may have been enabled by periodic spikes in conifers (e.g., *Pinus*) and flowering plants (e.g., *Alnus*) and the increased abundance of oaks in southern California during the last glacial interval (Heusser 1995, 1998; Heusser and Sirocko 1997). Mastodons are commonly associated with conifer consumption (e.g., Lepper et al. 1991; Teale and Miller 2012; Newsom and Mihlbachler 2006); stable carbon isotope values from McKittrick confirm a C_3 browsing signature ($\delta^{13}C_{enamel}$ = -8.4‰; Trayler et al., 2015). The restricted abundance of mastodons in the older Diamond Valley unit and their subsequent abundance in the Domenigoni Valley sediments (Table 4.1) parallels their near absence from the mid-continent before and during the LGM and their later preponderance during the Allerød oscillation (Widga et al. 2017).

Recent studies of dental microwear textures in *Mammut americanum* from across North

America enable DVLLF mastodons to be compared to mastodon populations occupying distinct paleoenvironmental settings (Green et al. 2017; Smith and DeSantis 2018). Specifically, DVLLF *Mammut Asfc* values are indistinguishable from *Asfc* values of *Mammut* from open pine parklands (p = 0.832), while DVLLF *Mammut epLsar* values are indistinguishable from *epLsar* values of *Mammut* from spruce-dominated boreal forests (p = 0.632) and cypress swamps (p = 0.167) (all Mann-Whitney U non-parametric tests) (Green et al. 2017). DVLLF mastodons have significantly higher *epLsar* values than mastodons from the open pine parkland sites of Jones Spring and Trolinger Spring, Missouri (King 1973; King and Saunders 1984) (p = 0.028), suggesting that DVLLF mastodons may have incorporated more grass into their diet than mastodons from these sites. Additionally, both *Asfc* values and *eplsar* values of DVLLF mastodons are indistinguishable from Ingleside mastodon *Asfc* values (p = 0.461) and *epLsar* values (p = 0.261) (Smith and DeSantis 2018). Ingleside, an ecotonal region on the Gulf Coastal Plain of East Texas, was characterized by an environment of predominately C_4 grasses interspersed by stands of C_3 forest (Lundelius 1972; Bryant and Holloway 1985; Koch et al. 2004; Smith and DeSantis 2018). Palynological remains support a similar paleoenvironmental setting for the DVLLF – with both sedimentary units having an abundance of grasslands interspersed by either conifer stands (Diamond Valley) or deciduous forest and heathland (Domenigoni Valley) (Heusser 1995, 1998; Heusser and Sirocko 1997).

Mammuthus

Mammoths were highly efficient grazers that arrived in North America *ca*. 1.5 to 1.3 Ma (Lister and Sher 2015); once in North America, mammoths quickly achieved a cosmopolitan distribution. Like modern elephants, mammoths exhibited considerable dietary flexibility over time and space (Metcalfe 2017), a key attribute that likely contributed to their widespread geographic range and abundance in Pleistocene faunal assemblages. Mammoth relative abundance in the DVLLF increases in the Domenigoni Valley unit (Table 4.1);

however, this increase was restricted and mammoth abundance remained relatively low. In the southwest, mammoth remains are relatively common at Rancho La Brea (Harris 2001; Farrell and Shaw 2009) and the Las Vegas Wash (Scott et al. 2017), but make up a smaller percentage of the large mammal assemblage at inland desert sites such as Lake Manix or Anza Borrego (Jefferson 2003). The relative paucity of *Mammuthus* at DVLLF is likely a true representation of their rarity in the intermontane basins of southern California, and suggests environmental conditions more favorable to the comparatively abundant browsers (*Mammut* and *Camelops*) and potential exclusion by competing grazers (*Bison* and *Equus*).

The microwear signature of DVLLF mammoths can be compared to DMTA attributes in Texas mammoths as well as mammoth populations occupying the Channel Islands (CHIS) off the coast of southern California (Smith and DeSantis 2018). Mammoths from the DVLLF have *Asfc* values that are significantly higher than *Asfc* values in mammoths from Ingleside ($p = 0.001$), Cypress Creek ($p = 0.001$), and Friesenhahn ($p = 0.008$), and are statistically indistinguishable from *Asfc* values found in CHIS mammoths ($p = 0.095$) (all Mann-Whitney U non-parametric tests) (Smith and DeSantis 2018). This suggests some similarity in the hardness of material ingested by mammoths both on the mainland and off the coast of southern California. During the LGM, vegetation on the Channel Islands was characterized by abundant conifers and a diverse understory of forbs and shrubs; it wasn't until after the Younger Dryas ($\sim$11.3 ka) that the mixed conifer forest began to fragment and give way to more open grasslands (Chaney and Mason 1930; Anderson et al. 2008, 2010). Although the CHIS mammoths represent a time-averaged assemblage spanning at least 140 kyr (Muhs et al. 2015), on average, they consumed a large percentage of bark, seeds, and woody material in addition to the herbs and grasses growing in the understory (Semprebon et al. 2016; Smith and DeSantis 2018). If the Diamond Valley area was an ecotonal region of coniferous stands and grasslands, DVLLF mammoths may have been dietary generalists, preferring a mixed diet that was specialized on neither grass nor browse.

4.5 Conclusions

This study characterizes the paleoecology of the Diamond Valley Lake Local Fauna, the largest non-asphaltic, open-environment Late Pleistocene terrestrial vertebrate assemblage known from the American southwest. Specifically, we tested whether the textural properties of diet changed in space or time for 5 megafaunal genera (*Bison*, *Camelops*, *Equus*, *Mammut*, and *Mammuthus*) recovered from two sedimentary units dating to before and after the last glacial maximum. The results of analyzing dental microwear and dental mesowear textures are incongruent: dental mesowear values do not significantly differ for any taxa between the two units or when compared to nearby Rancho La Brea, while dental microwear attributes suggest significant changes in diet for *Bison* and *Equus* but not for *Camelops*, *Mammut*, or *Mammuthus*. *Bison* and *Equus* display niche plasticity, with both taxa consuming less grass and more woody browse after the LGM. *Camelops* exhibits niche conservatism, remaining a browser specialized on hard foods. *Mammut* microwear compares favorably with mastodons occupying an ecotonal environment between grasslands and closed forests, while *Mammuthus* microwear compares well with mammoths occupying a closed forest environment on the nearby Channel Islands. When compared with pollen records for southern California, these results suggest that a paleoecological mosaic persisted at Diamond Valley Lake throughout the Late Pleistocene. This mosaic provided a diversity of abundant resources, the precise makeup of which changed through time, but which consistently enabled resident taxa to effectively partition dietary resources. As mesowear values do not substantially differ from mesowear values of populations at Rancho La Brea, the Diamond Valley Lake Local Fauna is a representative picture of the paleoenvironmental setting of southern California during the late Pleistocene: both before and after the LGM.

Chapter 5

PHYLOGENETIC CONSERVATISM OF BIOTIC CRISES IN NORTH AMERICAN MAMMALS

5.1 Introduction

Understanding the causes and consequences of biotic crises is one of the priority research questions in paleoecology (Seddon et al. 2014), because it both allows us to compare the drivers of the ongoing biodiversity crisis with geological extinction events (Barnosky et al. 2011; Hull and Darroch 2013) and provides an invaluable source of data for predictive models aimed at remediating the impacts of a potential future ecosystems collapse (Finnegan et al. 2015; Hull et al. 2015; Payne et al. 2016). Of all past biotic crises, the 'Big 5' mass extinction events (Raup and Sepkoski 1982) are the most well-studied because of their propensity to change the trajectory of life by eliminating established lineages and allowing other taxonomic groups to diversify. The intensity of mass extinction events has been shown to be decoupled from the ecological severity of the extinction in marine realms (Erwin 1998, 2001, 2008; Jablonski 1989, 1991; McGhee et al. 2012); this is because the former is generally a measure of the number of genera or families lost (Sepkoski 1996) while the latter is a measure of the amount of evolutionary history (i.e., the length of the branches separating two taxa in a phylogenetic tree (Faith 1992)) lost due to extinction. Evolutionary history quantifies the amount of evolution that has occurred since divergence from a last common ancestor. Random extinctions in a phylogenetic tree eliminate relatively little evolutionary history, even when extinction intensity is high, whereas the same level of extinction can remove much greater portions of evolutionary history when clustered (selective) (Mooers et al. 2005; Nee and May 1997). Because phylogenetically selective extinctions can remove large amounts of evolutionary history at once, the degree to which extinctions are phylogenetically selective could explain the disconnect between

the severity of an extinction event and its effect on the history of life (McGhee et al. 2004; 2012). Accounting for evolutionary history in studies of mass extinction and recovery (Roy et al. 2009; Krug and Patzkowsky 2015) has added insight into the factors driving diversification, many of which may be phylogenetically conserved (i.e., likely to be passed from parent to daughter species (McKinney 1997; Bennet et al. 2005; Davies et al. 2008; Purvis 2008)). Previous work has detailed the ecological severity and magnitude of the 'Big 5' mass extinctions (e.g., McGhee et al. 2004; Hull and Darroch 2013; Muscente et al. 2018), much of which has focused on the Paleozoic and Mesozoic fossil record of the marine realm. However, the terrestrial fossil record also has potential to illustrate how mammals responded to some of the Cenozoic Era's major biotic crises (e.g., Blois and Hadley 2009; Fraser et al. 2015).

Here, we examine patterns in phylogenetic conservatism of mammaliam communities for the Late Cretaceous and Cenozoic, an interval that encompasses numerous climatic and biogeographic changes as well as at least 5 noteworthy biotic crises: the Cretaceous-Paleogene extinction (K-Pg), the Paleocene-Eocene Thermal Maximum (PETM), the Eocene-Oligocene transition (EOT), the Mid-Miocene Climatic Optiumum (MMCO), and the late Pleistocene extinctions (LPE) (Table 5.1). Each of these biotic crises represent periods of time when communities experienced heightened ecological stress as a result of abiotic factors (e.g., climate or environmental change) or biotic factors (i.e., competition or predation). We were interested in understanding whether communities responded in predictable ways for a given source of ecological stress. Thus, this work sought to answer three related research questions: 1) what intervals in the Cenozoic constitute a biotic crisis event in North American mammals?; 2) how are taxonomic severity and ecological severity of these biotic crises related?; and, 3) for a given source of ecological stress, is the pattern of extinction and/or origination predictable? Answers to these questions may help provide a deep time framework for the development of conservation planning aimed at managing the future of terrestrial mammalian communities (see Barnosky et al. 2017).

Table 5.1: Cenozoic biotic crises; timing, impacts on mammals, and proposed driver(s).

Biotic Crisis Timing and Impacts on North American Mammals	**Proposed Extinction Driver(s)**
The **Cretaceous-Paleogene (K-Pg) mass extinction** occurred ∼66.0 Ma. Although all major Cretaceous mammalian lineages survived the extinction, the responses were heterogeneous: metatherians experienced heavy extinctions; multituberculates suffered a mass depletion (low origination rates); and eutherians experienced high turnover, with peaks in both origination and extinction rates[1-3].	**An asteroid impact at Chicxulub, Mexico.** The impact led to severe initial cataclysms (e.g., magnitude >11 earthquakes, shelf collapse around the Yucatán platform, and widespread tsunamis) followed by global environmental perturbations including darkness and rapid cooling[4]. Biota may have also experienced stress due to rapid climate warming during the last 350 kyr of the Cretaceous as a result of Deccan volcanic eruptions[5].
The **Paleocene-Eocene Thermal Maximum (PETM)** commenced ∼55.5 Ma and lasted ∼170 kyr. Endemic mammalian genera experienced body size decreases during the first ∼130,000 years[6], while some smaller taxa shifted their geographic ranges northward5. Mammalian generic diversity increased in central North America during the PETM, likely a result of high-latitude intercontinental emigrations from Eurasia into North America[7].	**Rapid warming and/or elevated pCO_2.** The introduction of vast quantities (2,000 to 6,800 Pg) of carbon into the ocean-atmosphere system occurred over a short period of time (1 kyr to 50 kyr)[8]. This carbon addition led to an enhanced greenhouse effect, inducing multiple changes including: an increase in average global temperature of >5° C; changes in oceanic circulation patterns and primary productivity; rapid ocean acidification; and an increase in aridity, especially during the summer months[9-11].
The **Eocene-Oligocene Transition (EOT)** ended ∼33.7 Ma, with extinctions beginning in North America during the Mid Eocene[12]. Many archaic mammal groups experienced total extinction, with several other groups experiencing heavy losses, but not complete extinction. These losses were more than compensated for by high immigration of mammal taxa from Asia (e.g., rabbits, rodents, bears), the appearance of multiple carnivorous taxa (e.g., amphicyonids, canids, nimravids), and a large radiation in artiodactyls (e.g., pigs, camels, ruminants, and oreodonts). Perissodactyls declined in diversity but remained a prominent element of the fauna into the Oligocene[13].	**Rapid cooling and floral turnover, especially in the northern high latitudes.** Opening of marine gateways and/or reduction of pCO_2 caused a state change from the earlier 'greenhouse' world to an 'icehouse' world[14]. Ice sheet growth on Antarctica and deep-water cooling, increase in $\delta^{18}O$ accomplished in two 40-kyr long steps separated by a 200-kyr long intermediate plateau[15]. Global rapid cooling and an increase in mean annual temperature range was followed by radical floral change across northern high latitudes, with the replacement of subtropical vegetation by more temperate forms (although this may have been the end result of Eocene cooling and not due to the EOT itself)[16].

The **Mid-Miocene Climatic Optimum (MMCO)** occurred between 17 - 14.5 Ma, with biotic turnover peaking in North America at slightly different times than on other continents. Herbivorous taxa experienced significant turnover within lineages, with replacement of large ungulate browsers with grazers as well as turnover in many smaller mammals, including rodents[17,18]. High immigration rates are seen in taxa from Eurasia (e.g., felids, borophagine canids, and proboscideans) also occurred during this time[19].	**Rapid warming and/or elevated pCO_2 punctuating a long-term global cooling trend coincident with the spread of grasslands into northern high latitudes.** The MMCO global warming event coincides with relatively warm deep-water temperatures and a decline in polar glacial ice cover[14,20]. pCO_2 was elevated (>500 - 850 ppmv) and may have been responsible for changes in oceanic circulation patterns and primary productivity[21,22]. Higher latitudes experienced warmer and wetter conditions, which may have facilitated environmental change including the spread of grasslands and grassland-adapted taxa[23,24]. Biotic turnover was likely a result of continental- and regional-scale environmental change as well as local-scale biotic interactions[17-19].
The **Late Pleistocene Extinctions (LPE)** ended ∼0.009 Ma, although today's biodiversity crisis may be an ongoing expression of this "6th mass extinction[25]." Extinctions in North America occurred in two pulses coincident with climatic change: 1) the loss of warm-adapted animals from 45-20 ka and cold-adapted animals between 12-9 ka[26]. Extinctions selected heavily against large-bodied taxa and disproportionately against some phylogenetic clades. Total extinction of some long-lived clades in North America (e.g., Equidae, Camelidae), although some members of these clades were subsequently re-introduced by Eurasian human immigrants[27].	**Human predation, with climatic change controlling the timing, geography, and magnitude of the extinctions**. Pleistocene glacial-interglacial cycling resulted in increased habitat specialization and the co-occurrence of species that would not exist together today (i.e., 'no-analog communities')[28]. These highly specialized mammalian communities may have been stressed by the onset of the last glacial maximum; however, increased pressure resulting from human predation is likely to account for many of the extinctions. The timing, extent, magnitude, and cause of extinction for many Pleistocene taxa remains a source of debate amongst paleontologists, archeologists, and conservation biologists[29].

1 = Pires et al. 2018; 2 = Bininda-Emonds et al. 2007; 3 = Springer et al. 2003; 4 = Schulte et al. 2010; 5 = Keller et al. 2018; 6 = Secord et al. 2012; 7 = Burger 2012; 8 = Liu et al. 2009; 9 = Zachos et al. 2005; 10 = Zachos et al. 2008; 11 = Lawrence et al. 2003; 12 = Prothero and Heaton 1996; 13 = Janis 1993; 14 = Zachos et al. 2001; 15 = Zanazzi et al. 2007; 16 = Pound and Salzman 2017; 17 = Barnosky and Carrasco 2002; 18 = Hopkins 2007; 19 = Janis 2004; 20 = Lear et al. 2010; 21 = Beerling and Royer 2011; 22 = Herold et al. 2011; 23 = Cerling et al. 1998; 24 = Wolfe 1994; 25 = Barnosky et al. 2011; 26 = Barnosky et al. 2004; 27 = Barnosky et al. 2014; 28 = Williams and Jackson 2007; 29 = Koch and Barnosky 2006

5.2 Methods

We downloaded fossil occurrence data for the Late Cretaceous and Cenozoic from the Paleobiology Database (https://paleobiodb.org/) in February 2019, using the taxon name 'mammalia' and the parameters: time interval range = 85 Ma to 0 Ma, continent = North America, taxonomic resolution = genus, output options = classification, coordinates, location. We ran the analysis at genus level rather than species level to avoid any debate about the validity of included Late Cretaceous and Cenozoic mammal species. We removed any occurrences of aquatic or volant organisms (Orders Sirenia, Cetacea, Desmostylia, and Chiroptera; Families Phocidae, Desmatophocidae, Odobenidae, and Otariidae) as well as those occurrences with uncertain genus or family IDs. The remaining occurrence data were used to define the first occurrence datum (FAD), last occurrence datum (LAD) and longevity for each mammalian genus. We partitioned data by North American Land Mammal Ages (NALMAs) (Woodburne 2004) because they delineate relatively stable community assemblages through time. We include the newly-defined Santarosean and Saintaugustinean (Barnosky et al. 2014) and updated the NALMA boundary ages for occurrences in our data to reflect recent geochronologic revisions (e.g., Fowler 2017) that are not yet followed by the Paleobiology Database.

We used the FAD and LAD to identify the four fundamental classes of taxa (Foote 2000) for each NALMA. Briefly summarized here, the classes are: (1) taxa confined to the interval (i.e., taxa whose FAD and LAD both occur within the interval); (2) taxa that exist prior to the interval and make their LAD during the interval; (3) taxa whose FAD is during the interval and persist into the subsequent interval; and (4) taxa that range through the entire interval and exist in both the previous and subsequent interval (Figure 5.1). We follow the terminology of Foote (2000) in identifying the numbers of each of these taxa (N_{FL}, N_{bL}, N_{bt}, and N_{Ft}, respectively), including the total number of taxa crossing the bottom of an interval ($N_b = N_{bL} + N_{bt}$) and the top of the interval ($N_t = N_{Ft} + N_{bt}$), and used these values to calculate the number of originations ($N_o = N_{FL} + N_{Ft}$) and extinctions

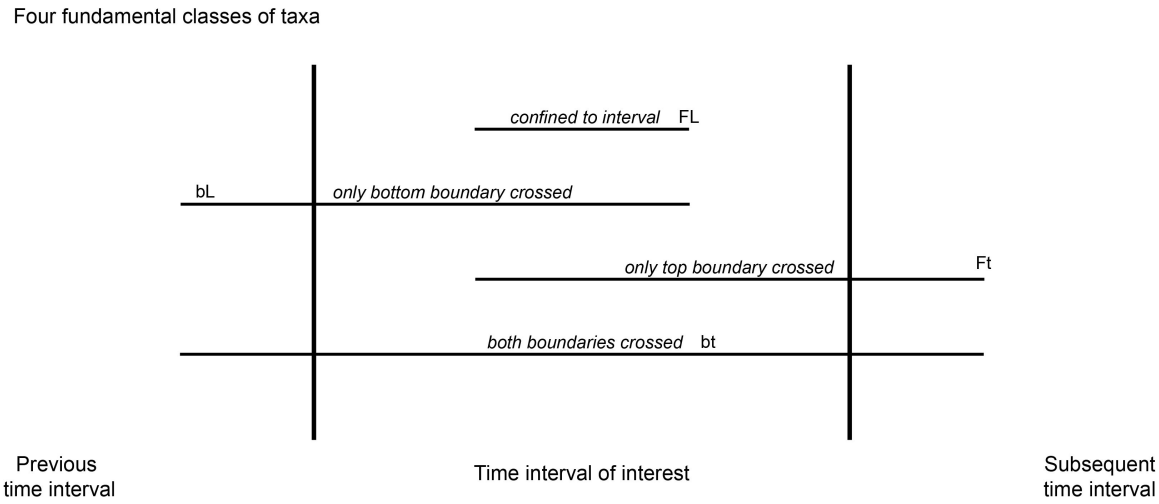

Figure 5.1: The four fundamental classes of taxa. FL = FAD and LAD occur within interval; bL = taxa crosses bottom of interval, LAD occurs within interval; Ft = FAD occurs within interval, taxa crosses top boundary of interval; bt = taxa crosses both the bottom and top boundaries of interval. Reproduced from Foote (2000).

($N_e = N_{FL} + N_{bL}$) in each interval as well as origination and extinction rates.

The per-capita rate of origination (p_d) and extinction (q_d) for the duration of each interval (Δt) are defined as:

$$p_d = -\ln\left(\frac{N_{bt}/N_t}{\Delta t}\right) \tag{5.1}$$

$$q_d = -\ln\left(\frac{N_{bt}/N_b}{\Delta t}\right) \tag{5.2}$$

In addition to calculating origination and extinction rates for each interval, we computed two indices of phylogenetic clustering. The first index, R_{CL}, is Pearson's correlation coefficient between two matrices (Roy et al. 2009; Krug and Patzkowsky 2015). We calculated R_{CL} values for both extinction and origination for each interval. Each of the matrices used in the calculation of R_{CL} are $n \times n$ binary matrices (with the lower triangles, including the diagonals, removed), where n is equal to the number of genera that appear in the interval. In the matrix M_{TAX}, the cross-product (i.e., the cell at the intersection of a row and a

column) equals 1 when both genera belong to the same taxonomic family, and 0 otherwise. In M_{EXT}, the cross-product is 1 when both genera go extinct at the end of the interval, and a 0 otherwise; for M_{ORIG}, the cross-product is 1 when both genera originate at the beginning of the interval, and a 0 otherwise. R_{CL} for extinctions is the correlation between M_{TAX} and M_{EXT}, while R_{CL} for originations is the correlation between M_{TAX} and M_{ORIG}. As R_{CL} is a correlation coefficient, it can take on any value from +1 to –1; a value of +1 suggests extinctions or originations are perfectly clustered (i.e., genera originating/going extinct are more closely-related than would be expected by chance), a value of –1 suggests extinctions or originations are perfectly even (i.e., the numbers of genera originating/going extinct are evenly dispersed amongst families), and a value of 0 suggests extinctions or originations are perfectly random with respect to family membership.

The second clustering index is Moran's I (here, an index of clustering, I_{CL}, a metric used in assessing patterns of spatial clustering and evenness (Moran 1950). This metric has been used to estimate taxonomic patterns of extinction risk in extant vertebrates (Gittleman and Kot 1990; Lockwood et al. 2002) as well as to test for phylogenetic signal in Mesozoic-Cenozoic bivalves (Roy et al. 2009) and in brachiopods across the Late Ordovician mass extinction (Krug and Patzkowsky 2015). Our calculation of I_{CL} uses the same matrices as used in the calculation of R_{CL}, and is computed as:

$$I_{CL} = \frac{\Sigma_i \Sigma_j z_i z_j w_{ij}}{\Sigma_i \Sigma_j w_{ij}} \times \frac{n}{\Sigma_i z_i^2} \tag{5.3}$$

Where w_{ij} is equivalent to M_{TAX} and z_i and z_j refer to the normalized row and column sums (n = number of rows/columns) of M_{EXT} or M_{ORIG}, respectively. Like R_{CL}, I_{CL} takes on more positive values when extinctions or originations are clustered, negative values when they are even, and a value approaching 0 when extinctions or originations are random with respect to taxonomic membership.

We assessed statistical significance by randomizing the genera within each interval that originate or go extinct, recalculating R_{CL} and I_{CL}, and repeating 5000 times to generate a

Table 5.2: Lack of correlation between R_{CL}, I_{CL}, and various diversity and turnover metrics.

	R_{CL} Extinctions		I_{CL} Extinctions		R_{CL} Originations		I_{CL} Originations	
	rho	**p-value**	**rho**	**p-value**	**rho**	**p-value**	**rho**	**p-value**
Number of genera (N_{tot})	-0.138	0.519	0.148	0.489	-0.002	0.994	-0.360	0.084
Number of extinctions (N_e)	-0.077	0.719	0.262	0.216	–	–	–	–
Number of originations (N_o)	–	–	–	–	0.081	0.707	-0.164	0.445
Proportion of extinctions	-0.210	0.322	0.056	0.796	–	–	–	–
Proportion of originations	–	–	–	–	0.048	0.825	0.235	0.268
Per-capita rate of extinction (q_d)	0.124	0.536	-0.089	0.680	–	–	–	–
Per-capita rate of origination (p_d)	–	–	–	–	-0.213	0.317	0.295	0.162

All correlations done using Spearman rank-order correlations. Results consistent regardless of test statistic. Neither metric of taxonomic clustering is statistically significantly correlated with any metric of diversity (at the 0.05 level).

null distribution. We used the 95% confidence limits of this null distribution to identify excursions above the range of the null model. R_{CL} and I_{CL} may be sensitive to sample size (Roy et al. 2009; Krug and Patzkowsky 2015); however, our data suggest no strong correlation (Table 5.2) between either index of clustering and various metrics of diversity or turnover rates, including: diversity within an interval, number of extinctions/originations, proportional extinction/origination, or per-taxon extinction/origination (Foote 2000).

Table 5.3: NALMAs and associated extinction/origination rates and degree of clustering.

					Extinctions					Originations				
NALMA	**Max. Age (Ma)**	**Min. Age (Ma)**	**Duration (Ma)**	$\mathbf{N_{tot}}$	$\mathbf{N_e}$	$\mathbf{q_d}$	$\mathbf{q_i}$	$\mathbf{R_{CL}}$	$\mathbf{I_{CL}}$	$\mathbf{N_o}$	$\mathbf{p_d}$	$\mathbf{p_i}$	$\mathbf{R_{CL}}$	$\mathbf{I_{CL}}$
Judithian	83.5	70.6	12.9	24	6	0.03	0.36	-0.009	-0.048	14	0.07	0.94	0.118	0.127
Edmontonian	70.6	68	2.6	28	8	0.03	0.07	-0.024	-0.167	12	0.11	0.29	-0.020	-0.167
Lancian	68	66	2	28	19	0.53	1.05	-0.081	-0.283	8	0.13	0.25	-0.024	-0.233
Puercan	66	63.9	2.1	76	31	0.71	1.48	**0.117**	0.091	54	1.05	2.20	-0.023	0.050
Torrejonian	63.9	60.9	3	96	34	0.18	0.55	**0.055**	**0.329**	51	0.29	0.87	0.016	**0.105**
Tiffanian	60.9	56	4.9	143	73	0.27	1.34	**0.045**	**0.132**	74	0.28	1.36	0.023	0.146
Clarkforkian	56	55	1	125	30	0.69	0.69	0.012	0.015	71	1.26	1.26	-0.004	0.077
Wasatchian	55	50.1	4.9	197	72	0.09	0.42	-0.008	0.031	75	0.09	0.45	0.012	0.066
Bridgerian	50.1	46.3	3.8	201	118	0.33	1.27	-0.050	**0.081**	77	0.23	0.86	-0.019	-0.022
Uintan	46.3	40.1	6.2	244	114	0.19	1.15	-0.014	0.053	146	0.23	1.43	-0.033	0.013
Duchesnean	40.1	36.9	3.2	166	71	0.25	0.79	-0.004	0.044	60	0.21	0.68	0.019	0.021
Chadronian	36.9	33.7	3.2	191	96	0.31	0.98	-0.016	0.060	82	0.26	0.84	0.035	**0.085**
Orellan	33.7	32	1.7	119	35	0.23	0.39	**0.048**	**0.191**	42	0.28	0.48	0.018	0.134
Whitneyan	32	30	2	168	37	0.21	0.41	0.018	**0.109**	85	0.43	0.87	0.008	0.044
Arikareean	30	18.8	11.2	294	131	0.08	0.93	-0.012	**0.135**	149	0.09	1.05	0.019	0.030
Hemingfordian	18.8	16	2.8	250	91	0.23	0.64	0.020	**0.063**	94	0.24	0.66	0.002	**0.042**
Barstovian	16	12.6	3.4	265	117	0.26	0.87	0.010	-0.001	100	0.22	0.76	0.010	-0.014
Clarendonian	12.6	9	3.6	215	67	0.12	0.45	0.013	0.067	73	0.14	0.49	0.015	**0.064**
Hemphillian	9	4.8	4.2	276	137	0.26	1.07	-0.004	0.029	118	0.23	0.95	0.000	-0.008
Blancan	4.8	1.4	3.4	233	79	0.20	0.68	-0.004	**0.093**	109	0.26	0.89	0.009	-0.018
Irvingtonian	1.4	0.21	1.19	203	56	0.29	0.34	-0.010	0.014	54	0.28	0.33	0.005	0.001
Rancholabrean	0.21	0.014	0.196	155	17	0.52	0.10	0.001	0.000	21	0.67	0.13	0.010	0.075
Santarosean	0.014	0.0005	0.0135	169	38	22.93	0.31	-0.006	0.080	30	18.54	0.25	-0.007	0.019
Saintaugustinean	0.0005	0	0.0005	139	0	0	0	–	–	6	90.24	0.05	-0.008	-0.002

N_{tot}, total number of genera; N_e, total number of extinctions; N_o, total number of originations; q_d, per-capita extinction rate; q_i, time independent extinction rate; p_d, per-capita origination rate; p_i, time independent origination rate; R_{CL}, index of phylogenetic clustering; I_{CL}, Moran's I. Bold = significant excursions (outside of 95% confidence intervals).

5.3 Results

Analysis of the taxonomic severity across intervals suggests that the highest time-dependent extinction rates occurred (in order from most severe to least severe) during the Santarosean ($q_d = 22.93$), the Puercan ($q_d = 0.71$), the Clarkforkian ($q_d = 0.69$), the Lancian ($q_d = 0.53$), and the Rancholabrean ($q_d = 0.52$) (Figure 5.2; Table 5.3). The duration of each interval influences these rates, which may also be subject to the 'pull of the recent' (Raup 1972; Alroy 2010) (although this effect has been shown to not significantly alter the pattern of diversification at the generic or familial level (Sahney and Benton 2017)); thus, we also calculated time-independent extinction rate on a per-interval basis by setting the denominator in the calculation of q to 1 for each interval. When this is done for the five most severe extinction intervals, the Lancian and the Puercan are the only intervals with an extinction rate greater than 1 (Table 5.3). The highest time-dependent origination rates occurred (in order from most severe to least severe) during the Santarosean ($p_d = 18.54$), the Clarkforkian ($p_d = 1.26$), and the Puercan ($p_d = 1.05$). When time-independent origination rates are calculated for these intervals, only the Puercan and Clarkforkian have origination rates greater than 1 (Table 5.3).

Our results of taxonomic severity are largely in agreement with past studies of mammalian compositional turnover since the Late Cretaceous. Most previous workers have identified the K-Pg transition and the interval of time encompassing the PETM as periods with elevated extinction rates (Alroy 1999, 2000; Alroy et al. 2000; Hooker 2000). High origination rates typify the Puercan and Clarkforkian, suggesting rapid speciation and/or immigration into North America immediately following these early Paleogene biotic crises. For the remainder of the Cenozoic until the late Pleistocene, extinction and origination rates remain relatively conservative, although moderate spikes in extinction rate are apparent during the middle Eocene (Bridgerian), the late Eocene through early Oligocene (Chadronian, Orellan, and Whitneyan), and the middle Miocene (Hemingfordian and Barstovian) (Figure 5.2). Our study highlights the late Pleistocene (Rancholabrean) extinctions as

well; because we include the recently-defined Santarosean and Saintaugustinean NALMAs (Barnosky et al. 2014), most megafaunal extinctions of the late Pleistocene occur during the extremely short Santarosean (0.014 – 0.0005 Ma), resulting in the highest extinction rate of the entire study interval by a factor of over 30.

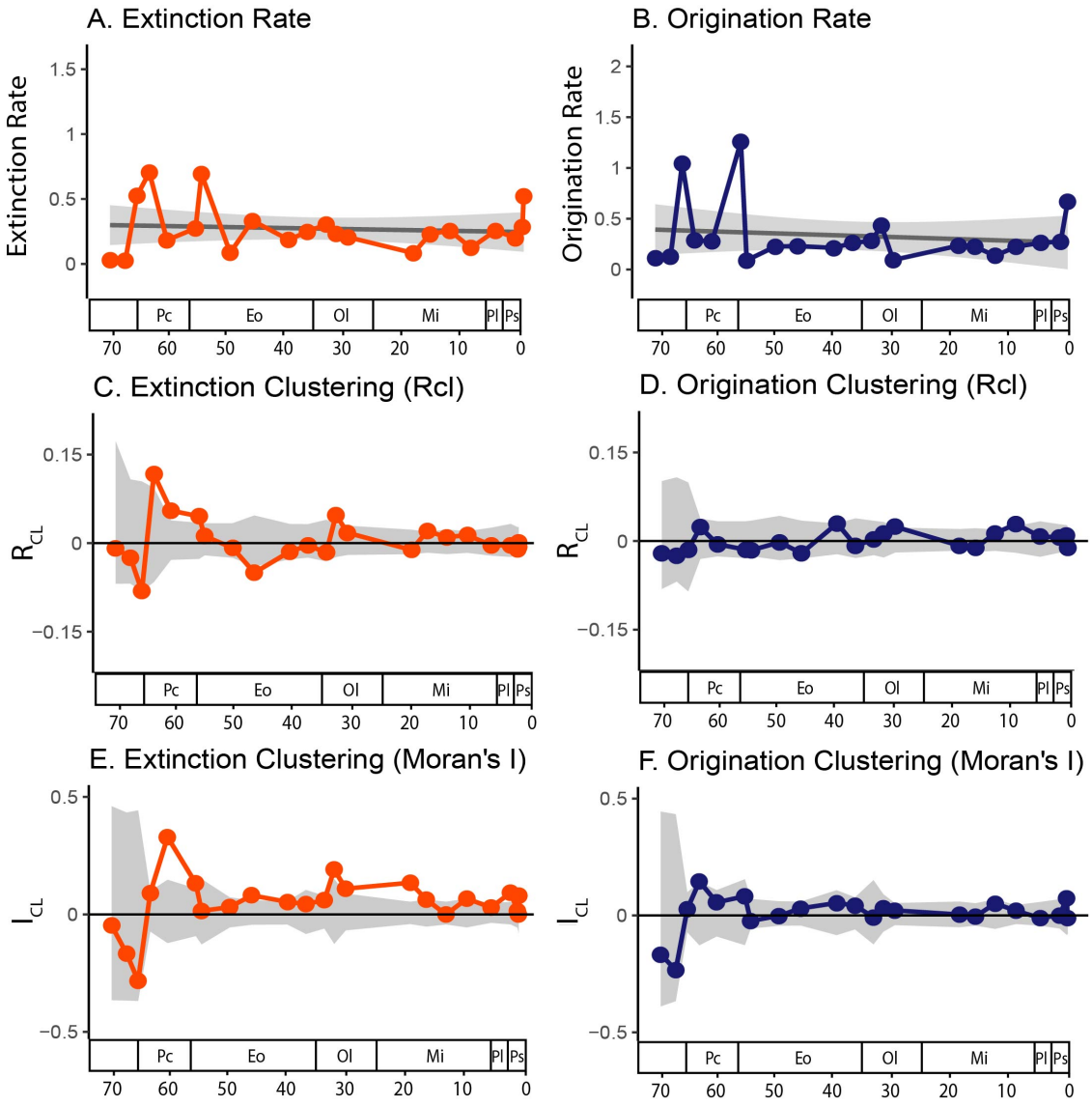

Figure 5.2: Rates of (A) extinction and (B) origination in North American mammals throughout the Cenozoic, and the degree to which these events were clustered using (C, D) the index of relative clustering, R_{CL}, and (E, F) Moran's I, I_{CL}.

Analysis of phylogenetic clustering for the Late Cretaceous through the Anthropocene suggests that overall neither extinction nor origination tend to be clustered within intervals

more often than would be expected by chance (Figure 5.2), although the two indices of taxonomic clustering differ in their sensitivity. While neither index is impacted by any metric of diversity or turnover (Table 5.2), Moran's I (I_{CL}) is more likely to suggest clustering within families (i.e., a value of greater than 0) as compared to Pearson's correlation coefficient (R_{CL}). Ten of the twenty-three time intervals analyzed for extinction have an R_{CL} value of above 0 ($p = 0.678$, exact binomial test), whereas nineteen of the twenty-three time intervals have an I_{CL} value of above 0 ($p = 0.003$, exact binomial test). The effect is less pronounced, but still apparent, for origination (15/24 intervals, $p = 0.308$ for R_{CL}; 19/24 intervals, $p = 0.023$ for I_{CL}; exact binomial tests).

R_{CL} and I_{CL} values differ in sign and magnitude in several time intervals. One critical interval is immediately following the K-Pg extinction during the Puercan (66.0 – 63.9 Ma), where the high R_{CL} value suggests a phylogenetically conservative extinction while the value of I_{CL} does not exceed the 95% confidence limits of the null model (Figure 5.3). During the Bridgerian (50.1 – 46.3 Ma), I_{CL} would suggest a significantly clustered extinction while R_{CL} does not exceed the limits of the null model and is also negative. The value of I_{CL} suggests significant extinction clustering during the Whitmeyan (32 – 30 Ma), Arikareean (30.0 – 18.8 Ma), Hemingfordian (18.8 – 16 Ma), and Blancan (4.8 – 1.4 Ma); R_{CL} does not exceed the limits of the null model in any of these intervals (Table 5.3). The effect is also apparent for originations, where R_{CL} never exceeds the limit of the null model, while I_{CL} suggests significant phylogenetic clustering in origination during the Torrejonian (63.9 – 60.9 Ma), Chadronian (36.9 – 33.7 Ma), Hemingfordian, and Clarendonian (12.6 – 9.0 Ma). The difference in signs between I_{CL} and R_{CL} cannot be explained as resulting from sample size, as there is no consistent metric of taxonomic diversity that explains these different responses (Table 5.2).

Overall, taxonomically clustered extinction is more pronounced in the Paleogene than in the Neogene (Figure 5.2). Nine of the twenty-four intervals in the Paleogene (12 each for R_{CL} and I_{CL}) show significant clustering as compared to three of the eighteen intervals

in the Neogene (Paleogene, p = 0.087; Neogene, p = 0.008; exact binomial tests). No such difference exists when comparing between taxonomically clustered originations in the Paleogene and Neogene (all $p > 0.05$; exact binomial tests). Both R_{CL} and I_{CL} suggest significantly clustered extinctions occurred during the Torrejonian (*ca.* 63.9 – 60.9 Ma), the Tiffanian (*ca.* 60.9 – 56 Ma), and the Orellan (*ca.* 33.7 – 32 Ma), all of which fall within the Paleogene (Figure 5.2; Table 5.3). None of these intervals are characterized by above average extinction rates: the Torrejonian and Tiffanian occur during the late Paleocene (after the K-Pg extinction and before the PETM), while the Orellan is the final NALMA of the Eocene (coinciding with the EOT). No clustered extinctions are associated with Neogene biotic crises (either the LPE or the current biodiversity crisis).

We constructed heatmaps of the percentage of extinction and origination occurring during each NALMA to document the changing taxonomic composition of North American mammals throughout the Cenozoic (Figure 5.3). We used taxonomic orders of occurrences in the PBDB to construct these heatmaps, recognizing that some of these orders (e.g., Condylarthra, Insectivora) are paraphyletic or polyphyletic. We also highlight which mammalian families experienced higher-than-average clustering for each of the moderately or significantly clustered intervals, and list their ecological traits (body size, diet, and life habit) in Supplemental Tables 14 and 15. In the NALMAs following the K-Pg extinction, disproportionately high extinction rates occur in small-bodied mammals (i.e., $<$1 kg in body mass) and arboreal and scansorial (climbing) mammals (Supplemental Table 14). The feeding ecology of these groups was diverse and distributed evenly amongst carnivores, omnivores, insectivores, and herbivores; thus, diet did not predict which groups would be disproportionately represented in these extinctions. During the Orellan, the NALMA that coincides with the EOT, 6 of the 8 families with disproportionate extinction were rodents of similar body size, feeding ecology, and life habit (Supplemental Table 14). The disproportionate loss of rodent families during the EOT represents the largest loss of evolutionary history concentrated in one taxonomic order in the entire study interval.

Figure 5.3: Heatmaps of the percentage of total interval (A) extinctions (orange) and (B) originations (violet) for Cenozoic mammal orders for each NALMA (Table 5.3). Percentage values are relative to all extinctions or originations that occurred in that interval.

5.4 Discussion

As originally observed by Darwin (1859), closely-related taxa are more likely to interact intensely with one another than with distantly-related taxa. This leads to a direct relationship between the intensity of interspecific interactions (e.g., mutualism, commensalism, amensalism) and the net ecological similarity of taxa; thus, closely-related taxa tend to be more ecologically similar than distantly-related taxa (Harvey and Pagel 1991; Burns and Strauss 2011). A community composed of taxa that are more closely-related than expected by chance might therefore indicate a community shaped by habitat filtering, wherein those taxa share traits important for their persistence in that environment (e.g., diet, life habit, body size). Such closely-related communities are thus shaped primarily by abiotic (i.e., climatic, geographical) factors. In contrast, a community could be composed of distantly-related taxa as a result of current or past competitive exclusion between similar (and thus closely-related) taxa and/or as a result of convergent evolution in traits important for persistence in a given environment (Cavender-Bares et al. 2004; Fraser et al. 2015). A community comprised of distantly-related taxa (or taxa that are random with respect to higher-order taxonomic membership) would therefore by shaped primarily by biotic (i.e., competition, predation) factors. Although competition among entire clades is generally considered a rare process, recent work has suggested that it can play a more substantial role than climate change in determining which clades speciate and which go extinct (Silvestro et al. 2015). Thus, phylogenetically clustered extinctions may indicate that abiotic factors drove extinction, while phylogenetically random extinctions might implicate biotic extinction drivers (e.g., competition or predation).

The low frequency of clustering indices (both R_{CL} and I_{CL}) above the range of the null model suggests that phylogenetic conservatism in North American mammals throughout the Cenozoic is the exception, rather than the rule (Figure 5.2, Table 5.3). Two distinct intervals of phylogenetically conserved (i.e., ecologically severe) extinction occur during the Paleogene: the earlier interval persists throughout the Paleocene, with the most recent

clustered extinction occurring in the interval just prior to the onset of the PETM *ca.* 55.5 Ma (Bowen et al. 2015); the latter interval coincides with the EOT, characterized by a rapid (∼300,000 year) decrease in global mean surface temperatures of 3° – 5° C *ca.* 33.7 Ma (Liu et al. 2009). Only one of these intervals (the Puercan) occurs during a period of high extinction rate, suggesting that the ecological severity of biotic crises is decoupled from the taxonomic severity of extinction during these intervals. While extinction magnitude was low-to-moderate during the late Paleocene and the Eocene-Oligocene transition, the loss of evolutionary history during these periods would critically shape the resultant character and structure of mammalian ecosystems in North America. In the following paragraphs, we review our data within the context of the major biotic crises in North American mammals over the last 70 million years.

The K-Pg extinction caused biological turnover on a nearly unprecedented scale in Earth history (Alroy 2008). Although all major Cretaceous mammalian lineages survived the K-Pg extinction, mammals were also severely impacted by the bolide impact that triggered these losses (Schulte et al. 2010). However, our analysis contributes to a growing body of literature documenting heterogeneous responses amongst the major mammalian clades present in North America during this time (Alroy 1999; Springer et al. 2003; Bininda-Emonds et al. 2007; Pires et al. 2018). We find evidence that metatherians (Didelphimorphia, Marsupialia, and Deltatheroida) were disproportionately impacted by the K-Pg extinction, with a high extinction proportion (8/19 extinct genera were metatherians) confirming a classic mass extinction response (Figure 5.3A; Supplemental Table 14) (Pires et al. 2018). We show low origination rates for multituberculates from the Lancian to the Puercan, substantiating previous evidence that multituberculates suffered a mass depletion across the K-Pg interval (Figure 5.3B; Supplemental Table 15) (Pires et al. 2018). We also find evidence for low extinction rates in all Eutherian mammal clades across the K-Pg boundary (Lancian and Puercan), and document evidence for higher origination rates across multiple eutherian lineages beginning in the Puercan (Figure 5.3B). This supports

previous evidence for a mass turnover in eutherian mammals across the K-Pg boundary, with origination and extinction peaking across this interval (Pires et al. 2018). While origination rate spikes during the Puercan (Table 5.2), the suite of mammals that appear at this time do so evenly across lineages (Figure 5.3B) – corroborating previous evidence that mammals did not explosively diversify across the K-Pg boundary, despite the environmental niches made available by the extinction of the dinosaurs (Alroy et al. 2000; Springer et al. 2003; Bininda-Emonds et al. 2007).

The Clarkforkian-Wasatchian boundary (*ca.* 55 Ma) has long been recognized as an interval of extreme biotic change marked by a major ordinal replacement event (Gingerich 1989; Clyde and Gingerich 1998; Alroy et al. 2000). Our data suggest that artiodactyl, perissodactyl, and rodent genera first begin to appear in North America during the Clarkforkian (Figure 5.3B). True primates and hyaeonodontid creodonts also continue to proliferate around this time. These first appearances are likely tied to the concurrent PETM, a warming episode that was extremely rapid (<30,0000 years), which may have facilitated immigration from Eurasia via the exposure of high-latitude land bridges (Gingerich 1989; Koch et al. 1992; Bears 1998; Hooker 1998). Once in North America, each of these groups began to speciate rapidly (Alroy et al. 2000). Our data suggest that the loss of evolutionary history during the PETM was relatively minor, with low R_{CL} and I_{CL} values indicating random extinctions (Figure 5.2C,E), although the rate of extinction was quite high (Figure 5.2A). This may suggest that warm temperatures facilitated an increase in species' geographic ranges, which in turn permitted increased intensity of interspecies interactions such as competition and predation.

The EOT was a period of rapid global cooling, with a decrease in mean annual temperature of $\sim 8^{\circ}$ C (Zanazzi et al. 2007), which may have led towards intense selection against warm-adapted species. 50% of mammalian genera that went extinct at this interval were rodents (n = 14); the remainder were mostly carnivores and artiodactyls (Figure 5.3A). Most taxa impacted were ground-dwelling herbivores of small body sizes (Supplemental Table

14). Cooling during this interval may have led towards habitat filtering in many of these archaic groups, which led towards their replacement by many of the newly-immigrating groups to North America (Janis 1993; Prothero and Heaton 1996). Prior to this extinction was a high rate of origination that was moderately clustered (Table 5.3), suggesting biotic-fueled emigration. During the late Eocene, the vast majority of disproportionately-impacted families belonged to Rodentia, as well as the bear family (Ursidae) and the rabbit family (Leporidae) (Figure 5.3A, Supplemental Table 14). While the number of extinctions in mammals was relatively minor in contrast to terrestrial gastropods, amphibians, and reptiles (Prothero and Heaton 1996), our analysis suggests that the evolutionary impact of these extinctions were significant. Cooling climates may have broken up forest canopies in favor of grasslands, which would have selected against archaic mammal groups, many of which were adapted to forest browsing or arboreal life (Prothero 1994). Subsequently, originating taxa (e.g., dogs, camels, rhinos, pocket gophers) came to dominate later Oligocene and Miocene faunas (Janis 1993).

Our data do not suggest any major losses or gains in evolutionary history during the MMCO, nor do they suggest an above-average rate of extinction or origination (Figure 5.2). Previous studies have documented significant turnover within many lineages, and heavy selection against large ungulate browsers and rodents (e.g., Barnosky and Carrasco 2002; Hopkins 2007). The findings of this study are not inconsistent with these prior studies, but rather support the stepwise replacement of herbivore and carnivore guilds that occurred throughout the late Paleogene. 'Originations,' resulting mostly from emigrating taxa from Eurasia (including of felids, proboscideans, and borophagine canids; Janis 2004), were spread fairly evenly across taxonomic lineages. These relatively random extinctions with respect to group membership may parallel the earlier PETM, suggesting that competition may have been a driving force in this turnover (as seen in some equid taxa in the Railroad Canyon section from Idaho, Harris 2016). Future stable isotope studies focusing on co-occurring species with similar dietary, behavioral, or environmental niches in

MMCO sediments may help corroborate this finding.

The LPE have been and continue to be thoroughly studied by paleontologists, archeologists, and modern conservation ecologists. In North America, extinctions occurred in two pulses though to be tied to climate change: an earlier extinction of warm-adapted mammals from 45-20 ka coinciding with the onset of the last glacial maximum (LGM), and a later loss of cold-adapted mammals between 12-9 ka (Barnosky et al. 2004). Our data parallel this, with a large number of Rancholabrean extinctions (n=17) and Santarosean extinctions (n=38). Because of the very short duration of these intervals, extinction rates are quite high, and the Santarosean extinctions are off the chart of Figure 5.2. Interestingly, neither extinction nor origination are significantly clustered during these intervals (Table 5.3). However, paleontologists are well-aware of the ecological ramifications of these extinctions, such as the disproportionate loss of ecosystem engineers and large-bodied mammals leading towards widespread habitat and environmental changes (e.g., Owen-Smith 1987; Gill et al. 2009; Johnson 2009; Malhi et al. 2016). Thus, phylogenetic clustering is only one means of measuring the ecological severity of extinctions. The LPE were likely driven principally by human predation, although climate change controlled the timing, geography, and magnitude of the extinctions (Koch and Barnosky 2006).

5.5 Conclusions

Our analysis into the frequency of phylogenetic selectivity in North American mammals suggests that the taxonomic selectivity and ecological severity of extinctions are decoupled. Whereas the highest extinction rates coincide with major biotic crises (the K-Pg extinction, the PETM, the Late Pleistocene extinction of megafauna, and the arrival of *Homo sapiens* in North America), the most phylogenetically selective extinctions coincide with an interval of moderate but consistent warming and the appearance of multiple eutherian lineages in North America (the Paleocene) and an interval of rapid cooling (the Eocene-Oligocene Transition). These intervals of phylogenetically clustered extinction may sug-

gest that abiotic drivers of extinction (e.g., rapid climate or environmental change) selected against characters that are phylogenetically conserved, such as body size and/or life habit. By contrast, biotic drivers of extinction (e.g., competition and predation) may have resulted in phylogenetically random extinctions during intervals such as the Santarosean, Rancholabrean, Clarkforkian, and Lancian. Our study yields promising results for examining the relationships between extinction trigger, extinction magnitude, and phylogenetic signal in mammalian faunas.

Chapter 6

SYNTHESIS

The overall goal of this dissertation was to interrogate past ecosystems and their response to disturbance using both "near-time" and "deep-time" approaches. The specific objectives were to: 1) improve our understanding of megaherbivore paleoecology using geochemical and textural proxies for diet; 2) use these proxy records to reconstruct the dietary niches of extinct megafauna and infer competition and niche partitioning in past mammalian communities; and, 3) assess whether and how past biotic crises impacted ecosystem structure and function in North American mammals. In pursuing these objectives, the above chapters examine several paleontological case-studies at different temporal and spatial scales. Here, I review the major conclusions from each chapter and comment on future avenues for progress.

Chapter 2 examined dietary variability in mammoths and mastodons by examining the relationship between the physical properties of diet (using dental microwear textures) and the geochemical properties of diet (stable carbon isotopes). Three important conclusions came out of this chapter. First, we were able to show that co-occurring mammoths and mastodons with stable isotope data suggesting grazing and browsing habits, respectively, had statistically indistinguishable dental microwear texture attribute data. This challenges the classic dietary category habits and confirms that extinct proboscideans, like modern ones, had diets that relied on foods of widely varying physical properties. Second, we find no evidence for a difference in diet between juvenile and adult mammoths or mastodons, suggesting that dietary ecology did not change with age in these species. Third, we demonstrate that the Channel Islands mammoths, off the coast of California, had much more variable diets than their mainland counterparts based on microwear. These findings support previous studies that suggested a closed-forest environment on Santa Rosa Island and

confirms that mammoths on the Channel Islands consumed more woody bark and browse than their mainland counterparts.

Recognizing that dental microwear textures and stable isotopes can be used in conjunction to provide a more complete reconstruction of dietary habits, in Chapter 3 we sought to provide evidence for competitive interactions in sympatric probosideans. Two major conclusions from this work were that co-occurring mammoths and gomphotheres consumed similar resources during the Early Pleistocene, and that gomphotheres later changed their dietary tendencies toward a more mixed-feeding habit while mammoths remained hyper-efficient generalists. While the ultimate extinction of the gomphothere clade was likely due to the culmination of millions of years of environmental turnovers and biotic stressors, our results from this chapter demonstrated that competition between mammoths and *Cuvieronius* was highly prevalent in the Atlantic Coastal Plain of North America throughout the Pleistocene. This chapter was significant in that it documented that multiple dietary proxies cab be used to infer interspecific interactions, including niche partitioning and competition. The use of such data can be invaluable for testing extinction hypotheses and construction predictive models for understanding what might go extinct in the future, particularly when preferred food becomes scarce as a result of climate or environmental change. Future studies testing for signtures of competition in the fossil record would benefit from relying on multiple sources of information into how species express their dietary and/or behavioral niches.

In Chapter 4, we examined another case study of co-occurring megaherbivores in the Pleistocene in order to test hypotheses regarding mammalian dietary responses to climate and environmental change. In contrast to the previous chapter, we documented prevalent niche partitioning amongst sympatric megafauna, suggesting that the splitting of resources permitted multiple species to thrive both before and after the last glacial maximum. Further, the average mesowear scores of these mammals did not significantly differ between Diamond Valley Lake and Rancho La Brea, suggesting similar overall feeding ecologies. In

contrast, differences in local vegetation may be driving the differences in short-term diet as recorded by dental microwear textures. This chapter suggested several avenues for future research into the migratory habits of local horses, bison, and camels using stable isotope analysis. Additionally, a paleobotanical analysis of Diamond Valley Lake - particularly of the younger, post-LGM sediments - will help to clarify any differences between taxa recovered from the two units. The main conclusion to stem from this chapter is that large mammals at Diamond Valley Lake were resilient to climate and environmental change and did not significantly alter their dietary niches despite these changes.

While 'near-time' paleoecological studies compare conditions before and after a major disturbance, 'deep-time' studies take advantage of the longer geological record to investigate biological response to change. Chapter Five followed a 'deep-time' approach by testing for unique patterns in mammal community response to stress over the last 70 million years. We showed that the taxonomic magnitude of extinction events was decoupled from the amount of evolutionary history lost – biotic crises did not always result in major losses of evolutionary history. By contrast, intervals not usually associated with extinction events coincided with major losses in evolutionary history. These previously unrecognized impacts on mammalian community structure suggest different drivers of extinction; clustered extinctions potentially resulted from habitat filtering, while extinctions that were random with respect to group membership may reflect biotic factors such as competition or predation. This chapter yielded promising results for examining the relationships between extinction trigger, extinction magnitude, and phylogenetic signal in mammalian faunas.

The central theme of this dissertation is paleoecology; that is, the application of ecological theory to paleontological records. Paleoecology continues to provide novel insights into the ecological dynamics of extinct communities. As the impacts of climate change, exacerbated by anthropogenic inputs, continue to be felt by modern communities, conservation practices will increasingly rely upon accurate assessments of the dietary, behavioral, and environmental niches of their extinct relatives. Stable isotope analysis and dental tex-

tures (microwear and mesowear) are two dietary proxy data sources that can be used to quantify such niches. Because these proxy sources represent different time scales (from days to months to years) from different proximal sources (geochemical to physical), using them in tandem can reveal more nuances than can be used to detect mammalian response to change. Future studies should continue to rely upon high-resolution proxy data from a variety of sources to test fundamental theories in paleoecology. This dissertation was a step towards understanding mammalian responses to climate and environmental change at various spatial and temporal scales.

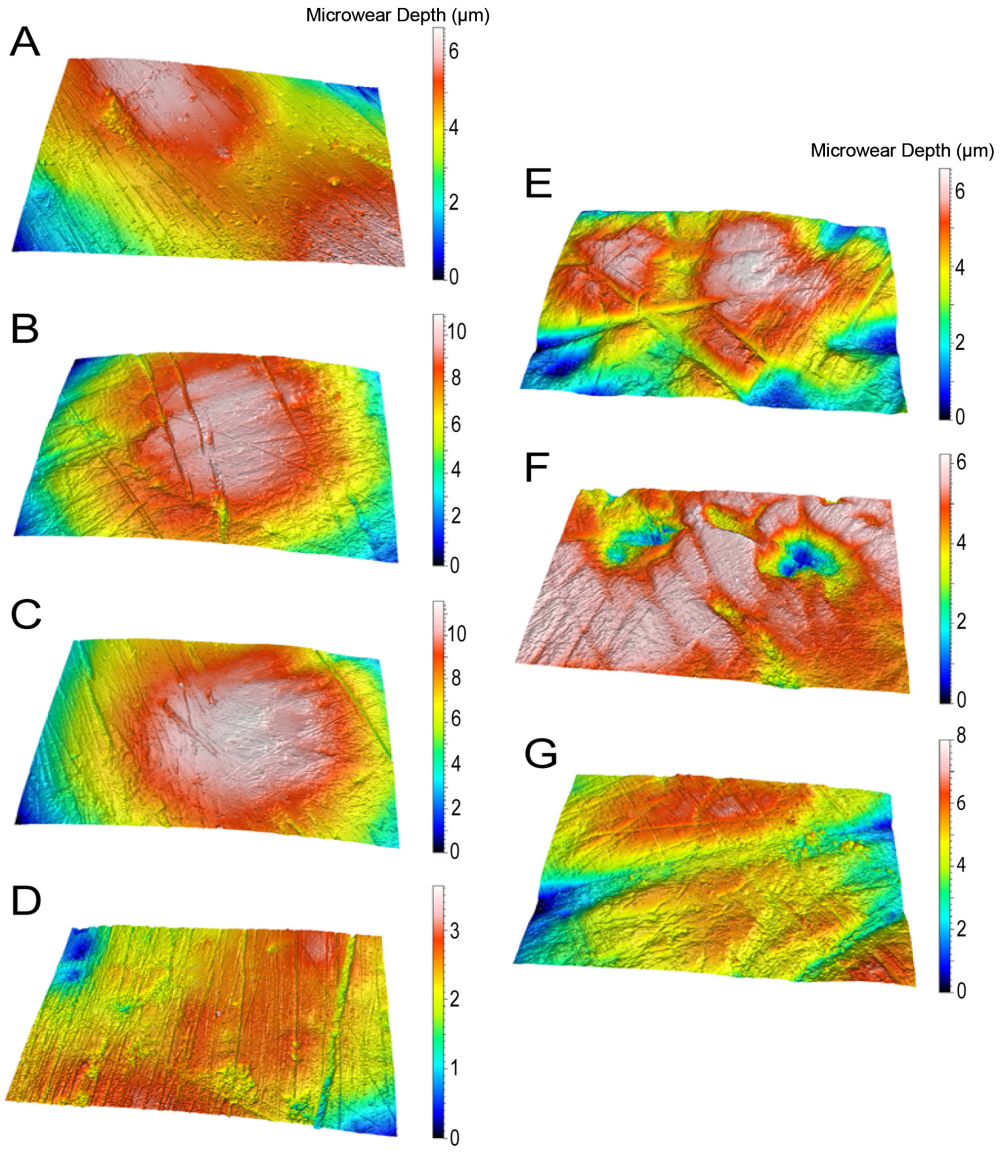

Supplemental Figure 1: 3D surface models showing examples of microwear for proboscidean populations used in this study. (A) Ingleside *Mammuthus columbi*, (B) Cypress Creek *Mammuthus columbi*, (C) Friesenhahn adult *Mammuthus columbi*, (D) Friesenhahn juvenile *Mammuthus columbi* (E) Ingleside *Mammut americanum*, (F) Friesenhahn *Mammut americanum*, (G) Santa Rosa Island *Mammuthus exilis*.

Appendix B: Supplemental Tables

Supplemental Table 1: Stable isotope data for all specimens used in Chapter 2.

Taxon	**Catalog Number**	**Locality**	**Tooth**	$\delta^{13}C_{enamel}$ (‰ V-PDB)	$\delta^{18}O_{enamel}$ (‰ V-SMOW)
Mammut americanum	TMM30967-50	Ingleside	rm3	-10.4	30.1
	TMM30967-247	Ingleside	m	-11.2	31.7
	TMM30967-257	Ingleside	rm3	-11.0	30.2
	TMM30967-339	Ingleside	m	-10.7	29.8
	TMM30967-351	Ingleside	m	-9.5	29.6
	TMM30967-352	Ingleside	m	-10.1	30.7
	TMM30967-470	Ingleside	m	-12.0	31.2
	TMM30967-525	Ingleside	m	-11.9	30.8
	TMM30967-591	Ingleside	M	-9.9	30.3
	TMM30967-593	Ingleside	m	-11.1	31.7
	TMM30967-672	Ingleside	m3	-12.6	30.6
	TMM30967-727	Ingleside	m	-11.7	30.4
	TMM30967-728	Ingleside	rm3	-10.5	30.9
	TMM30967-899	Ingleside	m	-12.4	28.6
	TMM30967-906	Ingleside	rm3	-10.6	28.5
	TMM30967-980	Ingleside	m	-11.4	29.0
	TMM30967-1606	Ingleside	m	-12.5	30.6
	TMM30967-1650	Ingleside	rm3	-10.7	29.6
	TMM30967-1766	Ingleside	lm2	-10.8	29.2
Mammuthus columbi	TMM47200-12	Cypress Creek	DP3	-3.4	31.0
	TMM47200-149	Cypress Creek	m	-3.9	29.2
	TMM47200-150	Cypress Creek	m	-4.3	28.5
	TMM47200-152	Cypress Creek	m	-4.1	29.4
	TMM47200-154	Cypress Creek	m	-3.8	29.7
	TMM47200-159	Cypress Creek	m	-3.0	29.4
	TMM47200-161	Cypress Creek	M3	-4.9	29.6
	TMM47200-162	Cypress Creek	M3	-2.9	30.8
	TMM47200-173	Cypress Creek	M3	-3.6	30.7
	TMM47200-174	Cypress Creek	M2	-4.2	28.9
Mammuthus columbi	TMM933-133	Friesenhahn	M2or3	-5.1	29.9
	TMM933-296	Friesenhahn	M1	-1.5	30.0
	TMM933-358	Friesenhahn	M2	-1.4	29.1
	TMM933-928	Friesenhahn	M1	-2.1	29.3
	TMM933-1006	Friesenhahn	dp4	-0.1	29.9

Taxon	Catalog Number	Locality	Tooth	δ^{13}C (‰ V-PDB)	δ^{18}O (‰ V-SMOW)
	TMM933-1013	Friesenhahn	m	-1.2	30.4
	TMM933-1309	Friesenhahn	m	-1.7	28.1
	TMM933-1505	Friesenhahn	M3	-0.1	30.1
	TMM933-1506	Friesenhahn	M2or3	-1.2	29.2
	TMM933-1507	Friesenhahn	M1or2	-3.4	29.3
	TMM933-2014	Friesenhahn	M3	0.0	30.0
	TMM933-2015	Friesenhahn	M2or3	-1.4	28.9
	TMM933-2022	Friesenhahn	dPorM1	-3.9	30.2
	TMM933-2243	Friesenhahn	M1	-1.1	29.2
	TMM933-2676	Friesenhahn	m	-1.9	30.1
	TMM933-3407	Friesenhahn	m	-3.5	31.1
Mammuthus columbi	TMM30967-148	Ingleside	M3	-2.6	30.0
	TMM30967-165	Ingleside	M3	-1.6	30.1
	TMM30967-500	Ingleside	lm2	-1.4	30.4
	TMM30967-679	Ingleside	m	-0.8	30.1
	TMM30967-1214	Ingleside	M3	-1.0	29.9
	TMM30967-1322	Ingleside	m	0.2	31.4
	TMM30967-1724	Ingleside	M3	-1.1	29.9
	TMM30967-1787	Ingleside	rm2	-1.1	28.0
	TMM30967-1818	Ingleside	RM3	-2.3	28.5

TMM, Texas Memorial Museum. Tooth = tooth position, lower case abbreviations indicate mandibular teeth, upper case abbreviations indicate maxillary teeth, right (r), left (l), deciduous pre-molar (dp), molar (m), and numerical tooth position, if known. Stable isotope data were normalized to NBS-19 and are reported in conventional delta (δ) notation; stable carbon isotope data are reported relative to V-PDB, and stable oxygen isotope data are reported against V-SMOW. The following equation was used to convert oxygen values from V-PDB to V-SMOW: $\delta_{\mathrm{VSMOW}} = 1.03086 * \delta_{\mathrm{VPDB}} + 30.86$ (Friedman and O'Neil 1977).

Supplemental Table 2: DMTA data for all specimens used in Chapter 2.

Taxon	**Catalog Number**	**Locality**	**Tooth**	**Age Description**	***Asfc***	***epLsar***	***Tfv***	***HAsfc*$_{3x3}$**	***HAsfc*$_{9x9}$**
Mammut	TMM933-327	Friesenhahn	dp2	Juvenile	1.063	0.0048	12890.27	0.214	0.566
americanum	TMM933-1292	Friesenhahn	DP2	Juvenile	1.047	0.0047	13724.64	0.332	0.869
	TMM933-1767	Friesenhahn	DP2	Juvenile	0.741	0.0040	10113.9	0.197	0.460
	TMM933-1768	Friesenhahn	DP2	Juvenile	2.759	0.0027	12658.1	0.376	0.739
	TMM933-3414	Friesenhahn	DP2	Juvenile	0.429	0.0011	13078.25	0.207	0.354
	TMM933-3609	Friesenhahn	DP2	Juvenile	0.660	0.0049	11784.2	0.184	0.335
	TMM933-3971	Friesenhahn	dp3	Juvenile	2.223	0.0016	4846.803	0.810	1.663
Mammut	TMM30967-50	Ingleside	rm2	Young Adult	2.211	0.0050	9147.276	0.418	0.813
americanum	TMM30967-141	Ingleside	mx	unknown	1.675	0.0018	12204.42	0.212	0.479
	TMM30967-156	Ingleside	M2	Mature	1.343	0.0030	12898.62	0.143	0.277
	TMM30967-159	Ingleside	m2	Mature	2.337	0.0015	10822.49	0.229	0.459
	TMM30967-205	Ingleside	lm1	Young Adult	0.976	0.0034	11233.11	0.472	0.684
	TMM30967-247	Ingleside	M2	Mature	6.004	0.0025	12262.53	0.405	0.616
	TMM30967-257	Ingleside	rm3	Mature	3.812	0.0040	14141.71	0.861	3.050
	TMM30967-338	Ingleside	lm3	Mature	1.117	0.0049	8649.135	0.279	0.421
	TMM30967-339	Ingleside	rm3	Mature	0.715	0.0064	1334.408	0.933	1.861
	TMM30967-344	Ingleside	mx	unknown	0.947	0.0084	10674.32	0.501	0.714
	TMM30967-351	Ingleside	mx	unknown	3.301	0.0009	13483.17	0.348	0.649
	TMM30967-352	Ingleside	rm3	Mature	1.202	0.0037	5637.2	0.295	0.465
	TMM30967-384	Ingleside	M2	Mature	2.308	0.0018	11755.13	0.264	0.547
	TMM30967-395	Ingleside	dp4	Youth	3.028	0.0028	11458.23	0.645	0.898
	TMM30967-414	Ingleside	rm3	Mature	2.081	0.0013	13183.73	0.185	0.384
	TMM30967-470	Ingleside	M2	Young Adult	3.065	0.0019	7102.654	0.382	0.568
	TMM30967-525	Ingleside	m2	Mature	1.389	0.0024	11273.48	0.178	0.295
	TMM30967-591	Ingleside	lm3	Mature	3.670	0.0068	10433.5	0.867	1.380
	TMM30967-593	Ingleside	M2	Mature	4.794	0.0023	12624.29	0.188	0.465
	TMM30967-672	Ingleside	rm3	Mature	2.928	0.0017	8247.79	0.289	0.387

Taxon	Catalog Number	Locality	Tooth	Age Description	*Asfc*	*epLsar*	*Tfv*	$HAsfc_{3x3}$	$HAsfc_{9x9}$
	TMM30967-727	Ingleside	M1	Youth	3.808	0.0039	15098.74	0.669	1.173
	TMM30967-728	Ingleside	lm3	Mature	11.717	0.0021	16546.72	0.290	0.611
	TMM30967-773	Ingleside	RM2	Young Adult	0.809	0.0028	9231.639	0.351	0.621
	TMM30967-777	Ingleside	M1	Young Adult	1.648	0.0040	10592.12	0.375	1.084
	TMM30967-856	Ingleside	M1	Young Adult	1.362	0.0067	10320.64	0.457	0.705
	TMM30967-899	Ingleside	dp4	Youth	4.321	0.0036	12007	0.298	0.624
	TMM30967-904	Ingleside	rm3	Young Adult	1.617	0.0039	9830.81	0.985	1.289
	TMM30967-906	Ingleside	rm3	Young Adult	1.786	0.0036	11852.37	0.354	0.587
	TMM30967-980	Ingleside	rm3	Young Adult	3.275	0.0040	507.0205	0.456	1.076
	TMM30967-1606	Ingleside	m2	Mature	3.938	0.0047	4317.442	0.255	0.499
	TMM30967-1714	Ingleside	LM1	Youth	0.857	0.0015	8740.816	0.336	0.575
	TMM30967-1786	Ingleside	DP4	Youth	1.852	0.0017	14237.29	0.312	0.530
Mammuthus	TMM47200-12	Cypress Creek	DP3	W Juvenile	1.179	0.004	15760.02	0.638	0.991
columbi	TMM47200-149	Cypress Creek	mx	unknown	1.494	0.0030	7060.769	0.284	0.495
	TMM47200-150	Cypress Creek	mx	unknown	2.541	0.0026	12932.43	0.191	0.346
	TMM47200-152	Cypress Creek	mx	unknown	1.643	0.0020	3870.442	0.459	0.689
	TMM47200-154	Cypress Creek	mx	unknown	0.794	0.0072	22468.09	0.857	1.333
	TMM47200-159	Cypress Creek	mx	unknown	1.956	0.0053	21534.26	0.233	0.335
	TMM47200-161	Cypress Creek	M3	Mature	1.407	0.0040	16963.26	0.290	0.595
	TMM47200-162	Cypress Creek	M3	Mature	2.441	0.0043	11771.72	0.642	1.061
	TMM47200-163	Cypress Creek	mx	unknown	3.840	0.0023	17039.23	0.265	0.577
	TMM47200-168	Cypress Creek	mx	unknown	1.111	0.0035	22432.91	0.273	0.534
	TMM47200-173	Cypress Creek	M3	Mature	3.183	0.0042	13759.7	0.496	0.836
	TMM47200-174	Cypress Creek	M1 or M2	Youth	2.283	0.0044	32491.46	0.414	0.910
Mammuthus	TMM933-296	Friesenhahn	DP4 or M1	Youth	1.442	0.0034	11036.05	0.384	0.523
columbi	TMM933-358	Friesenhahn	DP4 or M1	P-W Juvenile	3.235	0.0057	14502.78	0.256	0.468
	TMM933-363	Friesenhahn	dp3	W Juvenile	2.957	0.0041	14956.13	0.318	0.642
	TMM933-918	Friesenhahn	DP3	W Juvenile	6.471	0.0046	15453.00	0.520	0.706

Taxon	Catalog Number	Locality	Tooth	Age Description	*Asfc*	*epLsar*	*Tfv*	$HAsfc_{3x3}$	$HAsfc_{9x9}$
	TMM933-928	Friesenhahn	M1	P-W Juvenile	4.690	0.0035	16973.20	0.308	0.523
	TMM933-1004	Friesenhahn	M1 or M2	Young Adult	2.254	0.0013	12135.35	0.432	0.553
	TMM933-1005	Friesenhahn	DP4	W Juvenile	2.592	0.0044	12209.77	0.672	0.927
	TMM933-1006	Friesenhahn	m1	Youth	3.593	0.0055	10713.01	0.407	0.734
	TMM933-1190	Friesenhahn	DP3	W Juvenile	2.386	0.0052	12726.89	0.339	0.665
	TMM933-1505	Friesenhahn	M2	Young Adult	1.931	0.0069	13093.77	0.556	0.915
	TMM933-1508	Friesenhahn	dp3	W Juvenile	0.774	0.0092	11516.14	0.386	0.715
	TMM933-1511	Friesenhahn	dp3	W Juvenile	3.877	0.0079	16966.19	0.471	0.928
	TMM933-1762	Friesenhahn	dp3	W Juvenile	3.274	0.0048	14257.36	0.324	0.570
	TMM933-1993	Friesenhahn	dp4/DP4	W Juvenile	4.416	0.0034	11767.52	0.384	0.705
	TMM933-2014	Friesenhahn	M3	Mature	0.937	0.0050	6891.021	0.638	1.189
	TMM933-2015	Friesenhahn	M1 or M2	Young Adult	1.752	0.0021	14854.19	0.614	1.246
	TMM933-2053	Friesenhahn	dp3	W Juvenile	3.805	0.0027	11825.29	0.433	0.974
	TMM933-2161	Friesenhahn	dp3	W Juvenile	1.742	0.0042	4431.57	0.377	0.812
	TMM933-2241	Friesenhahn	M1	Youth	1.608	0.0086	13633.32	0.316	0.700
	TMM933-2243	Friesenhahn	DP4 or M1	Youth	4.321	0.0041	11554.79	1.059	2.095
	TMM933-2305	Friesenhahn	dp3	W Juvenile	3.615	0.0070	14607.27	0.422	0.916
	TMM933-2459	Friesenhahn	dp3	P-W Juvenile	4.862	0.0064	12462.43	0.350	1.029
	TMM933-2466	Friesenhahn	dp3	W Juvenile	1.622	0.0060	13942.72	0.370	0.844
	TMM933-2470	Friesenhahn	DP3	W Juvenile	1.525	0.0090	14269.42	0.489	0.718
	TMM933-2489	Friesenhahn	dp4	W Juvenile	2.147	0.0027	10538.71	0.223	0.376
	TMM933-2672	Friesenhahn	DP4	P-W Juvenile	0.457	0.0019	8538.974	0.493	0.891
	TMM933-2810	Friesenhahn	dp4	P-W Juvenile	6.241	0.0050	14153.86	0.341	0.615
	TMM933-2901	Friesenhahn	dp3	W Juvenile	1.865	0.0069	10658.04	0.522	1.198
	TMM933-3464	Friesenhahn	DP3	W Juvenile	4.806	0.0048	12011.9	0.445	0.941
	TMM933-3811	Friesenhahn	DP3	W Juvenile	3.218	0.0013	11953.67	0.195	0.375
	TMM933-3840	Friesenhahn	DP4	W Juvenile	2.156	0.0049	14325.87	1.664	1.981

Taxon	Catalog Number	Locality	Tooth	Age Description	*Asfc*	*epLsar*	*Tfv*	$HAsfc_{3x3}$	$HAsfc_{9x9}$
Mammuthus	TMM30967-140	Ingleside	M2	Youth	0.839	0.0049	7861.142	0.243	0.489
columbi	TMM30967-148	Ingleside	RM3	Mature	1.568	0.0050	7742.857	0.330	0.549
	TMM30967-160	Ingleside	rm3	Mature	5.937	0.0015	10045.17	0.488	0.779
	TMM30967-162	Ingleside	Mx	unknown	0.837	0.0012	3888.173	0.168	0.436
	TMM30967-165	Ingleside	RM3	Mature	3.545	0.0040	13965.18	0.387	0.568
	TMM30967-166	Ingleside	mx	unknown	1.335	0.0035	4015.505	0.254	0.472
	TMM30967-167	Ingleside	mx	unknown	2.057	0.0028	9624.596	0.204	0.453
	TMM30967-181	Ingleside	rm1	Youth	2.191	0.0005	11178.44	0.227	0.372
	TMM30967-210	Ingleside	M2	Young Adult	4.057	0.0036	11234.08	0.255	0.521
	TMM30967-213	Ingleside	LM3	Mature	2.066	0.0030	10077.36	0.402	0.916
	TMM30967-462	Ingleside	M2	Young Adult	2.440	0.0034	12920.41	0.340	0.775
	TMM30967-500	Ingleside	lm2	Young Adult	2.651	0.0079	18019.48	0.336	0.817
	TMM30967-678	Ingleside	LM2	Youth	0.962	0.0021	9339.051	0.278	0.388
	TMM30967-717	Ingleside	mx	unknown	1.532	0.0013	12516.76	0.431	0.835
	TMM30967-723	Ingleside	RM2	Young Adult	1.522	0.0045	13199.53	0.359	0.607
	TMM30967-1172	Ingleside	rm3	Mature	1.015	0.0030	8180.983	0.157	0.446
	TMM30967-1201	Ingleside	lm2	Mature	4.311	0.0045	12390.49	0.545	0.833
	TMM30967-1214	Ingleside	M3	Mature	1.638	0.0055	13291.53	0.288	0.816
	TMM30967-1600	Ingleside	M1	Youth	0.456	0.0017	6799.187	0.227	0.453
	TMM30967-1601	Ingleside	M1	Youth	3.056	0.0010	739.3141	0.478	1.402
	TMM30967-1652	Ingleside	lm3	Mature	2.059	0.0012	13644.04	0.390	0.675
	TMM30967-1684	Ingleside	RM3	Mature	2.603	0.0058	11527.58	0.499	0.823
	TMM30967-1724	Ingleside	RM3	Mature	2.499	0.0023	11374.14	0.230	0.427
	TMM30967-1729	Ingleside	lm3	Mature	2.381	0.0065	11669.27	0.440	0.663
	TMM30967-1805	Ingleside	LM3	Mature	1.803	0.0027	13012.07	0.266	0.461
	TMM30967-1818	Ingleside	RM3	Mature	4.062	0.0016	13595.39	0.349	0.769

Taxon	Catalog Number	Locality	Tooth	Age Description	*Asfc*	*epLsar*	*Tfv*	$HAsfc_{3x3}$	$HAsfc_{9x9}$
Mammuthus columbi	SBMNHVP1101	Santa Rosa	lm3		2.073	0.0021	13782.56	0.377	0.771
Mammuthus exilis	SBMNHVP836	Santa Rosa	mx		1.061	0.0056	10697.78	0.499	0.664
	SBMNHVP837	Santa Rosa	mx		2.610	0.0048	15270.69	0.324	0.703
	SBMNHVP838	Santa Rosa	M3		0.608	0.0046	12110.58	0.445	0.461
	SBMNHVP868	Santa Rosa	dp4		19.666	0.0017	11894.27	0.976	3.497
	SBMNHVP885	Santa Rosa	mx		4.379	0.0039	14785.14	0.514	0.742
	SBMNHVP930	Santa Rosa	rm2		27.829	0.0018	14002.32	0.764	3.068
	SBMNHVP945	Santa Rosa	mx		1.280	0.0058	11264.37	0.368	0.723
	SBMNHVP950	Santa Rosa	rdp4		16.718	0.0005	12366.26	0.442	1.316
	SBMNHVP961	Santa Rosa	M2		0.537	0.0038	10716.99	0.289	0.401
	SBMNHVP978	Santa Rosa	mx		1.037	0.0037	9668.808	0.276	0.571
	SBMNHVP1000	Santa Rosa	mx		3.028	0.0041	7828.842	0.228	0.454
	SBMNHVP1040	Santa Rosa	LM1		5.926	0.0019	12810.85	0.290	0.618
	SBMNHVP1059	Santa Rosa	mx		2.214	0.0062	8494.075	0.376	0.725
	SBMNHVP1065	Santa Rosa	M2		1.430	0.0037	12570.3	0.353	0.484
	SBMNHVP1078	Santa Rosa	lm3		0.779	0.0009	5345.409	0.175	0.347

Asfc, area-scale fractal complexity; *epLsar*, anisotropy; *Tfv*, textural fill volume, $HAsfc_{3x3}$, $HAsfc_{9x9}$, Heterogeneity of complexity in a 3x3 and 9x9 grid, respectively. Mx and mx refer to upper and lower molar fragments, respectively. Age descriptions come from Supplemental Table 3; W Juvenile = "Weaning Juvenile"; P-W Juvenile = "Post-Weaning Juvenile".

Supplemental Table 3: Molar dimensions, wear stage, and developmental age groupings for *Mammuthus columbi* and *Mammut americanum* specimens used in Chapter 2.

Taxon	TMM Catalog Number	Locality	Tooth	Max. Length (mm)	Max. Width (mm)	Wear Stage	Age Description
Mammut	933-327	Friesenhahn	dp2	27.8	19.2	3	Juvenile
americanum	933-1292	Friesenhahn	DP2	34.7	28.8	0/+ to 1	Juvenile
	933-1767	Friesenhahn	DP2	33.3	29.1	0/+ to 1	Juvenile
	933-1768	Friesenhahn	DP2	37.4	30.0	2	Juvenile
	933-2312	Friesenhahn	DP3	43.3	37.9	0/+	Juvenile
	933-3414	Friesenhahn	DP2	39.5	35.7	2 to 2+	Juvenile
	933-3609	Friesenhahn	DP2	23.1	39.6	0/+ to 1	Juvenile
	933-3971	Friesenhahn	dp3	54.0	38.4	1	Juvenile
	933-3972	Friesenhahn	DP3	42.6	44.5	0/+	Juvenile
	933-3973	Friesenhahn	dp4	79.5	57.3	0/+ to 1	Juvenile
	30967-50	Ingleside	rm2	95.55	72.09	3	Young Adult
	30967-141	Ingleside	mx				unknown
	30967-156	Ingleside	M2	102.86	98.09	4	Mature
	30967-159	Ingleside	m2	135.98	116.05	4	Mature
	30967-205	Ingleside	lm2	100.79	91.27	4	Mature
	30967-247	Ingleside	M2	112.28	94.71	3 to 4	Mature
	30967-257	Ingleside	rm3	*	84.64	3	Mature
	30967-321	Ingleside	LM2	99.7	89.82	4	Mature
	30967-338	Ingleside	lm3	136.15	83.24	3 to 4	Mature
	30967-339	Ingleside	rm3	129.21	82.23	2	Mature
	30967-341	Ingleside	m3	153.93	77.61	3 to 4	Mature
	30967-344	Ingleside	mx				unknown
	30967-351	Ingleside	mx				unknown

Taxon	TMM Catalog Number	Locality	Tooth	Max. Length (mm)	Max. Width (mm)	Wear Stage	Age Description
Mammuthus columbi	47200-12	Cypress Creek	DP3	65.8	54.3	V	Weaning Juvenile
	47200-149	Cypress Creek	mx				unknown
	47200-150	Cypress Creek	mx				unknown
	47200-152	Cypress Creek	mx				unknown
	47200-154	Cypress Creek	mx				unknown
	47200-159	Cypress Creek	mx				unknown
	47200-161	Cypress Creek	M3	*	94.1	n/a	Mature
	47200-162	Cypress Creek	M3	*	87.0	n/a	Mature
	47200-163	Cypress Creek	mx				unknown
	47200-168	Cypress Creek	mx				unknown
	47200-173	Cypress Creek	M3	*	77.8	n/a	Mature
	47200-174	Cypress Creek	M1	100.4	56.5	XIII	Youth
	933-296	Friesenhahn	M1	128.0	68.5	XI	Youth
	933-358	Friesenhahn	M1	128.5	58.6	VIII	Post-Weaning Juvenile
	933-363	Friesenhahn	dp3	52.0	28.0	V	Weaning Juvenile
	933-463	Friesenhahn	dp3	68.0	31.0	II	Weaning Juvenile
	933-537	Friesenhahn	DP3	67.5	58.0	V	Weaning Juvenile
	933-575	Friesenhahn	mx				unknown
	933-918	Friesenhahn	DP3	50.0	28.5	II	Weaning Juvenile
	933-928	Friesenhahn	M1	96.0	57.0	VIII	Post-Weaning Juvenile
	933-1004	Friesenhahn	M2	163.0	70.0	XVI	Young Adult
	933-1005	Friesenhahn	DP4	115.0	56.0	V	Weaning Juvenile
	933-1006	Friesenhahn	dp4 or m1	119.0	76.0	IX or XIII	Youth
	933-1190	Friesenhahn	DP3	72.0	38.0	III	Weaning Juvenile
	933-1505	Friesenhahn	M2	156.5	93.0	XVI	Young Adult
	933-1508	Friesenhahn	dp3	76.0	36.0	V	Weaning Juvenile
	933-1511	Friesenhahn	dp3	52.0	36.0	V	Weaning Juvenile
	933-1762	Friesenhahn	dp3	74.5	35.5	III	Weaning Juvenile

Taxon	TMM Catalog Number	Locality	Tooth	Max. Length (mm)	Max. Width (mm)	Wear Stage	Age Description
	933-1993	Friesenhahn	dp4/DP4	98.0	47.0	V	Weaning Juvenile
	933-2014	Friesenhahn	m3	228.0	87.0	XXV	Mature
	933-2015	Friesenhahn	m2	172.0	54.0	XIV	Young Adult
	933-2053	Friesenhahn	dp3	73.0	30.0	II	Weaning Juvenile
	933-2161	Friesenhahn	dp3	58.0	25.5	II	Weaning Juvenile
	933-2241	Friesenhahn	M1	125.0	53.0	X	Youth
	933-2243	Friesenhahn	M1	96.0	60.0	X	Youth
	933-2305	Friesenhahn	dp3	73.0	43.0	V	Weaning Juvenile
	933-2459	Friesenhahn	DP4	88.0	43.6	VI	Post-Weaning Juvenile
	933-2466	Friesenhahn	dp3	60.0	28.5	IV	Weaning Juvenile
	933-2470	Friesenhahn	DP3	57.0	32.0	IV	Weaning Juvenile
	933-2489	Friesenhahn	dp4	109.0	34.0	IV	Weaning Juvenile
	933-2665	Friesenhahn	dp3	77.0	38.5	V	Weaning Juvenile
	933-2672	Friesenhahn	DP4	92.0	49.0	VI	Post-Weaning Juvenile
	933-2810	Friesenhahn	dp4	65.0	53.0	VI	Post-Weaning Juvenile
	933-2901	Friesenhahn	dp3	74.6	41.0	IV	Weaning Juvenile
	933-2902	Friesenhahn	mx				Unknown
	933-3464	Friesenhahn	DP3	58.5	52.0	V	Weaning Juvenile
	933-3811	Friesenhahn	DP3	72.0	40.0	II	Weaning Juvenile
	933-3840	Friesenhahn	DP4	98.0	46.0	V	Weaning Juvenile
	933-3842	Friesenhahn	DP4	106.0	46.5	V	Weaning Juvenile
	30967-140	Ingleside	M2	120.0	66.0	XIII	Youth
	30967-148	Ingleside	RM3	146.9+	73.1	XXV	Mature
	30967-160	Ingleside	rm3	136.0+	87.3	XXII	Mature
	30967-162	Ingleside	Mx				Unknown
	30967-165	Ingleside	RM3	209.1	90.5	XXVIII	Mature
	30967-166	Ingleside	mx				Unknown
	30967-167	Ingleside	mx				Unknown

Taxon	TMM Catalog Number	Locality	Tooth	Max. Length (mm)	Max. Width (mm)	Wear Stage	Age Description
	30967-181	Ingleside	rm1	198.1	70.0	X	Youth
	30967-210	Ingleside	M2	198.9	89.6	XVII	Young Adult
	30967-213	Ingleside	LM3	211.0	98.1	XXV	Mature
	30967-462	Ingleside	M2	175.7	86.0	XVII	Young Adult
	30967-500	Ingleside	lm2	145.5	63.8	XVII	Young Adult
	30967-678	Ingleside	LM2	97.8+	82.4	XIII	Youth
	30967-717	Ingleside	mx				Unknown
	30967-723	Ingleside	RM2	175.1	78.6	XIV	Young Adult
	30967-1172	Ingleside	rm3	309.1	86.3	XXIII	Mature
	30967-1201	Ingleside	lm3	280.0	87.4	XXV	Mature
	30967-1214	Ingleside	M3	210.4	98.7	XXVI	Mature
	30967-1600	Ingleside	M1	133.3	69.0	XI	Youth
	30967-1601	Ingleside	M1	*	69.6	XI	Youth
	30967-1652	Ingleside	lm3	264.9	85.5	XXV	Mature
	30967-1684	Ingleside	RM3	260.5	116.8	XXVI	Mature
	30967-1724	Ingleside	RM3	195.1+	87.2	XXVIII	Mature
	30967-1729	Ingleside	lm3	198.7	85.6	XXVII	Mature
	30967-1805	Ingleside	LM3	228.9	107.2	XXVI	Mature
	30967-1818	Ingleside	RM3	179.4	94.5	XXV	Mature

Molar dimensions are reported as maximum values; + indicates that the tooth was either partially broken or was missing lophs/lophids and thus the true length is probably larger than the value reported. * indicates that a large portion of the tooth was broken and so the length was not reported; width was used to define wear stage and/or age grouping in those cases. Mx and mx refer to upper and lower molar fragments, respectively – we do not report dimensions, wear stage or age grouping for fragmentary molars. *Mammuthus* wear stages are from Laws (1966) and age descriptions come from Saunders (1977a) with the additional caveat that we split the "Juvenile" age group into "Weaning" (Wear Stage I –V) and "Post-Weaning" (Wear Stage VI –VIII) groups. *Mammut* wear stages and age descriptions are from Saunders (1977b) and Green and Hulbert (2005), although we simplify their schemes by combining the "Mature" and "Old Age" groups and not sub-dividing the "Youth" or "Juvenile" age groups.

Supplemental Table 4: Summary of comparisons (p-values) for all DMTA attributes between Texas mammoth (*Mammuthus columbi*) populations from Chapter 2.

		Ingleside	Friesenhahn
Asfc	Cypress Creek	0.671	0.951
	Ingleside		0.905
epLsar	Cypress Creek	0.823	0.705
	Ingleside		0.335
Tfv	Cypress Creek	**0.008**	0.061
	Ingleside		0.345
$Hasfc_{3x3}$	Cypress Creek	0.276	**0.036**
	Ingleside		**0.005**
$Hasfc_{9x9}$	Cypress Creek	0.371	0.083
	Ingleside		**0.032**

Asfc, area-scale fractal complexity; *epLsar*, anisotropy; *Tfv*, textural fill volume, $Hasfc_{3x3}$, $Hasfc_{9x9}$, Heterogeneity of complexity in a 3x3 and 9x9 grid, respectively. *Asfc* and *epLsar* were compared using a parametric ANOVA with post hoc Tukey HSD; *Tfv*, $Hasfc_{3x3}$ and $Hasfc_{9x9}$ were compared using a non-parametric Kruskal-Wallis with Dunn's Test. Bold values indicate significant differences between populations ($p < 0.05$).

Supplemental Table 5: Summary of comparisons (p-values) for all DMTA attributes between Texas mammoth (*Mammuthus columbi*) juveniles and adults from Chapter 2.

Juveniles		Adults	
		Friesenhahn Mammoths (n = 13)	Ingleside Mammoths (n = 21)
Friesenhahn "Weaning Juvenile" Mammoths (n = 18)	*Asfc*	0.182	0.238
	epLsar	0.584	**0.014**
	Tfv	0.385	0.089
	$Hasfc_{3x3}$	0.873	0.079
	$Hasfc_{9x9}$	0.920	0.051

Asfc, area-scale fractal complexity; *epLsar*, anisotropy; *Tfv*, textural fill volume, $Hasfc_{3x3}$, $Hasfc_{9x9}$, Heterogeneity of complexity in a 3x3 and 9x9 grid, respectively. $Hasfc_{3x3}$ and $Hasfc_{9x9}$ were compared amongst all groups using non-parametric Mann-Whitney U tests. All other attributes were compared using a parametric t-test between all groups. Bold values indicate significant differences between populations ($p < 0.05$).

Supplemental Table 6: Summary of comparisons (p-values) for all DMTA attributes between Texas mastodon (*Mammut americanum*) juveniles and adults from Chapter 2.

Juveniles		Adults
		Ingleside Mastodons (n = 20)
Friesenhahn "Juvenile" Mastodons (n = 7)	*Asfc*	**0.016**
	epLsar	0.993
	Tfv	0.359
	$Hasfc_{3x3}$	0.199
	$Hasfc_{9x9}$	0.647

Asfc, area-scale fractal complexity; *epLsar*, anisotropy; *Tfv*, textural fill volume, $Hasfc_{3x3}$, $Hasfc_{9x9}$, Heterogeneity of complexity in a 3x3 and 9x9 grid, respectively. *epLsar* was compared using a parametric t-test; all other attributes were compared using non-parametric Mann-Whitney U tests. Bold values indicate significant differences between populations ($p < 0.05$).

Supplemental Table 7: Specimen information, including taxonomy, locality, age, stable isotope data, dental microwear attributes, and applicable supporting references (as .xls file).

GitHub repository for this project at the following link:
https://github.com/paleodentist/gomphothere_competitive_exclusion

Supplemental Table 8: Summary of comparisons (p-values) for all stable isotope and DMTA attribute values between proboscidean populations used in Chapter 3, broken down by NALMA subdivision.

			Ir1			Ir2		Ra		
			Cuvieronius	*Mammut*	*Mammuthus*	*Mammut*	*Mammuthus*	*Cuvieronius*	*Mammut*	*Mammuthus*
$\delta^{13}C_{vmeq}$	Bl5	*Cuvieronius*	**0.040**	<**0.001**	<**0.001**	<**0.001**	0.371	0.057	<**0.001**	<**0.001**
	Ir1	*Cuvieronius*	–	<**0.001**	0.255	<**0.001**	0.125	<**0.001**	<**0.001**	**0.005**
		Mammut		–	<**0.001**	0.125	**0.003**	<**0.001**	**0.043**	<**0.001**
		Mammuthus			–	<**0.001**	0.141	<**0.001**	<**0.001**	0.303
	Ir2	*Mammut*				–	**0.010**	**0.002**	0.646	<**0.001**
		Mammuthus					–	0.617	**0.010**	**0.023**
	Ra	*Cuvieronius*						–	<**0.001**	<**0.001**
		Mammut							–	<**0.001**
		Mammuthus								–
$\delta^{18}O_{enamel}$	Bl5	*Cuvieronius*	<0.001	0.150	0.204	<0.001	**0.002**	0.372	0.339	0.746
	Ir1	*Cuvieronius*	–	**0.006**	<**0.001**	**0.013**	0.190	<**0.001**	<**0.001**	<**0.001**
		Mammut		–	0.056	**0.002**	**0.001**	0.071	0.076	0.115
		Mammuthus			–	<**0.001**	**0.006**	0.755	0.578	0.183
	Ir2	*Mammut*				–	0.975	<**0.001**	<**0.001**	<**0.001**
		Mammuthus					–	**0.004**	**0.005**	**0.004**
	Ra	*Cuvieronius*						–	0.897	0.425
		Mammut							–	0.330
		Mammuthus								–
Asfc	Bl5	*Cuvieronius*	0.105	0.356	0.815	0.727	0.082	0.451	0.072	0.746
	Ir1	*Cuvieronius*	–	**0.010**	0.083	0.195	0.331	0.052	**0.002**	0.175
		Mammut		–	0.238	0.792	**0.009**	0.530	0.972	0.097
		Mammuthus			–	0.907	0.150	0.764	0.725	0.415
	Ir2	*Mammut*				–	0.192	0.880	0.725	0.620
		Mammuthus					–	0.075	0.132	0.126
	Ra	*Cuvieronius*						–	0.315	0.268
		Mammut							–	**0.009**
		Mammuthus								–

			Ir1			Ir2		Ra		
			Cuvieronius	*Mammut*	*Mammuthus*	*Mammut*	*Mammuthus*	*Cuvieronius*	*Mammut*	*Mammuthus*
epLsar	Bl5	*Cuvieronius*	0.109	0.080	**0.015**	0.787	0.976	0.233	**0.024**	**0.004**
	Ir1	*Cuvieronius*	–	0.299	0.249	0.979	0.502	0.541	0.314	0.054
		Mammut		–	0.552	0.580	0.220	0.171	0.664	0.876
		Mammuthus			–	0.834	0.316	0.078	0.726	0.116
	Ir2	*Mammut*				–	0.593	0.668	0.741	0.458
		Mammuthus					–	0.788	0.259	0.127
	Ra	*Cuvieronius*						–	**0.033**	**0.001**
		Mammut							–	0.209
		Mammuthus								–
Tfv	Bl5	*Cuvieronius*	0.806	0.159	**0.003**	0.214	0.766	0.074	0.211	0.094
	Ir1	*Cuvieronius*	–	0.131	**0.014**	0.305	0.417	0.720	0.434	0.054
		Mammut		–	0.858	0.225	0.181	0.094	0.127	0.112
		Mammuthus			–	**0.016**	**0.010**	**<0.001**	**0.001**	**0.013**
	Ir2	*Mammut*				–	0.552	**0.019**	0.056	0.966
		Mammuthus					–	0.141	0.367	0.755
	Ra	*Cuvieronius*						–	0.284	**0.011**
		Mammut							–	**0.008**
		Mammuthus								–
Hasfc$_{3x3}$	Bl5	*Cuvieronius*	0.139	0.861	0.112	0.141	0.107	0.127	**0.046**	0.059
	Ir1	*Cuvieronius*	–	0.866	0.180	0.502	0.809	0.780	0.239	0.435
		Mammut		–	0.603	0.647	0.931	0.823	0.659	0.815
		Mammuthus			–	0.920	0.688	0.451	0.879	0.430
	Ir2	*Mammut*				–	0.865	0.630	0.765	0.821
		Mammuthus					–	0.708	0.891	0.863
	Ra	*Cuvieronius*						–	0.726	0.763
		Mammut							–	0.514
		Mammuthus								–

			Ir1			Ir2		Ra		
			Cuvieronius	*Mammut*	*Mammuthus*	*Mammut*	*Mammuthus*	*Cuvieronius*	*Mammut*	*Mammuthus*
Hasfc$_{9x9}$	Bl5	*Cuvieronius*	0.285	0.693	**0.010**	0.153	0.660	0.074	0.148	**0.028**
	Ir1	*Cuvieronius*	–	0.201	**0.008**	0.809	0.610	0.251	0.067	0.187
		Mammut		–	0.684	1.000	0.329	0.867	0.721	0.696
		Mammuthus			–	0.651	0.079	0.632	0.290	0.096
	Ir2	*Mammut*				–	0.379	0.848	0.585	0.983
		Mammuthus					–	0.389	0.576	0.232
	Ra	*Cuvieronius*						–	0.807	0.650
		Mammut							–	0.602
		Mammuthus								–

$\delta^{13}C_{vmeq}$, modern equivalent vegetation stable carbon isotope signature of paleodiet; $\delta^{18}O_{enamel}$, stable oxygen isotope signature of the structural carbonate portion of enamel; *Asfc*, area-scale fractal complexity; *epLsar*, anisotropy; *Tfv*, textural fill volume, *Hasfc$_{3x3}$*, *Hasfc$_{9x9}$*, Heterogeneity of complexity in a 3x3 and 9x9 grid, respectively. * = result of a Mann-Whitney U test (comparing vs. any non-normally distributed data per Shapiro-Wilks test). Bold = significant differences between compared populations ($p < 0.05$). Results (significant vs. non-significant) are unchanged whether running a Student's T test or a Mann-Whitney U test when comparing normal to non-normal data. Bl5, Late Blancan (2.6 – 1.8 Ma); Ir1, Early Irvingtonian (1.8 – 0.85 Ma), Ir2, Late Irvingtonian (0.85 – 0.3 Ma); Ra, Rancholabrean (0.3 – 0.011 Ma).

Supplemental Table 9: DMTA data for all DVLLF taxa examined in Chapter 4.

Taxon	**Catalog Number**	**Valley**	**Tooth**	***Asfc***	***epLsar***	***Tfv***	***HAsfc*$_{3x3}$**	***HAsfc*$_{9x9}$**
Bison	WSC P-10054	Diamond	rm3	9.319	0.0016	14726.21	0.62	1.09
Bison	WSC P-10560	Diamond	lm3	2.660	0.0067	11822.83	0.34	0.49
Bison	WSC P-11048	Diamond	rm2	2.279	0.0067	12309.12	0.52	0.85
Bison	WSC P-11332	Diamond	rm3	1.967	0.0066	12108.27	0.27	0.48
Bison	WSC P-12630	Diamond	rm2	3.720	0.0065	16714.69	0.55	0.75
Bison	WSC P-13627	Diamond	rm3	2.850	0.0052	12442.27	0.15	0.37
Bison	WSC P-13646	Diamond	lm2	2.805	0.0060	11539.90	0.19	0.39
Bison	WSC P-4965	Diamond	LM1	1.732	0.0043	12787.35	0.21	0.52
Bison	WSC P-567	Diamond	rm2	4.841	0.0040	10907.67	0.19	0.34
Bison	WSC P-7421	Diamond	lm2	4.574	0.0072	13051.00	0.50	1.16
Bison	WSC P-7593	Diamond	RM1	2.279	0.0073	13913.84	0.42	0.68
Bison	WSC P-7603	Diamond	lm2	2.430	0.0035	11912.40	0.28	0.47
Bison	WSC P-11482	Domenigoni	rm3	2.531	0.0035	12815.52	0.27	0.49
Bison	WSC P-11903	Domenigoni	rm2	2.540	0.0041	14352.25	0.32	0.57
Bison	WSC P-11991	Domenigoni	rm2	3.765	0.0049	11808.44	0.69	0.97
Bison	WSC P-18173	Domenigoni	lm2	2.635	0.0033	13414.32	0.30	0.69
Bison	WSC P-18184	Domenigoni	lm3	14.271	0.0026	15863.41	0.40	0.79
Bison	WSC P-19037	Domenigoni	lm3	2.780	0.0031	11298.35	0.22	0.44
Bison	WSC P-22367	Domenigoni	LM2	4.970	0.0021	12212.37	0.15	0.33
Bison	WSC P-484	Domenigoni	rm2	3.472	0.0033	13723.50	0.21	0.38
Bison	WSC P-495	Domenigoni	rm3	4.756	0.0020	13463.36	0.19	0.39
Bison	WSC P-6581	Domenigoni	rm2	2.903	0.0039	9951.66	0.22	0.45
Camelops	WSC P-12534	Diamond	lm1	7.271	0.0027	16747.81	0.20	0.52
Camelops	WSC P-12645	Diamond	rm1	7.028	0.0013	15653.02	0.38	0.61
Camelops	WSC P-12737	Diamond	rm3	8.448	0.0011	14661.91	0.55	1.09
Camelops	WSC P-13389	Diamond	RM2	2.953	0.0015	16312.62	0.59	1.03
Camelops	WSC P-19858	Diamond	LM2	4.107	0.0014	13357.67	0.26	0.48

Taxon	Catalog Number	Valley	Tooth	*Asfc*	*epLsar*	*Tfv*	$HAsfc_{3x3}$	$HAsfc_{9x9}$
Camelops	WSC P-19938	Diamond	lm1	1.655	0.0035	7324.34	0.31	0.54
Camelops	WSC P-8635	Diamond	lm3	5.984	0.0041	14397.59	0.36	0.66
Camelops	WSC P-11410	Domenigoni	LM2	5.786	0.0019	14394.13	0.28	0.75
Camelops	WSC P-11715	Domenigoni	lm2	6.411	0.0035	16213.94	0.19	0.39
Camelops	WSC P-11899	Domenigoni	rm3	5.909	0.0019	14829.76	0.36	0.51
Camelops	WSC P-12586	Domenigoni	lm3	2.626	0.0036	8861.89	0.24	0.47
Camelops	WSC P-17189	Domenigoni	lm1	3.568	0.0012	14908.04	0.20	0.35
Camelops	WSC P-17589	Domenigoni	LM2	2.113	0.0033	14638.09	0.39	0.70
Equus	WSC P-10167	Diamond	LP4	2.652	0.0073	14973.79	0.26	0.70
Equus	WSC P-10435	Diamond	LM3	5.243	0.0030	14490.49	0.34	0.52
Equus	WSC P-10441	Diamond	LM3	2.709	0.0055	11888.57	0.47	0.85
Equus	WSC P-10538	Diamond	lm2	3.495	0.0047	14494.02	0.46	0.78
Equus	WSC P-12966	Diamond	LM1	3.475	0.0021	15687.16	0.27	0.56
Equus	WSC P-12968	Diamond	rm3	4.374	0.0025	14461.50	0.36	0.62
Equus	WSC P-13632	Diamond	rp4	1.569	0.0055	16269.74	0.27	0.49
Equus	WSC P-13647	Diamond	RM1	3.814	0.0064	17335.12	0.46	0.81
Equus	WSC P-15544	Diamond	RM3	3.234	0.0074	13164.02	0.32	0.66
Equus	WSC P-15579	Diamond	rm1	1.789	0.0047	11447.85	0.39	0.79
Equus	WSC P-17601	Diamond	lm2	1.554	0.0083	14270.17	0.36	0.57
Equus	WSC P-19931	Diamond	rm2	6.836	0.0044	16242.00	0.47	0.81
Equus	WSC P-26714	Diamond	RM1	3.817	0.0027	11164.95	0.76	1.01
Equus	WSC P-7474	Diamond	LM1	1.895	0.0052	12866.67	0.25	0.38
Equus	WSC P-7759	Diamond	lm2	4.598	0.0016	17753.49	0.23	0.42
Equus	WSC P-7791	Diamond	lm2	2.175	0.0026	15015.39	0.35	0.70
Equus	WSC P-8555	Diamond	LM1	2.910	0.0079	7613.80	0.22	0.39
Equus	WSC P-10986	Domenigoni	LP4	7.088	0.0025	14810.68	0.30	0.52
Equus	WSC P-11128	Domenigoni	rm3	4.203	0.0030	11969.50	0.24	0.59
Equus	WSC P-11386	Domenigoni	RM2	4.345	0.0031	13923.99	0.30	0.66

Taxon	**Catalog Number**	**Valley**	**Tooth**	***Asfc***	***epLsar***	***Tfv***	***HAsfc$_{3x3}$***	***HAsfc$_{9x9}$***
Equus	WSC P-11780	Domenigoni	rm2	3.679	0.0028	14172.67	0.27	0.51
Equus	WSC P-11890	Domenigoni	LM1	2.771	0.0055	13977.26	0.47	0.63
Equus	WSC P-12248	Domenigoni	lm1	3.575	0.0048	14535.84	0.23	0.38
Equus	WSC P-13858	Domenigoni	lm1	3.501	0.0050	15245.05	0.35	0.68
Equus	WSC P-14612	Domenigoni	rp4	6.154	0.0034	15961.63	0.36	0.76
Equus	WSC P-17465	Domenigoni	LM1	4.951	0.0067	13114.10	0.41	1.33
Equus	WSC P-17483	Domenigoni	RM1	5.081	0.0021	16937.11	0.32	0.62
Equus	WSC P-17557	Domenigoni	RM1	3.663	0.0044	15218.50	0.34	0.68
Equus	WSC P-19933	Domenigoni	lm3	7.776	0.0047	13840.71	0.64	0.92
Equus	WSC P-22389	Domenigoni	LM3	6.540	0.0013	13924.57	0.54	0.85
Mammut	WSC P-10312	Diamond	M2	4.562	0.004	4564.86	0.26	0.49
Mammut	WSC P-10646	Diamond	LM3	3.511	0.006	10638.68	0.24	0.68
Mammut	WSC P-23419	Diamond	LM2	1.904	0.004	8700.42	0.28	0.47
Mammut	WSC P-5522	Diamond	mx	1.659	0.004	12786.93	0.38	0.63
Mammut	WSC P-7342	Diamond	RM3	1.750	0.002	17364.92	0.86	1.37
Mammut	WSC P-7387	Diamond	RM3	4.228	0.003	10466.33	0.30	0.61
Mammut	WSC P-10713	Domenigoni	LM3	1.281	0.002	12236.50	0.28	0.51
Mammut	WSC P-10818	Domenigoni	LM2	3.663	0.003	12057.40	0.35	0.51
Mammut	WSC P-10840	Domenigoni	LM3	2.609	0.003	6954.53	0.25	0.58
Mammut	WSC P-10844	Domenigoni	LM3	4.246	0.005	12130.10	0.63	0.97
Mammut	WSC P-11634	Domenigoni	lm2	2.125	0.007	8167.21	0.19	0.53
Mammut	WSC P-1408	Domenigoni	LM3	1.462	0.002	7446.35	0.36	0.59
Mammut	WSC P-17218	Domenigoni	dp4	1.583	0.004	8570.93	0.23	0.55
Mammut	WSC P-18743	Domenigoni	rm3	2.068	0.004	13763.29	0.25	0.59
Mammut	WSC P-19631	Domenigoni	LM2	1.522	0.002	4402.43	0.30	0.59
Mammut	WSC P-19708	Domenigoni	Px	3.291	0.003	14228.45	0.79	1.30
Mammut	WSC P-19721	Domenigoni	rm3	2.061	0.004	6837.19	0.19	0.41
Mammut	WSC P-19730	Domenigoni	lm2	4.854	0.002	18353.41	0.33	0.90

Taxon	Catalog Number	Valley	Tooth	*Asfc*	*epLsar*	*Tfv*	$HAsfc_{3x3}$	$HAsfc_{9x9}$
Mammut	WSC P-22588	Domenigoni	LM3	2.498	0.004	11731.70	0.34	0.54
Mammut	WSC P-22702	Domenigoni	RM3	1.632	0.004	6759.51	0.17	0.44
Mammut	WSC P-6523	Domenigoni	RM3	2.960	0.006	9957.95	0.35	0.67
Mammut	WSC P-7285	Domenigoni	m2	2.090	0.001	12436.52	0.46	0.68
Mammut	WSC P-817	Domenigoni	mx	2.311	0.004	5822.96	0.26	0.53
Mammuthus	WSC P-11509	Diamond	Mx	3.332	0.002	13407.41	0.33	0.58
Mammuthus	WSC P-18715	Diamond	Mx	10.603	0.005	13818.92	0.27	0.49
Mammuthus	WSC P-1015	Domenigoni	LM3	2.661	0.008	10727.27	0.46	1.06
Mammuthus	WSC P-11345	Domenigoni	M3	5.236	0.004	13870.82	0.29	0.47
Mammuthus	WSC P-11443	Domenigoni	lm3	10.424	0.002	14690.50	0.30	0.56
Mammuthus	WSC P-17554	Domenigoni	RM3	10.044	0.005	14012.13	0.50	0.67
Mammuthus	WSC P-18748	Domenigoni	LM2	3.922	0.002	11723.56	0.45	1.16
Mammuthus	WSC P-26939	Domenigoni	Mx	1.767	0.007	10540.62	0.27	0.50
Mammuthus	WSC P-394	Domenigoni	RP4	5.880	0.002	10752.35	0.53	1.11

Asfc, area-scale fractal complexity; *epLsar*, anisotropy; *Tfv*, textural fill volume, $HAsfc_{3x3}$, $HAsfc_{9x9}$, Heterogeneity of complexity in a 3x3 and 9x9 grid, respectively. Tooth position: L, upper left; l, lower left; R, upper right; r, lower right; M, molar; P, premolar; x, position unknown. WSC-P, Western Science Center Paleontology collections.

Supplemental Table 10: Mesowear variable values for all DVLLF ungulates examined in Chapter 4.

				Cusp Shape (CS)					Occlusal Relief (OR)					MWS					MNS				
Taxon	**WSC #**	**Valley**	**Tooth**	**1**	**2**	**3**	**4**	**5**	**1**	**2**	**3**	**4**	**5**	**1**	**2**	**3**	**4**	**5**	**1**	**2**	**3**	**4**	**5**
Bison	P-4965	Diamond	LM1	0.5	0	0	0.5	0.5	0	0	0	0	0	3	4	4	3	3	5	5	5	5	4
Bison	P-7593	Diamond	RM1	1	0.5	0.5	0.5	0.5	1	1	1	1	1	0	1	1	1	1	1	2	2	3	2
Bison	P-12389	Diamond	RM2	0.5	1	0.5	0.5	0.5	1	1	1	1	1	1	0	1	1	1	2	1	1	1	2
Bison	P-12796	Diamond	RM2	1	1	0.5	1	1	1	1	1	1	1	0	0	1	0	0	2	0	0	1	2
Bison	P-8814	Domenigoni	LM2	0	0	0	0	0	0	0	0	0	0	4	4	4	4	4	5	6	5	6	5
Bison	P-11688	Domenigoni	LM1	0.5	0.5	0.5	0.5	0.5	1	1	1	0	1	1	1	1	3	1	3	3	4	4	3
Bison	P-22367	Domenigoni	LM2	0.5	0.5	0.5	0.5	0.5	1	1	1	1	1	1	1	1	1	1	2	3	4	1	1
Camelops	P-11056	Diamond	LM2	1	1	1	1	0.5	1	1	1	1	1	0	0	0	0	1	3	0	2	2	0
Camelops	P-13388	Diamond	RM3	0.5	0.5	1	0.5	1	1	1	1	0	0	1	1	0	3	2	3	4	1	4	3
Camelops	P-13389	Diamond	RM2	0.5	0.5	1	1	0	0	0	0	0	0	3	3	2	2	4	4	5	3	3	4
Camelops	P-19858	Diamond	LM2	0	0	0.5	0.5	0.5	0	0	0	0	0	4	4	3	3	3	5	6	4	4	5
Camelops	P-20570	Diamond	LM1	0.5	0.5	1	0.5	1	0	1	0	0	0	3	1	2	3	2	4	3	4	2	3
Camelops	P-20571	Diamond	LM2	1	1	1	1	1	1	1	1	1	1	0	0	0	0	0	0	0	1	0	3
Camelops	P-11410	Domenigoni	LM2	0.5	0.5	1	0.5	0.5	1	1	0	0	0	1	1	2	3	3	4	4	3	5	4
Camelops	P-17589	Domenigoni	RM2	0.5	1	1	1	1	1	1	1	0	0	1	0	0	2	2	2	4	2	3	2
Camelops	P-24534	Domenigoni	RM1	0.5	0.5	0.5	0.5	0.5	0	0	0	0	0	3	3	3	3	3	4	4	5	4	5
Equus	P-7474	Diamond	LM1	0	0.5	0.5	0.5	0	0	1	1	1	0	4	1	1	1	4	5	5	5	2	5
Equus	P-8528	Diamond	RM2	0	0	0	0	0	0	0	0	0	0	4	4	4	4	4	6	6	6	5	4
Equus	P-8555	Diamond	LM1	0.5	0	0	0	0	0	0	0	0	0	3	4	4	4	4	5	5	4	6	5
Equus	P-10435	Diamond	LM3	0.5	0	1	0	1	0	0	0	0	0	3	4	2	4	2	5	5	5	4	3
Equus	P-10986	Diamond	LP4	0	0.5	0.5	0.5	0	0	0	0	0	0	4	3	3	3	4	4	5	5	4	5
Equus	P-12306	Diamond	LM2	0	0	0	0	0	0	0	0	0	0	4	4	4	4	4	5	6	6	6	6
Equus	P-12966	Diamond	LM1	0.5	0	0	0.5	0.5	0	0	0	0	0	3	4	4	3	3	5	5	5	5	6
Equus	P-13647	Diamond	RM1	0	0	1	0	1	0	0	0	0	0	4	4	2	4	2	6	6	5	6	5
Equus	P-15544	Diamond	RM3	0.5	0.5	0.5	0.5	0.5	0	0	1	0	0	3	3	1	3	3	5	4	3	4	4
Equus	P-19433	Diamond	RP4	0.5	0.5	1	0.5	1	0	0	0	0	0	3	3	2	3	2	4	5	4	3	3

				Cusp Shape (CS)					Occlusal Relief (OR)					MWS					MNS				
Taxon	**WSC #**	**Valley**	**Tooth**	**1**	**2**	**3**	**4**	**5**	**1**	**2**	**3**	**4**	**5**	**1**	**2**	**3**	**4**	**5**	**1**	**2**	**3**	**4**	**5**
Equus	P-26714	Diamond	RM1	0.5	0	0.5	0.5	0.5	0	0	1	0	0	3	4	1	3	3	4	6	5	4	5
Equus	P-10167	Domenigoni	LP4	0	0	0.5	0	0.5	0	0	0	0	0	4	4	3	4	3	6	6	5	6	5
Equus	P-11386	Domenigoni	RM2	0	0	0	0	0	0	0	0	0	0	4	4	4	4	4	6	6	6	6	5
Equus	P-11572	Domenigoni	LP4	0.5	1	0.5	0.5	0.5	1	1	1	1	1	1	0	1	1	1	3	1	3	1	5
Equus	P-11890	Domenigoni	LM1	0	0	1	0.5	0.5	0	0	0	0	0	4	4	2	3	3	5	5	5	5	4
Equus	P-13858	Domenigoni	LM1	0	0.5	1	0	0.5	0	0	0	0	1	4	3	2	4	1	5	4	3	6	3
Equus	P-14056	Domenigoni	LM1	0	0	0	0	0	0	0	0	0	0	4	4	4	4	4	6	6	5	6	5
Equus	P-17465	Domenigoni	LM1	0.5	0.5	0.5	0.5	0.5	0	0	1	0	0	3	3	1	3	3	4	4	3	4	5
Equus	P-17483	Domenigoni	RP4	0.5	0.5	0.5	1	0.5	1	1	1	1	1	1	1	1	0	1	4	3	5	2	4
Equus	P-17557	Domenigoni	LM1	0.5	0.5	1	1	0.5	0	0	1	0	0	3	3	0	2	3	4	5	3	2	3
Equus	P-22389	Domenigoni	LM3	0	0	0.5	0	0	0	0	0	0	0	4	4	3	4	4	5	6	5	2	4

MWS, univariate mesowear score; MNS, mesowear numerical scale; Numbers under CS, OR, MWS, and MNS correspond to the observer number; WSC; Western Science Center; Tooth positions: L, left; R, right; M, molar; P, premolar.

Supplemental Table 11: Pairwise comparisons (p-values) between Domenigoni and Diamond valley fauna.

	Asfc	*epLsar*	*Tfv*	$Hasfc_{3x3}$	$Hasfc_{9x9}$	MWS	MNS
Bison	0.222	**0.002***	0.956*	0.418	0.429*	0.212	0.229
Camelops	0.366*	0.567*	0.836	0.133*	0.181	0.905	0.548
Equus	**0.009***	0.141*	0.609*	0.967	0.591*	0.571	0.158
Mammut	0.473*	0.319*	0.656*	0.708	0.609	–	–
Mammuthus	0.667	0.555	0.889	0.500	0.500	–	–

Asfc, area-scale fractal complexity; *epLsar*, anisotropy; *Tfv*, textural fill volume, $Hasfc_{3x3}$, $Hasfc_{9x9}$, Heterogeneity of complexity in a 3x3 and 9x9 grid, respectively; MWS, mesowear univariate scale (0-4); MNS, mesowear numerical score (0-6). * = result of a Mann-Whitney U Test. Bold = significant differences between populations ($p < 0.05$). Results (significant vs. non-significant) are unchanged whether running a Student's T test or a Mann-Whitney U test when comparing normal to non-normal data.

Supplemental Table 12: Time-independent pairwise comparisons (p-values) between DMTA attribute values and mesowear variables of DVLLF taxa.

		Camelops	*Equus*	*Mammut*	*Mammuthus*
Asfc	*Bison*	0.098	0.225	**0.017**	0.064
	Camelops	–	0.188*	**0.001**	0.431*
	Equus		–	**0.007**	0.131*
	Mammut			–	**0.003**
	Mammuthus				–
epLsar	*Bison*	<**0.001***	0.845*	0.087*	0.561*
	Camelops	–	<**0.001***	**0.009***	**0.045***
	Equus		–	0.113*	0.638*
	Mammut			–	0.667*
	Mammuthus				–
Tfv	*Bison*	**0.015**	**0.010***	**0.005***	0.701*
	Camelops	–	0.648	**0.001**	**0.036**
	Equus		–	<**0.001***	**0.028***
	Mammut			–	**0.021***
	Mammuthus				–
$Hasfc_{3x3}$	*Bison*	0.682	0.099	0.507	0.192
	Camelops	–	0.397	0.922	0.367
	Equus		–	177	0.714
	Mammut			–	0.229
	Mammuthus				–
$Hasfc_{9x9}$	*Bison*	0.453	0.071	0.151	0.124
	Camelops	–	0.481*	0.649	0.393
	Equus		–	0.322	0.987
	Mammut			–	0.773
	Mammuthus				–
MWS	*Bison*	0.832	0.062	–	–
	Camelops	–	**0.013**	–	–
	Equus		–	–	–
MNS	*Bison*	0.832	**0.019**	–	–
	Camelops	–	**0.005**	–	–
	Equus		–	–	–

Asfc, area-scale fractal complexity; *epLsar*, anisotropy; *Tfv*, textural fill volume, $Hasfc_{3x3}$, $Hasfc_{9x9}$, Heterogeneity of complexity in a 3x3 and 9x9 grid, respectively; MWS, mesowear univariate scale (0-4); MNS, mesowear numerical score (0-6). * = result of a Mann-Whitney U Test. Bold = significant differences between populations ($p < 0.05$). Results (significant vs. non-significant) are unchanged whether running a Student's T test or a Mann-Whitney U test when comparing normal to non-normal data.

Supplemental Table 13: Pairwise comparisons (p-values) between DVLLF and RLBLF ungulates.

	Asfc	*epLsar*	*Tfv*	$Hasfc_{3x3}$	$Hasfc_{9x9}$	MWS	MNS
Bison	0.246	0.262*	0.262*	**0.011**	**0.006**	0.908	0.546
Camelops	0.622	0.275	0.622	0.109	0.207	**0.039**	**0.014**
Equus	0.907*	**0.031**	0.870*	**0.004**	**0.018**	**0.003**	**0.049**

Asfc, area-scale fractal complexity; *epLsar*, anisotropy; *Tfv*, textural fill volume, $Hasfc_{3x3}$, $Hasfc_{9x9}$, Heterogeneity of complexity in a 3x3 and 9x9 grid, respectively; MWS, mesowear univariate scale (0-4); MNS, mesowear numerical score (0-6). * = result of a Mann-Whitney U Test. Bold = significant differences between populations ($p < 0.05$). Results (significant vs. non-significant) are unchanged whether running a Student's T test or a Mann-Whitney U test when comparing normal to non-normal data.

Supplemental Table 14: NALMAs with significant phylogenetic conservatism (extinction).

NALMA	Total N	Total N_e	Families with Disproportionate Extinction [# Ne / # N]	Diet Preference	Body Size	Life Habit
Puercan*	76	31	Taeniolabididae [5/8]	He	Md	Ar
			Cimolestidae [7/13]	In	Sm	Sc
			Hyopsodontidae [11/21]	Om	Sm	Sc
			All other families [8/34]			
Torrejonian	96	34	Viverravidae [4/6]	Ca	Sm	Gd
			Cimolestidae [4/8]	In	Sm	Sc
			Palaechthonidae [4/8]	In – Om	Sm	Ar
			Neoplagiaulacidae [3/9]	Om	Sm	Ar
			All other families [19/65]			
Tiffanian	143	73	Hyopsodontidae [5/5]	Om	Sm	Sc
			Palaechthonidae [4/4]	In – Om	Sm	Ar
			Picrodontidae [3/4]	He	Sm	Ar
			Triisodontidae [3/4]	Om	Sm	Sc
			Microcosmodontidae [4/6]	He	Sm	Ar
			Micromomyidae [4/7]	Om	Sm	Ar
			Apheliscidae [8/15]	In	Sm	Gd
			Pantolestidae [5/10]	Pi – Du	Md	Am
			Plesiadapidae [3/6]	He	Md	Ar
			Erinaceidae [4/9]	In - Ca	Sm	Sf
			All other families [19/65]			
Bridgerian*	201	118	Esthonychidae [5 / 6]	He	Lg	Gd
			Oxyaenidae [7 / 9]	Ca	Lg	Gd
			Ceratomorpha [7 / 10]	Br	Mf	Gd
			Microsyopidae [4 / 6]	Om	Sm	Ar
			Omomyidae [23 / 36]	In	Sm	Ar
			Hyaenodontidae [12 / 19]	Ca	Lg	Gd
			Sciuravidae [7 / 12]	He	Sm	Gd
			Brontotheriidae [4 / 8]	Br	Mf	Gd
			All other families [49 / 95]			
Orellan	119	35	Ursidae [3 / 4]	He – Ca	Mf	Gd
			Florentiamyidae [2/ 3]	He	Sm	Gd
			Dipodidae [2 / 3]	He – In	Sm	Gd
			Ischyromyidae [3 / 5]	He	Sm	Gd
			Heliscomyidae [4 / 7]	He	Sm	Gd
			Castoridae [2 / 4]	Br	Md	Am
			Eomyidae [2 / 5]	He	Sm	Gd
			Leporidae [2 / 6]	Gz - Br	Sm	Sa
			All other families [11 / 68]			
Whitneyan*	168	37	Aplodontidae [6 / 12]	He	Sm	Fo
			Anthracotheriidae [3 / 6]	Br	Mf	Gd
			Tayassuidae [3 / 6]	He - Om	Lg	Gd
			Rhinocerotidae [3 / 7]	Br	Mf	Gd
			Merycoidodontidae [5 / 17]	He	Lg	Gd
			All other families [20 / 120]			

NALMA	Total N	Total N_e	Families with Disproportionate Extinction [# Ne / # N]	Diet Preference	Body Size	Life Habit
Arikareean*	294	131	Allomyidae [5 / 5]	He	Sm	Gd
			Aplodontidae [4 / 5]	He	Sm	Fo
			Nimravidae [7 / 9]	Ca	Lg	Gd
			Castoridae [8 / 13]	Br	Md	Am
			Canidae [15 / 26]	Ca - Om	Lg	Gd
			Merycoidodontidae [14 / 28]	He	Lg	Gd
			Mustelidae [6 / 12]	Ca - Om	Md	Sc
			Erinaceidae [4 / 8]	In - Ca	Sm	Sf
			Mylagaulidae [4 / 8]	He	Sm	Gd
			All other families [64 / 180]			
Hemingfordian*	250	91	Florentiamyidae [3/3]	He	Sm	Gd
			Ailuridae [2/2]	Ca – Om	Lg	Gd
			Hypertragulidae [2/2]	Fr	Md	Gd
			Geomyidae [4/5]	Br	Sm	Fo
			Allomyidae [2/3]	He	Sm	Gd
			Ochotonidae [2/3]	He	Sm	Sa
			Amphicyonidae [5/9]	Ca	Mf	Gd
			Mustelidae [9/18]	Ca - Om	Md	Sc
			Rhinocerotidae [5/10]	Br	Mf	Gd
			Ursidae [3/6]	He – Ca	Mf	Gd
			Leporidae [3/7]	Gz - Br	Sm	Sa
			Eomyidae [2/5]	He	Sm	Gd
			Moschidae [2/5]	Br - Gz	Lg	Gd
			Procyonidae [2/5]	Fr - Ca	Md	Sc
			Merycoidodontidae [5/13]	He	Lg	Gd
			Castoridae [3/8]	Br	Md	Am
			All other families [37/146]			
Blancan*	233	79	Equidae [6 / 12]	Gz – Br	Mf	Gd
			Canidae [5 / 10]	Ca – Om	Lg	Gd
			Ursidae [4 / 8]	He – Ca	Mf	Gd
			Cricetidae [17 / 35]	He	Sm	Gd
			Leporidae [5 / 14]	Gz – Br	Sm	Sa
			Mustelidae [7 / 17]	Ca – Om	Md	Sc
			Felidae [6 / 15]	Ca	Lg	Sc
			All other families [29 / 122]			

* = moderately significant clustering, i.e. either I_{CL} or R_{CL} deemed significant excursions, and not both. For each interval, families with extinction proportions greater than the mean of the interval are listed in order of decreasing extinction intensity. Body size category is based on the mean body size of all species in that family, with body sizes from Supplemental Table 7 in Smith et al. (2018). Diet preference and life habit are from the Paleobiology Database:
Diet: Br = browser; Ca = carnivore; Du = durophagous; Fr = frugivore; Gn = granivore; Gz = grazer; Herbivore = He; In = insectivore; Om = omnivore; Pi = piscovore. Body size: Sm = small ($\leq$1 kg), Md = medium (1 – 10 kg), Lg = large (10 – 100 kg), Mf = megafauna ($\geq$100 kg). Life habit: Am = amphibious, Ar = arboreal, Fo = fossorial, Gd = ground dwelling, Sa = saltatorial, Sc = scansorial, Sf = semifossorial.

Supplemental Table 15: NALMAs with significant phylogenetic conservatism (origination).

NALMA	Total N	Total N_e	Families with Disproportionate Extinction [# Ne / # N]	Diet Preference	Body Size	Life Habit
Torrejonian	96	51	Paromomyidae [3/3	Om	Sm	Ar
			Apatemyidae [2/2]	He	Sm	Ar
			Pantolambdidae [2/2]	He	Lg	Gd
			Plesiadapidae [2/2]	He	Md	Ar
			Picrodontidae [3/4]	He	Sm	Ar
			Pantolestidae [4/6]	Pi – Du	Md	Am
			Viverravidae [4/6]	Ca	Sm	Gd
			Herpetotheriidae [2/3]	Om	Sm	Gd
			Palaechthonidae [5/8]	In - Om	Sm	Ar
			Mixodectidae [3/5]	In	Sm	Gd
			All other families [21/41]			
Chadronian*	191	82	Nimravidae [3/3]	Ca	Lg	Gd
			Talpidae [2/2]	In	Sm	Fo
			Sciuridae [4/5]	Gr - Fr	Sm	Sc
			Entelodontidae [5/7]	Om	Mf	Gd
			Chalicotheriidae [2/3]	Br	Mf	Gd
			Patriomanidae [2/3]	In	Sm	Sc
			Praetragulidae [2/3]	Gz - Br	Md	Gd
			Merycoidodontidae [6/10]	He	Lg	Gd
			Brontotheriidae [8/14]	Br	Mf	Gd
			Amphicyonidae [3/6]	Ca	Mf	Gd
			Anthracotheriidae [3/6]	Br	Mf	Gd
			Hyracodontidae [2/4]	Br	Mf	Gd
			Miacidae [2/4]	Ca	Md	Gd
			Pantolestidae [2/4]	Pi - Du	Md	Am
			Eomyidae [11/25]	He	Sm	Gd
			All other families [25/92]			
Hemingfordian*	250	94	Procyonidae [4 / 5]	Fr - Ca	Md	Sc
			Palaeomerycidae [8 / 12]	Br	Mf	Gd
			Mustelidae [11 / 18]	Ca - Om	Md	Sc
			Canidae [10 / 19]	Ca - Om	Lg	Gd
			Equidae [7 / 14]	Br - Gr	Mf	Gd
			Castoridae [4 / 8]	Br	Md	Am
			Camelidae [8 / 20]	Br	Mf	Gd
			Rhinocerotidae [4 / 10]	Br	Mf	Gd
			All other families [48 / 144]			

NALMA	Total N	Total N_e	Families with Disproportionate Extinction [# Ne / # N]	Diet Preference	Body Size	Life Habit
Clarendonian*	215	73	Felidae [3 / 4]	Ca	Lg	Sc
			Cricetidae [9 / 12]	He	Sm	Gd
			Ailuridae [2/3]	Ca – Om	Lg	Gd
			Gomphotheriidae [8/14]	Br – Gz	Mf	Gd
			Antilocapridae [6/12]	Gz - Br	Lg	Gd
			Camelidae [7/15]	Br	Mf	Gd
			Tayassuidae [6/13]	He - Om	Lg	Gd
			Mustelidae [7/17]	Ca - Om	Md	Sc
			Geomyidae [2/5]	Br	Sm	Fo
			Ochotonidae [2/5]	He	Sm	Sa
			Procyonidae [2/5]	Fr - Ca	Sm	Sc
			Ursidae [2/5]	He - Ca	Mf	Gd
			All other families [17 / 105]			

* = moderately significant clustering, i.e. either I_{CL} or R_{CL} deemed significant excursions, and not both. For each interval, families with origination proportions greater than the mean of the interval are listed in order of decreasing origination intensity. Body size category is based on the mean body size of all species in that family, with body sizes from Supplemental Table 7 in Smith et al. (2018). Diet preference and life habit are from the Paleobiology Database:
Diet: Br = browser; Ca = carnivore; Du = durophagous; Fr = frugivore; Gn = granivore; Gz = grazer; Herbivore = He; In = insectivore; Om = omnivore; Pi = piscovore. Body size: Sm = small ($\leq$1 kg), Md = medium (1 – 10 kg), Lg = large (10 – 100 kg), Mf = megafauna ($\geq$100 kg). Life habit: Am = amphibious, Ar = arboreal, Fo = fossorial, Gd = ground dwelling, Sa = saltatorial, Sc = scansorial, Sf = semifossorial.

REFERENCES

Agenbroad, L.D. 2001. Channel Islands (USA) pygmy mammoths (*Mammuthus exilis*) compared and contrasted with *M. columbi*, their continental ancestral stock, in: Cavarretta, G., Giola, P., Mussi, M., Palombo, M.R. (Eds.), The World of Elephants: International Conference, Rome, pp. 473-475.

Agenbroad, L.D. 2005. North American Proboscideans: mammoths: the state of knowledge, 2003. Quaternary International 126-128:73-92.

Agenbroad, L.D. 2012. Giants and pygmies: mammoths of Santa Rosa Island, California (USA). Quaternary International 255:2-8.

Agenbroad, L.D. and J.I. Mead. 1994. The Hot Springs Mammoth Site: A Decade of Field and Laboratory Research in the Paleontology, Geology, and Paleoecology. The Mammoth Site of South Dakota, Inc. Hot Springs, South Dakota

Aharon, P. and R. Dhungana. 2017. Ocean-atmosphere interactions as drivers of mid-to-late Holocene rapid climate changes: Evidence from high-resolution stalagmite records at DeSoto Caverns, Southeast USA. Quaternary Science Reviews 170:69–81.

Aharon, P., D. Aldridge, and J. Hellstrom. 2012. Rainfall variability and the rise and collapse of the Mississippian chiefdoms: evidence from a Desoto Caverns stalagmite. In L. Giosan, D.Q. Fuller, K. Nicoll, R.K. Flad, and P.D. Clift, eds. Climates, Landscapes, and Civilizations. Geophysical Monograph Series 25, pp. 35–42, 25.

Akersten, W.A., T.M. Foppe, and G.T. Jefferson. 1988. New source of dietary data from extinct herbivores. Quaternary Research 30(1):92–97.

Alley, R.B., J. Marotzke, W.D. Nordhaus, J.T. Overpeck, D.M. Peteet, R.A. Pielke, R.T. Pierrehumbert, P.B. Rhines, T.F. Stocker, L.D. Talley, and J.M. Wallace. 2003. Abrupt climate change. Science 299:2005-2010.

Alroy, J., 1999. The fossil record of North American mammals: evidence for a Paleocene Evolutionary Radiation. Syst. Biol. 48(1): 107-118.

Alroy, J., 2000. New methods for quantifying macroevolutionary patterns and processes. Paleobiology 26(4): 707-733.

Alroy, J., 2010. Fair sampling of taxonomic richness and unbiased estimation of origination and extinction rates. The Paleontological Society Papers 16 pp. 55-80.

Alroy, J., Koch, P.L., Zachos, J.C., 2000. Global climate change and North American mammalian evolution. Paleobiology 26(S4), 259-288.

Anderson, E. 1984. Who's who in the Pleistocene: a mammalian bestiary, in: Martin, P.S., Klein, R.G. (Eds.), Quaternary Extinctions: A prehistoric revolution. The University of Arizona Press, Tucson, AZ. pp. 40-89.

Anderson, R.L., R. Byrne, and T. Dawson. 2008. Stable isotope evidence for a foggy climate on Santa Cruz Island, California at 16,600 cal. yr. B.P. Palaeogeography, Palaeoclimatology, Palaeoecology 262:176–181.

Anderson, R.S. and P.A. Koehler. 2003. Modern pollen and vegetation relationships in the mountains of southern California, USA. Grana 43(3):129–146.

Anderson, R.S., S. Starratt, R.M.B. Jass, and N. Pinter. 2010. Fire and vegetation history on Santa Rosa Island, Channel Islands, and long-term environmental change in southern California. Journal of Quaternary Science 25:782-797.

Anderson, R.S., M.J. Power, S.J. Smith, K.B. Springer, and E. Scott. 2002. Paleoecology of a middle Wisconsin deposit from southern California. Quaternary Research 58:310–317.

Araujo, B.B., L.G.R. Oliveira-Santos, M.S. Lima-Ribeiro, J.A.F. Diniz-Filho, and F.A. Fernandez. 2015. Bigger kill than chill: the uneven roles of humans and climate on late Quaternary megafaunal extinctions. Quaternary International 431:216-222.

Arman, S.D., P.S. Ungar, C.A. Brown, L.R.G. DeSantis, C. Schmidt, and G.J. Prideaux. 2016. Minimizing inter-microscope variability in dental microwear texture analysis. Surface Topography: Metrology and Properties 4:024007.

Arnold, T.E., A.F. Diefendorf, M. Brenner, K.H. Freeman, and A.A. Baczynski. 2018.

Climate response of the Florida peninsula to Heinrich events in the North Atlantic. Quaternary Science Reviews 194:1-11.

Asher, R.J. and T. Lehmann. 2008. Dental eruption in afrotherian mammals. BMC Biol. 6:1-11.

Ayliffe, L.K., A. Lister, and A. Chivas. 1992. The preservation of glacial-interglacial climatic signatures in the oxygen isotopes of elephant skeletal phosphate. Paleogeography, Paleoclimatology, Paleoecology 99:179–191.

Ayliffe, L.K., A.R. Chivas, and M.G. Leaker. 1994. The retention of primary oxygen isotope compositions of fossil elephant skeletal phosphate. Geochimica et Cosmochimica Acta 58:5291–5298.

Baldwin, B.G., D.H. Goldman, D.J. Keil, R. Patterson, T.J. Rosatti, and D.H. Wilken (Eds.) 2012. The Jepson manual. Vascular plants of California, second edition. Berkeley, CA: University of California Press. 1568 pp.

Barnosky, A.D. et al. 2017. Merging paleobiology with conservation biology to guide the future of terrestrial ecosystems. Science 355 (6325):1-10.

Barnosky, A.D. and M.A. Carrasco. 2002. Effects of Oligo-Miocene global climate changes on mammalian species richness in the northwestern quarter of the USA. Evolutionary Ecology Research 4: 811–841.

Barnosky, A.D., M. Holmes, R. Kirchholtes, E. Lindsey, K.C. Maguire, A.W. Poust, M.A. Stegner, J, Sunseri, B. Swartz, J. Swift, N.A. Villavicencio, and G.O.U. Wogan. 2014. Prelude to the Anthropohcene: two new North American Land Mammal Ages (NALMAs). The Anthropocene Review 1–18.

Barnosky, A.D., N. Matzke, S. Tomiya, G.O.U. Wogan, B. Swartz, T.B. Quental, C. Marshall, J.L. McGuire, E.L. Lindsey, K.C. Maguire, B. Mersey, and E.A. Ferrer. 2011. Has the Earth's sixth mass extinction already arrived? Nature 471:51–57.

Barnosky, A.D., P.L. Koch, R.S. Feranec, S.L. Wing, and A.B. Shabel, 2004. Assessing the causes of Late Pleistocene extinctions on the continents. Science 306:70–75.

Barrón-Ortiz, C.R., J.M. Theodor, and J. Arroyo-Cabrales. 2014. Dietary resource partitioning in the Late Pleistocene horses from Cedral, north-central Mexico: evidence from the study of dental wear. Revista Mexicana de Ciencias Geológicas 31(2):260-269.

Baumann, E.J. and B.E. Crowley. 2015. Stable isotopes reveal ecological differences amongst now-extinct proboscideans from the Cincinnati region, USA. Boreas 44:240–254.

Beerling, D.J. and D.L. Royer. 2011. Convergent Cenozoic CO_2 history. Nature Geoscience 4:418–420.

Bell, C.J., E.L. Lundelius, A.D. Barnosky, R.W. Graham, and E.H. Lindsay. 2004. The Blancan, Irvingtonian, and Rancholabrean mammal ages. In M.O. Woodburne, ed. Late Cretaceous and Cenozoic Mammals of North America: Biostratigraphy and Geochronology. Columbia University Press, pp. 232–314.

Bender, M. 1971. Variations in the 13C/12C ratios of plants in relation to the pathway of photosynthetic carbon dioxide fixation. Phytochemistry 10:1239-1244

Bennet, P.M., I.P.F. Owens, D. Nussey, S.T. Garnett, and G.M. Crowley. 2005. Mechanisms of extinction in birds: phylogeny, ecology, and threats in: Purvis A, Gittleman JL, Brooks T, (Eds). Phylogeny and Conservation. Cambridge: Cambridge Universty Press, 317-336.

Berger, J. and C. Cunningham. 1998. Behavioural ecology in managed reserves: gender-based asymmetries in interspecific dominance in African elephants and rhinos. Animal Conservation 1:33-38.

Bernor, R.L., G.M. Semprebon, and J. Damuth. 2014, Maragheh ungulate mesowear: interpreting paleodiet and paleoecology from a diverse fauna with restricted sample sizes. Annales Zoologici Fennici, 51:201–208.

Bibi, F. 2007. Dietary niche partitioning among fossil bovids in late Miocene C3 habitats: Consilience of functional morphology and stable isotope analysis. Palaeogeography, Palaeoclimatology, Palaeoecology 253:529–538.

Bininda-Emonds, O.R.P., M. Cardillo, K.E. Jones, R.D.E. MacPhee, R.M.D. Beck, R. Grenyer, S.A. Price, R.A. Vos, J.L. Gittleman, and A. Purvis. 2007 The delayed rise of present-day mammals. Nature 446:507-512.

Blois, J.L. and E.A. Hadley. 2009. Mammalian response to Cenozoic climate change. Annual Review of Earth and Planetary Sciences 37:8.1-8.28.

Blondel, C., Merceron, G., Andossa, L., Taisso, M.H., Vignaud, P., Brunet, M., 2010. Dental mesowear analysis of the late Miocene Bovidae from Toros-Menalla (Chad) and early hominid habitats in Central Africa. Palaeogeography, Palaeoclimatology, Palaeoecology 292, 184-191.

Blum, M.D. and Aslan, A. 2006. Signatures of climate vs. sea-level change within incised valley-fill successions: Quaternary examples from the Texas Gulf Coast. Sedimentary Geology 190, 177-211.

Bocherens, H., G. Pacaud, P.A. Lazarev, and A. Mariotti. 1996. Stable isotope abundances (13C, 15N) in collagen and soft tissues from Pleistocene mammals from Yakutia: Implications for the palaeobiology of the Mammoth Steppe. Palaeogeography, Palaeoclimatology, Palaeoecology 126:31-44.

Bond, G.C. and R. Lotti. 1995. Iceberg discharges into the North Atlantic on millennial time scales during the last glaciation. Science 267:1005-1010.

Bond, W.J. 1993. Keystone species. In E.D. Schulze and H.A. Mooney, eds. Biodiversity and ecosystem function. Springer-Verlag. pp. 237–253.

Bowen, G.J., B.J. Maibauer, M.J. Kraus, U. Röhl, T. Westerhold, A. Steimke, P.D. Gingerich, S.L. Wing, and W.C. Clyde. 2015. Two massive, rapid releases of carbon during the onset of the Palaeocene-Eocene thermal maximum, Nature Geosci 8:44-47.

Broecker, W. and A.E. Putnam. 2012. How did the hydrologic cycle respond to the two-phase mystery interval? Quaternary Science Reviews 57:17-25.

Bryant, J.D. and P.N. Froelich. 1995. A model of oxygen isotope fractionation in body water of large mammals. Geochimica et Cosmochimica Acta 59:4523–4537.

Bryant, V.M. and R.G. Holloway. 1985. A late-Quaternary Paleoenvironmental record of Texas: an overview of the pollen evidence, in: Bryant, V.M., Holloway, R.G. (Eds.), Pollen records of late-Quaternary North American sediments. American Association of Stratigraphic Palynologists Foundation, pp. 39-70.

Burger, B.J. 2012. Northward range extension of a diminutive-sized mammal (*Ectocion parvus*) and the implication of body size change during the Paleocene-Eocene Thermal Maximum. Palaeogeography, Palaeoclimatology, Palaeoecology 363-364:144–150.

Burns, J.H. and S.Y. Strauss. 2011. More closely related species are more ecologically similar in an experimental test. Proceedings of the National Academy of Sciences of the United States of America 108(13):5302–5307.

Butler, K., J. Louys, and K. Travouillon. 2014. Extending dental mesowear analyses to Australian marsupials, with applications to six Plio-Pleistocene kangaroos from south-east Queensland. Palaeogeography, Palaeoclimatology, Palaeoecology 408:11–25.

Butler, P.M., 1972. Some functional aspects of molar evolution. Evolution 26:474–483.

Cabin, R.J. and R.J. Mitchell. 2000. To Bonferroni or not to Bonferroni: when and how are the questions. Bulletin of the Ecological Society of America 81:246–248.

Calandra, I. and G. Merceron. 2016. Dental microwear texture analysis in mammalian ecology. Mammal Review 46:215–228.

Calandra, I., U.B. Göhlich, and G. Merceron. 2008. How could sympatric megaherbivores coexist? Example of niche partitioning within a proboscidean community from the Miocene of Europe. Naturwissenschaften 95:831–838.

Campos-Arceiz, A. and S. Blake. 2011. Megagardeners of the forest – the role of elephants in seed dispersal. Acta Oecologica 37:542–553.

Capozza, M., 2001. Microwear analysis of *Mammuthus meridionalis* (Nesti, 1825) molar from Campo del Conte (Frosinone, Italy), in: The World of Elephants: Proceedings of the 1st International Congress, Rome, Italy, 529-533.

Carrasco, M.A., B.P. Kraatz, E.B. Davis, and A.D. Barnosky. 2005. Miocene mam-

mal mapping project (MIOMAP). University of California Museum of Paleontology, http://www.ucmp.berkeley.edu/miomap/

Cavender-Bares, J., D.D. Ackerly, D.A. Baum, and F.A. Bazzaz. 2004. Phylogenetic overdispersion in Floridian oak communities. American Naturalist 163:823-843.

Cerling, T.E. and J.M. Harris. 1999. Carbon isotope fractionation between diet and bioapatite in ungulate mammals and implications for ecological and paleoecological studies. Oecologia 120:347-363.

Cerling, T.E., J.M. Harris, B.J. MacFadden, M.G. Leakey, J. Quade, V. Eisenmann, and J.R. Ehleringer. 1997. Global vegetation change through the Miocene/Pliocene boundary. Nature 389:153–158.

Cerling, T.E., J.M. Harris, and M.G. Leakey. 1999. Browsing and grazing in elephants: the isotopic record of modern and fossil proboscideans. Oecologia 120:364-374.

Cerling, T.E., J.M. Harris, and M.G. Leakey. 2003. Isotope paleoecology of the Nawata and Nachukui Formations at Lothagam, Turkana Basin, Kenya. In M.G. Leakey and J.M. Harris, eds. Lothagam: The Dawn of Humanity in Eastern Africa. Columbia University Press, New York, pp. 605–624.

Cerling, T.E., J.R. Ehleringer, and J.M. Harris. Carbon dioxide starvation, the development of C_4 ecosystems, and mammalian evolution. Phil. Trans. R. Soc. Lond. B 353:159-171.

Chalk-Wilayto, J., K. Ossi-Lupo, and M. Raguet-Schofield. 2016. Growing up tough: comparing the effects of food toughness on juvenile feeding in *Sapajus libidinosus* and *Trachypithecus phayrei crepusculus*. Journal of Human Evolution 98:76-89.

Challender, D.W.S. and D.C. MacMillan. 2014. Poaching is more than an enforcement problem. Conservation Letters 7:484-494.

Chaney, R.W. and H.L. Mason. 1930. A Pleistocene flora from Santa Cruz Island, California. 514. Carnegie Institution of Washington Publication, pp. 1–24.

Christianson, D. and S. Creel. 2009. Effects of grass and browse consumption on the winter

mass dynamics of elk. Oecologia 158:603–613.

Clark, I.D. and P. Fritz. 1997. Environmental Isotopes in Hydrogeology, CRC Press, United States.

Clark, P.U., A.S. Dyke, J.D. Shakun, A.E. Carlson, J. Clark, B. Wohlfarth, J.X. Mitrovica, S.W. Hostetler, and A.M. McCabe. 2009. The last glacial maximum. Science 325:710–714.

Clementz, M.T. and P.L. Koch. 2001. Differentiating aquatic mammal habitat and foraging ecology with stable isotopes in tooth enamel. Oecologia 129:461– 472.

Collatz, G.J., J.A. Berry, and J.S. Clark. 1998. Effects of climate and atmospheric CO2 partial pressure on the global distribution of C4 grasses: present, past, and future. Oecologia 114:441–454.

Connin, S.L., J. Betancourt, and J. Quade. 1998. Late Pleistocene C4 plant dominance and summer rainfall in the southwestern United States from isotopic study of herbivore teeth. Quaternary Research 50:179-193.

Conservation Paleobiology Workshop. 2012. Conservation Paleobiology: Opportunities for the Earth Sciences. Report to the Division of Earth Sciences, National Science Foundation. Paleontological Research Institution, Ithaca, New York, 32 pp.

Coplen, T.B. 1994. Reporting of stable hydrogen, carbon, and oxygen isotopic abundances. Pure and Applied Chemistry 66(2):273–276.

Croft, D.A. and D. Weinstein. 2008. The first application of the mesowear method to endemic South American ungulates (Notoungulata) Palaeogeography, Palaeoclimatology, Palaeoecology 269:103–114.

Danowitz, M., S. Hou, M. Mihlbachler, V. Hastings, and N. Solounias. 2016. A combined-mesowear analysis of late Miocene giraffids from north Chinese and Greek localities of the Pikermian Biome. Palaeogeography, Palaeoclimatology, Palaeoecology 449:194–204.

Dansgaard W. 1964. Stable isotopes in precipitation. Tellus 16:273–276.

Dansgaard, W., S. Jonsen, H.B. Clausen, D. Dahl-Jensen, N.S. Gundenstrup, C.U. Ham-

mer, C.S. Hvidberg, J.P. Steffensen, A.E. Sveinjjornsdottir, J. Jouzel, G. Bond. 1993. Evidence for general instability of past climate from a 250 kyr ice-core record. Nature 364:218-220.

Darroch, S.A.F., E.A. Sperling, T.H. Boag, R.A. Racicot, S.J. Mason, A.S. Morgan, S. Tweedt, P. Myrow, D.T. Johnston, D.H. Erwin, and M. Laflamme. 2015. Biotic replacement and mass extinction of the Ediacara biota. Proc. R. Soc. B. 282:20151003.

Darwin, C. 1859. On the Origin of Species. London: John Murray; 1st Ed.

Davies, J.T., S.A. Fritz, R. Greyner, C.D.L. Orme, J. Bielby, O.R.P. Bininda-Emonds, et al. 2008. Phylogenetic trees and the future of mammalian biodiversity. PNAS USA 105(1):11556-11563.

de Albernaz, T.L., E.R. Secchi, L.R. de Oliveira, S. Botta. 2017. Ontogenetic and gender-related variation in the isotopic niche within and between three species of fur seals (genus *Arctocephalus*). Hydrobiologia 787:123-139.

DeMiguel, D., B. Azanza, and J. Morales. 2011. Paleoenvironments and paleoclimate of the middle Miocene of central Spain: a reconstruction from dental wear of ruminants. Palaeogeography, Palaeoclimatology, Palaeoecology 302:452–463.

DeSantis, L.R.G. 2016. Dental microwear textures: reconstructing diets of fossil mammals. Surface Topography: Metrology and Properties 4:1–12.

DeSantis, L.R.G. and B.W. Schubert. 2015. Tales from tapir teeth: dietary ecology of extant and extinct tapirs as inferred from dental microwear texture analysis. Southeastern Vertebrate Paleontology Meeting Program and Abstracts Book 2015.

DeSantis, L.R.G., J. Alexander, E. Biedron, P.S. Johnson, A.S. Frank, J.M. Martin, and L. Williams. 2018. Effects of climate on dental mesowear of extant koalas and two broadly distributed kangaroos throughout their geographic range. PLoS ONE 13(8):e0201962.

DeSantis, L.R.G., J.H. Field, S. Wroe, and J. Dodson. 2017. Dietary responses of Sahul (Pleistocene Australia-New Guinea) megafauna to climate and environmental change. Paleobiology - Rapid Communications 43:181–195.

DeSantis, L.R.G., J.R. Scott, B.W. Schubert, S.L. Donohue, B.M. McCray, C.A. Van Stolk, A.A. Winburn, M.A. Greshko, and M.C. O'Hara. 2013. Direct comparisons of 2D and 3D dental microwear proxies in extant herbivorous and carnivorous mammals. PLoS ONE 8:e71428.

DeSantis, L.R.G., R.A. Beavins Tracy, C.S. Koontz, J.C. Roseberry, and M.C. Velasco. 2012. Mammalian niche conservation through deep time. PLoS ONE 7(4):e35624.

DeSantis, L.R.G., R.S. Feranec, and B.J. MacFadden. 2009. Effects of global warming on ancient mammalian communities and their environments. PLoS ONE 4(6):e5750.

Díaz-Sibaja, R., E. Jiménez-Hidalgo, J. Ponce-Saavedra, and M.L. García-Zepeda. 2018. A combined mesowear analysis of Mexican *Bison antiquus* shows a generalist diet with geographical variation. Journal of Paleontology 92:1130–1139.

Diefendorf, A.F., K.H. Freeman, S.L. Wing, E.D. Currano, and K.E. Mueller. 2015. Paleogene plants fractionated carbon isotopes similar to modern plants. Earth and Planetary Science Letters 429:33-44.

Dietl, G.P. and K.W. Flessa (Eds.) 2009. Conservation Paleobiology: using the past to manage for the future. Paleontological Society Papers 15, 285 pp.

Dietl, G.P. and K.W. Flessa. 2011. Conservation Paleobiology: putting the dead to work. Trends in Ecology and Evolution 26(1): 30-37.

Dimmit, M.A. 2000. Biomes and communities of the Sonoran Desert region, in: Phillips, S.J., Comus, P.W. (Eds.), A Natural History of the Sonoran Desert. ASDM Press/University of California Press, pp. 3–18.

Dooley, A.C., E. Scott, J.L. Green, K.B. Springer, B.S. Dooley, and G.J. Smith. 2019. Mammut pacificus sp. nov., a newly recognized species of mastodon from the Pleistocene of western North America. PeerJ 7:e6614.

Dorale, J.A., R.L. Edwards, E. Ito, and L.A. Gonzalez. 1998. Climate and vegetation history of the midcontinent from 75 to 25 ka: A speleothem record from crevice cave, Missouri, USA. Science 282:1871–1874.

Drucker, D.G., C. Vercoutère, L. Chiotti, R. Nespoulet, L. Crépin, N.J. Conard, S.C. Münzel, T. Higham, J. van der Picht, M. Lázničková-Galetová, and H. Bocherens. 2015. Tracking possible decline of woolly mammoth during the Gravettian in Dordogne (France) and the Ach Valley (Germany) using multi-isotope tracking (13C, 14C, 15N, 34S, 18O). Quaternary International 359-360:304-317.

Dudley, J.P. 1996. Mammoths, gomphotheres, and the Great American Faunal Interchange, in: J. Shoshani J. and P. Tassy, eds. The Proboscidea: Evolution and Paleoecology of Elephants and their Relatives. Oxford University Press, pp. 289–295.

Dunn, O.J. 1964. Multiple comparisons using rank sums. Technometrics 6:241–252.

Ecker, M., H. Bocherens, M.A. Julien, F. Rivals, J.P. Raynal, and M.H. Moncel. 2013. Middle Pleistocene ecology and Neanderthal subsistence: insights from stable isotope analyses in Payre (Ardèche, southeastern France). Journal of Human Evolution 65:363–373.

Ehleringer, J.R. and R.K. Monson. 1993. Evolutionary and ecological aspects of photosynthetic pathway variation. Annual Review of Ecology and Systematics 24:411–439.

Ehleringer, J.R., T.E. Cerling, and B.R. Helliker. 1997. C4 photosynthesis, atmospheric CO2, and climate. Oecologia 112:285–299.

Ehleringer J.R., R.F. Sage, L.B. Flanagan, and R.W. Pearcy. 1991. Climate change and the evolution of C4 photosynthesis. Trends in Ecology and Evolution 6:95–99.

Elliot, M., L. Labeyrie, G. Bond, E. Cortijo, J.L. Turon, N. Tisnerat, and J.C. Duplessy. 1998. Millenial-scale iceberg discharges in the Irminger Basin during the last glacial period: relationship with the Heinrich events and environmental settings. Paleoceanography 13:433-446.

Enk, J., A. Devault, C. Widga, J. Saunders, P. Szpak, J. Southon, J.M. Rouillard, B. Shapiro, B. Golding, G. Zazula, D. Froese, D. Fisher, H. Poinar, and R. Macphee. 2016. *Mammuthus* population dynamics in Late Pleistocene North America: Divergence, Phylogeography and Introgression. Frontiers in Paleontology.

Enk, J., A. Devault, R. Debruyne, C.E. King, T. Treangen, D. O'Rourke, S.L. Salzberg, D. Fisher, R. MacPhee, and H. Poinar. 2011. Complete Columbian mammoth mitogenome suggests interbreeding with woolly mammoths. Genome Biology 12: R51.

Erwin, D.H. 1998. The end and the beginning: recoveries from mass extinctions. Trends in Ecology and Evolution. 13:344-349.

Erwin, D.H. 2001. Lessons from the past: biotic recoveries from mass extinctions. PNAS 98:5399-5403.

Erwin, D.H. 2008. Extinction as the loss of evolutionary history. PNAS 105:11520-11527.

Evans, G.L. 1961. The Friesenhahn Cave: Part I: Bulletin of the Texas Memorial Museum 2:7–22.

Faith, D.P. 1992. Conservation evaluation and phylogenetic diversity. Biol Conserv 61:1–10.

Farquhar, G.D., J.R. Ehleringer, K.T. Hubick. 1989. Carbon isotope discrimination and photosynthesis. Annual Review of Plant Physiology and Plant Molecular Biology 40:503–537.

Farrell, A. and C.A. Shaw. 2009. A preliminary description of an unusually complete specimen of *Mammuthus columbi* from Rancho La Brea, Los Angeles, California. Journal of Vertebrate Paleontology 29 (3):94A.

Feranec, R.S. 2004. Geographic variation in the diet of hypsodont herbivores from the Rancholabrean of Florida. Palaeogeography, Palaeoclimatology, Palaeoecology 207:359–369.

Feranec, R.S. and B.J. MacFadden. 2000. Evolution of the grazing niche in Pleistocene mammals from Florida: evidence from stable isotopes. Palaeogeography, Palaeoclimatology, Palaeoecology 162:155–169.

Feranec, R.S., E.A. Hadly, and A. Paytan. 2009. Stable isotopes reveal seasonal competition for resources between late Pleistocene *Bison* (*Bison*) and horse (*Equus*) from Rancho La Brea, southern California. Palaeogeography, Palaeoclimatology, Palaeoecology 271:153–160.

Finnegan, S., S.C. Anderson, P.G. Harnik, C. Simpson, D.P. Tittensor, J.E. Byrnes, Z.V.

Finkel, D.R. Lindberg, L.H. Liow, R. Lockwood, H.K. Lotze, C.R. McClain, J.L. McGuire, A. O'Dea, and J.M. Pandolfi. 2015. Paleontological baselines for evaluating extinction risk in the modern oceans. Science 348(6234):567-570.

Filippi, M.L., M.R. Palombo, M. Barbieri, M. Capozza, P. Iacumin, and A. Longinelli. 2001. Isotope and microwear analyses on teeth of late Middle Pleistocene *Elephas antiquus* from the Rome area (La Polledrara, Casal de' Pazzi), in: The World of Elephants: Proceedings of the 1st International Congress, Rome, Italy, 529-533.

Fisher, D.C. 2004. Season of musth and musth-related mortality in Pleistocene mammoths. Journal of Vertebrate Paleontology 24(Suppl. to 003):58A.

Fisher, D.C. 2018. Paleobiology of Pleistocene Proboscideans. Annual Review of Earth and Planetary Sciences 46:229-260.

Fisher, D.C., M.D. Cherney, C. Newton, A.N. Rountry, Z.T. Calamari, R.K. Stucky, C. Lucking, and L. Petrie. 2014. Taxonomic overview and tusk growth analyses of Ziegler Reservoir proboscideans. Quaternary Research 82:518–532.

Foote, M. 2000. Origination and extinction components of taxonomic diversity: general problems. Paleobiology 26(4):578-605.

Fortelius, M. and N. Solounias. 2000. Functional characterization of ungulate molars using the abrasion-attrition wear gradient: a new method for reconstructing paleodiets. American Museum Novitates 3301:1–36.

Foster, J.B. 1964. The evolution of mammals on islands. Nature 202:234-235.

Fox, D.L. and D.C. Fisher. 2001. Stable isotope ecology of a Late Miocene population of Gomphotherium productus (Mammalia, Proboscidea) from Port of Entry Pit, Oklahoma, USA. PALAIOS 16:279–293

Fox, D.L. and D.C. Fisher. 2004. Dietary reconstruction of Miocene Gomphotherium (Mammalia, Proboscidea) from the Great Plains region, USA, based on the carbon isotope composition of tusk and molar enamel. Paleogeography, Paleoclimatology, Paleoecology 206:311–335.

Fox-Dobbs, K., J.A. Leonard, and P.L. Koch. 2008. Pleistocene megafauna from eastern Beringia: Paleoecological and paleoenvironmental interpretations of stable carbon and nitrogen isotope and radiocarbon records. Palaeogeography, Palaeoclimatology, Palaeoecology 261:30-46.

Fowler, D.W. 2017. Revised geochronology, correlation, and dinosaur stratigraphic ranges on the Santonian-Maastrichtian (Late Cretaceous) formations of the Western Interior of North America. PLoS ONE 12(11):e0188426.

França, L.M., M.A.T. Dantas, A. Bocchiglieri, A. Cherckinsky, A.S. Ribeiro and H. Bocherens, 2014. Chronology and ancient feedings ecology of two upper Pleistocene megamammals from the Brazilian intertropical Region. Quaternary Science Reviews 99:78–83.

Franz-Odendaal, T.A. and T.M. Kaiser. 2003. Differential mesowear in the maxillary and mandibular cheek dentition of some ruminants (Artiodactyla). Ann. Zool. Fennici. 40:395–410.

Fraser, D., R. Gorelick, and N. Rybczynski. 2015. Macroevolution and climate change influence phylogenetic community assembly of North American hoofed mammals. Biological Journal of the Linnean Society 114:485-494.

Friedman, I. and J.R. O'Neil. 1977. Compilation of stable isotope fractionation factors of geochemical interest. USGPO.

Fritz, H. 1997. Low ungulate biomass in west African savannas: primary production or missing megaherbivores or large predator species? Ecography 20:417–421.

Fritz, H., M. Loreau, S. Chamaille-Jammes, M. Valeix, J. Clobert. 2011. A food web perspective on large herbivore community limitation. Ecography 34:196–202.

Fritz, H., P. Duncan, I.J. Gordon, and A.W. Illius. 2002. Megaherbivores influence trophic guilds structure in African ungulate communities. Oecologia 131:620– 625.

Galbany, J., L.M. Martínez, H.M. López-Amor, V. Espurz, O. Horaldo, A. Romero, J. de Juan, and A. Pérez-Pérez. 2005. Error rates in buccal-dental microwear quantification using scanning electron microscopy. Scanning 27:23–29.

Geist, V. 1974. On the relationship of social evolution and ecology in ungulates. American Zoologist 14:205–220.

Gill, J.L., J.W. Williams, S.T. Jackson, K.B. Lininger, and G.S. Robinson. 2009. Pleistocene megafaunal collapse, novel plant communities, and enhanced fire regimes in North America. Science 326(5956):1100-1103.

Gillette, D.D. and D.B. Madsen. 1993. The Columbian mammoth, *Mammuthus columbi*, from the Wasatch Mountains of Central Utah. Journal of Paleontology 67:669-680.

Gingerich, P.D. 2003. Mammalian responses to climate change at the Paleocene-Eocene boundary: Polecat Bench record in the northern Bighorn Basin, Wyoming. Geological Society of America Special Paper 369:463-478.

Gittleman, J.L. and M. Kot. 1990. Adaptation: statistics and a null model for estimating phylogenetic effects. Systematic Zoology 39(3):227-241.

Glover, K.C., G.M. MacDonald, M.E. Kirby, E.J. Rhodes, L. Stevens, E. Silveira, A. Whitaker, and S. Lydon. 2017. Evidence for orbital and North Atlantic climate forcing in alpine Southern California between 125 and 10 ka from multi-proxy analyses of Baldwin Lake. Quaternary Science Reviews 167:47–62.

Gobetz, K.E. and S.R. Bozarth. 2001. Implications for late Pleistocene mastodon diet from opal phytoliths in tooth calculus. Quaternary Research 55:115-122.

Gogarten, J.F. and F.E. Grine. 2013. Seasonal mortality patterns in primates: implications for interpretation of dental microwear. Evolutionary Anthropology 22:9–19.

González-Guarda, E., A. Petermann-Pichincura, C. Tornero, L. Domingo, J. Agustí, M. Pino, A.M. Abarzúa, J.M. Capriles, N.A. Villavicencio, R. Labarca, V. Tolorza, P. Sevilla, and F. Rivals. 2018. Multiproxy evidence for leaf-browsing and closed habitats in extinct proboscideans (Mammalia, Proboscidea) from Central Chile. Proceedings of the National Academy of Sciences of the United States of America 115(37):9258–9263.

Gordon, K.D. 1988. A review of methodology and quantification in dental microwear analysis. Scanning Microscopy 2:1139–1147.

Graham, R.W., 1976. Pleistocene and Holocene mammals, taphonomy, and paleoecology of the Friesenhahn Cave Local Fauna, Bexar County, Texas. University of Texas PhD Dissertation, 254 p.

Graham, R.W. 1986. Descriptions of the dentitions and stylogyoids of *Mammuthus columbi* from the Colby Site, in: Frison, G.C., Todd, L.C. (Eds.), The Colby Mammoth Site – Taphonomy and Archaeology of a Clovis Kill in Northern Wyoming. University of New Mexico Press, Albuquerque. pp. 171-229

Graham, R.W. 2005. Quaternary mammal communities: relevance of the individualistic response and non-analogue faunas. Paleontological Society Papers 11:141-158.

Graham, R.W. and E.C. Grimm. 1990. Effects of global climate change on the patterns of terrestrial biological communities. Trends in Ecology and Evolution 5(9):289-292.

Graham, R.W. and E.L. Lundelius. 1984. Coevolutionary disequilibrium and Pleistocene extinctions. In P.S. Martin and R.G. Klein, eds. Quaternary Extinctions: a Prehistoric Revolution. University of Arizona Press, Tuscon, pp. 223-249.

Graham, R.W., E.L. Lundelius, Jr., and L. Meissner, with contribution by Keith Muhlestein, 2013. Friesenhahn Cave: Late Pleistocene paleoecology and predator – prey relationships of mammoths with an extinct scimitar cat, in: Hunt, B.B., Catlos, E.J. (Eds.), Late Cretaceous to Quaternary Strata and Fossils of Texas: Field Excursions Celebrating 125 Years of GSA and Texas Geology, GSA South-Central Section Meeting, Austin, Texas, April 2013: Geological Society of America Field Guide 30, p. 15–31, doi:10.1130/2013.0030(02).

Grant, P.R., and B.R. Grant. 2006. Evolution of character displacement in Darwin's finches. Science 313:224-226.

Green, J.L., Hulbert, R., 2005. The deciduous premolars of *Mammut americanum* (Mammalia, Proboscidea). Journal of Vertebrate Paleontology 25, 702-715.

Green, J.L., G.M. Semprebon, and N. Solounias. 2005. Reconstructing the paleodiet of Florida *Mammut americanum* via low-magnification sterepmicroscopy. Palaeogeogra-

phy, Palaeoclimatology, Palaeoecology 223:34-48.

Green, J.L., L.R.G. DeSantis, and G.J. Smith. 2017. Regional variation in the browsing diet of Pleistocene *Mammut americanum* (Mammalia, Proboscidea). Palaeogeography, Palaeoclimatology, Palaeoecology 487:59–70.

Grimm, E.C., G.L. Jacobson, W.A. Watts, B.C.S. Hansen, and K.A. Maasch. 1993. A 50,000-year record of climate oscillations from Florida and its temporal correlation with the Heinrich events. Science 261(5118):198-200.

Grimm, E.C., W.A. Watts, G.L. Jacobson, B.C.S. Hansen, H.R. Almquist, and A.C. Diffenbacher-Krall. 2006. Evidence for warm wet Heinrich events in Florida. Quaternary Science Reviews 25:2197-2211.

Grine, F.E. 1981. Trophic differences between gracile and robust australopithecines - a scanning electron-microscope analysis of occlusal events South African Journal of Sciences 77:203–230.

Grine, F.E. 1986. Dental evidence for dietary differences in *Australopithecus* and *Paranthropus*: a quantitative analysis of permanent molar microwear Journal of Human Evolution 15:783–822.

Grine, F.E., P.S. Ungar, and M.F. Teaford. 2002. Error rates in dental microwear quantification using scanning electron microscopy. Scanning 24:144-153.

Guthrie, R.D. 1984. Mosaics, allelochemics and nutrients: an ecological theory of Late Pleistocene Megafaunal Extinctions, in: P.S. Martin and R.G. Klein, eds. Quaternary Extinctions: a Prehistoric Revolution. University of Arizona Press, Tuscon, pp. 259-298.

Hanley, T.A 1982. The nutritional basis for food selection by ungulates. Journal of Range Management 35:146-151.

Hardin, G. 1960. The competitive exclusion principle. Science 131:1292–1297.

Hardy, F.C. 2015. Stable isotope analysis of *Bison* latifrons and paleoecological inferences. UNLV Theses, Dissertations, Professional Papers, and Capstones. 2478.

Harris, E.B. 2016. Effects of the mid-Miocene Climatic Optimum on ecosystem structure and plant-animal interactions: a phytolith and stable isotope perspective. University of Washington Dissertation. 229 pp.

Harris, J.M. 2001. Reconstructing a late Pleistocene environment. In: Harris, J.M. (Ed.), Rancho La Brea: Death Trap and Treasure Trove. Terra, vol. 38(2), pp. 12–21.

Harvey, P.H. and M.D. Pagel. 1991. The comparative method in evolutionary biology. Oxford University Press.

Haupt, R.J., L.R.G. DeSantis, J.L. Green, and P.S. Ungar. 2013. Dental microwear texture as a proxy for diet in xenarthrans. Journal of Mammalogy 94:856-866.

Haynes, G. 2012. Elephants (and extinct relatives) as earth-movers and ecosystem engineers. Geomorphology 157-158:99-107.

Haynes, G. 2017. Finding meaning in mammoth age profiles. Quaternary International 443:65-78.

Hedberg, C. and L.R.G. DeSantis. 2017. Dental microwear texture analysis of extant koalas: clarifying causal agents of microwear. Journal of Zoology 301:206-214.

Heinrich, H. 1988. Origin and consequences of ice-rafting in the northeast Atlantic Ocean during the last 130,000 years. Quaternary Research 29:142-152.

Herold, N., M. Huber, and R.D. Müller. 2011. Modeling the Miocene Climatic Optimum. Part I: Land and Atmosphere*. Journal of Climate 24:6353–6372.

Hester, A., M. Bergman, G. Iason, and J. Moen. 2006. Impacts of large herbivores on plant community structure and dynamics, in: Danell, K., Bergstrom, R., Duncan, P., Pastor, J. (Eds.), Large herbivore ecology, ecosystem dynamics and conservation. Cambridge University Press, pp. 97–141.

Heusser, L.E. 1995. Pollen stratigraphy and paleoceanographic interpretation of the 160-k.y. record from Santa Barbara Basin, Hole 893A. Proc. Ocean Drill. Program Sci. Results 146(2):265–281.

Heusser, L.E. 1998. Direct correlation of millennial-scale changes in western North Amer-

ican vegetation and climate with changes in the California current system over the past 60 kyr. Paleoceanography 13:252-262.

Heusser, L.E. and F. Sirocko. 1997. Millennial pulsing of environmental change in southern California from the past 24 k.y.: a record of Indo-Pacific ENSO events? Geology 25(3):243-246.

Higgins, P. and B.J. MacFadden. 2004. "Amount Effect" recorded in oxygen isotopes of Late Glacial horse (*Equus*) and *Bison* (*Bison*) teeth from the Sonoran and Chihuahuan deserts, southwestern United States. Paleogeography, Paleoclimatology, Paleoecology 206(3):337–353.

Hillborn, R., P. Arcese, M. Borner, J. Hando, G. Hopcraft, M. Loibooki, S. Mduma, and A.R.E. Sinclair. 2006. Effective enforcement in a conservation area. Science 314(5803):1266

Holland, S.M. 2018. Estimation, not significance. Paleobiology (43):1-6.

Hooker, J.J. 2000. Paleogene mammals: crises and ecological change, in: Biotic Response to Global Change: The Last 145 Million Years, ed. SJ Culver, PF Rawson, pp. 333–49. New York: Cambridge Univ. Press

Hopkins, S.S.B. 2007. Causes of lineage decline in the Aplodontidae: Testing for the influence of physical and biological change. Palaeogeography, Palaeoclimatology, Palaeoecology 246 (2–4):331-353.

Hoppe, K.A. 2004. Late Pleistocene mammoth herd structure, migration patterns, and Clovis hunting strategies inferred from isotopic analyses of multiple death assemblages. Paleobiology 30:129–145.

Hulbert, R.C. 2010. A new early Pleistocene tapir (Mammalia: Perissodactyla) from Florida, with a review of Blancan tapirs from the state. Bulletin of the Florida Museum of Natural History 49(3):67-126

Hull, P.M. and S.A.F. Darroch. 2013. Mass extinctions and the structure and function of ecosystems, in: Ecosystem Paleobiology and Geobiology, The Paleontological Soci-

ety Short Course, October 26, 2013. The Paleontological Society Papers, Volume 19, Andrew M. Bush, Sara B. Pruss, and Jonathan L. Payne (eds.).

Hull, P.M., S.A.F. Darroch, and D.H. Erwin. 2015. Rarity of mass extinctions and the future of ecosystems. Nature 528:345-351.

Iacumin, P. A. Di Matteo, V. Nikolaev, and T.V. Kuznetsova. 2010. Climate information from C, N and O stable isotope analyses of mammoth bones from northern Siberia. Quaternary International 212:206–212.

Iqbal, A. and B.B. Khan. 2001. Feeding behaviour of camel. . . . . Review. Pak. J. Agric. Sci. 38:58–63.

Jablonksi, D. 1989. The biology of mass extinction: a paleontological view. Philos Trans Roy Soc Lon B 325:357-368.

Jablonski, D. 1991. Extinctions: a paleontological perspective. Science 253:754-757.

Janis, C.M. 1993. Tertiary mammal evolution in the context of changing climates, vegetation, and tectonic events. Annual Review of Ecological Systems 24:467-500.

Janis, C.M., J. Damuth, and J.M. Theodor. 2004. The species richness of Miocene browsers, and implications for habitat type and primary productivity in the North American grassland biome.Palaeogeography, Palaeoclimatology, Palaeoecology 207(3-4):371-398.

Janzen, D.H. 1986. Chihuahuan Desert Nopaleras: defaunated big mammal vegetation. Annual Review of Ecology and Systematics 17:595–636.

Janzen, D.H. and P.S. Martin. 1982. Neotropical anachronisms: the fruits the gomphotheres ate. Science 215(4528):19-27.

Jefferson, G.T., 2003. Stratigraphy and paleontology of the middle to late Pleistocene Manix Formation, and paleoenvironments of the central Mojave River, southern California, in: Enzel, Y., Wells, S.G., Lancaster, N. (Eds.), Paleoenvironments and Paleohydrology of the Mojave and Southern Great Basin Deserts, pp. 43–60. Geological Society of America Special Paper 368.

Jefferson, G.T. and J.L. Goldin. 1989. Seasonal migration of *Bison antiquus* from Rancho

La Brea, California. Quaternary Research 31:107–112.

Jiménez-Moreno, G., R.S. Anderson, S. Desprat, L.D. Grigg, E.C. Grimm, L.E. Heusser, B.F. Jacobs, C. López-Martínez, C.L. Whitlock, and D.A. Willard. 2010. Millennial-scale variability during the last glacial in vegetation records from North America. Quaternary Science Reviews 29:2865-2881.

Johnson, C.N., 2009. Ecological consequences of Late Quaternary extinctions of megafauna. Proceedings of the Royal Society B: Biological Sciences 276, 2509 –2519.

Johnson, D. 1978. The origin of island mammoths and the quaternary land bridge history of the northern Channel Islands, California. Quaternary Research 10:204-225.

Jones, B.D. and L.R.G. DeSantis. 2017. Dietary ecology of ungulates from the La Brea tar pits in southern California: a multi-proxy approach. Palaeogeography, Palaeoclimatology, Palaeoecology 466:110–127.

Jones, C.G., J.H. Lawton, and M. Shachak. 1994. Organisms as ecosystem engineers. Oikos 69:373–386.

Kaiser, T.M. and M. Fortelius. 2003. Differential mesowear in occluding upper and lower molars: opening mesowear analysis for lower molars and premolars in hypsodont horses. Journal of Morphology 25:67–83.

Kaiser, T.M. and E. Schulz. 2006. Tooth wear gradients in zebras as an environmental proxy – a pilot study. Mitteilungen aus dem Hamburgischen Zoologischen Museum und Institut 103:187–210.

Kaiser, T.M. and N. Solounias. 2003. Extending the tooth mesowear method to extinct and extant equids. Geodiversitas 25:321–345.

Kaiser, T.M., D.W.H. Müller, M. Fortelius, E. Schulz, D. Codron, and M. Clauss. 2013. Hypsodonty and tooth facet development in relation to diet and habitat in herbivorous ungulates: implications for understanding tooth wear. Mammal Review 43:34–46.

Kaiser, T.M., J. Brasch, J.C. Castell, E. Schulz, and M. Clauss. 2009. Tooth wear in captive wild ruminant species differs from that of free-ranging conspecifics. Mammalian

Biology 74:425–437.

Kaiser, T.M., N. Solounias, M. Fortelius, R.L. Bernor, and F. Schrenk. 2000. Tooth mesowear analysis on *Hippotherium primigenium* from the Vallesian Dinotherien-sande (Germany) - A blind test study. Carolinea 58:103–114.

Keller, G., P. Mateo, J. Punekar, H. Khozyem, B. Gertsch, J. Spangenberg, A.M. Bitchong, and T. Adatte. Environmental changes during the Cretaceous-Paleogene mass extinction and Paleocene-Eocene Thermal Maximum: implications for the Anthropocene. Gondwana Research 56:69-89.

King, J.E. 1973. Late Pleistocene palynology and biogeography of the Western Missouri Ozarks. Ecological Monographs 43:539–565.

King, J.E. and J.J. Saunders. 1984. Environmental insularity and the extinction of the American mastodont. In: Martin, P.S., Klein, R.G. (Eds.), Quaternary Extinctions: A Prehistoric Review. University of Arizona Press, Tuscon, pp. 315–339.

Kingston, J.D. and T. Harrison. 2007. Isotopic dietary reconstructions of Pliocene herbivores at Laetoli: implications for early hominin paleoecology. Palaeogeography, Palaeoclimatology, Palaeoecology 243:272-306.

Koch, P.L. 2007. Isotopic study of the biology of modern and fossil vertebrates, in: Michener, R.H., Latjha, K. (Eds.), Stable Isotopes in Ecology and Environmental Research. Blackwell Publishing, Boston, pp. 99-154.

Koch, P.L. and A.D. Barnosky. 2006. Late Quaternary Extinctions: State of the Debate. Annual Review of Ecology and Evolutionary Systems 37:215–250.

Koch, P.L., N.S. Diffenbaugh, and K.A. Hoppe. 2004. The effects of late Quaternary climate and pCO2 change on C4 plant abundance in the south-central United States. Palaeogeography, Palaeoclimatology, Palaeoecology 207:331–357.

Koch, P.L., N. Tuross, M.L. Fogel. 1997. The effects of sample treatment and diagenesis on the isotopic integrity of carbonate in biogenic hydroxylapatite. Journal of Archaeological Sciences 24:417–429.

Koch P.L., K.A. Hoppe, and S.D. Webb. 1998. The isotope ecology of late Pleistocene mammals in North America, Part 1. Florida. Chemical Geology 152:119–138.

Koch, P.L., N.S. Diffenbaugh, and K.A. Hoppe. 2004. The effects of late Quaternary climate and pCO2 change on C4 plant abundance in the south-central United States. Palaeogeography, Palaeoclimatology, Palaeoecology 207:331–357.

Kohn, M.J. 2010. Carbon isotope compositions of terrestrial C3 plants as indicators of (paleo)ecology and (paleo)climate. Proceedings of the National Academy of Sciences of the United States of America 107(46):19691–19695.

Kohn, M.J. 2016. Carbon isotope discrimination in C3 land plants is independent of natural variations in pCO2. Geochemical Perspectives Letters 2:35–43.

Kohn, M.J. and T.E. Cerling. 2002. Stable isotope compositions of biological apatite, in: M.J. Kohn, J. Rakovan, and J.M. Hughes, eds. Phosphates: geochemical, geobiological, and materials importance. Reviews in Mineralogy and Geochemistry 48, pp. 455–488.

Kohn, M.J., M.J. Schoeninger, and J.W. Valley. 1996. Herbivore tooth oxygen isotope compositions: effects of diet and physiology. Geochimica et Cosmochimica Acta 60:3889-3896.

Kohn M.J., M.J. Schoeninger, and J.W. Valley. 1998. Variability in herbivore tooth oxygen isotope compositions: Reflections of seasonality or developmental physiology? Chemical Geology 152:97–112.

Kowalewski, M. 2004. Conservation paleobiology, in: Geller, E. (Ed.), McGrawHill 2004 Yearbook of Science and Technology. McGrawHill, New York, pp. 60-62.

Knapp, A., J.M. Blair, J.M. Briggs, S.L. Collins, D.C. Hartnett, L.C. Johnson, and G. Towne. 1999. The keystone role of *Bison* in North American tallgrass prairie. BioScience 49:39–50.

Krug, A.Z. and M.E. Patzkowsky. 2015. Phylogenetic clustering of origination and extinction across the Late Ordovician mass extinction. PLoS ONE 10(12):e0144354

Kubiak, H. 1982. Morphological characters of the mammoth: An adaptation to the Arctic-Steppe environment, in: Hopkins, D.M., Matthews, J.V., Schweger, C.E. (Eds.), Paleoecology of Beringia. Academic Press, Inc, pp. 281-289.

Kurtén, B. and E. Anderson. 1980. Pleistocene mammals of North America. Columbia University Press, 442 p.

Landman, M., D.S. Schoeman, and G.I.H. Kerley. 2013. Shift in black rhinoceros diet in the presence of elephant: evidence for competition? PLoS ONE 8(7):e69771.

Larramendi, A. 2016. Shoulder height, body mass, and shape of proboscideans. Acta Paleontologica Polonica 61(3):537–574.

Laub, R.S. 1996. The masticatory apparatus of the American mastodon (*Mammut americanum*), in: Stewart, K.M., Seymour, K.L. (Eds.), Palaeoecology and Palaeoenvironments of Late Cenozoic Mammals: Tributes to the career of C.S. (Rufus) Churcher. University of Toronto Press, Toronto, pp. 375-405.

Lawrence, K.T., L.C. Sloan, and J.O. Sewall. 2003. Terrestrial climatic response to precessional orbital forcing in the Eocene. Geological Society of America Special Paper 369:65-77.

Laws, R.M. 1966. Age criteria for the African Elephant (Loxodonta africana). East African Wildlife Journal 4:1-37.

Laws, R.M. 1970. Elephants as agents of habitat and landscape change in East Africa. Oikos 21:1-15.

Lear, C.H., E.M. Mawbey, and Y. Rosenthal. 2010. Cenozoic benthic foraminiferal Mg/Ca and Li/Ca records: Toward unlocking temperatures and saturation states. Paleoceanography 25, 1–11.

Leavitt, S.W. 1993. Environmental information from 13C/12C ratios of wood, in: Swart, P.K., Lohmann, K.C., McKenzie, J., Savin, S. (Eds.), Climate Change in Continental Isotopic Records. Geophysical Monographs. American Geophysical Union, Washington, DC, pp. 325– 331.

Lee, P.C., S. Sayialal, W.K. Lindsay, and C.J. Moss. 2012. African elephant age determination from teeth: validation from known individuals. African Journal of Ecology 50:9-20.

Lepper, B.T., T.A. Frolking, D.C. Fisher, G. Goldstein, J.E. Sanger, and D.A. Wymer. 1991. Intestinal contents of a late Pleistocene mastodont from midcontinental North America. Quaternary Research 36:120-125.

Leuenberger, M., U. Siegenthaler, and C.C. Langway. 1992. Carbon isotope composition of atmospheric CO2 during the last ice age from an Antarctic ice core. Nature 357:488–490.

Levin, N.E., T.E. Cerling, B.H. Passey, J.M. Harris, and J.R. Ehleringer. 2006. A stable isotope aridity index for terrestrial environments. Proceedings of the National Academy of Science USA 103:11201–11205.

Lister, A.M. 2013. The role of behaviour in adaptive morphological evolution of African proboscideans. Nature 500(7462):331–334.

Lister, A.M. 2017. On the type material and evolution of North American mammoths. Quaternary International 443:14-31.

Lister, A.M. and A.V. Sher. 2015. Evolution and dispersal of mammoths across the Northern Hemisphere. Science 350:805-809.

Liu, Z., G.J. Bowen, and J.M. Welker. 2010. Atmospheric circulation is reflected in precipitation isotope gradients over the conterminous United States. Journal of Geophysical Research 115:1-14.

Liu, Z., M. Pagani, D. Zinniker, R. DeConto, M. Huber, H. Brinkhuis, S.R. Shah, R.M. Lecki, and A. Pearson. 2009. Global cooling during the Eocene-Oligocene Climate Transition. Science 323:1187-1190.

Lockwood, J.L., G.R. Russell, J.L. Gittleman, C.C. Daehler, M.L. McKinney, and A. Purvis. 2002. A metric for analyzing taxonomic patterns of extinction risk. Conservation Biology 16(4):1137–1142.

Loffredo, L.F. and L.R.G. DeSantis. 2014. Cautionary lessons from assessing dental mesowear observer variability and integrating paleoecological proxies of an extreme generalist *Cormohipparion emsliei*. Palaeogeography, Palaeoclimatology, Palaeoecology 395:42–52.

Longinelli, A. 1984. Oxygen isotopes in mammal bone phosphate: A new tool for paleohydrological and paleoclimatological research? Geochimica et Cosmochimica Acta 48:385–390.

Louys, J., P. Ditchfield, C. Meloro, S. Elton, and L.C. Bishop. 2012. Stable isotopes provide independent support for the use of mesowear variables for inferring diets in African antelopes. Proceedings of the Royal Society B: Biological Sciences 279:4441–4446.

Lucas, P.W. 2004. Dental Functional Morphology – How Teeth Work. Cambridge University Press, Cambridge, 99. 355 p.

Lucas, P.W., R. Omar, K. Al-Fadhalah, A.S. Almusallam, A.G. Henry, S. Michael, L.A. Thai, J. Watzke, D.S. Strait, and A.G. Atkins. 2013. Mechanisms and causes of wear in tooth enamel: implications for hominin diets. Journal of the Royal Society Interface 10: 20120923.

Lucas, S.G. 2008. Taxonomic nomenclature of *Cuvieronius* and *Haplomastodon*, proboscideans from the Plio-Pleistocene of the new world. New Mexico Museum Natural History and Science 44:409-415.

Lundelius, E.L. 1972. Fossil vertebrates from the Late Pleistocene Ingleside Fauna, San Patricio County, Texas. University of Texas Borough of Economic Geology Reports and Investigations 77:1-74.

Lundelius, E.L., V.M. Bryant, R. Mandel, K.J. Thies, and A. Thomas. 2013. The first occurrence of a toxodont (Mammalia, Notoungulata) in the United States. Journal of Vertebrate Paleontology 33:229-232.

Luz, B., Y. Kolodny, and M. Horowitz. 1984. Fractionation of oxygen isotopes between mammalian bone-phosphate and environmental drinking water. Geochimica et Cos-

mochimica Acta 48:1689–1693.

MacArthur, R. and R. Levins. 1967. The limiting similarity, convergence, and divergence of coexisting species. American Naturalist 101:377-385.

MacFadden, B.J. 2000. Middle Pleistocene climate change recorded in fossil mammal teeth from Tarija, Bolivia, and upper limit of the Ensenadan Land-Mammal Age. Quaternary Research 54:121–131.

MacFadden, B.J. and T.E. Cerling. 1996. Mammalian herbivore communities, ancient feeding ecology, and carbon isotopes: A 10-million year sequence from the Neogene of Florida: Journal of Vertebrate Paleontology 16:103–115.

MacFadden, B.J., N. Solounas, and T.E. Cerling. 1999a. Ancient diets, ecology, and extinction of 5-million-year-old horses from Florida. Science 283:824–827.

MacFadden B.J., T.E. Cerling, J.M. Harris, and J. Prado. 1999b. Ancient latitudinal gradients of C3/C4 grasses interpreted from stable isotopes of New World Pleistocene horse (*Equus*) teeth. Global Ecology and Biogeography 8, 137–149.

MacFadden, B.J., Y. Wang, T.E. Cerling, and F. Anaya. 1994. South American fossil mammals and carbon isotopes: a 25 million-year sequence from the Bolivian Andes. Palaeogeography, Palaeoclimatology, Palaeoecology 107:257-268.

Maglio, V.J. 1972. Evolution of mastication in the Elephantidae. Evolution 26:638-658.

Maglio, V.J. 1973. Origin and evolution of the Elephantidae. Transactions of the American Philosophical Society 63:1-149.

Malhi, Y., C.E. Doughty, M. Galetti, F.A. Smith, J-C. Svenning, and J.W. Terborgh. 2016. Megafauna and ecosystem function from the Pleistocene to the Antropocene. PNAS 113(4):838-846.

Marino, B.D., M.B. McElroy, R.J. Salawitch, and W.G. Spaulding. 1992. Glacial-to-interglacial variations in the carbon isotopic composition of atmospheric CO2. Nature 357:461–466.

Martin, P.S. 1967. Prehistoric overkill, in: Martin, P.S., Wright, H.E. Jr. (Eds.), Pleistocene

Extinctions: The Search for a Cause. Yale University Press, pp. 75–120.

Martinez-Meyer, E., P.A. Townsend, and W.W. Hargrove. 2004. Ecological niches as stable distributional constraints on mammal species, with implications for Pleistocene extinctions and climate change projections for biodiversity. Global Ecology and Biogeography 13:305–314.

Mason, H.L. 1944. A Pleistocene flora from the McKittrick asphalt deposits of California. California Academy of Sciences Proceedings, pp. 221–234.

May, R.M. 1974. On the theory of niche overlap. Theoretical Population Biology 5:297-332.

May, R.M. and R.H. MacArthur. 1972. Niche overlap as a function of environmental variability. Proceedings of the National Academy of Sciences 69:1109-1113.

McNab, B.K. 2010. The geographic and temporal correlations of mammal size reconsidered: a resource rule. Oecologia 164:13-23.

McGhee, G.R. Jr., M.E. Clapham, P.M. Sheehan, D.J. Bottjer, and M.L. Droser. 2012. A new ecological-severity ranking of major Phanerozoic biodiversity crises. Palaeogeography, Palaeoclimatology, Palaeoecology 370:260-270.

McGhee, G.R. Jr., P.M. Sheehan, D.J. Bottjer, and M.L. Droser. 2004. Ecological ranking of Phanerozoic biodiversity crises: ecological and taxonomic severities are decoupled. Palaeogeography, Palaeoclimatology, Palaeoecology 211:289-297.

McKinney, M.L. 1997. Extinction vulnerability and selectivity: combining ecological and paleontological views. Annual Review of Ecology and Systematics 28:495-516.

Meade, G.E., 1961. The saber-toothed cat, Dinobastis serus. Part II: Bulletin of the Texas Memorial Museum 2:23–60.

Merceron, G., A. Ramdarshan, C. Blondel, J.-R. Boisserie, N. Brunetiere, A. Francisco, D. Gautier, X. Milhet, A. Novello, and D. Pret. 2016. Untangling the environmental from the dietary: dust does not matter. Proceedings of the Royal Society B 283:20161032.

Merceron, G., E. Hofman-Kamińska, and R. Kowalczyk. 2014. 3D dental microwear

texture analysis of feeding habits of sympatric ruminants in the Bialowiez'a Primeval Forest, Poland. Forest Ecology and Management 328:262-269.

Merceron, G., E. Schulz, L. Kordos, and T.M. Kaiser. 2007. Paleoenvironment of *Dryopithecus brancoi* at Rudabánya, Hungary: evidence from dental meso- and micro-wear analyses of large vegetarian mammals. Journal of Human Evolution 53:331–349.

Merceron, G., G. Escarguel, J-M. Angibault, and H. Verheyden-Tixier. 2010. Can dental microwear textures record inter-individual dietary variations? PLoS ONE 5:e9542.

Metcalfe, J.Z. 2017. Proboscidean isotopic compositions provide insight into ancient humans and their environments. Quaternary International 443:147-159.

Metcalfe, J.Z., F.J. Longstaffe, J.A.M. Ballenger, and C.V. Haynes. 2011. Isotopic paleoecology of Clovis mammoths from Arizona. Proceedings of the National Academy of Science USA 108:17916–17920.

Metcalfe, J.Z., F.J. Longstaffe, and G. Hodgins. 2013. Proboscideans and paleoenvironments of the Pleistocene Great Lakes: landscape, vegetation, and stable isotopes. Quaternary Science Reviews 76:102-113.

Metcalfe, J.Z., F.J. Longstaffe, and G.D. Zazula. 2010. Nursing, weaning, and tooth development in woolly mammoths from Old Crow, Yukon, Canada: Implications for Pleistocene extinctions. Palaeogeography, Palaeoclimatology, Palaeoecology 298:257-270.

Mihlbachler M.C., B.L. Beatty, A. Caldera-Siu, D. Chan, and R. Lee. 2012. Error rates and observer bias in dental microwear analysis using light microscopy. Paleontologica Electronica 15:12A.

Mihlbachler, M.C., D. Campbell, C. Chen, M. Ayoub, and P. Kaur. 2018. Microwear-mesowear congruence and mortality bias in rhinoceros mass-death assemblages. Paleobiology 44:131–154.

Mihlbachler, M.C., D. Campbell, M. Ayoub, C. Chen, I. Ghani. 2016. Comparative dental microwear of ruminant and perissodactyl molars: implications for paleodietary analysis of rare and extinct ungulate clades. Paleobiology 42:98–116.

Mihlbachler, M.C., F. Rivals, N. Solounias, and G.M. Semprebon. 2011. Dietary change in evolution of horses in North America. Science 331:1178–1181.

Millar, C.I. and W.B. Woolfenden. 2016. Ecosystems past: vegetation prehistory, in: Mooney, H., Zavaleta, E. (Eds.), Ecosystems of California. University of California Press, pp. 131–154.

Mooers, A.O., S.B. Heard, and E. Chrostowski. 2005. Evolutionary heritage as a metric for conservation. In: Purvis, A., Gittleman, J.L., Brooks, T. (Eds.) Phylogeny and Conservation. Cambridge: Cambridge University Press:120-138.

Morgan, G.S. and R.C. Hulbert. 1995. Overview of the geology and vertebrate biochronology of the Leisey Shell Pit local fauna, Hillsborough County, Florida. Bulletin of the Florida Museum of Natural History 37:1–92.

Moran, P.A.P. 1950. Notes on continuous stochastic phenomena. Biometrika 37(1/2):17-23.

Mothé, D., L.S. Avilla, L. Asevedo, L. Borges-Silva, M. Rosas, R. Labarca-Encina, R. Souberlich, E. Soibelzon, J.L. Roman-Carrion, S.D. Ríos, A.D. Rincon, G.C. Oliveira, and R.P. Lopes. 2017. Sixty years after 'The mastodonts of Brazil': The state of the art of South American proboscideans (Proboscidea, Gomphotheriidae). Quaternary International 43:52–64.

Muhs, D.R., K.R. Simmons, L.T. Groves, J.P. McGeehin, R.R. Schumann, and L.D. Agenbroad. 2015. Late Quaternary sea-level history and the antiquity of mammoths (*Mammuthus exilis* and *Mammuthus columbi*), Channel Islands National Park, California, USA. Quaternary Research, 83(3):502-521.

Müller, D.W.H., D. Codron, C. Meloro, A. Munn, A. Schwarm, J. Hummel, M. Clauss. 2013. Assessing the Jarman-Bell Principle: Scaling of intake, digestibility, retention time and gut fill with body mass in mammalian herbivores. Comparative Biochemistry and Physiology, Part A 164:129-140.

Murphy, B.P., D.M.J.S. Bowman, and M.K. Gagan. 2007. The interactive effect of tem-

perature and humidity on the oxygen isotope composition of kangaroos. Functional Ecology 21:757–766.

Muscente, A.D., A. Prabhu, H. Zhong, A. Eleish, M.B. Meyer, P. Fox, R.M. Hazen, and A.H. Knoll. 2018. Quantifying ecological impacts of mass extinctions with network analysis of fossil communities. PNAS 115(20):5217-5222.

Naidoo, R., B. Fisher, A. Manica and A. Balmford. 2016. Estimating economic losses to tourism in Africa from the illegal killing of elephants. Nature Communications 7(13379):1-9.

Naiman, R.J. 1988. Animal influences on ecosystem dynamics. Bioscience 38:750-752.

Nakagawa, S. 2004. A farewell to Bonferroni: the problems of low statistical power and publication bias. Behavioral Ecology 15:1044–1045.

Nee, S. and R.M. May. 1997. Extinction and the loss of evolutionary history. Science 278:692-694.

Newsom, L. and M.C. Mihlbachler. 2006. Mastodon (*Mammut americanum*) diet and foraging patterns based on dung material from the Page/Ladson site (8JE581), Jefferson County, Florida, in: Webb, S.D. (Ed.), The First Floridians and Last Mastodons: the Page-Ladson Site in the Aucilla River. Topics in Geobiology. Springer, pp. 263–333

Nowak, R.M. 2018. Walker's mammals of the world. John's Hopkins University Press, Baltimore. 784 pp.

O'Leary, M.H. 1988. Carbon isotopes in photosynthesis. BioScience 38(5):328–336.

Orr, P.C. 1968. Prehistory of Santa Rosa Island. Santa Barbara Museum of Natural History, Santa Barbara.

Osmond C.B., W.G. Allaway, B.G. Sutton, J.H. Troughton, O. Queiroz, U. Lüttge, and K. Winter. 1973. Carbon isotope discrimination in photosynthesis of CAM plants. Nature 246:41-42.

Oster, J.L., S.F. Warken, N. Skhon, M.M. Arienzo, and M. Lachniet. 2019. Speleothem paleoclimatology for the Caribbean, Central America, and North America. Quaternary

2(5):1–33.

Oster, J.L., I.P. Montanez, L.R. Santare, W.D. Sharp, C. Wong, and K.M. Cooper. 2015a. Stalagmite records of hydroclimate in central California during termination 1. Quaternary Science Reviews 127:199–214.

Oster, J.L., D.E. Ibarra, M.J. Winnick, and K. Maher. 2015b. Steering of westerly storms over western North America at the Last Glacial Maximum. Nature Geoscience 8:201-205.

Owen-Smith, R.N. 1987. Pleistocene extinctions: the pivotal role of megaherbivores. Paleobiology 13:351-362.

Owen-Smith, R.N. 1988. Megaherbivores: the influence of very large body size on ecology. Cambridge: Cambridge University Press.

Owen-Smith, R.N. and J. Chafota. 2012. Selective feeding by a megaherbivore, the African elephant (*Loxodonta africana*). Journal of Mammology 93:698-705.

Palombo, M.R., M.L. Filippi, P. Iacumin, A. Loginelli, M. Barbieri, and A. Maras. 2005. Coupling tooth microwear and stable isotope analyses for palaeodiet reconstruction: the case study of Late Middle Pleistocene *Elephas* (*Palaeoloxodon*) *antiquus* teeth from Central Italy (Rome area). Quaternary International 126-128:153-170.

Papworth, S.K., J. Rist, L. Coad, and E.J. Milner-Gulland. 2009. Evidence for shifting baseline syndrome in conservation. Conservation Letters 2(2):93-100.

Passey, B.H., T.F. Robinson, L.K. Ayliffe, T.E. Cerling, M. Sponheimer, M.D. Dearing, B.L. Roeder, and J.R. Ehleringer. 2005. Carbon isotope fractionation between diet, breath CO2, and bioapatite in different mammals. Journal of Archeological Science 32:1459–1470.

Payne, J.L., A.M. Bush, N.A. Heim, M.L. Knope, and D.J. McCauley. 2016. Ecological selectivity of the emerging mass extinction in the oceans. Science 353:1284–1286.

Pérez-Crespo, V.A. J. Cabrales-Arroyo, M. Benammi, E. Johnson, O.J. Polaco, A. Santos-Moreno, P. Morales-Puente, and E. Cienfuegos-Alvarado. 2012. Geographic variation

of diet and habitat of the Mexican populations of Columbian Mammoth (*Mammuthus columbi*). Quaternary International 276-277:8-16.

Pérez-Crespo, V.A., J.L. Prado, M.T. Alberdi, J. Arroyo-Cabrales, and E. Johnson. 2016. Diet and habitat for six American Pleistocene proboscidean species using carbon and oxygen stable isotopes. Ameghiniana 53:39–51.

Peters, R.H. 1983. The Ecological Implications of Bodv Size. Cambridge: Cambridge University Press. 329 p.

Peterson, A.T., J. Soberón, and V. Sánchez-Cordero. 1999. Conservatism of ecological niches in evolutionary time. Science 285:1265–1267.

Petersen, K.L., P.J. Mehringer, and C.E. Gustafon. 1983. Late-glacial vegetation and climate at the Manis Mastodon site, Olympic Peninsula, Washington. Quaternary Research 20:215-231.

Pianka, E.R. 1976. Competition and niche theory. In R.M. May, ed. Theoretical Ecology – Principles and Applications. Blackwell Scientific Publishing. pp. 114–141

Pires, M.M., B.D. Rankin, D. Silvestro, and T.B. Quental. 2018. Diversification dynamics of mammalian clades during the K-Pg mass extinction. Biol Lett 14:20180458

Poole, J.H. 1987. Rutting behavior in African elephants: the phenomenon of musth. Behaviour 102(3/4):283-316.

Post, E. 2013. Life history variation and phenology. In E. Post., ed. Ecology of climate change: the importance of biotic interactions. Monographs in Population Biology (52), Princeton University Press, pp. 54-95.

Pound, M.J. and U. Salzmann. 2007. Heterogeneity in global vegetation and terrestrial climate change during the late Eocene to early Oligocene transition. Scientific Reports 7:43386.

Prideaux, G.J., L.K. Ayliffe, L.R.G. DeSantis, B.W. Schubert, P.F. Murray, M.K. Gagan, and T.E. Cerling. 2009. Extinction implications of a chenopod browse diet for a giant Pleistocene kangaroo. Proceedings of the National Academy of Science USA

106:11646–11650.

Pringle, R.M. 2008. Elephants as agents of habitat creation for small vertebrates at the patch scale. Ecology 89:26-33.

Prothero, D.R. 1994. The Late Eocene-Oligocene extinctions. Annual Review of Earth and Planetary Sciences 22:145-165.

Prothero, D.R. and T.H. Heaton. 1996. Faunal stability during the early Oligocene climatic crash. Palaeogeography Palaeoclimatology Palaeoecology 127:257–283.

Purnell, M., O. Seehausen, and F. Galis. 2012. Quantitative three-dimensional microtextural analyses of tooth wear as a tool for dietary discrimination in fishes. Journal of the Royal Society Interface 9:2225–2233.

Purvis, A. 2008. Phylogenetic approaches to the study of extinction. Annual Review of Ecological Systemics 39:301-319.

Rabosky, D.L. 2013. Diversity-dependence, ecological speciation, and the role of competition in macroevolution. Annual Review of Ecology, Evolution, and Systematics 44:481–502.

Ramdarshan, A., C. Blondel, N. Bruneitière, A. Francisco, D. Gautier, J. Surault, and G. Merceron. 2016. Seeds, browse, and tooth wear: a sheep perspective. Ecology and Evolution 6:5559-5569.

Raup, D. M. 1972. Taxonomic diversity during the Phanerozoic. Science 177:1065–1071.

Raup, D.M. and Sepkoski, J.J. Jr., 1982. Mass extinctions in the marine fossil record. Science 215:1501-1503.

Raup, D.M. and Sepkoski, J.J. Jr., 1986. Periodic extinction of families and genera. Science 231:833–836.

Ripple, W.J., et al., 2017. World Scientists' Warning to Humanity: a second notice. BioScience 67(12): 1026–1028.

Rivals, F. and G.M. Semprebon 2011. Dietary plasticity in ungulates: insight from tooth microwear analysis. Quaternary International 245:279–284.

Rivals, F., D. Mol, F. Lacombat, A.M. Lister, and G.M. Semprebon. 2015. Resource partitioning and niche separation between mammoths (*Mammuthus rumanus* and *Mammuthus meridionalis*) and gomphotheres (*Anancus arvernensis*) in the Early Pleistocene of Europe. Quaternary International 379:167–170.

Rivals, F., G.M. Semprebon, A. Lister. 2012. An examination of dietary diversity patterns in Pleistocene proboscideans (*Mammuthus*, *Palaeoloxodon*, and *Mammut*) from Europe and North America as revealed by dental microwear. Quaternary International 255:188-195.

Rivals, F., M.C. Mihlbachler, N. Solounias, D. Mol, G.M. Semprebon, J. de Vos, and D.C. Kalthoff. 2010. Palaeoecology of the Mammoth Steppe fauna from the late Pleistocene of the North Sea and Alaska: Separating species preferences from geographic influence in paleoecological dental wear analysis. Palaeogeography Palaeoclimatology Palaeoecology 286:42-54.

Rivals, F., N. Solounias, and M.C. Mihlbachler. 2007. Evidence for geographic variation in the diets of late Pleistocene and early Holocene *Bison* in North America, and differences from the diets of recent *Bison*. Quaternary Research 68:338–346.

Roth, V.L., 1982. Dwarf mammoths from the Santa Barbara Channel Islands: Size, Shape, Development, and Evolution. Yale University PhD Dissertation, 277 p.

Roth, V.L., 1996. Pleistocene dwarf elephants from the California Islands, in: Shoshani, J., Tassy, P. (Eds.), The Proboscidea: Evolution and Paleoecology of Elephants and their Relatives. Oxford University Press, pp. 249-253.

Roy, K., G. Hunt, and D. Jablonski. 2009. Phylogenetic conservatism of extinctions in marine bivalves. Science 325(5941): 733–737.

Rozanski, K., L. Araguas-Araguas, and R. Gonfiantini. 1992. Relation between long-term trends of oxygen-18 isotope composition of precipitation and climate. Science 258:981-985.

Saarinen, J. and A. Karme. 2017. Tooth wear and diets of extant and fossil xenarthrans

(Mammalia, Xenarthra) – applying a new mesowear approach. Palaeogeography, Palaeoclimatology, Palaeoecology 476:42-54.

Saarinen, J., A. Karme, T. Cerling, K. Uno, L. Säilä, S. Kasiki, S. Ngene, T. Obari, E. Mbua, F.K. Manthi, and M. Fortelius. 2015. A new tooth wear–based dietary analysis method for Proboscidea (Mammalia). Journal of Vertebrate Paleontology e:918546.

Sage, R.F. 2017. A portrait of the C4 photosynthetic family on the 50th anniversary of its discovery: species number, evolutionary lineages, and Hall of Fame. Journal of Experimental Botany 68(2):e11–e28.

Sánchez, B., J.L. Prado, J.L., and M.T. Alberdi. 2004. Feeding ecology, dispersal, and extinction of South American Pleistocene gomphotheres (Gomphotheriidae, Proboscidea). Paleobiology 30:146–161.

Sánchez, G., V.T. Holliday, E.P. Gaines, J. Arroyo-Cabrales, N. Martínez-Tagüeña, A. Kowler, T. Lange, G.W.L. Hodgins, S.M. Mentzer, and I. Sanchez-Morales. 2014. Human (Clovis)-Gomphothere (Cuvieronius sp.) Association 13,390 Calibrated yBP in Sonora, Mexico. Proceedings of the National Academy of Sciences 111:10972-10977.

Sanders, W.J. 2007. Taxonomic review of fossil Proboscidea (Mammalia) from Langebaanweg, South Africa. Transactions of the Royal Society of South Africa, 62(1):1-16.

Sahney, S.S. and M.J. Benton. 2017. The impact of the Pull of the Recent on the fossil record of tetrapods. Evolutionary Ecology Research 18:7–23

Sandom, C.J., S. Faurby, B. Sandel, and J.C. Svenning. 2014. Global late Quaternary megafauna extinctions linked to humans, not climate change. Proceedings of the Royal Society of London Series B: Biological Sciences 281:20133254.

Saunders, J.J. 1977a. Lehner Ranch Revisited, in: Johnson, E. (Ed.), Paleo-Indian lifeways. The Museum Journal, 17:48-64.

Saunders, J.J. 1977b. Late Pleistocene vertebrates of the Western Ozark Highland, Missouri. Illinois State Museum Reports of Investigations, No. 33.

Saunders, J.J. 1996. North American Mammutidae, in: Shoshani, J., Tassy, P. (Eds.), The

Proboscidea: Evolution and Paleoecology of Elephants and their Relatives. Oxford University Press, pp. 272-279.

Saunders, A.K. and L.R.G. DeSantis. 2017. Dietary ecology of the Local Lancefield Fauna in Victoria, Australia: did the kangaroos die from a massive drought? In: Southeastern GSA 67th Meeting Program and Abstracts Book.

Schluter, D. 2000. Ecological character displacement in adaptive radiation. American Naturalist 156:S4–S16.

Schoener, T.W. 1974. Resource partitioning in ecological communities. Science 185:27–38.

Schoener, T.W. 1982. The controversy over interspecific competition. American Naturalist 70:586–595.

Schubert, B.A. and A.H. Jahren, 2012. The effect of atmospheric CO2 concentration on carbon isotope fractionation in C3 land plants. Geochimica et Cosmochimica Acta 96:29-43.

Schubert, B.A. and A.H. Jahren. 2015. Global increase in plant carbon isotope fractionation following the Last Glacial Maximum caused by increase in atmospheric pCO2. Geology 43:435–438.

Schulte, P., et al. 2010. The Chicxulub asteroid impact and mass extinction at the Cretaceous-Paleogene boundary. Science 327(5970):1214-1218

Schultz, E., V. Piotrowski, M. Clauss, M. Mau, G. Merceron, and T.M. Kaiser. 2013. Dietary abrasiveness is associated with variability of microwear and dental surface texture in rabbits. PLoS ONE 8:e56167.

Scott, E., K.B. Springer, and J.C. Sagebiel. 2017. The Tule Springs local fauna: Rancholabrean vertebrates from the Las Vegas Formation, Nevada. Quaternary International 443:105-121.

Scott, J.R. 2012. Dental microwear texture analysis of extant African Bovidae. Mammalia 76:157-174.

Scott R.S., P.S. Ungar, T.S. Bergstrom, C.A. Brown, C.A., B.D. Childs, M.F. Teaford, A.

Walker. 2006. Dental microwear texture analysis: technical considerations. Journal of Human Evolution 51:339–349.

Scott, R.S., P.S. Ungar, T.S. Bergstrom, C.A. Brown, F.E. Grine, M.F. Teaford, and A. Walker. 2005. Dental microwear texture analysis shows within-species diet variability in fossil hominins. Nature Letters 436:693–695.

Secord, R., J.I. Bloch, S.G.B. Chester, D.M. Boyer, A.R. Wood, S.L. Wing, M.J. Kraus, F.A. McInerney, and J. Krigbaum. 2012. Evolution of the earliest horses driven by climate change in the Paleocene-Eocene Thermal Maximum. Science 335(6071):959-962.

Seddon, A.W.R., et al. 2014. Looking forward through the past: identification of 50 priority research questions in paleoecology. Journal of Ecology 102:256-267.

Semprebon, G.M. 2002. Advances in the reconstruction of extant ungulate ecomorphology with applications to fossil ungulates. University of Massachusetts, Amnherst PhD Dissertation, 457 p.

Semprebon, G.M. and F. Rivals. 2010. Trends in the paleodietary habits of fossil camels from the Tertiary and Quaternary of North America. Palaeogeography, Palaeoclimatology, Palaeoecology 295:131–145.

Semprebon G.M., L.R. Godfrey, N. Solounias, M.R. Sutherland, and W.L. Jungers. 2004. Can low-magnification stereomicroscopy reveal diet? Journal of Human Evolution 47:115-144.

Semprebon, G.M., F. Rivals, J.M. Fahlke, W.J. Sanders, A.M. Lister, and U.B. Gohlich. 2016. Dietary reconstruction of pygmy mammoths from Santa Rosa Island of California. Quaternary International 406B:1-14.

Sepkoski, J.J. Jr., 1996. Patterns of Phanerozoic extinction: a perspective from global data bases. In: Walliser, O.H., Ed. Global Events and Event Stratigraphy in the Phanerozoic. Berlin: Sprigner-Vertag, 35-52.

Shaw, C.A., Quinn, J.P., 1986. Rancho La Brea: a look at coastal southern California's

past. California Geology 39, 123–133.

Shoshani, J., 1998. Understanding proboscidean evolution: a formidable task. Trends in Ecology and Evolution 13, 480-487.

Silvestro, D., Antonelli, A., Salamin, N., and Quental, T.B., 2015. The role of clade competition in the diversification of North American canids. PNAS 112(28):8684-8689.

Simard, M.A., S.D. Cote, R.B. Weladji, and J. Huot. 2008. Feedback effects of chronic browsing on life-history traits of a large herbivore. Journal of Animal Ecology 77:678–686.

Sinclair, A.R.E. 1975. The resource limitation of trophic levels in tropical grassland ecosystems. Journal of Animal Ecology 44:497–520.

Sinclair, A.R.E., S. Mduma, J.S. Brashares. 2003. Patterns of predation in a diverse predator-prey system. Nature 425:288–290.

Sjostrom, D.J. and J.M. Welker. 2009. The influence of air mass source on the seasonal isotopic composition of precipitation, eastern USA. Journal of Geochemical Exploration 102:103–112.

Slotow, R. and G. van Dyk. 2001. Role of delinquent young "orphan" male elephants in high mortality of white rhinoceros in Pilanesberg National Park, South Africa. Koedoe 44(1):85-94.

Smith, G.J. and L.R.G. DeSantis. 2018. Dietary ecology of Pleistocene mammoths and mastodons as inferred from dental microwear textures. Palaeogeography, Palaeoclimatology, Palaeoecology 492:10–25.

Smith, G.J. and R.W. Graham. 2017. The effects of dental wear on impairing mammoth taxonomy: a reappraisal of the Newton mammoth, Bradford County, northeastern Pennsylvania. Quaternary International 443:40-51.

Solounias, N., G. Semprebon. 2002. Advances in the reconstruction of ungulate ecomorphology with application to early fossil equids. American Museum Novitates 3366:1–49.

Solounias, N., M. Teaford, and A. Walker. 1988. Interpreting the diet of extinct ruminants: the case of a non-browsing giraffid. Paleobiology 14:287–300.

Souron, A., Merceron, G., Blondel, C., Brunetière, N., Colyn, M., Hofman-Kamińska, E., Boisserie, J.-R., 2015. Three-dimensional dental microwear texture analysis and diet in extant Suidae (Mammalia: Cetartiodactyla). Mammalia 79, 279–291.

Springer K., E. Scott, J.C. Sagebiel, and K.M. Lyndon. 2009. The Diamond Valley Lake Local Fauna: Late Pleistocene vertebrates from inland southern California. Bulletin of the Museum of Northern Arizona 65:217–235.

Springer, K.B., E. Scott, J.C. Sagebiel, and L.K. Murray. 2010. Late Pleistocene large mammal faunal dynamics from inland southern California: The Diamond Valley Lake local fauna. Quaternary International 217:256–265.

Springer, M.S., W.J. Murphy, E. Eizirik, and S.J. O'Brien. 2003. Placental mammal diversification and the Cretaceous-Tertiary Boundary. PNAS 100(3):1056-1061.

Stansfield, F.J. 2015. A novel objective method of estimating the age of mandibles from African elephants (*Loxodonta africana africana*). PLoS One 10:e0124980.

Still, C.J., J.A. Berry, G.J. Collatz, and R.S. DeFries. 2003. Global distribution of C3 and C4 vegetation: Carbon cycle implications. Global Biogeochemical Cycles 17:1006.

Stowe, L.G. and J.A. Teeri. 1978. The geographic distribution of C4 species of the Dicotyledonae in relation to climate. American Naturalist 112:609–623.

Strömberg, C.A.E. and F.A. McInerney. 2011. The Neogene transition from C3 to C4 grasslands in North America: assemblage analysis of fossil phytoliths. Paleobiology 37(1):50–71.

Sukumar, R., 2003. The Living Elephants: Evolutionary ecology, behavior, and conservation. University of Oxford Press, New York, 478 p.

Teaford M.F. and A. Walker. 1984. Quantitative differences in dental microwear between primate species with different diets and a comment on the presumed diet of *Sivapithecus*. American Journal of Physical Anthropology 64:191–200.

Teaford, M.F. and O.J. Oyen. 1989. In vivo and in vitro turnover in dental microwear. American Journal of Physical Anthropology 80:447–460.

Teale, C.L. and N.G. Miller. 2012. Mastodon herbivory in mid-latitude late-Pleistocene boreal forests of eastern North America. Quaternary Research 78:72-81.

Tedford, R.H., L.B. Albright, A.D. Barnosky, I. Ferrusquia-Villafranca, R.M. Hunt, J.E. Storer, C.C. Swisher, M.R. Voorhies, S.D. Webb, and D.P. Whistler. 2004. Mammalian Biochronology of the Arikareean through Hemphillian Interval (Late Oligocene through Early Pliocene Epochs), in: Woodburne, M.O. (Ed.), Late Cretaceous and Cenozoic Mammals of North America. Columbia University Press, pp. 169-231.

Teeri, J.A. and L.G. Stowe. 1976. Climatic patterns and the distribution of C4 grasses in North America. Oecologia 23:1–12.

Teeri, J.A., L.G. Stowe, and D.A. Murawski. 1978. The climatology of two succulent plant families: Cactaceae and Crassulaceae. Canadian Journal of Botany 56:1750–1758.

Tejada-Lara, J.V., B.J. MacFadden, L. Bermudez, G. Rojas, R. Salas-Gismondi, and J.J. Flynn. 2018. Body mass predicts isotope enrichment in herbivorous mammals. Proceedings of the Royal Society B 285:20181020.

Tipple, B.J., S.R. Meyers, and M. Pagani. 2010. Carbon isotope ratio of Cenozoic CO2: a comparative evaluation of available geochemical proxies. Paleoceanography 25:PA3202.

Tobien, H., 1996. Evolution of zygodons with emphasis on dentition, in: Shoshani, J., Tassy, P. (Eds.), The Proboscidea: Evolution and Paleoecology of Elephants and their Relatives. Oxford University Press, pp. 76-85.

Todd, N.E. and V.L. Roth. 1996. Origin and radiation of the Elephantidae, in: Shoshani, J., Tassy, P. (Eds.),The Proboscidea: Evolution and Paleoecology of Elephants and their Relatives. Oxford University Press, pp. 193-202.

Todd, N.E., N. Falco, N. Silva, and C. Sanchez. 2007. Dental microwear variation in complete molars of *Loxodonta africana* and *Elephas maximus*. Quaternary International 169-170:192-202.

Torres, R.D. 1989. The mammalian carnivore-herbivore relationships in a late Pleistocene asphalt deposit at Maricopa, Kern County, California. Masters Thesis (California State

University, Long Beach).

Trayler, R.B., R.G. Dundas, K. Fox-Dobbs, and P.K. Van DeWater. 2015. Inland California during the Pleistocene – Megafaunal stable isotope records reveal new paleoecological and paleoenvironmental insights. Palaeogeography, Palaeoclimatology, Palaeoecology 437:132-140.

Ungar, P.S., C.A. Brown, T.S. Bergstrom, A. Walker. 2003. A quantification of dental microwear by tandem scanning confocal microscopy and scale-sensitive fractal analyses. Scanning 25:185–193.

Ungar, P.S., F.E. Grine, and M.F. Teaford. 2008. Dental microwear and diet of the Plio-Pleistocene hominin Paranthropus boisei. PLoS One 3:e2044.

Ungar, P.S., G. Merceron, and R.S. Scott. 2007. Dental microwear texture analysis of Varswater bovids and Early Pliocene paleoenvironments of Langebaanweg, Western Cape Province, South Africa. Journal of Mammalian Evolution 14:163–181.

Valli, A.M.F. and M.R. Palombo. 2008. Feeding behavior of middle-size deer from the Upper Pliocene site of Vallier (France) inferred by morphological and micro/mesowear analysis. Palaeogeography, Palaeoclimatology, Palaeoecology 257:106–122.

Valli, A.M.F., M.R. Palombo, and M.T. Alberdi. 2012. How homogenous are microwear patterns on a fossil horse tooth? Preliminary test on a premolar of *Equus altidens* from Barranco Leon 5 (Spain). Alp. Mediterr. Quat. 25:25–33.

van Horne, B. 1982. Niches of adult and juvenile deer mice (*Peromyscus maniculatus*) in seral stages of coniferous forest. Ecology 63:992-1003.

Voelker, S.L., J.R. Brooks, F.C. Meinzer, R. Anderson, M.K. Bader, G. Battipaglia, K.M. Becklin, D. Beerling, D. Bert, J.L. Betancourt, T.E. Dawson, J.C. Domec, R.P. Guyette, C. Körner, S.W. Leavitt, S. Linder, J.D. Marshall, M. Mildner, J. Ogée, I. Panyushkina, H.J. Plumpton, K.S. Pregitzer, M. Saurer, A.R. Smith, R.T. Siegwolf, M.C. Stambaugh, A.F. Talhelm, J.C. Tardif, P.K. van de Water, J.K. Ward, and L. Wingate. 2015. A dynamic leaf gas-exchange strategy is conserved in woody plants under changing am-

bient CO2: evidence from carbon isotope discrimination in paleo and CO2 enrichment studies. Global Change Biology 22(2):889-902.

von Koenigswald, W. 2016. The diversity of mastication patterns in Neogene and Quaternary proboscideans. Palaeontographica Abteilung A. 307:1–41.

Walker, A.W., 1984. Mechanisms of honing in the male baboon canine. American Journal of Physical Anthropology 65:47–60.

Walker, A.W., H.N. Hoeck, and L. Perez. 1978. Microwear of mammalian teeth as an indicator of diet. Science 201:908-910.

Wang, S., T. Deng, T. Tang, G. Xie, Y. Zhang, and D. Wang. 2015. Evolution of *Protanancus* (Proboscidea, Mammalia) in East Asia. Journal of Vertebrate Paleontology 35(1):e881830.

Wasser, S., et al., 2010. Elephants, ivory, and trade. Science 327(5971):1331-1332.

Webb, S.D. 1974. Chronology of Florida Pleistocene mammals. In S.D. Webb, ed. Pleistocene mammals of Florida. University of Florida Press, Gainesville, pp. 5 – 31.

Webb, D.S. 1985. Late Cenozoic mammal dispersals between the America. In F.G. Stehil and S.D. Webb, eds. The Great American Biotic Interchange. Plenum Press, pp. 357–386.

Weins, J.J., D.D. Ackerly, A.P. Allen, B.L. Anacker, L.B. Buckley, H.V. Cornell, E.I. Damschen, T.J. Davies, J.A. Grytnes, S.P. Harrison, B.A. Hawkins, R.D. Holt, C.M. McCain, and P.R. Stephens. 2010. Niche conservatism as an emerging principle in ecology and conservation biology. Ecological Letters 13:1310–1324.

Werner, E.E. and J.F. Gilliam. 1984. The ontogenetic niche and species interactions in size-structured populations. Annual Review of Ecology and Systematics 15:393-425.

Widga, C., S.N. Lengyel, J. Saunders, G. Hodgins, J.D. Walker, and A.D. Wanamaker. 2017a. Late Pleistocene proboscidean populations dynamics in the North American Midcontinent. BOREAS 46:772 -782.

Widga, C., J. Saunders, and J. Enk. 2017b. Reconciling phylogenetic and morphological trends in North American *Mammuthus*. Quaternary International 443:32 – 39.

Williams, J.W. and S.T. Jackson. 2007. Novel climates, no-analog communities, and ecological surprises. Frontiers in Ecology and the Environment 5:475–482.

Wolf, A., C.E. Doughty, and Y. Malhi. 2013. Lateral diffusion of nutrients by mammalian herbivores in terrestrial ecosystems. PLoS ONE 8:e71352.

Wolfe, J. 1994. Tertiary climatic changes at middle latitudes of western North America. Palaeogeography, Palaeoclimatology, Palaeoecology 108:195–205.

Woodburne, M.O. 2004. Late Cretaceous and Cenozoic Mammals of North America: Biostratigraphy and Geochronology. New York: Columbia University Press.

Woodburne, M.O. 2010. The Great American Biotic Interchange: dispersals, tectonics, climate, sea level and holding pens. Journal of Mammal Evolution 17:245–264.

Xia, J., J. Zheng, D. Huang, Z.R. Tian, L. Chen, Z. Zhou, P.S. Ungar, and L. Qian. 2015. New model to explain tooth wear with implications for microwear formation and diet reconstruction. Proceedings of the National Academy of Sciences 112:10669-10672.

Yann, L.T. and L.R.G. DeSantis. 2014. Effects of Pleistocene climates on local environments and dietary behavior of mammals in Florida. Palaeogeography, Palaeoclimatology, Palaeoecology 414:370–381.

Yann, L.T., L.R.G. DeSantis, R.J. Haupt, J.L. Romer, S.E. Corapi, and D.J. Ettenson. 2013. The application of an oxygen isotope aridity index to terrestrial paleoenvironmental reconstructions in Pleistocene North America. Paleobiology 39:576-590.

Yann, L.T., L.R.G. DeSantis, P.L. Koch, and E.L. Lundelius. 2016. Dietary ecology of Pleistocene camelids: Influences of climate, environment, and sympatric taxa. Palaeogeography, Palaeoclimatology, Palaeoecology 461:389–400.

Zachos, J.C., G.R. Dickens, and R.E. Zeebe. 2008. An early Cenozoic perspective on greenhouse warming and carbon-cycle dynamics. Nature 45:279-283.

Zachos, J.C., M. Pagani, L. Sloan, E. Thomas, and K. Billups. 2001. Trends, rhythms, and aberrations in global climate 65 Ma to present. Science 292:686–693.

Zachos, J.C., U. Röhl, S.A. Schellenberg, A. Sluijs, D.A. Hodell, D.C. Kelly, E. Thomas,

M. Nicolo, I. Raffi, L.J. Lourens, H. McCarren, and D. Kroon. 2005. Rapid acidification of the ocean during the Paleocene-Eocene Thermal Maximum. Science 308(5728):1611-615.

Zanazzi, A., M.J. Kohn, B.J. MacFadden, and D.O. Terry. 2007. Large temperature drop across the Eocene-Oligocene transition in central North America. Nature 445:639-642.

Zhang, H., Y. Wang, C.M. Janis, R.H. Goodall, and M.A. Purnell. 2017. An examination of feeding ecology in Pleistocene proboscideans from southern China (*Sinomastodon*, *Stegodon*, *Elephas*), by means of dental microwear texture analysis. Quaternary International 445:60–70.